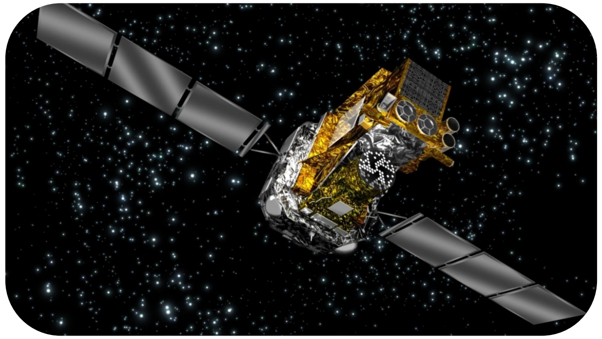

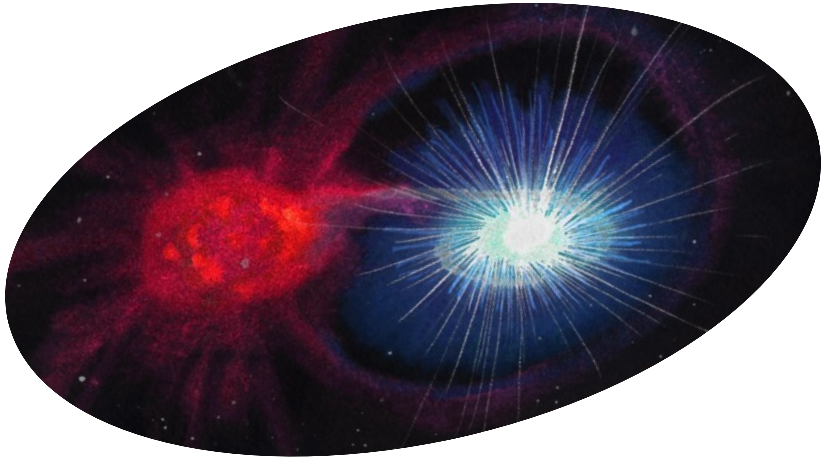

Accessing explosive novae nucleosynthesis in grounded laboratories

C. Fougères[1], et al.

[1]CEA DAM DIF, Arpajon (France)

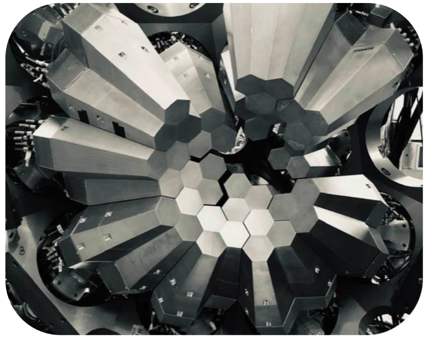

chloe.fougeres@cea.fr

PhyNuBE 3rd meeting 2024
(Oléron, France)

Origin of the elements

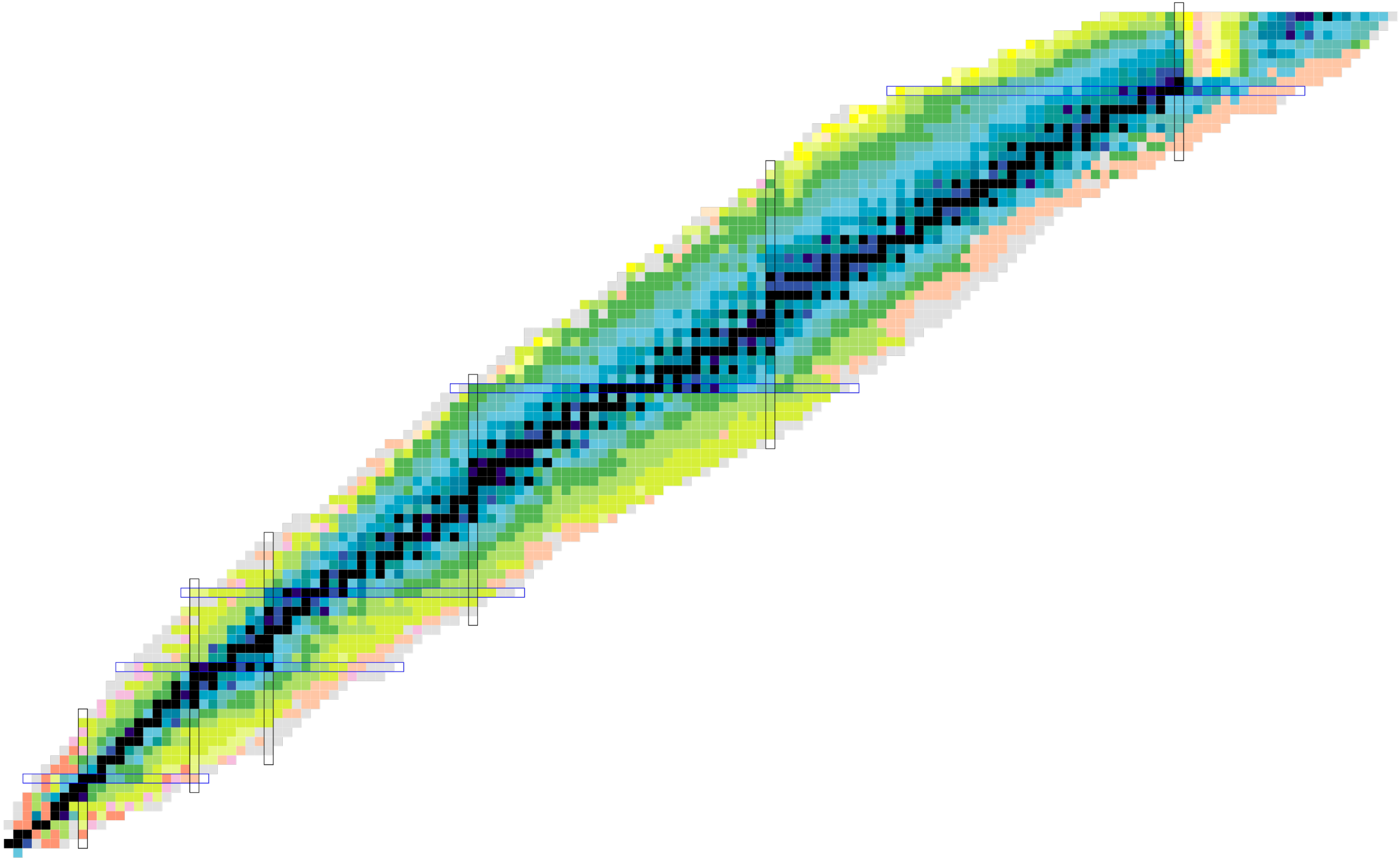

Origin of the elements

Ref. [https://cococubed.com]

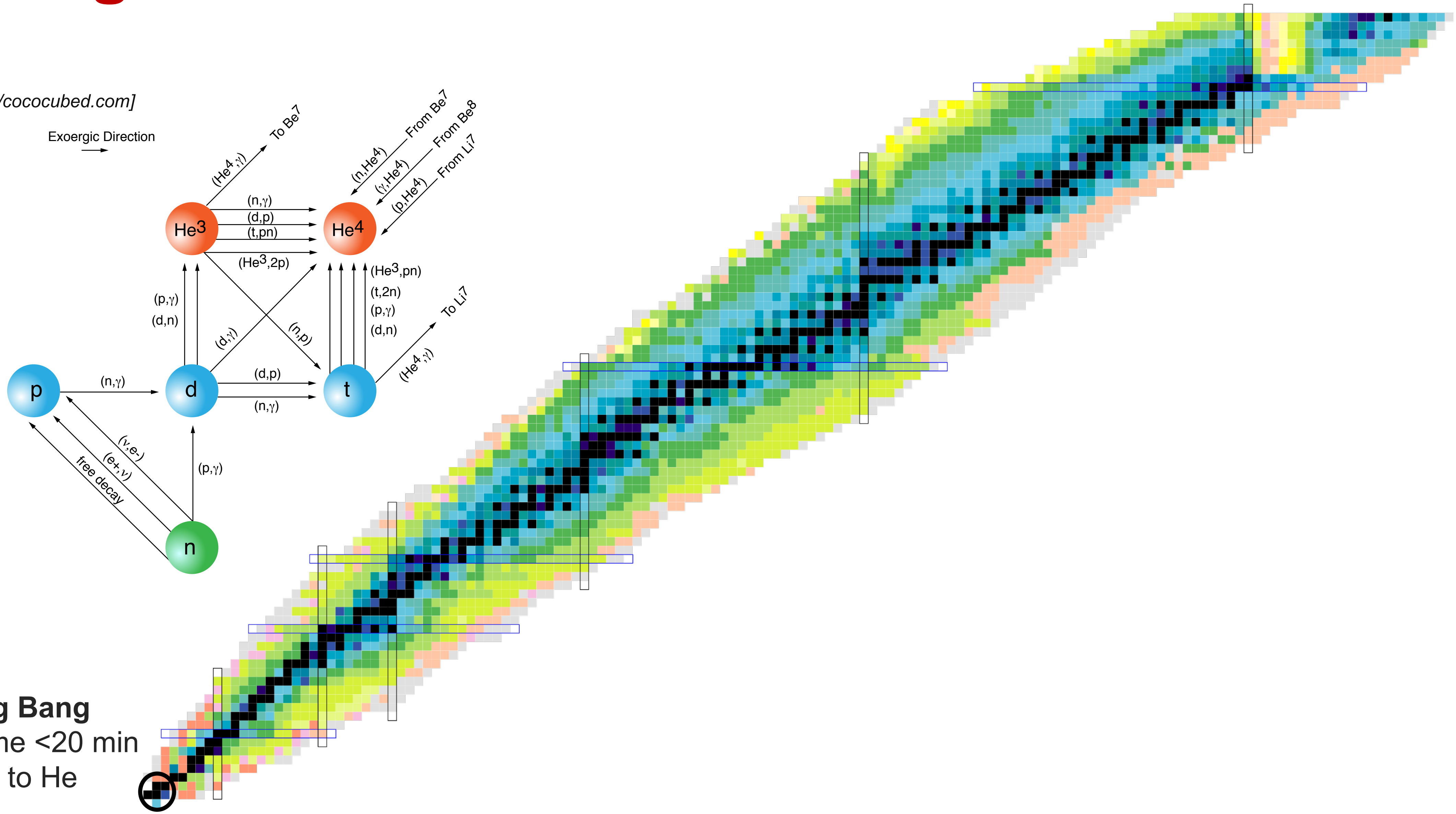

Big Bang
Time <20 min
Up to He

Z
N

Origin of the elements

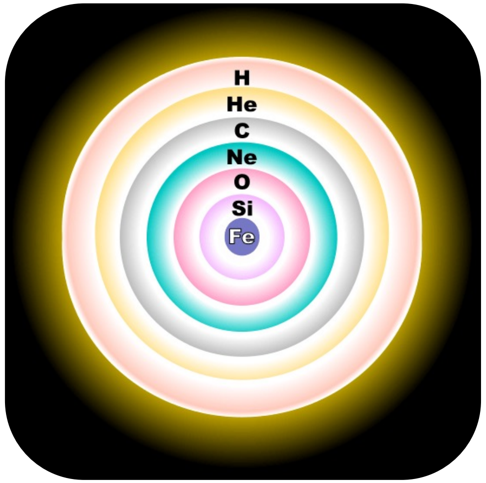

End of live
Fe core and fusion shells

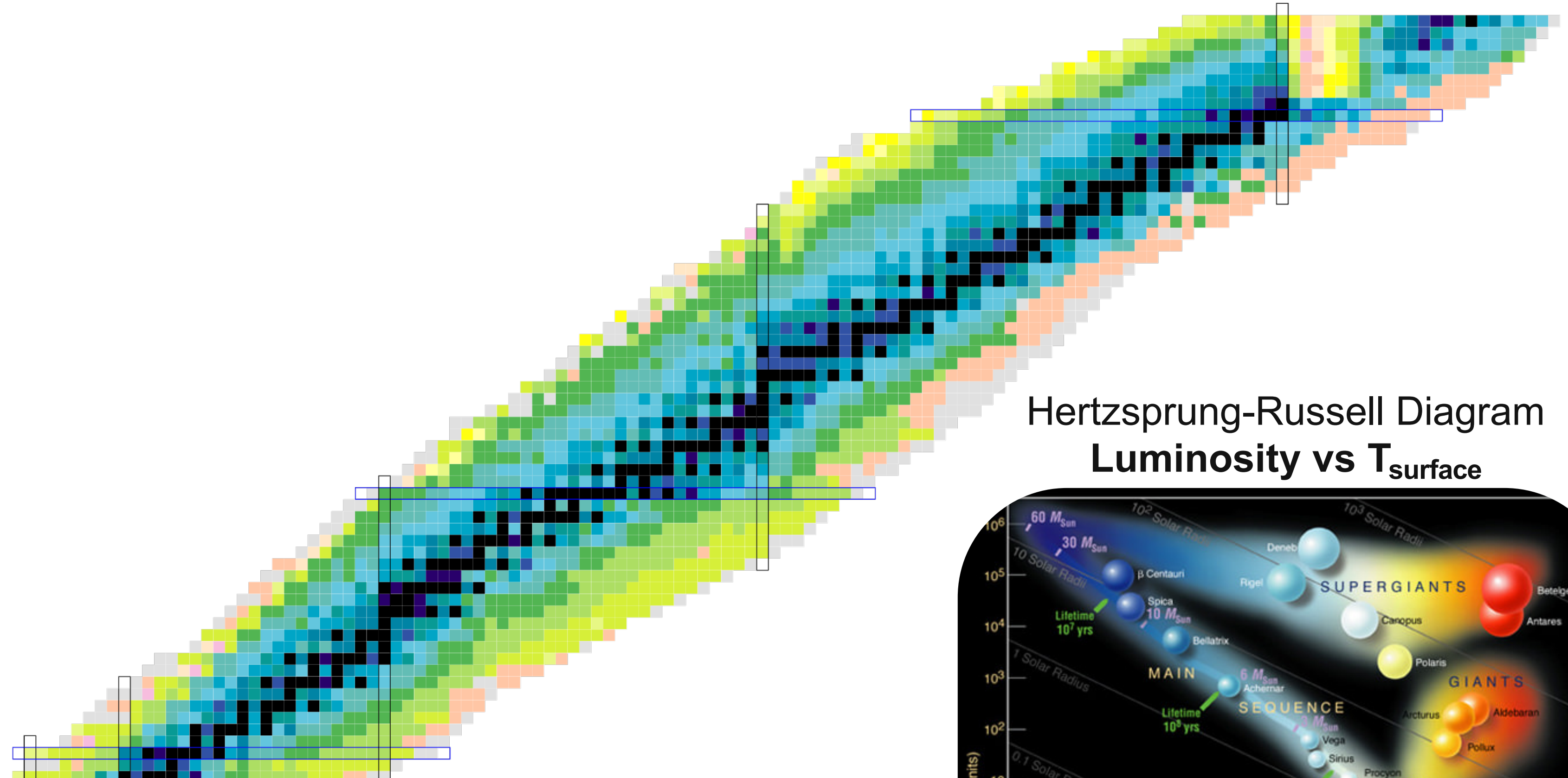
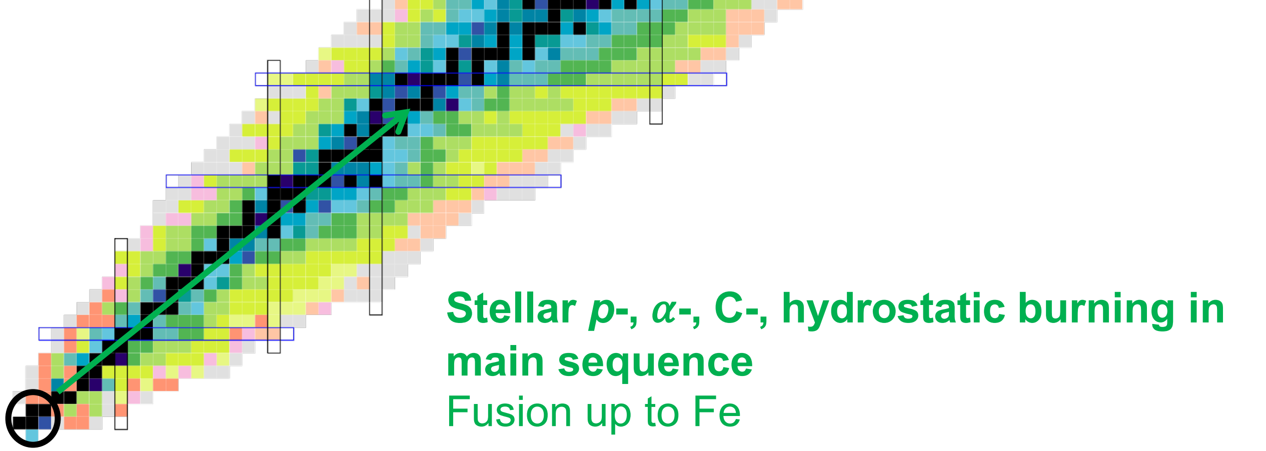

Stellar *p*-, *α*-, C-, hydrostatic burning in main sequence
Fusion up to Fe

Hertzsprung-Russell Diagram
Luminosity vs $T_{surface}$

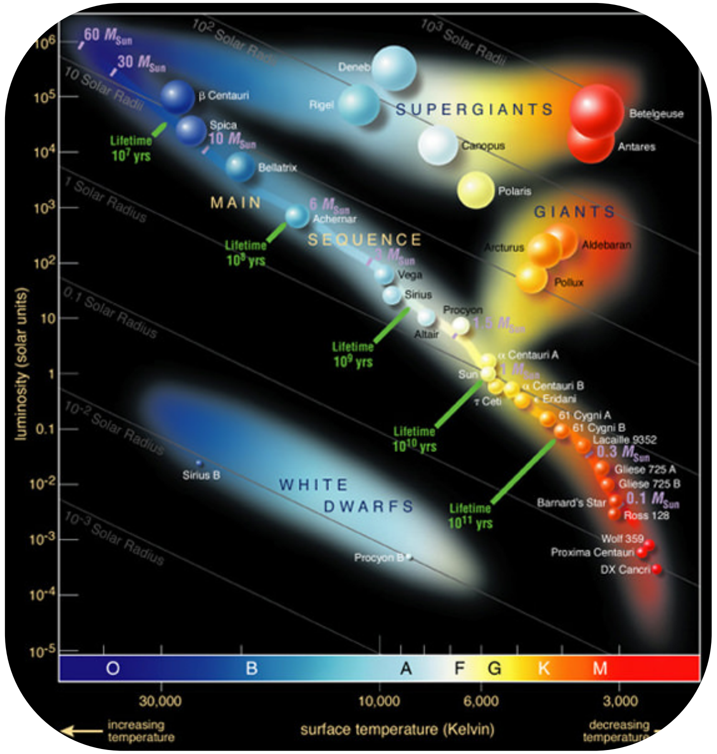

Origin of the elements

Binary stellar systems
Explosive nucleosynthesis

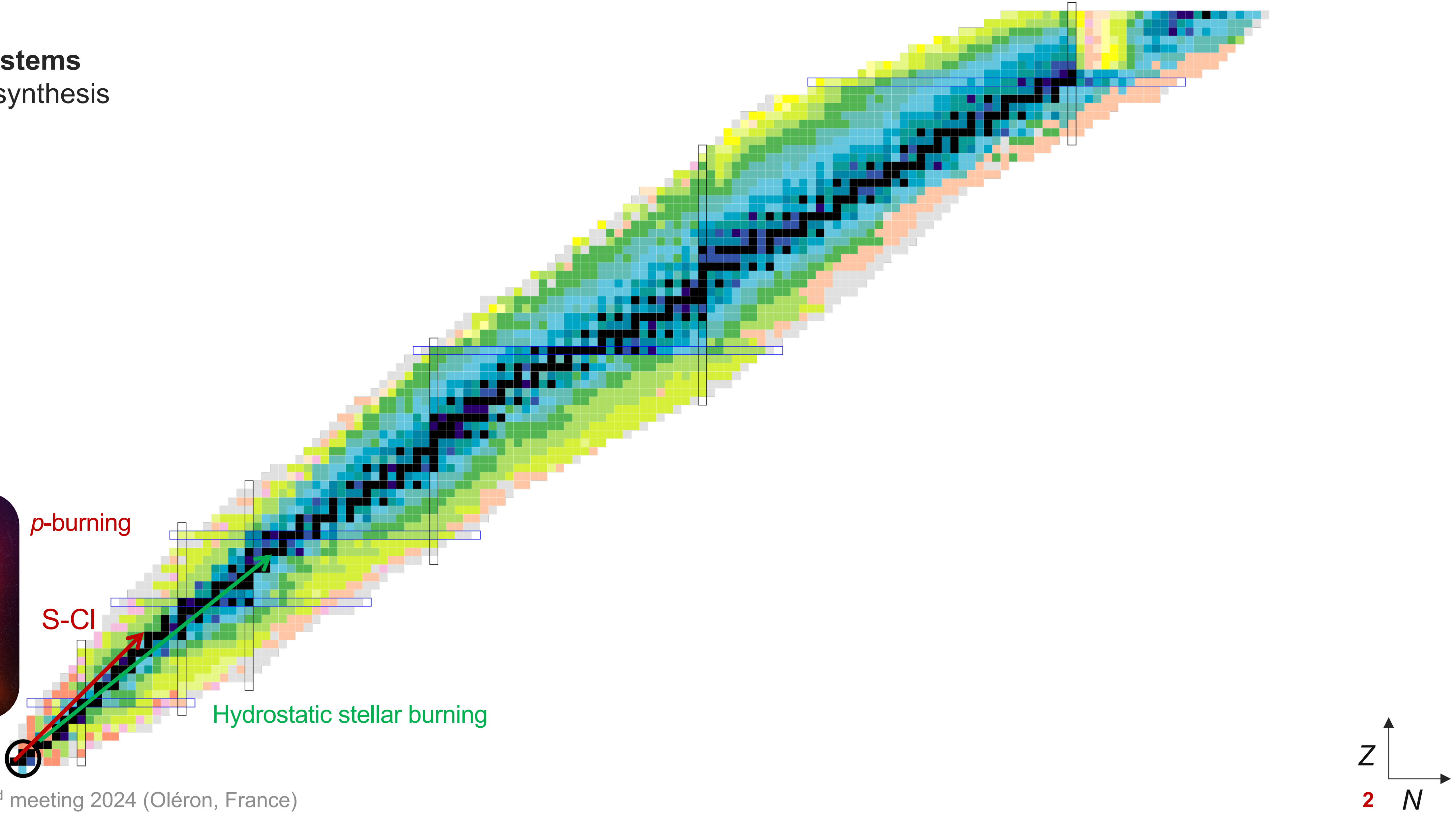

Origin of the elements

Binary stellar systems
Explosive nucleosynthesis

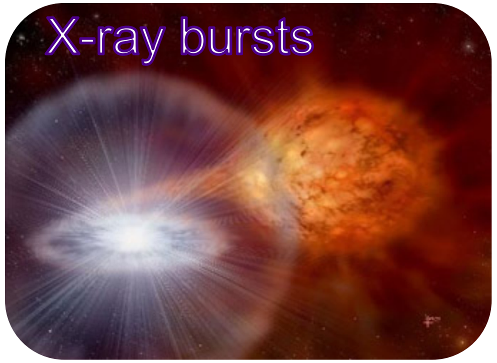

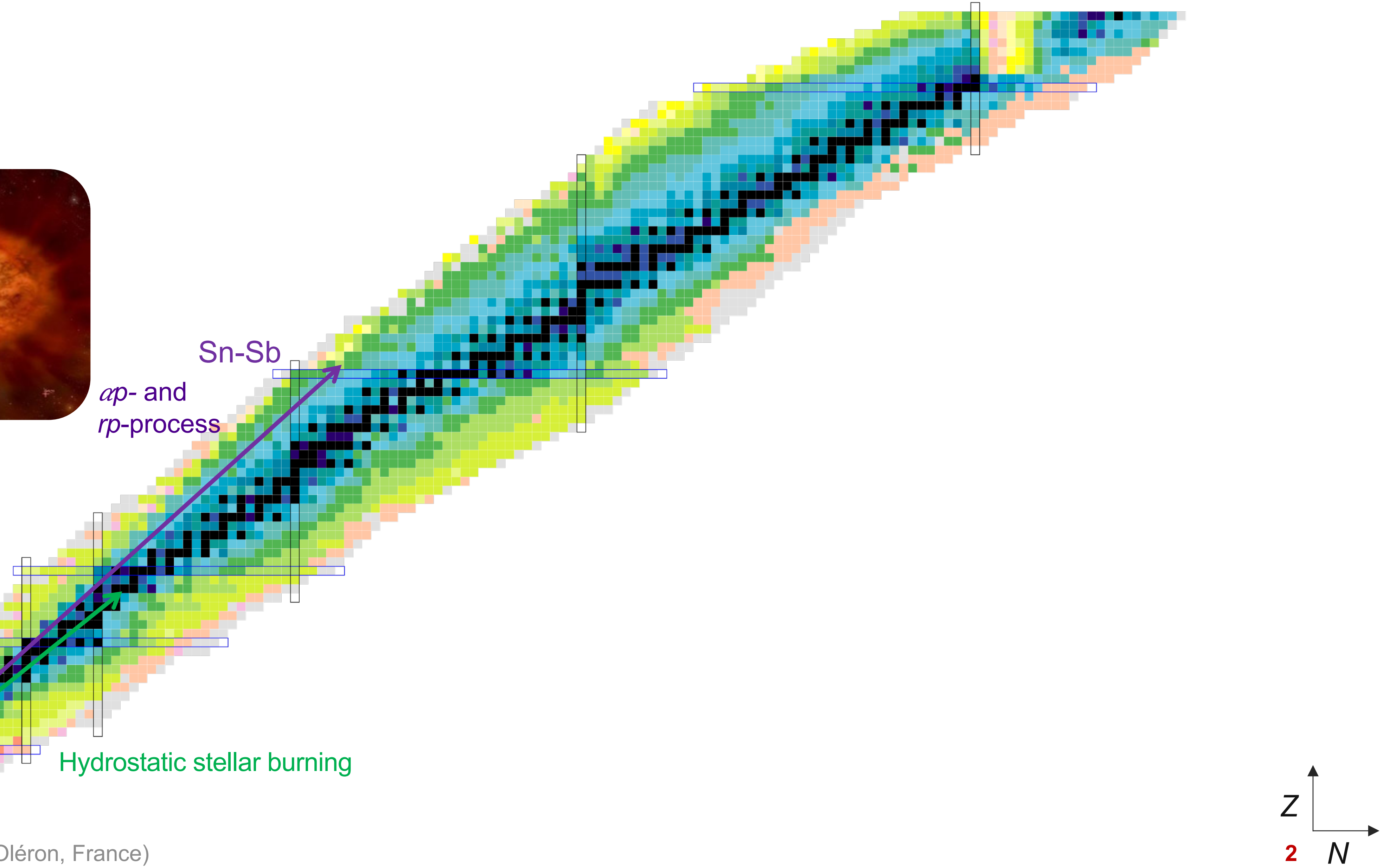

Origin of the elements

Binary stellar systems
Explosive nucleosynthesis

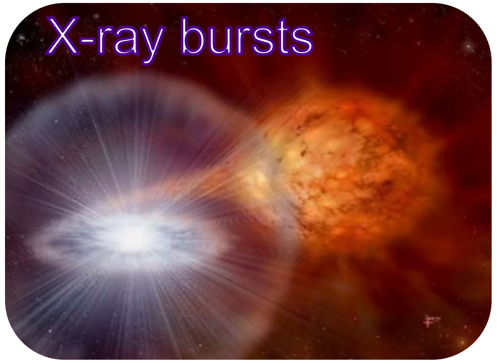

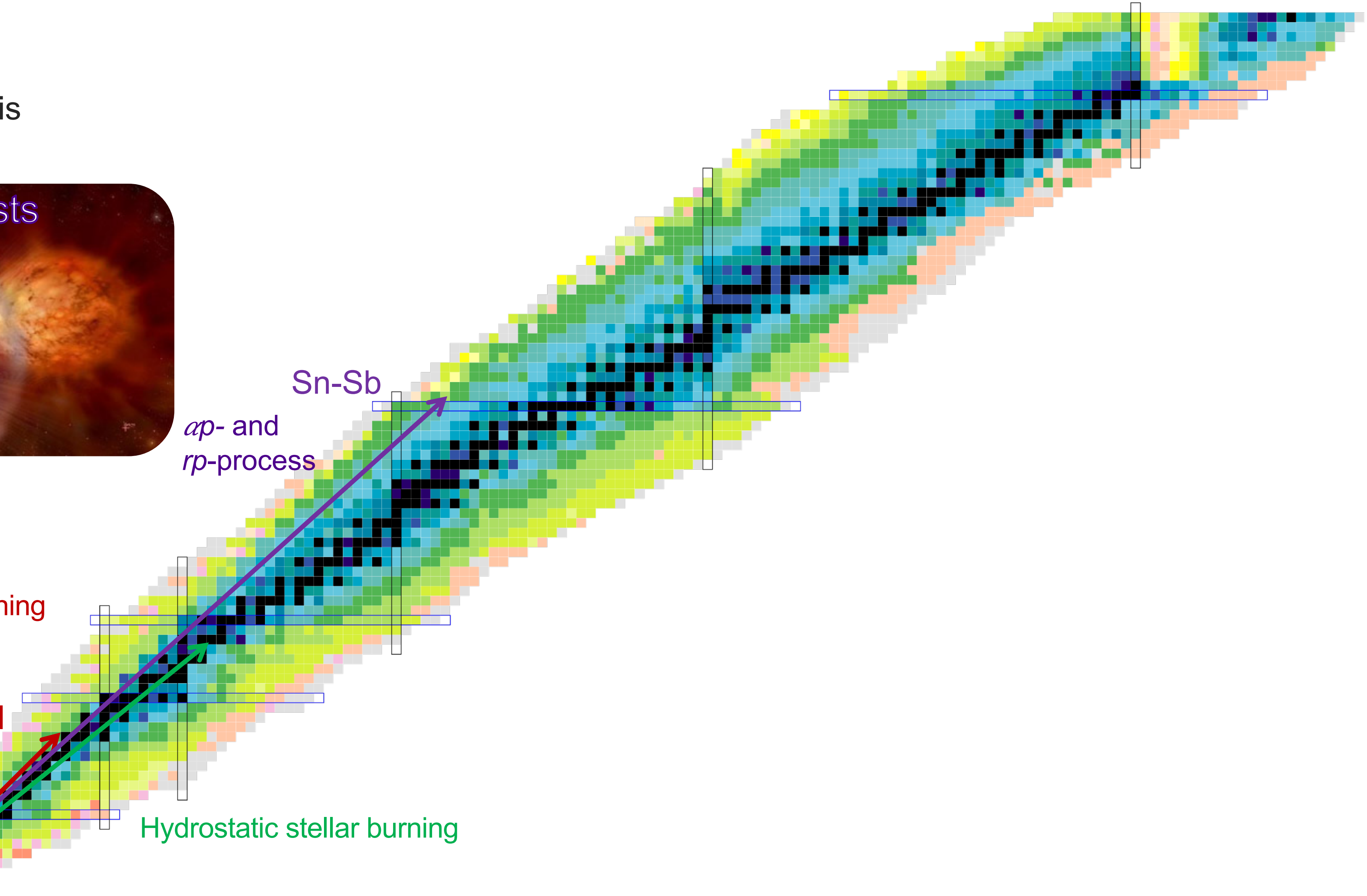

Origin of the elements

Binary stellar systems
Explosive nucleosynthesis

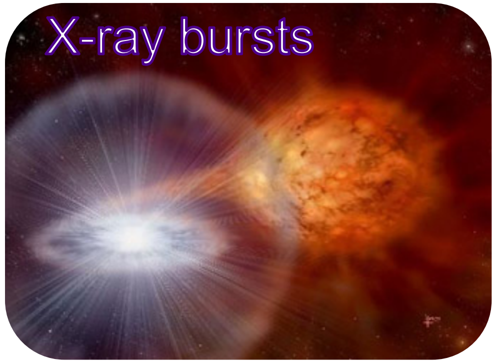

αp- and
rp-process

p-burning

S-Cl

BBN

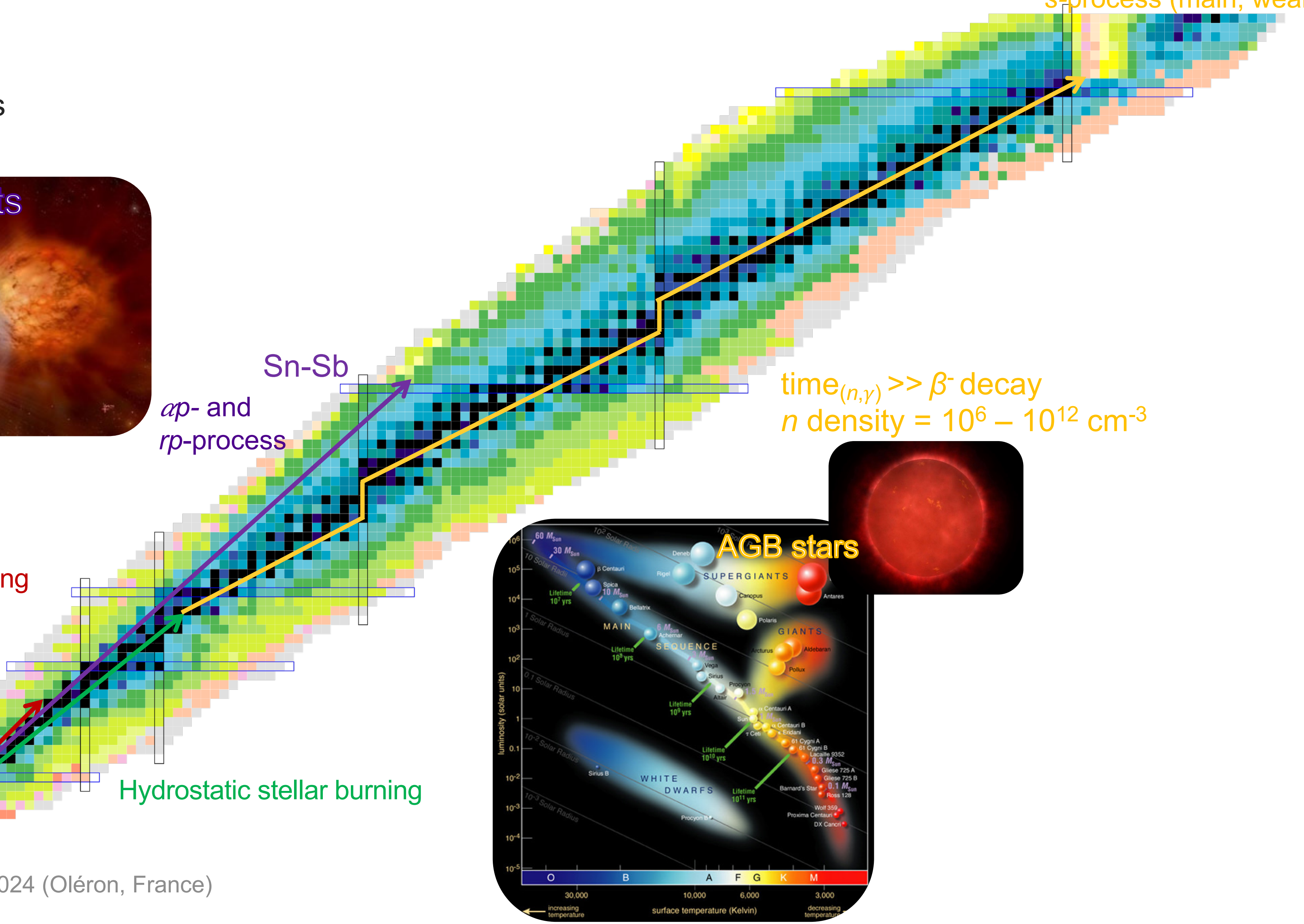

Hydrostatic stellar burning

(n,γ), β^- decay
s-process (main, weak)

time$_{(n,\gamma)}$ >> β^- decay
n density = $10^6 - 10^{12}$ cm^{-3}

Z
N

Origin of the elements

Binary stellar systems
Explosive nucleosynthesis

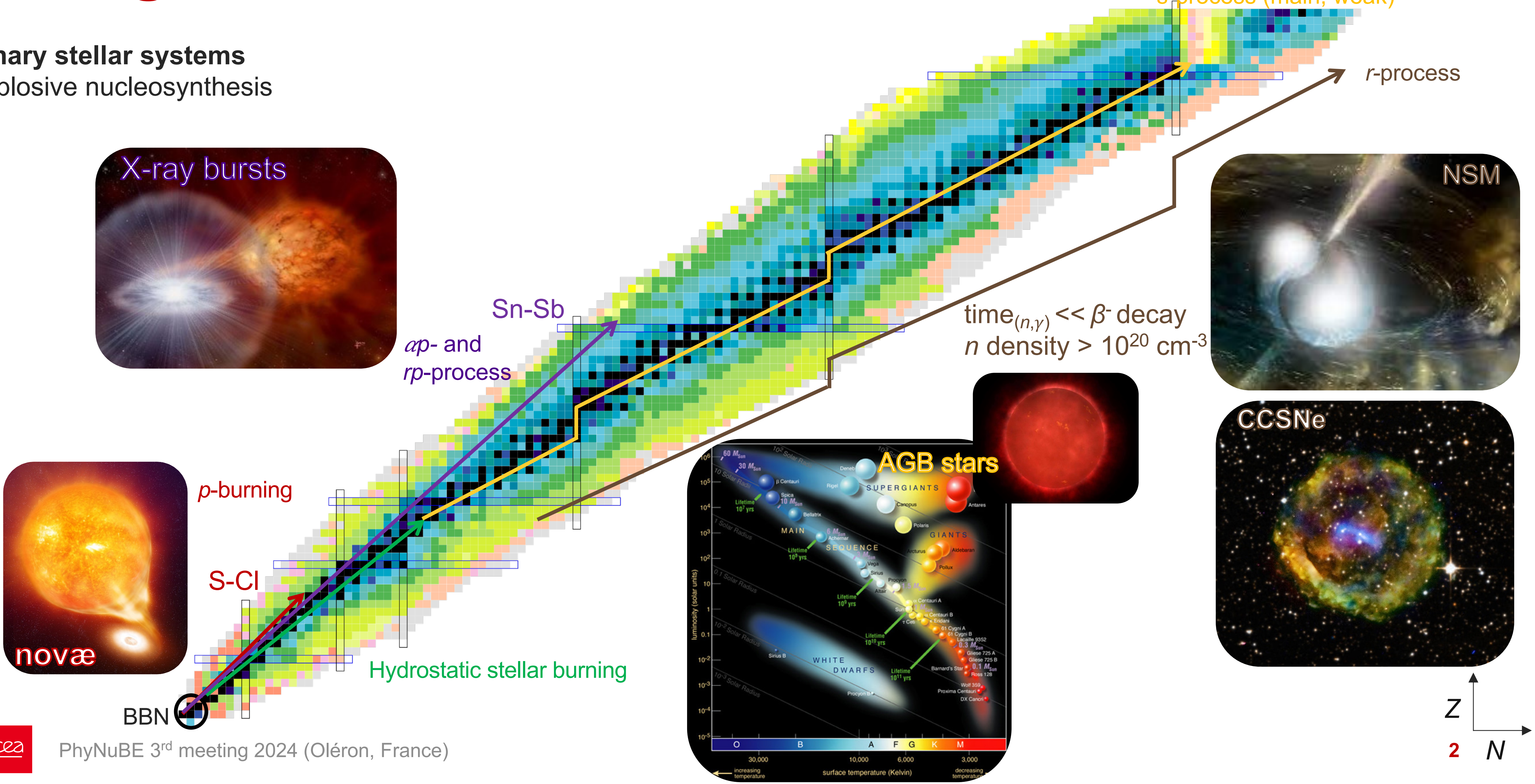

Origin of the elements

Binary stellar systems
Explosive nucleosynthesis

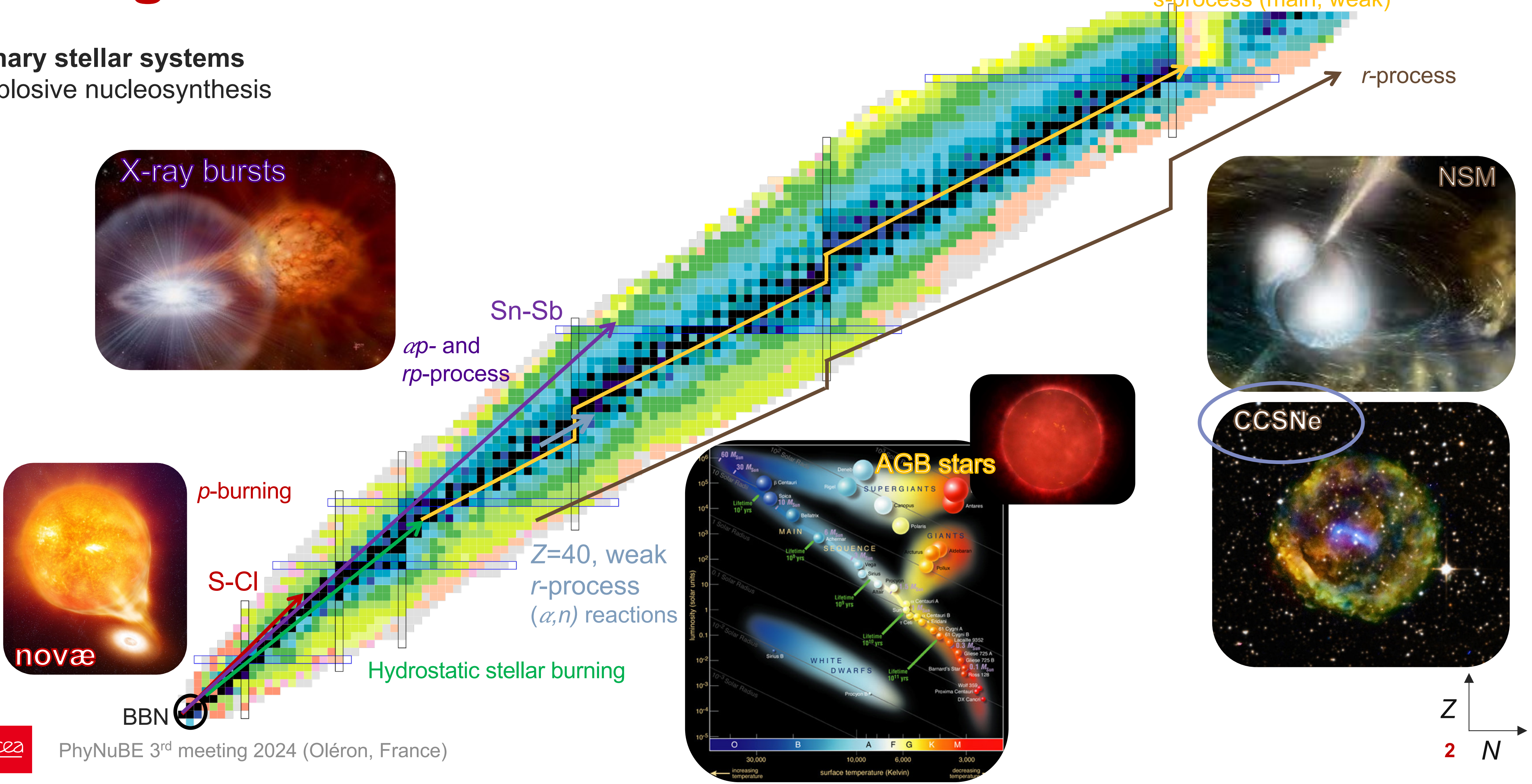

Origin of the elements

Binary stellar systems
Explosive nucleosynthesis

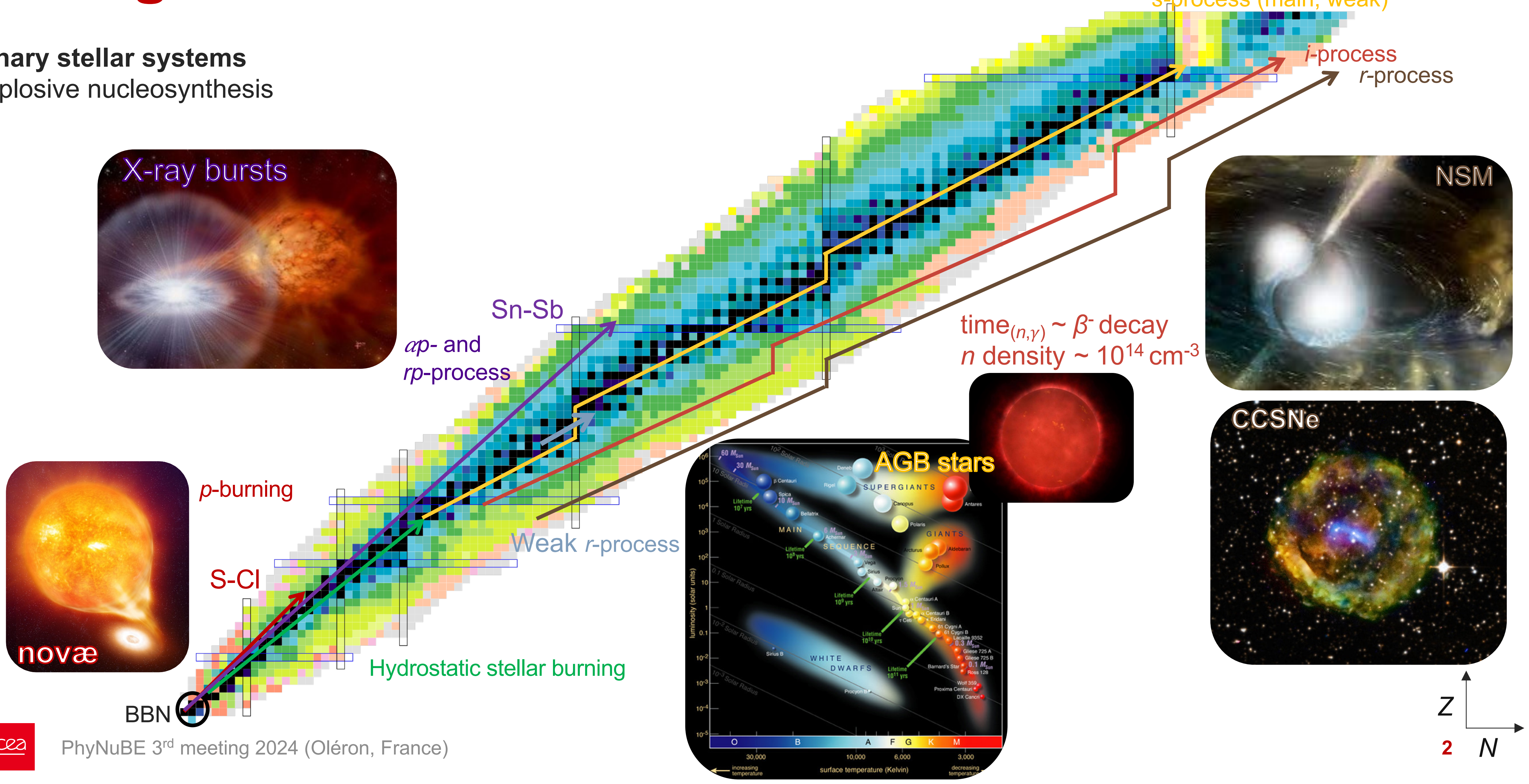

Origin of the elements

Binary stellar systems
Explosive nucleosynthesis

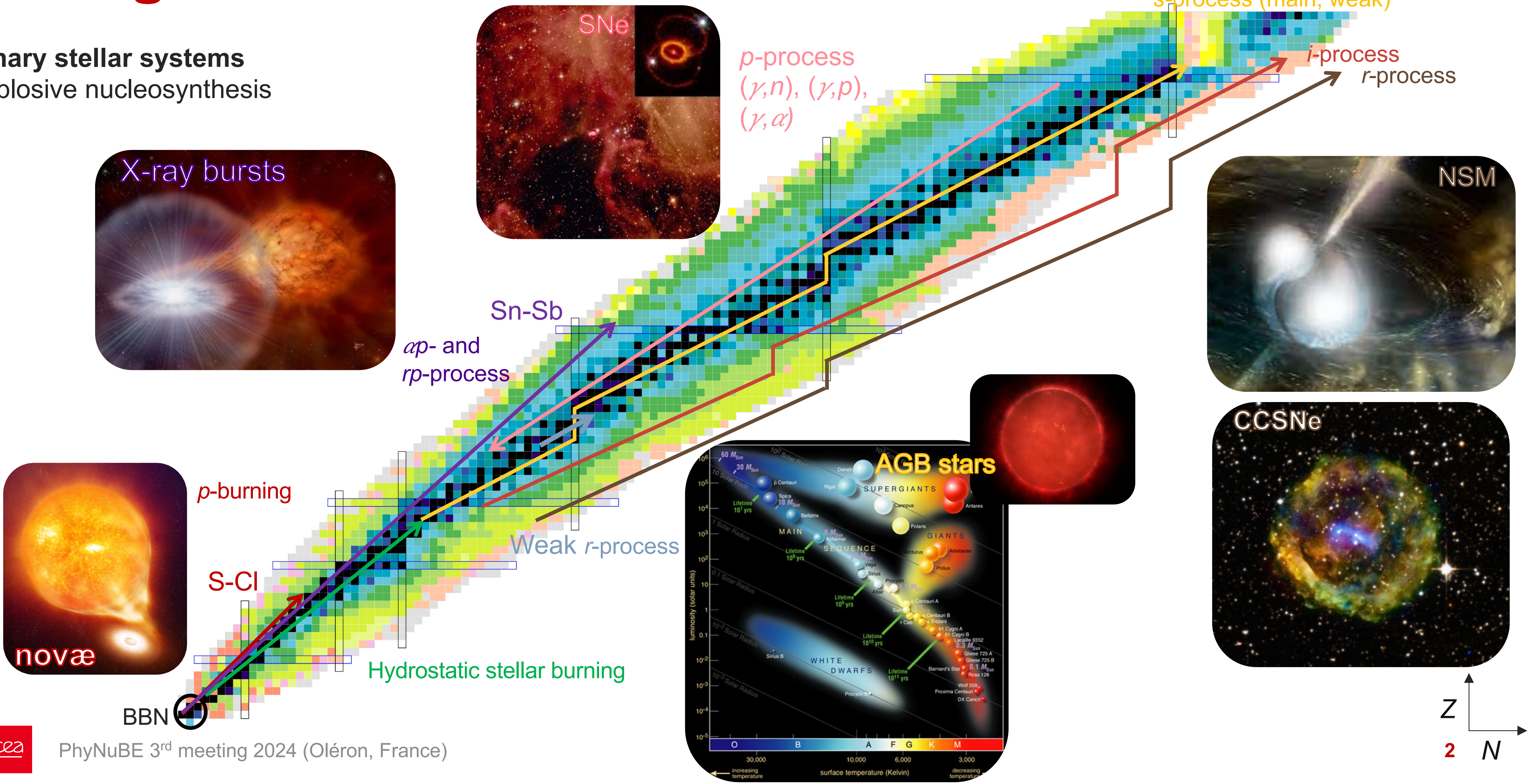

Astrophysical site for today

Binary stellar systems
Explosive nucleosynthesis

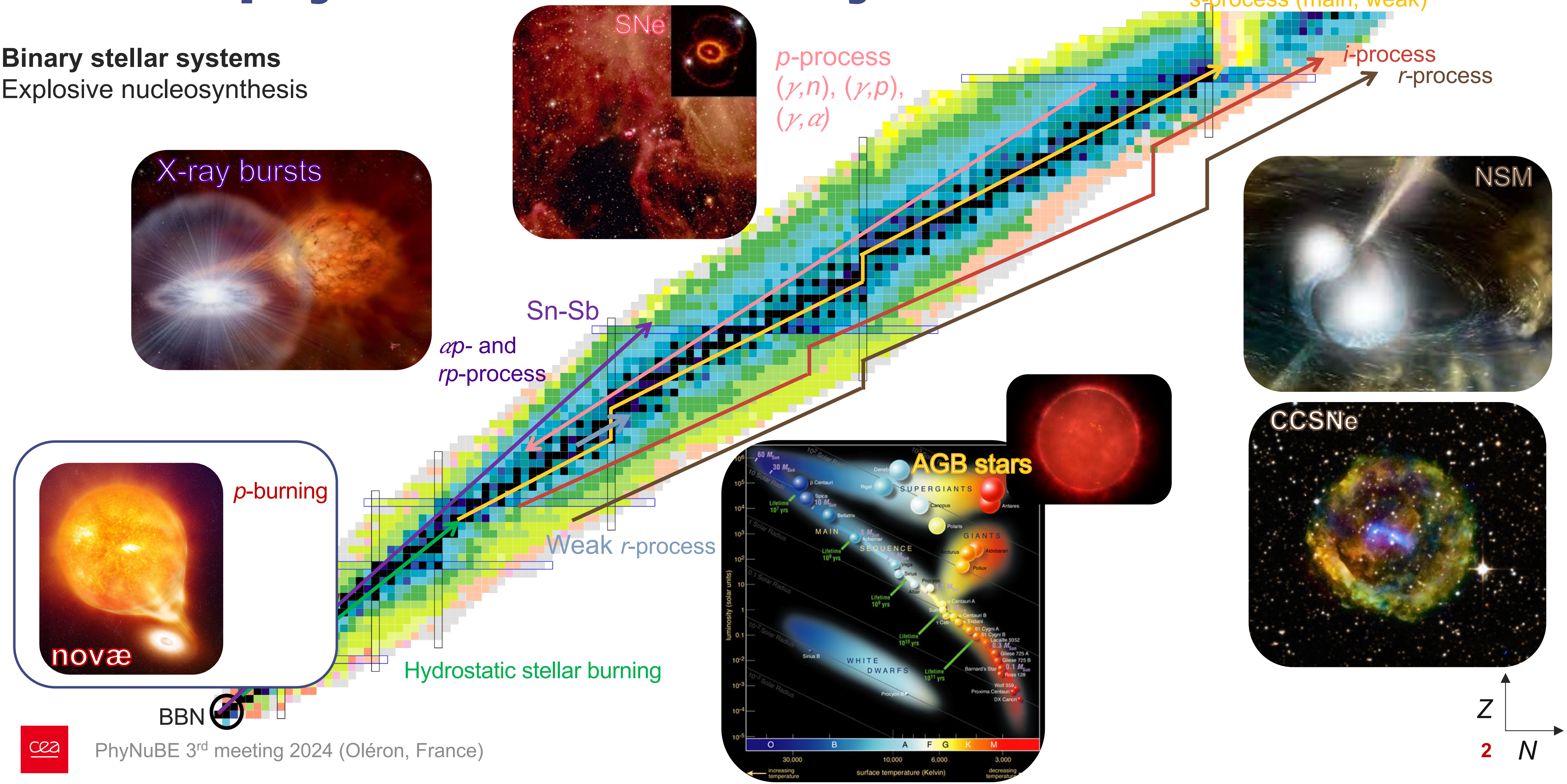

Low energy γ–ray astronomy

Direct probe of nuclear cosmic processes

Low energy γ–ray astronomy

Direct probe of nuclear cosmic processes

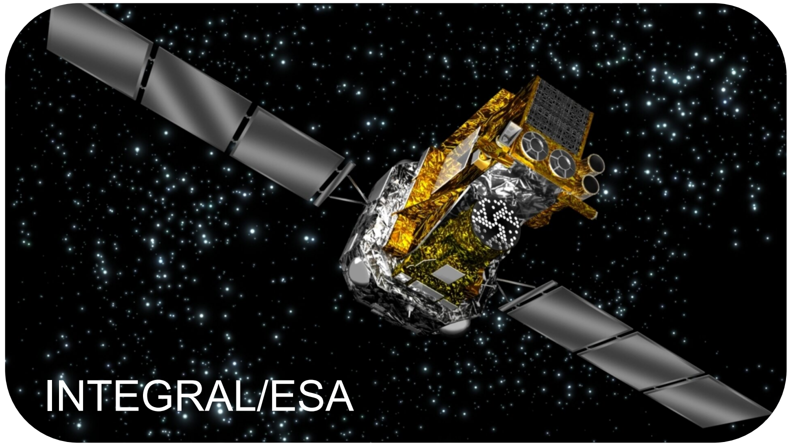

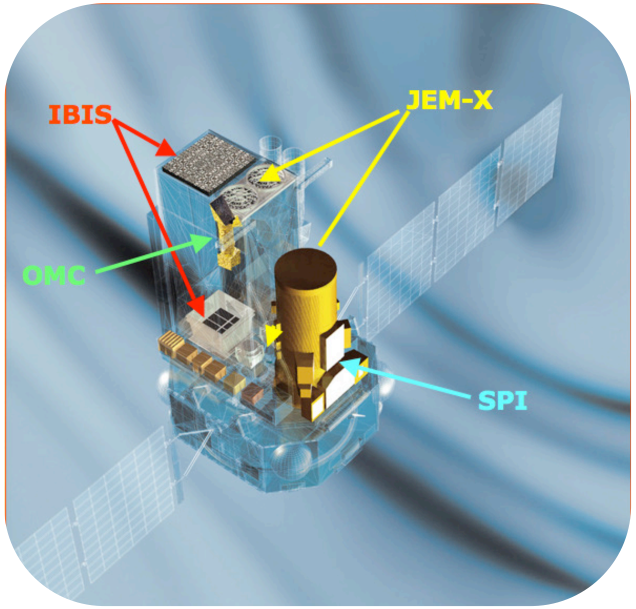

Low energy γ–ray astronomy

Direct probe of nuclear cosmic processes

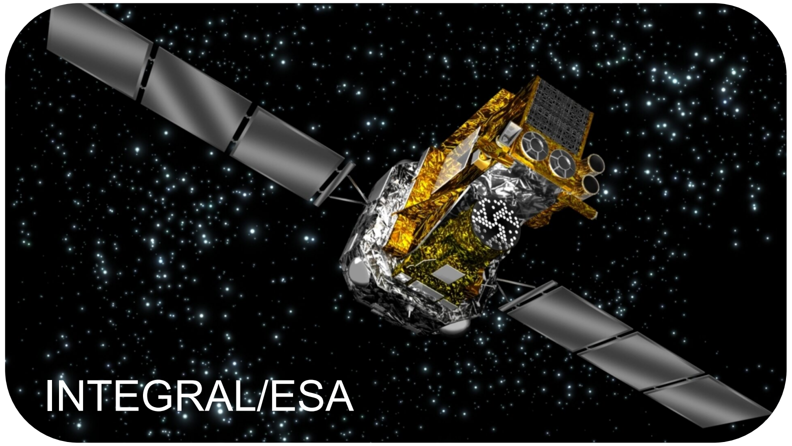

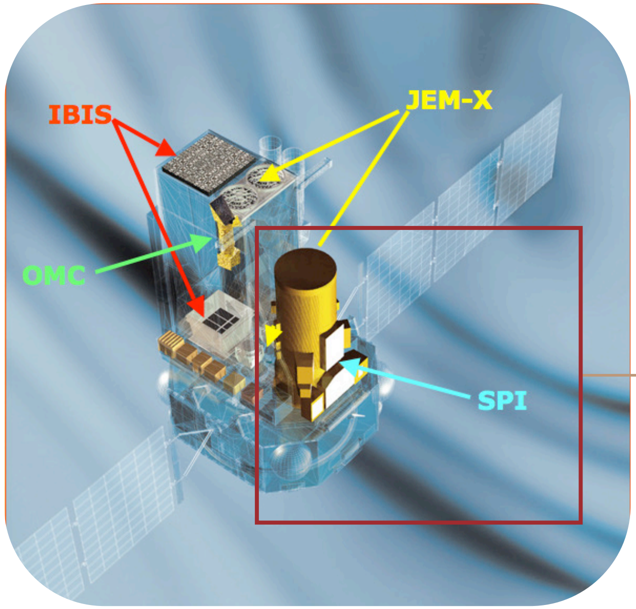

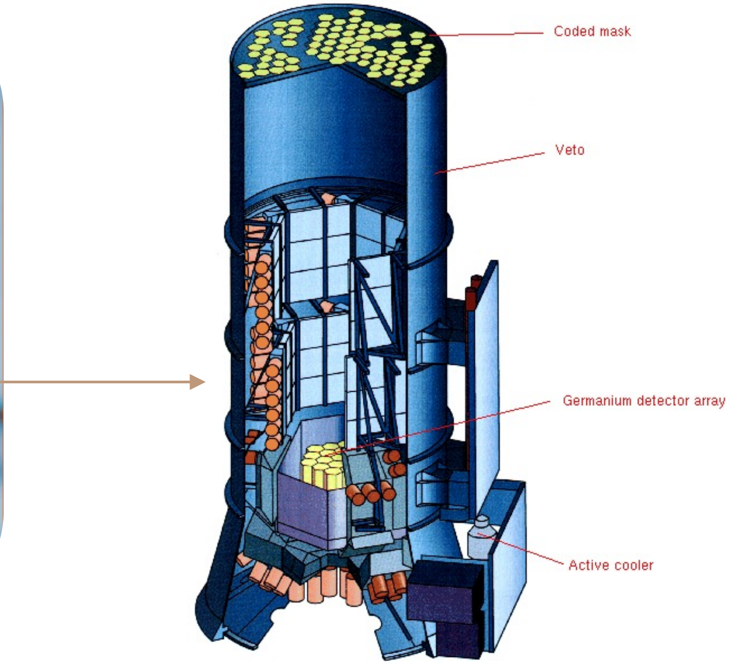

Low energy γ–ray astronomy

Direct probe of nuclear cosmic processes

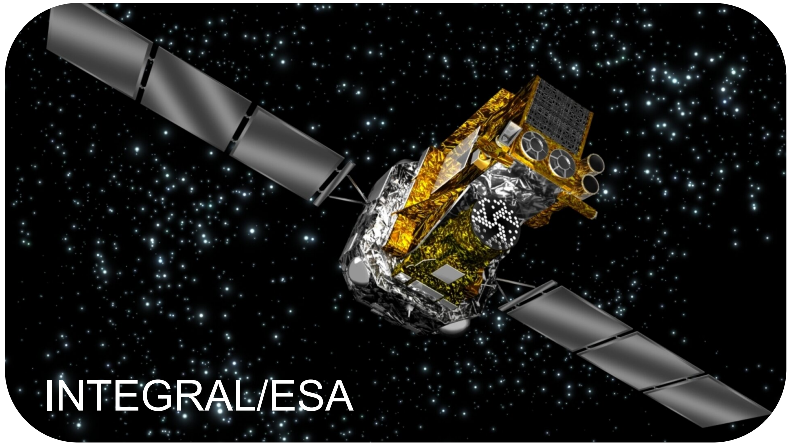

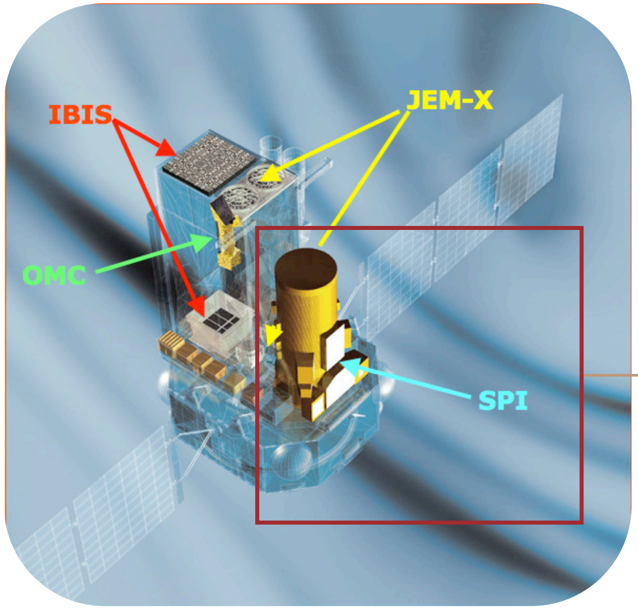

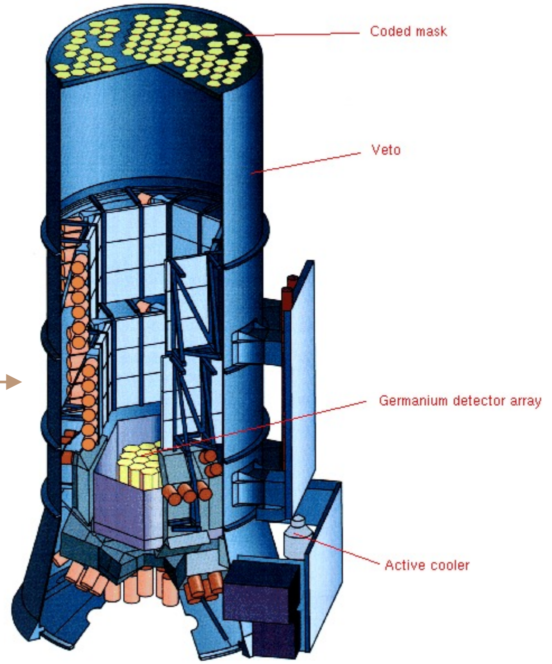

Long-lived >Myr (^{26}Al, ^{60}Fe)

Low energy γ–ray astronomy

Direct probe of nuclear cosmic processes

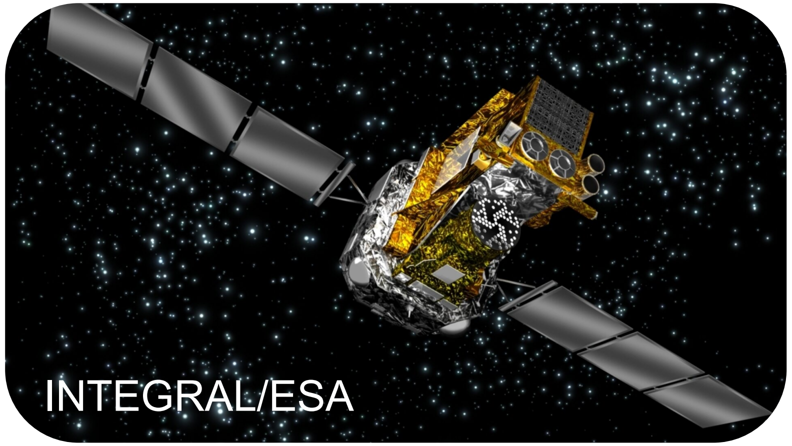

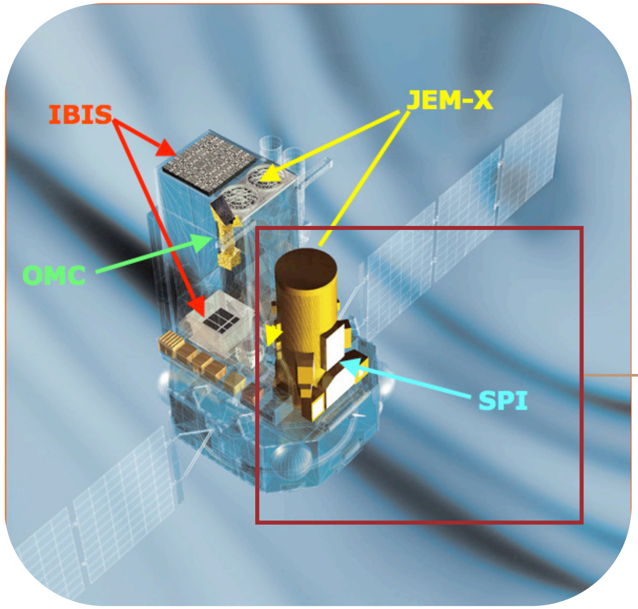

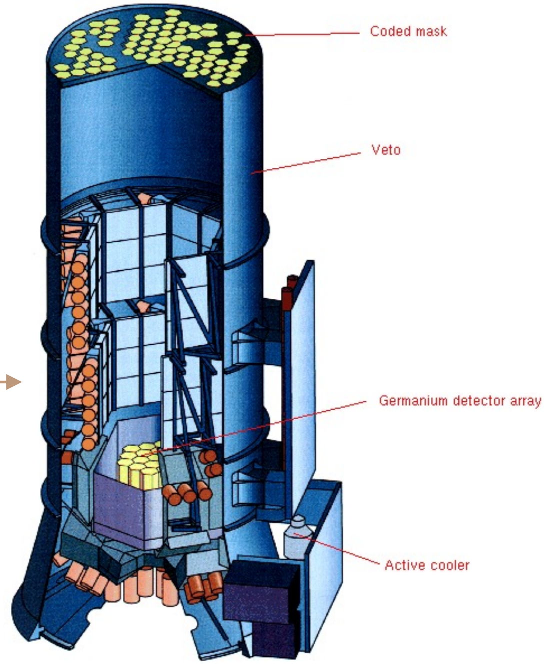

Long-lived >Myr (^{26}**Al**, ^{60}Fe)
E_γ = 1.809 MeV

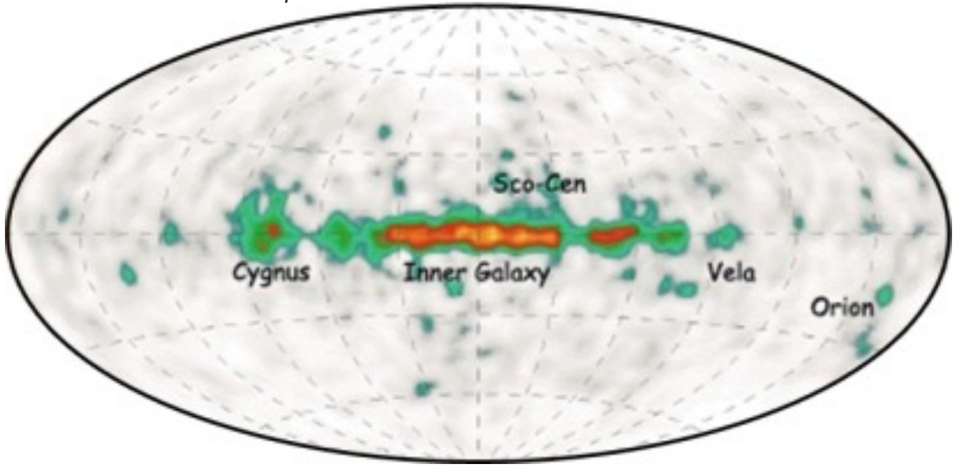

Plüschke et al. (2001)

Low energy γ–ray astronomy

Direct probe of nuclear cosmic processes

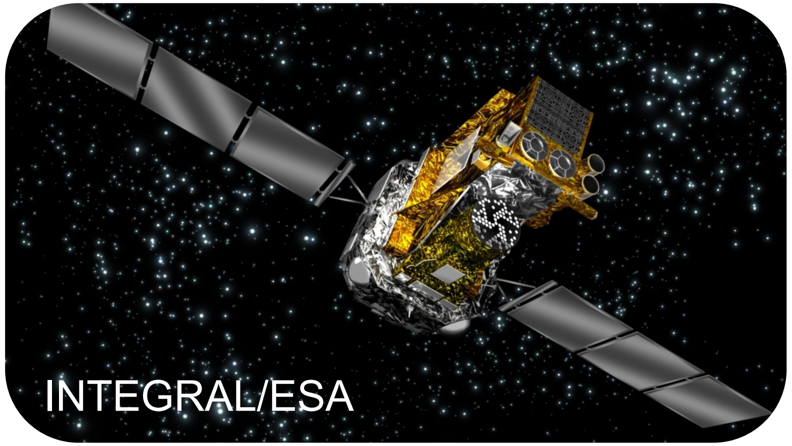

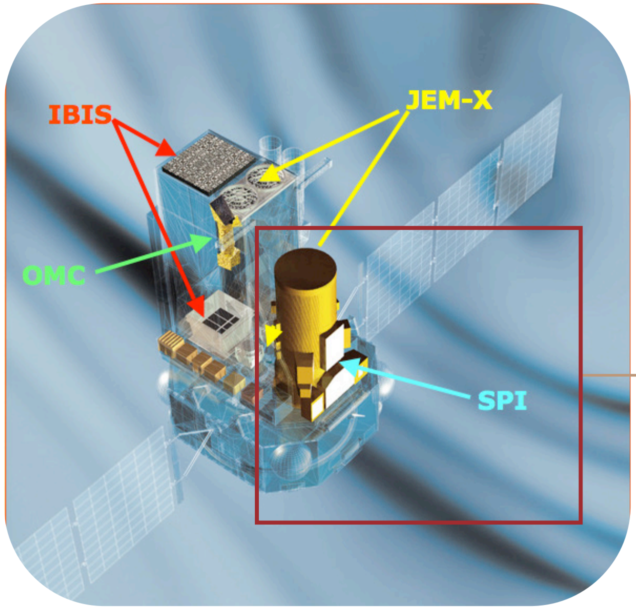

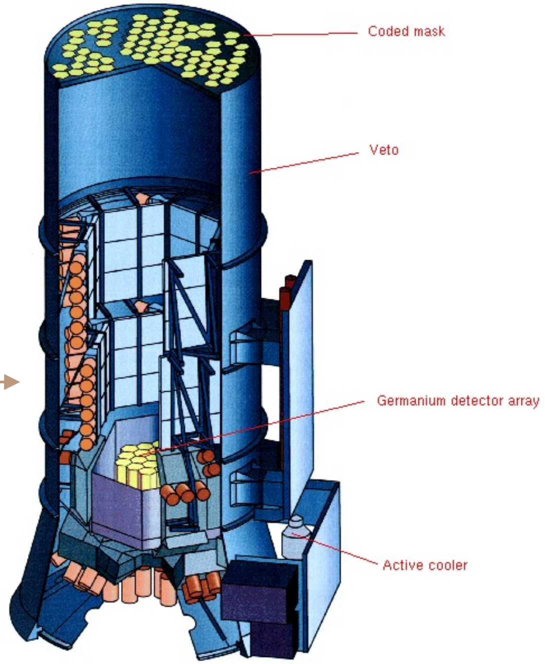

Long-lived >Myr (^{26}Al, ^{60}Fe)

E_γ = 1.809 MeV

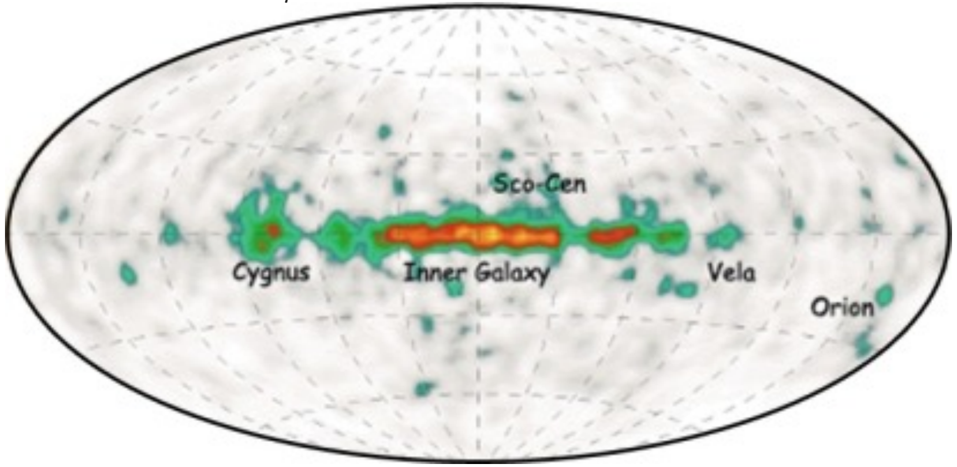

Short-lived ≲yr (^{7}Be, ^{18}F, ^{22}Na, ^{44}Ti, ^{56}Ni)

Plüschke et al. (2001)

Low energy γ–ray astronomy

Direct probe of nuclear cosmic processes

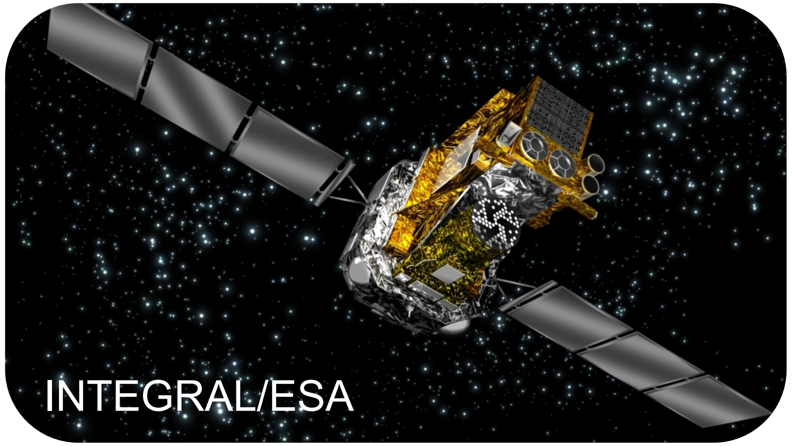

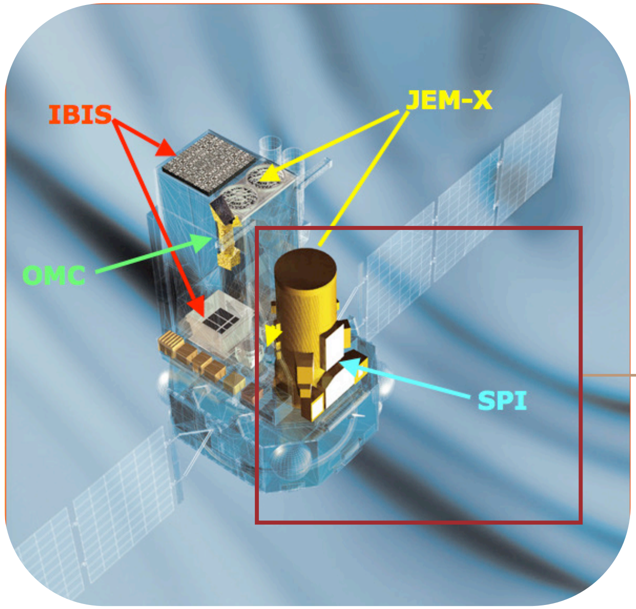

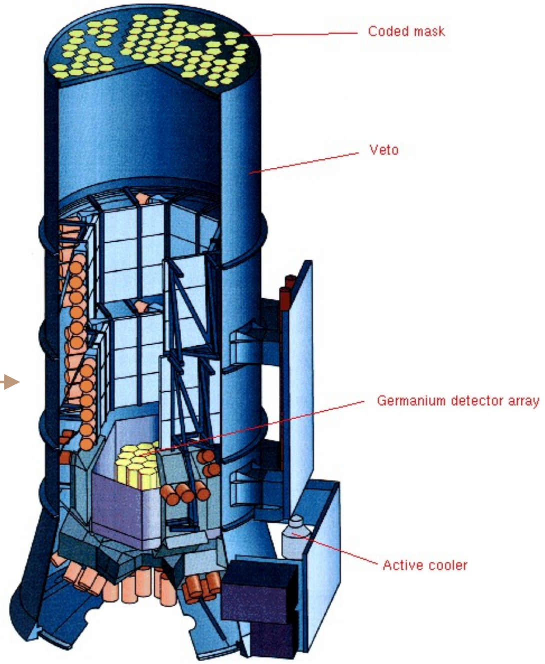

Long-lived >Myr (^{26}Al, ^{60}Fe)
E_γ = 1.809 MeV

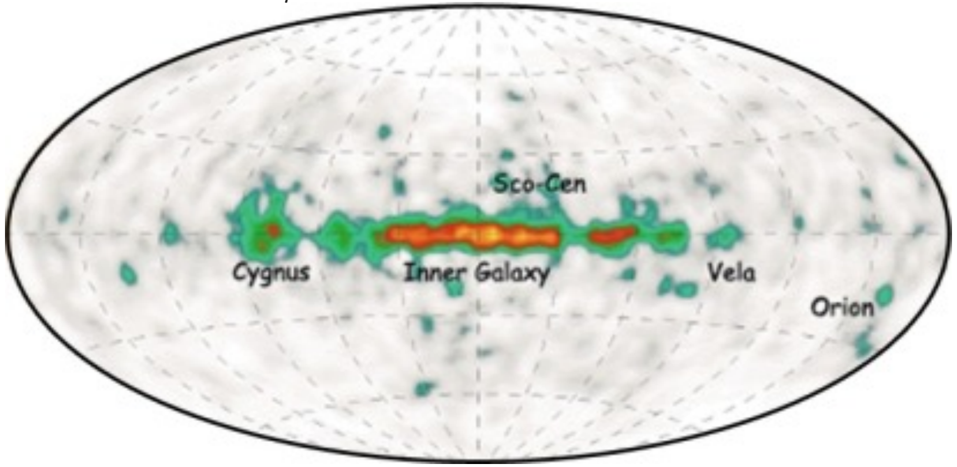

Short-lived ≲yr (^{7}Be, ^{18}F, ^{22}Na, ^{44}**Ti**, ^{56}Ni)
E_γ = 67.9 keV

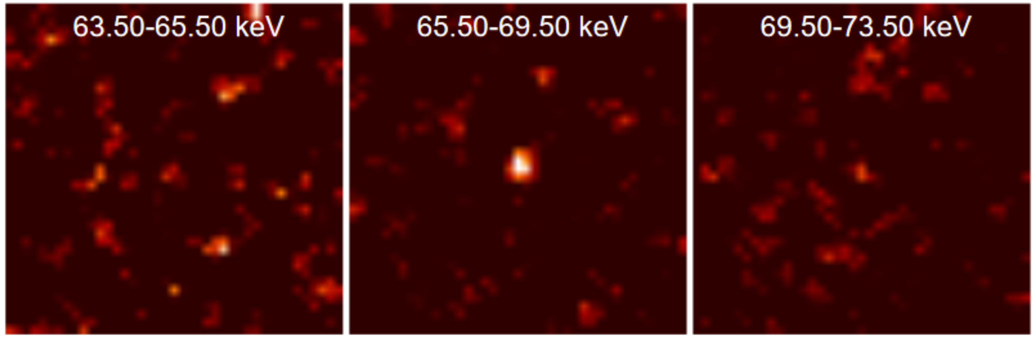

Plüschke et al. (2001)

Radioelements for today

Direct probe of nuclear cosmic processes

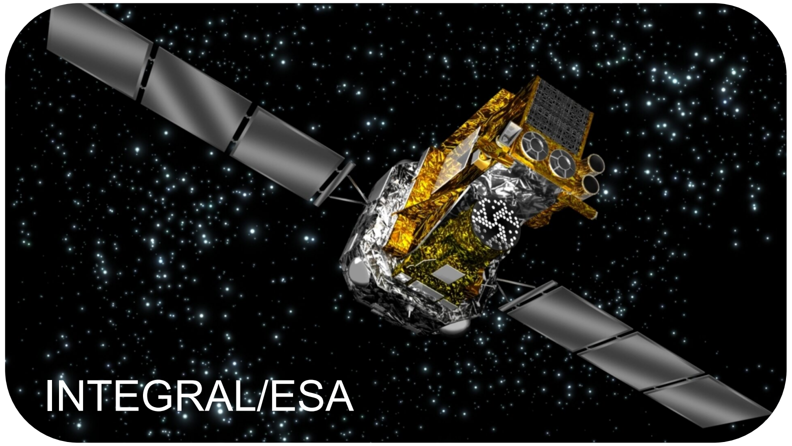

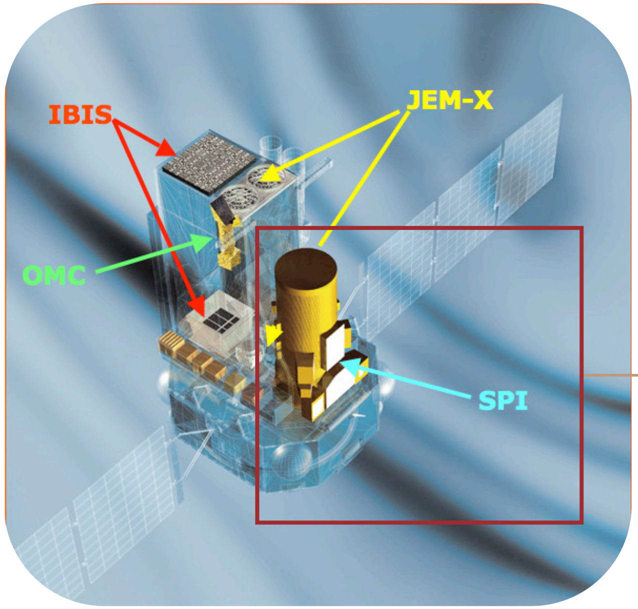

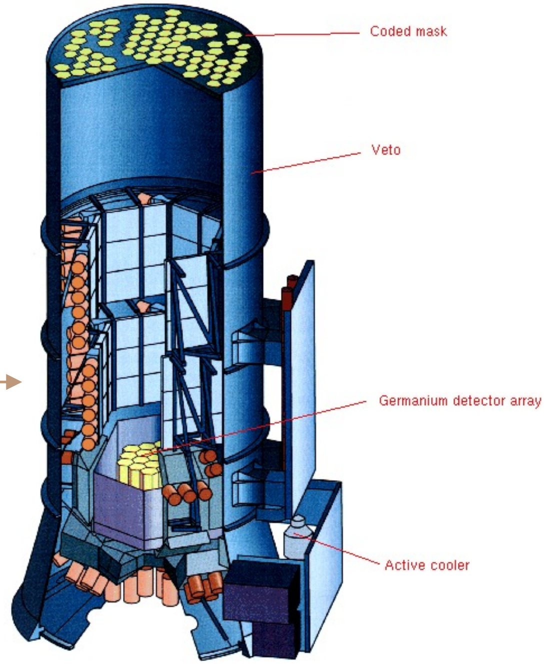

Long-lived >Myr (^{26}**Al**, ^{60}Fe)
E_γ = 1.809 MeV

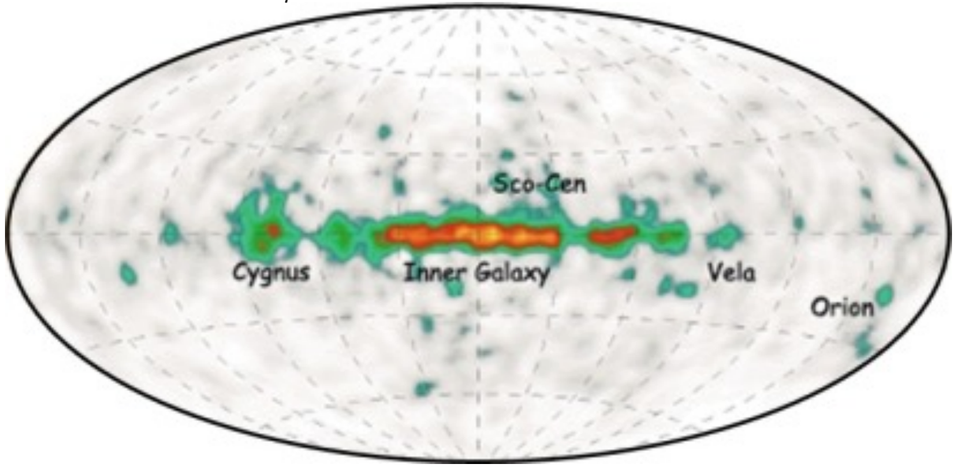

Short-lived ≲yr (^{7}Be, ^{18}**F**, ^{22}**Na**, ^{44}Ti, ^{56}Ni)
E_γ = 67.9 keV

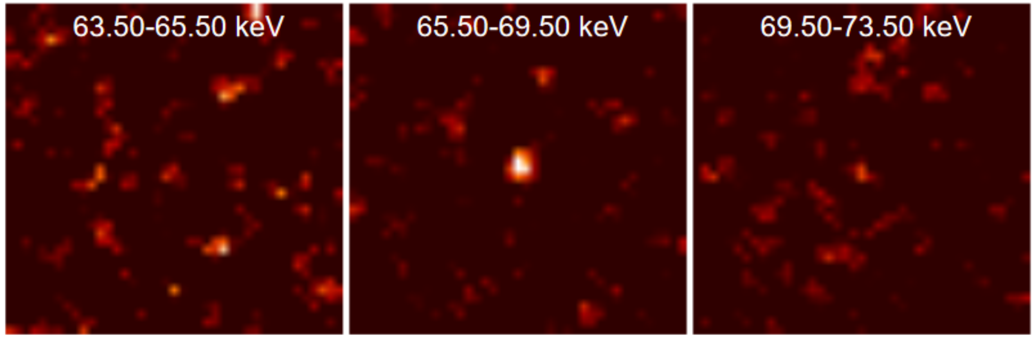

Plüschke et al. (2001)

Layout

Astrophysical landscape
Novae and γ–ray emitters

Layout

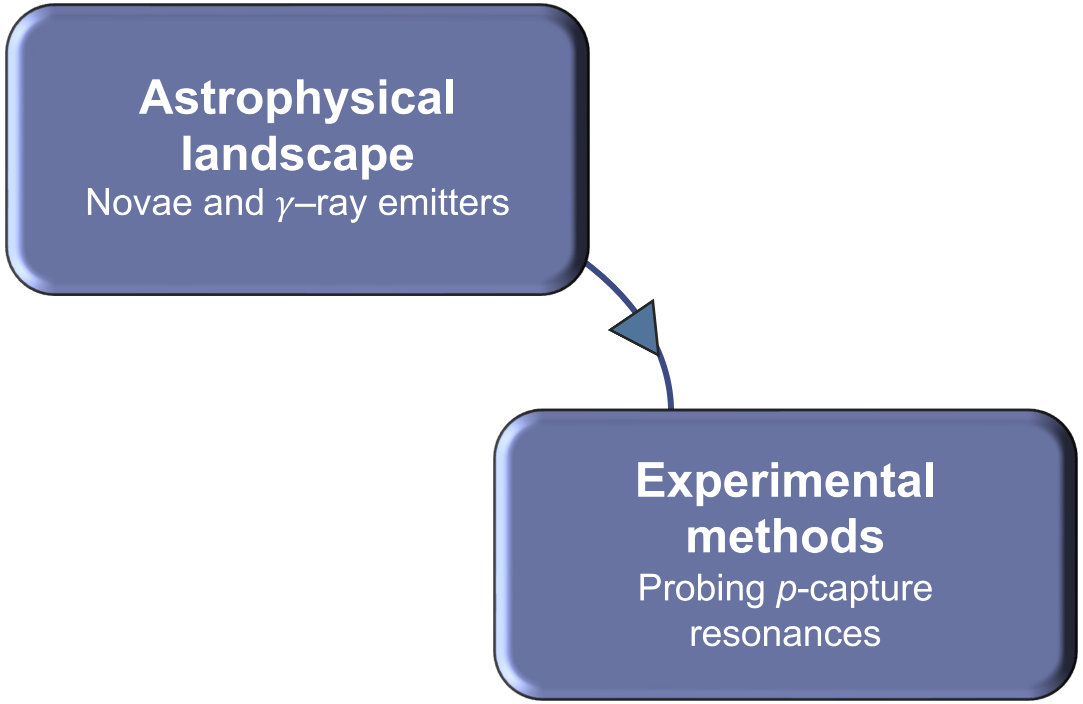

Astrophysical landscape
Novae and γ–ray emitters
Experimental methods
Probing p-capture resonances

Layout

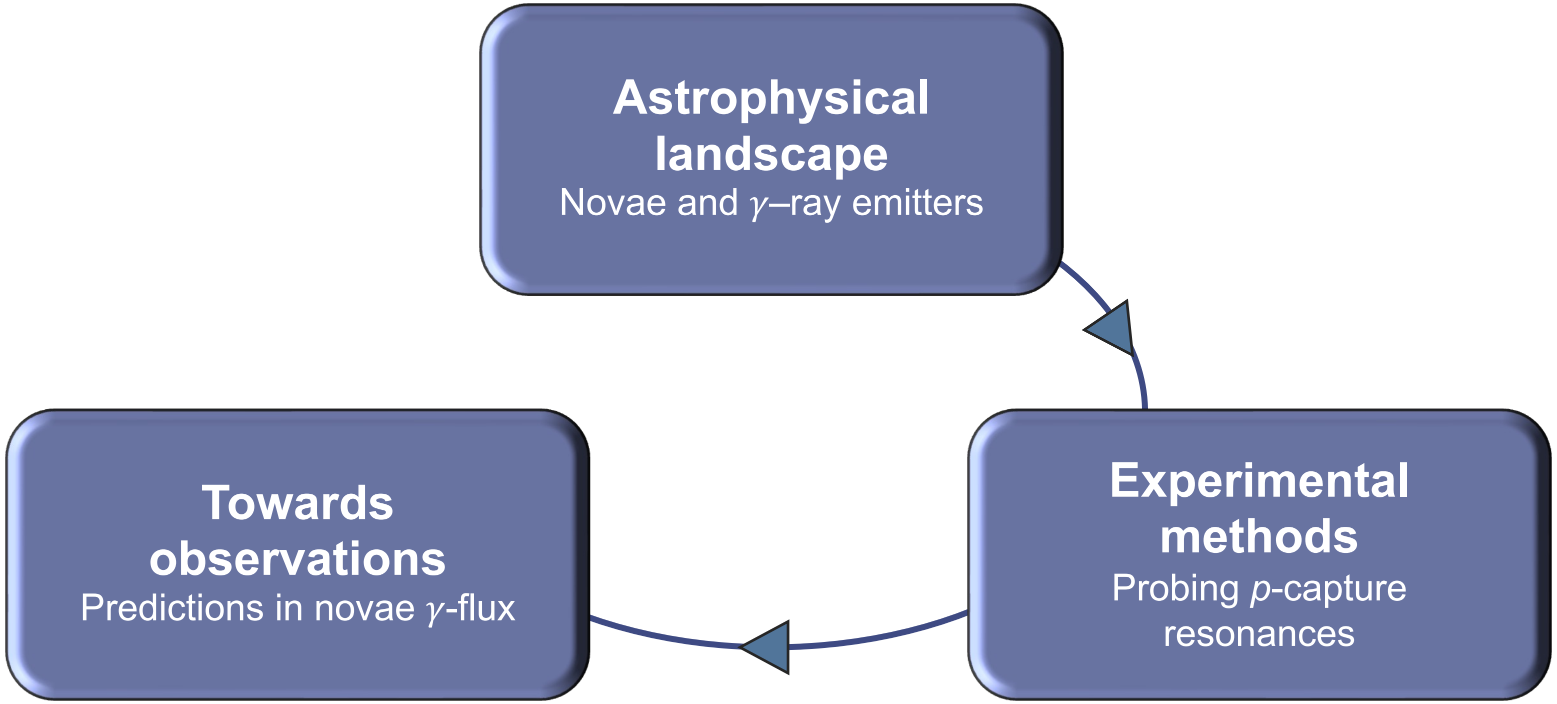
Astrophysical landscape
Novae and γ–ray emitters
Experimental methods
Probing p-capture resonances
Towards observations
Predictions in novae γ-flux

Layout

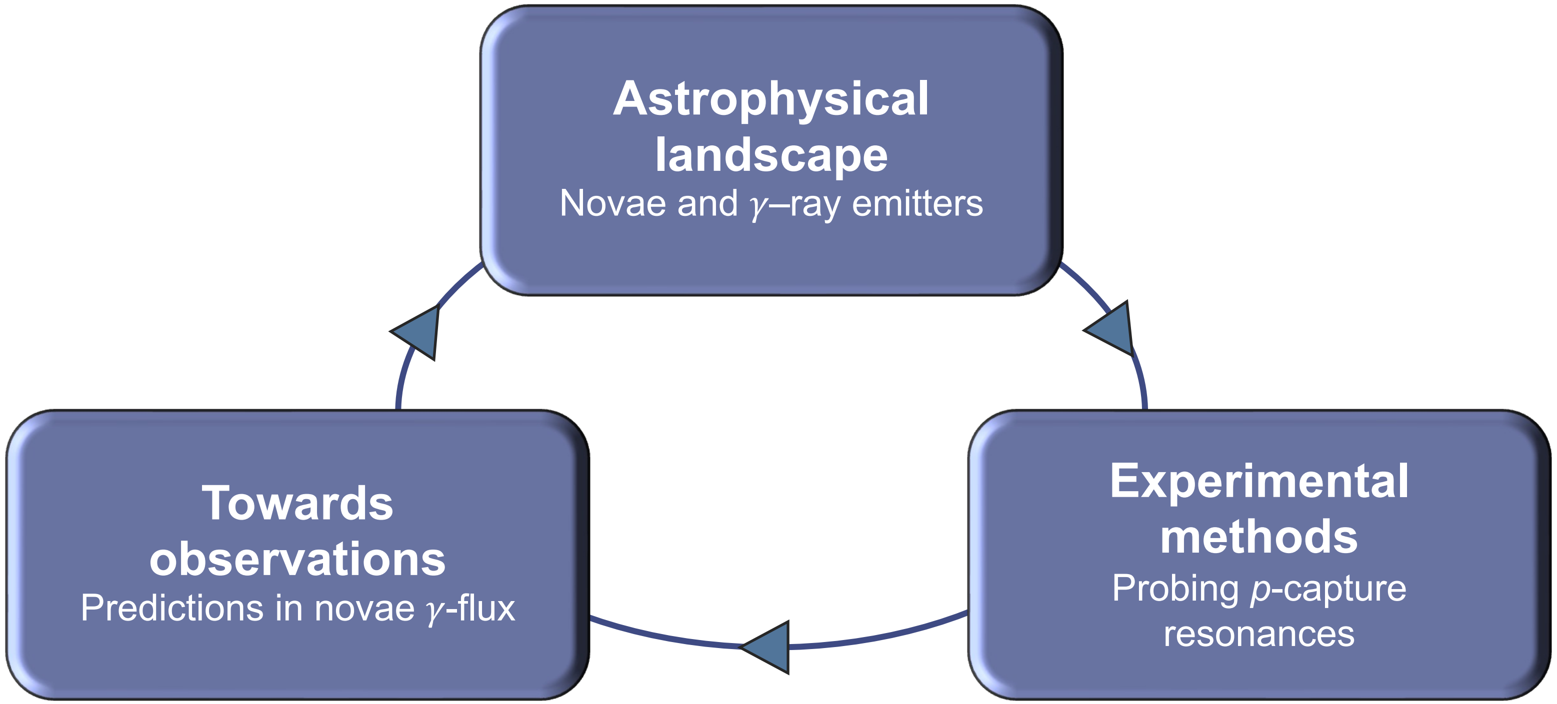

Astrophysical landscape
Novae and γ–ray emitters
Experimental methods
Probing p-capture resonances
Towards observations
Predictions in novae γ-flux

Layout

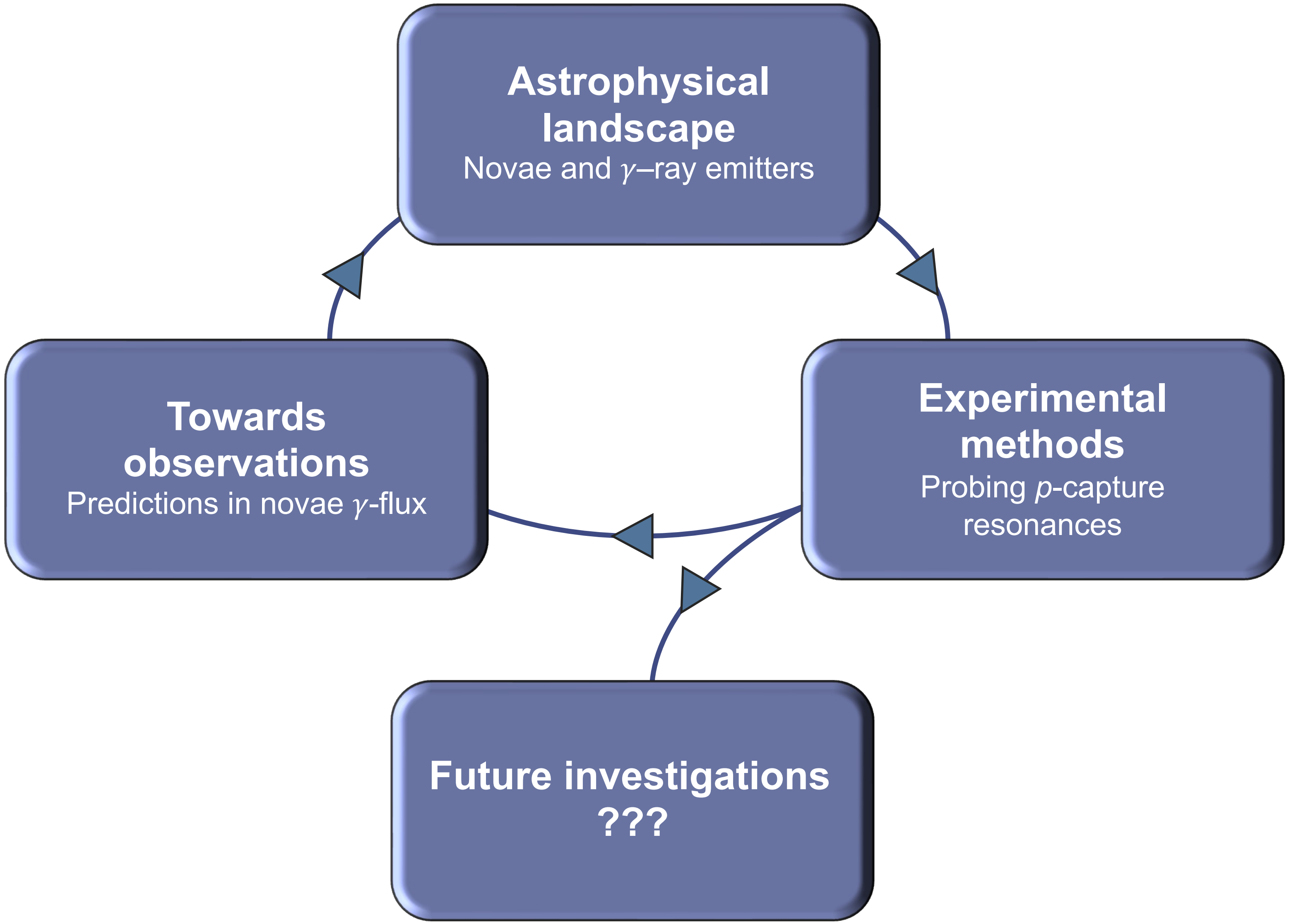
Astrophysical landscape
Novae and γ–ray emitters
Experimental methods
Probing p-capture resonances
Towards observations
Predictions in novae γ-flux
Future investigations
???

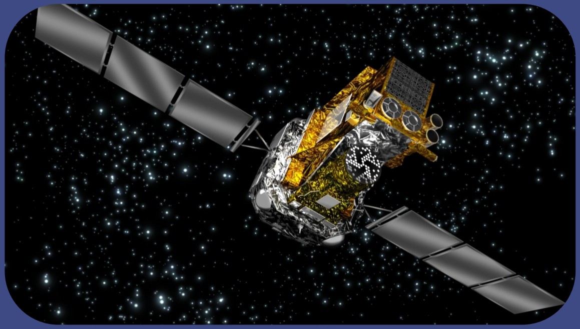

1. Astrophysical landscape

Novae and low energy γ–ray astronomy

Astrophysical site: novæ

Astrophysical site: novæ

Explosive H burning (T ≲0.5 GK)
Matter accretion at surface of compact star white dwarf
$(p,\gamma/\alpha)$, β^+ decay

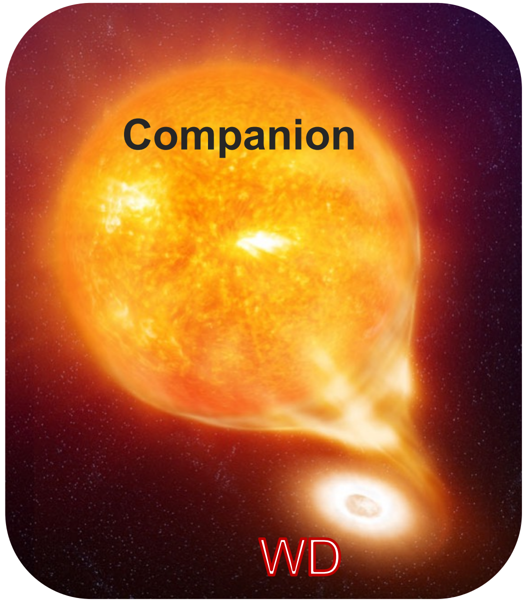

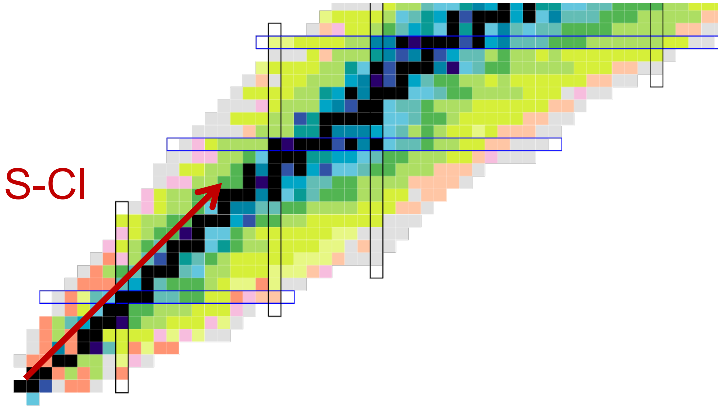

Astrophysical site: novæ

Explosive H burning (T ≲0.5 GK)
Matter accretion at surface of compact star white dwarf
$(p,\gamma/\alpha)$, β^+ decay

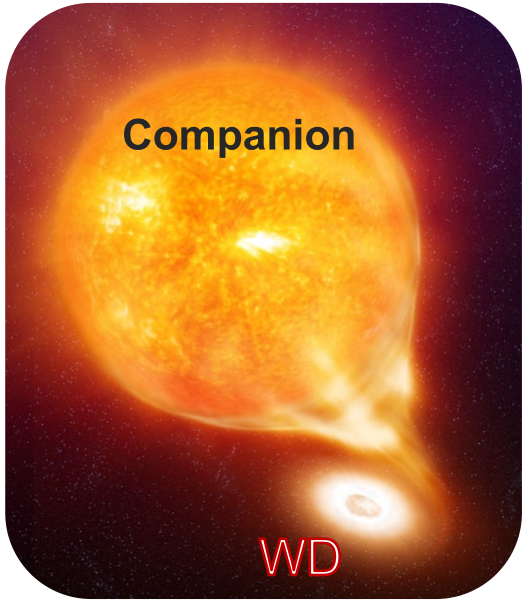

©HUBBLE/NASA
Nova Cygni, Parasce et al. (1992)

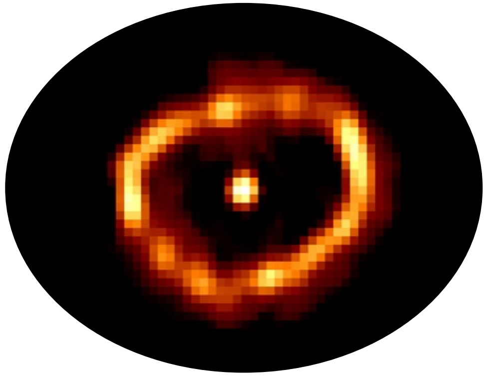

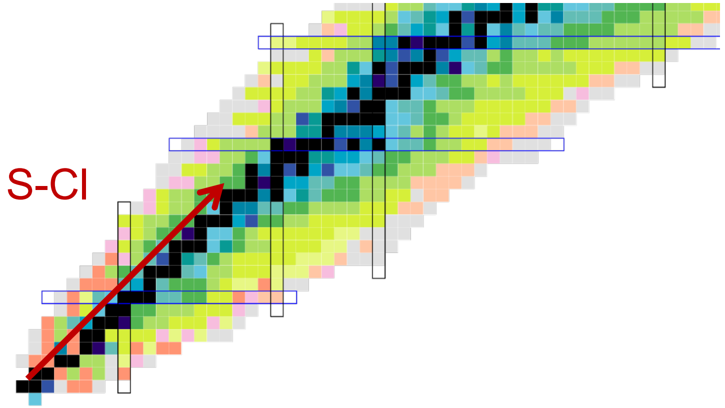

Astrophysical site: novæ

Explosive H burning (T ≲0.5 GK)
Matter accretion at surface of compact star white dwarf
$(p,\gamma/\alpha)$, β^+ decay

Impact
Abundances of nuclei
Number of supernovae Ia

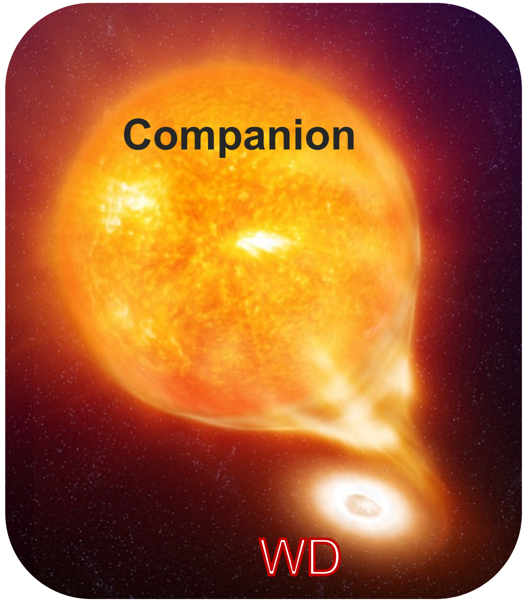

©HUBBLE/NASA
Nova Cygni, Parasce et al. (1992)

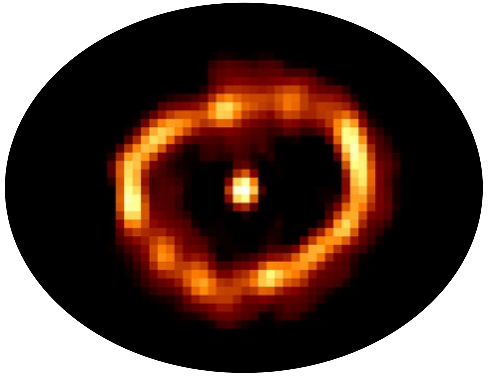

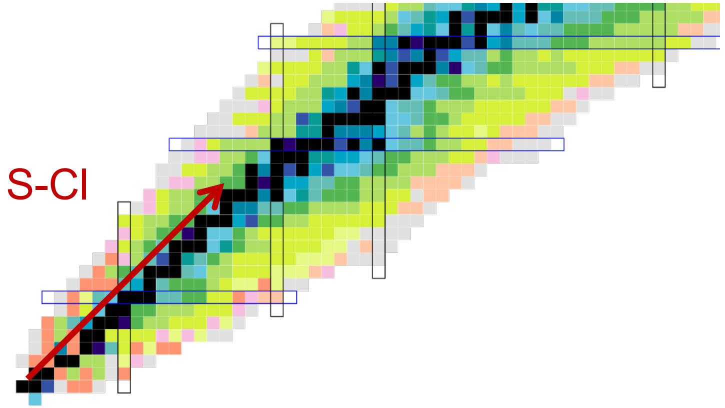

Astrophysical site: novæ

Explosive H burning (T ≲0.5 GK)
Matter accretion at surface of compact star white dwarf
($p,\gamma/\alpha$), β^+ decay

Impact
Abundances of nuclei
Number of supernovae Ia

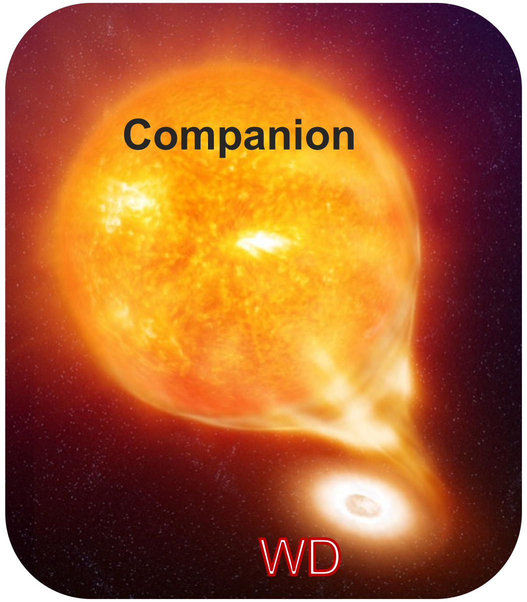

©HUBBLE/NASA
Nova Cygni, Parasce et al. (1992)

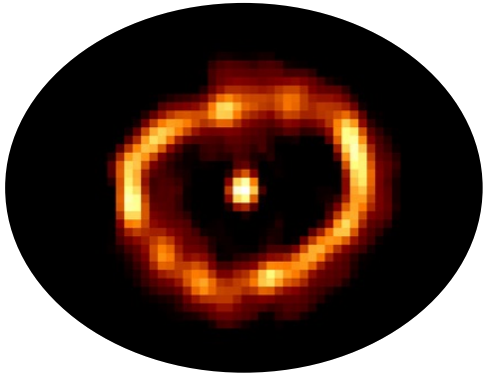

Opened questions
Compact star mass?
Accretion?
Mixing?
Ejected mass?

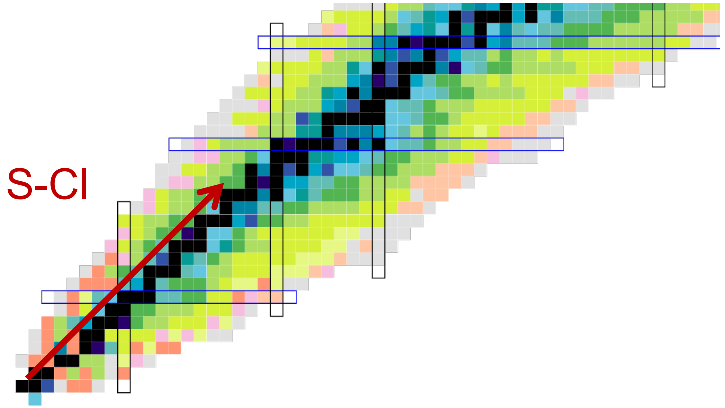

Astrophysical site: novæ

Explosive H burning (T $\lesssim$0.5 GK)
Matter accretion at surface of compact star white dwarf
($p,\gamma/\alpha$), β^+ decay

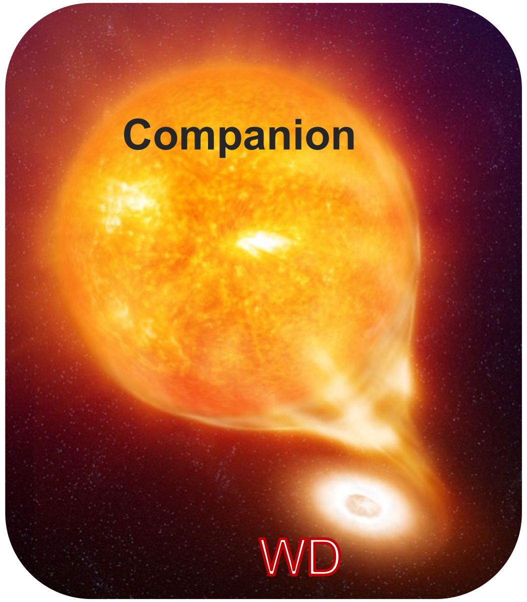

©HUBBLE/NASA
Nova Cygni, Parasce et al. (1992)

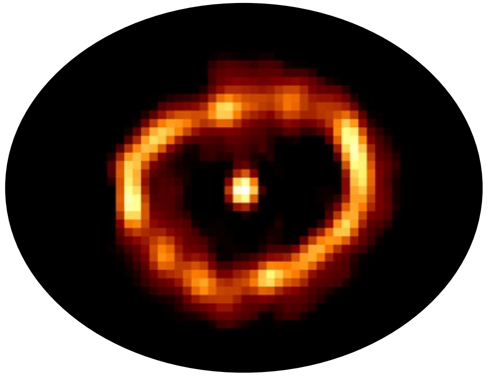

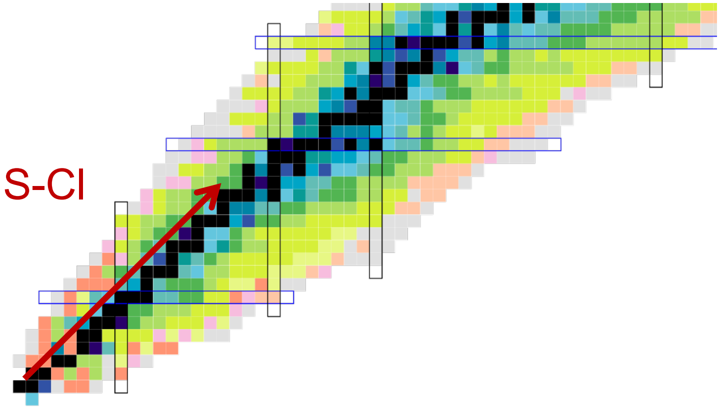

Impact
Abundances of nuclei
Number of supernovae Ia

Opened questions
Compact star mass?
Accretion?
Mixing?
Ejected mass?

Nuclear observations
Isotopic composition of presolar grains
Low energy γ–ray astronomy

Astrophysical site: novæ

Explosive H burning (T $\lesssim$0.5 GK)
Matter accretion at surface of compact star white dwarf
($p,\gamma/\alpha$), β^+ decay

Impact
Abundances of nuclei
Number of supernovae Ia

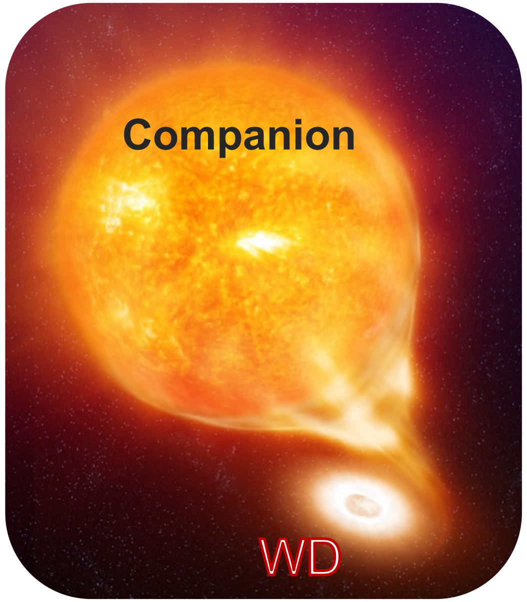

©HUBBLE/NASA
Nova Cygni, Parasce et al. (1992)

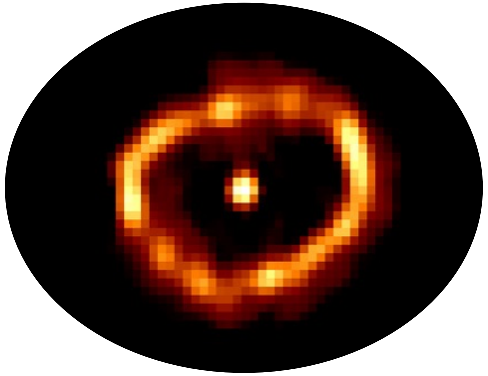

Opened questions
Compact star mass?
Accretion?
Mixing?
Ejected mass?

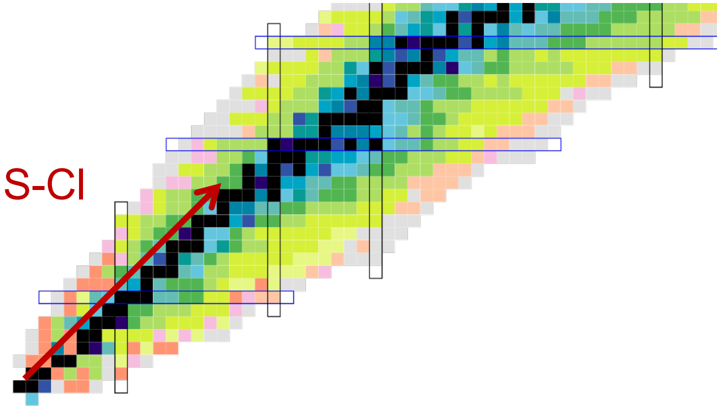

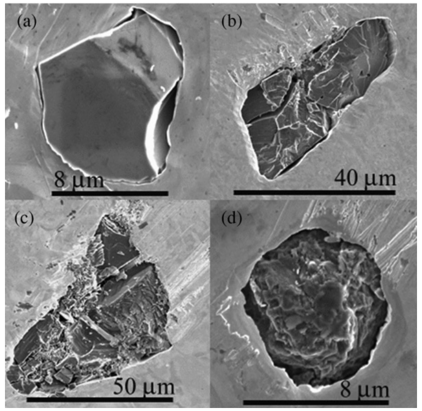

Nuclear observations
Isotopic composition of presolar grains
Low energy γ–ray astronomy

Astrophysical site: novæ

Explosive H burning (T ≲0.5 GK)
Matter accretion at surface of compact star white dwarf
($p,\gamma/\alpha$), β^+ decay

Impact
Abundances of nuclei
Number of supernovae Ia

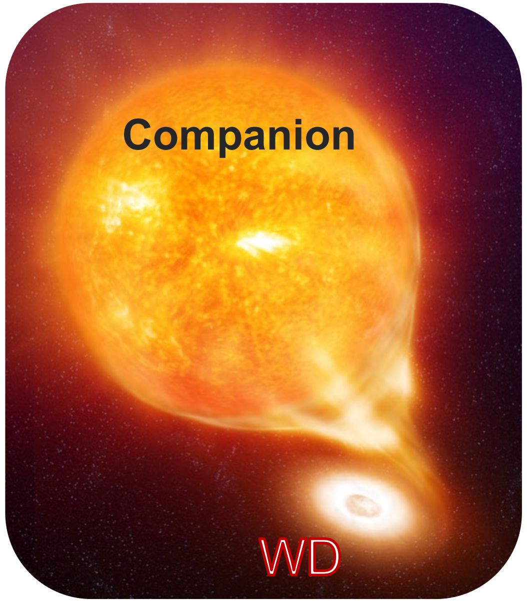

©HUBBLE/NASA
Nova Cygni, Parasce et al. (1992)

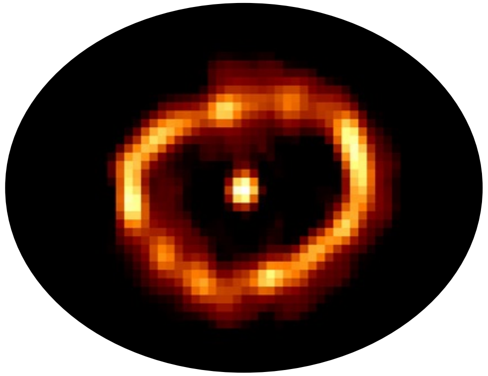

Opened questions
Compact star mass?
Accretion?
Mixing?
Ejected mass?

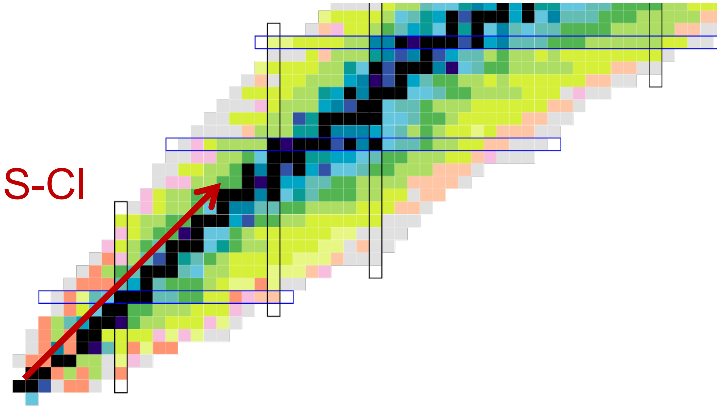

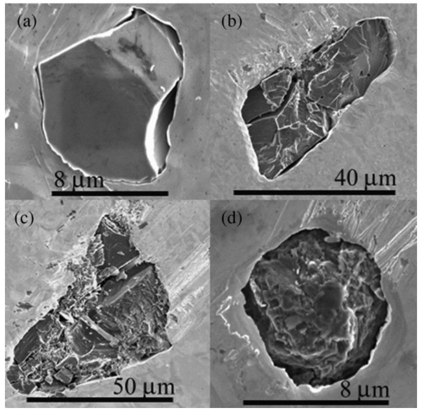

Nuclear observations
Isotopic composition of presolar grains
Low energy γ–ray astronomy

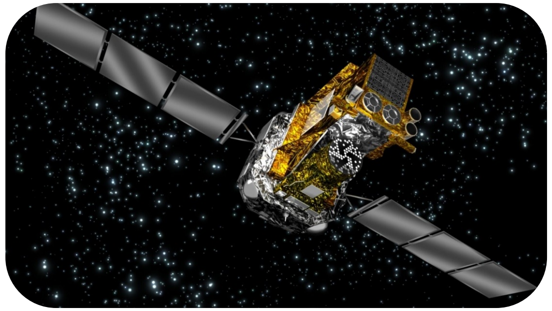

Nucleosynthesis network in novae

Nuclear ONe seed of white dwarf accreting solar-like matter (H dominant)

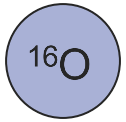

Nucleosynthesis network in novae

Nuclear ONe seed of white dwarf accreting solar-like matter (H dominant)

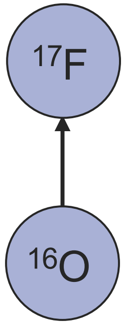

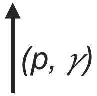

Nucleosynthesis network in novae

Nuclear ONe seed of white dwarf accreting solar-like matter (H dominant)

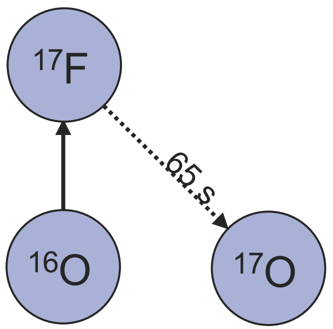

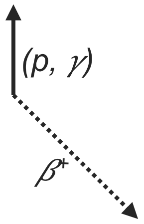

Nucleosynthesis network in novae

Nuclear ONe seed of white dwarf accreting solar-like matter (H dominant)

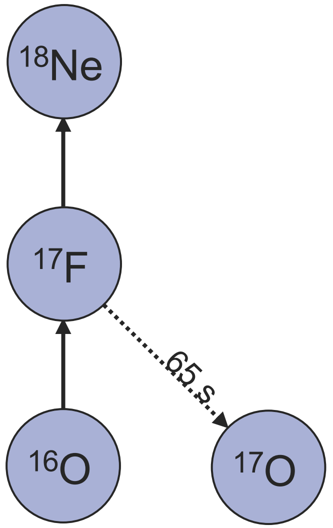

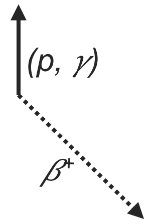

Nucleosynthesis network in novae

Nuclear ONe seed of white dwarf accreting solar-like matter (H dominant)

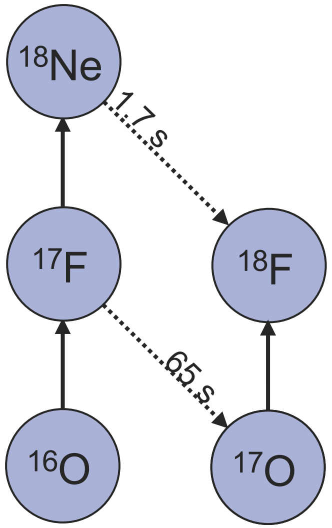

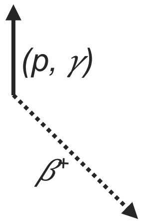

Nucleosynthesis network in novae

Nuclear ONe seed of white dwarf accreting solar-like matter (H dominant)

Nucleosynthesis network in novae

Nuclear ONe seed of white dwarf accreting solar-like matter (H dominant)

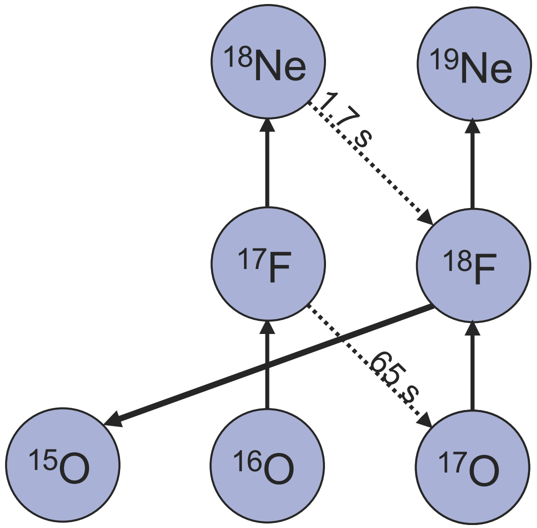

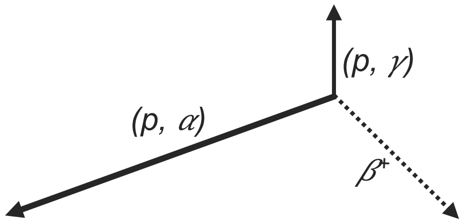

Nucleosynthesis network in novae

Nuclear ONe seed of white dwarf accreting solar-like matter (H dominant)

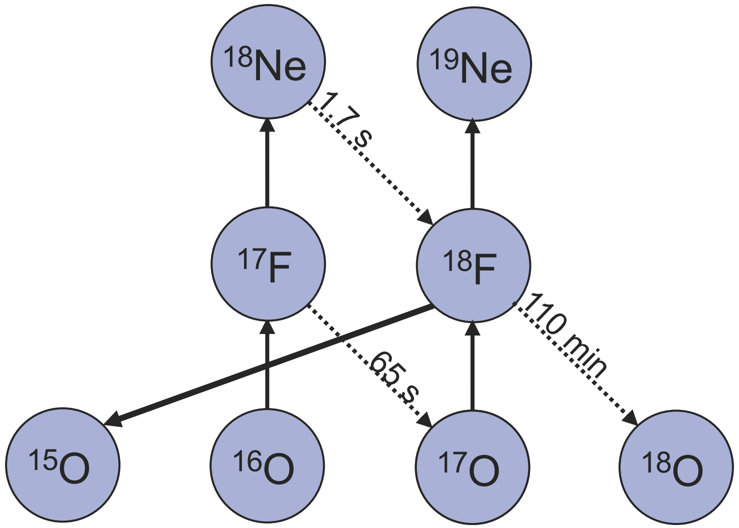

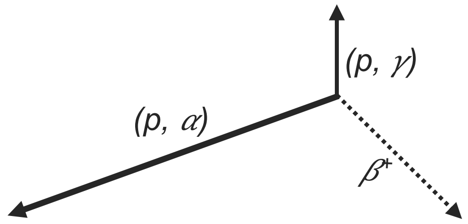

Nucleosynthesis network in novae

Nuclear ONe seed of white dwarf accreting solar-like matter (H dominant)

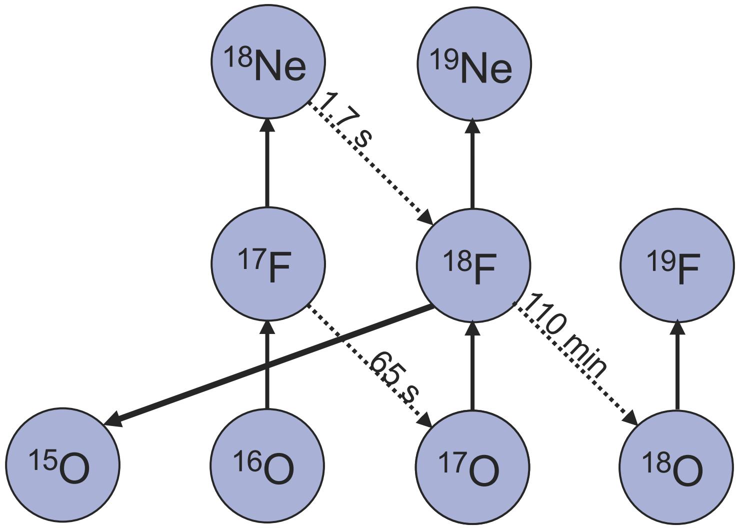

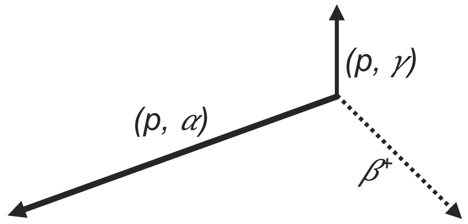

Nucleosynthesis network in novae

Nuclear ONe seed of white dwarf accreting solar-like matter (H dominant)

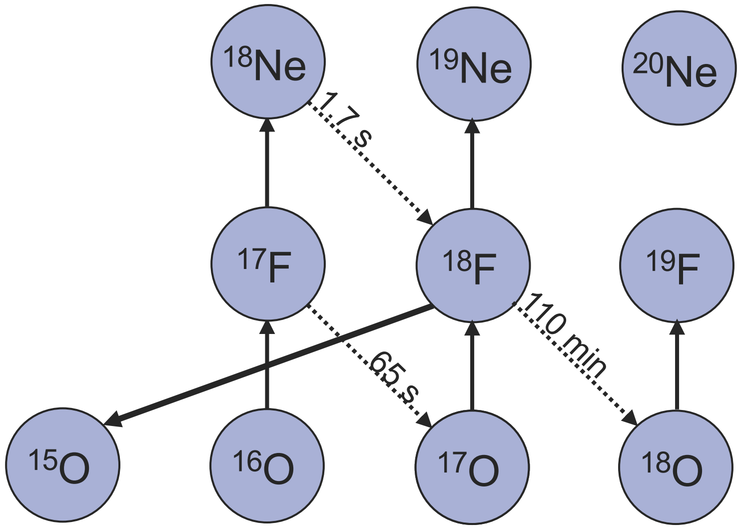

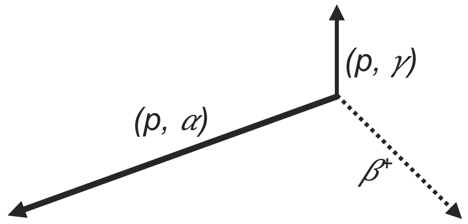

Nucleosynthesis network in novae

Nuclear ONe seed of white dwarf accreting solar-like matter (H dominant)

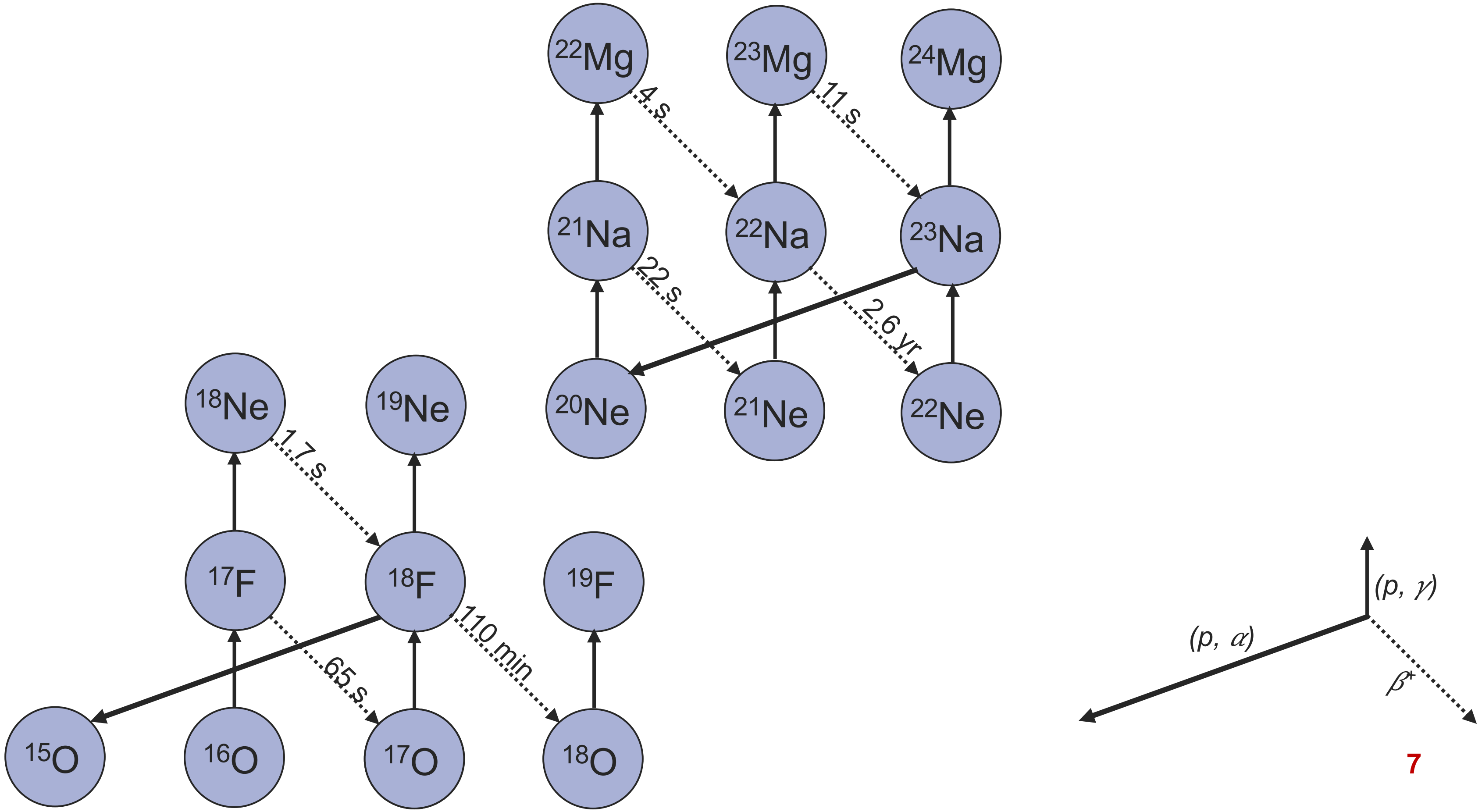

Nucleosynthesis network in novae

Nuclear ONe seed of white dwarf accreting solar-like matter (H dominant)

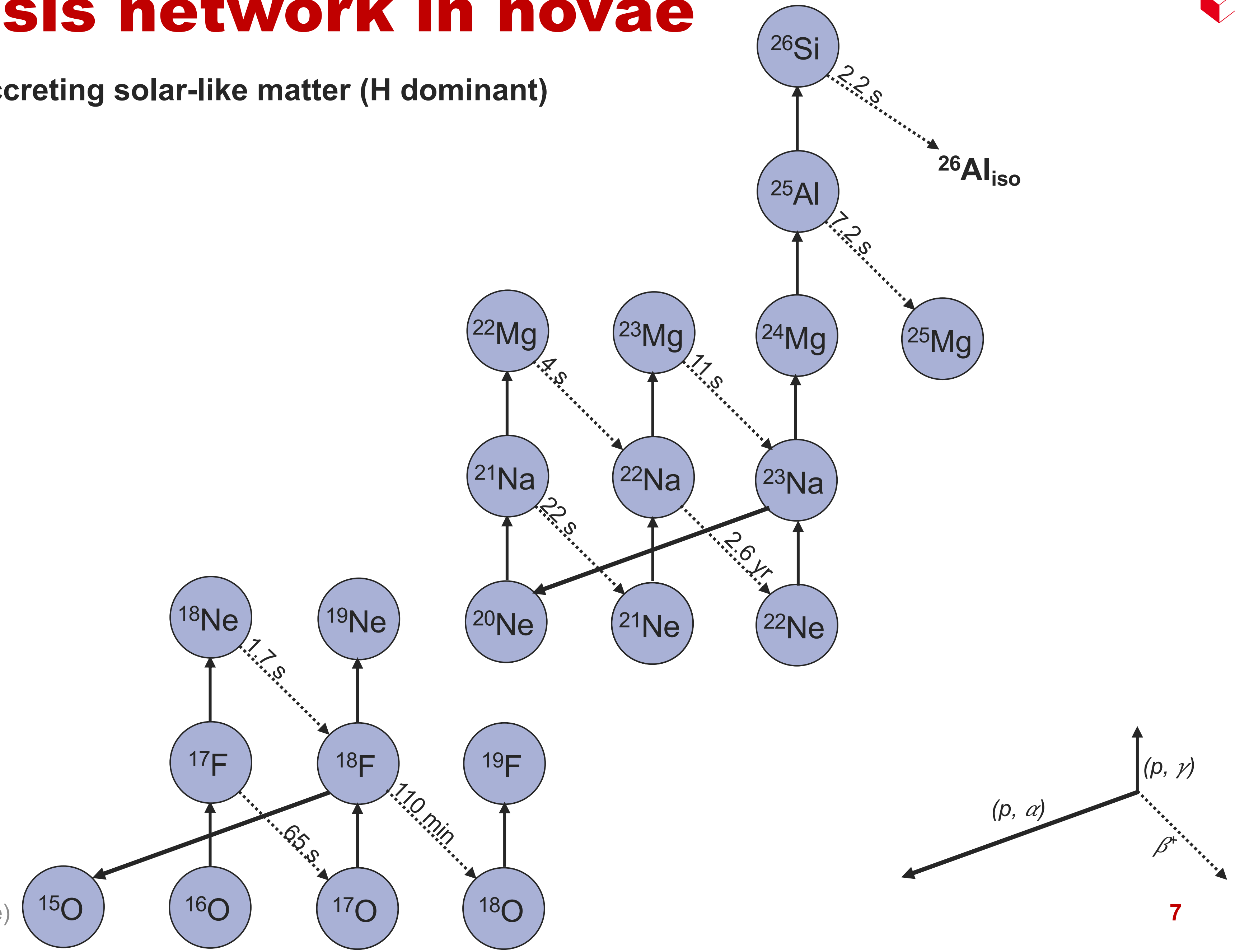

Nucleosynthesis network in novae

Nuclear ONe seed of white dwarf accreting solar-like matter (H dominant)

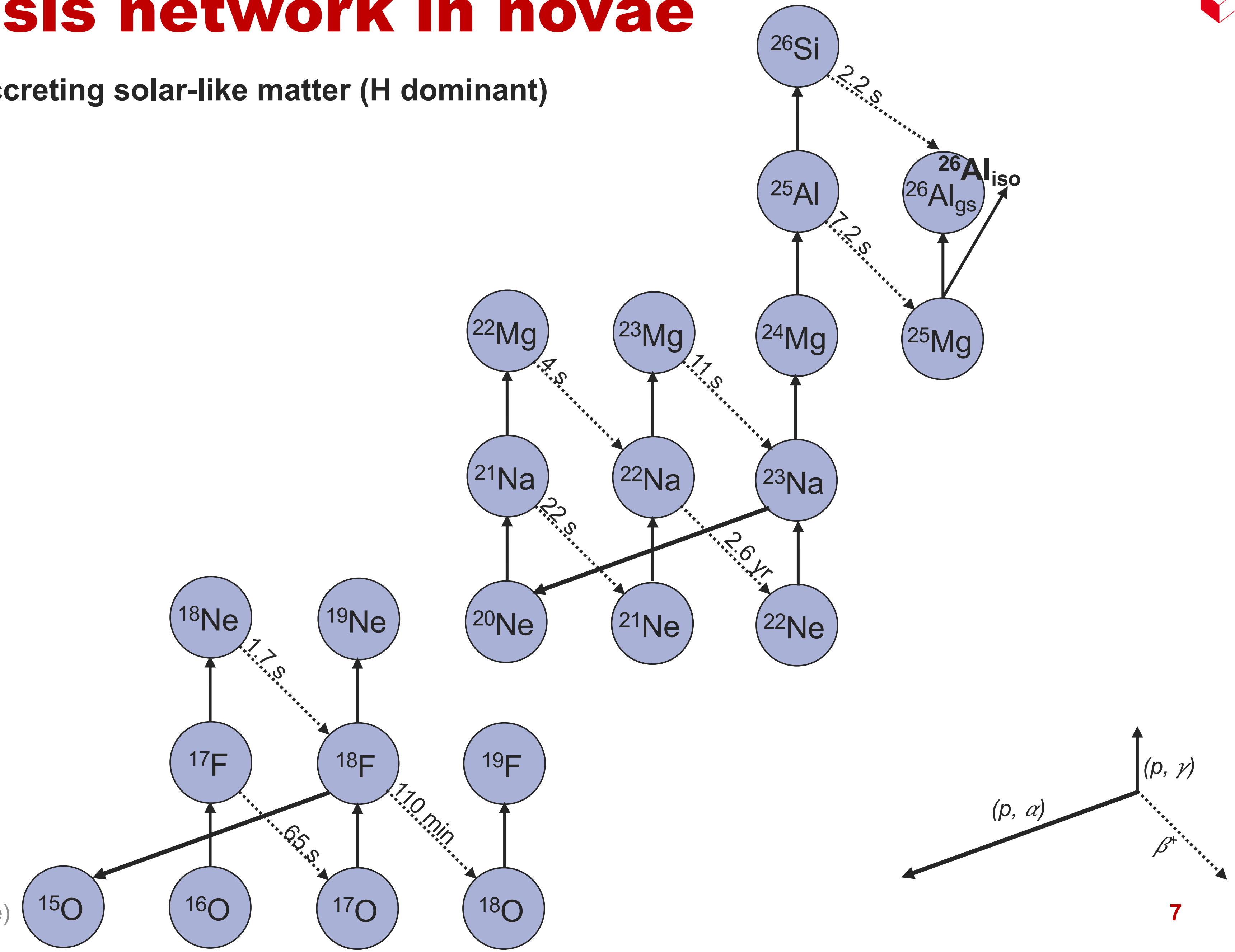

Nucleosynthesis network in novae

Nuclear ONe seed of white dwarf accreting solar-like matter (H dominant)

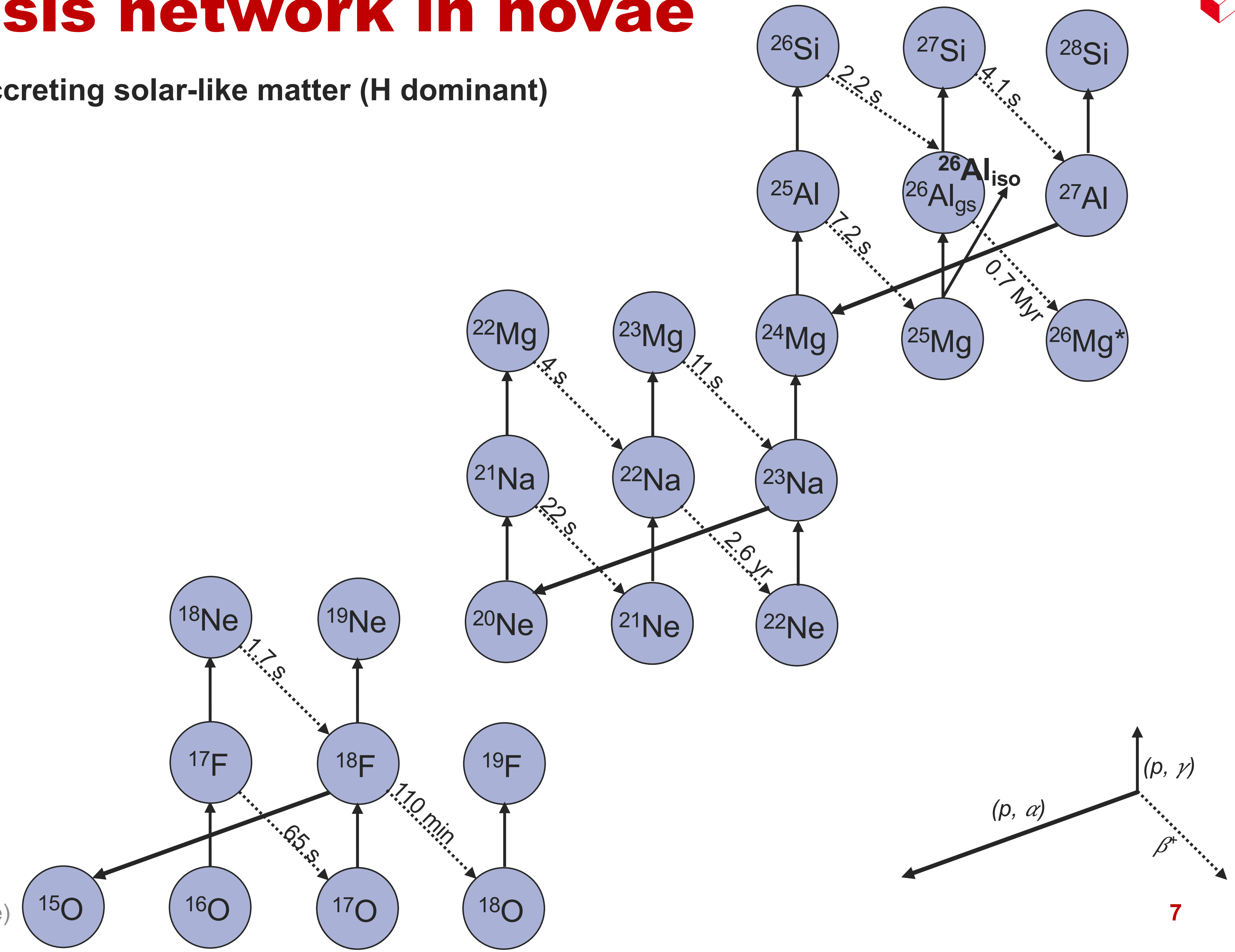

Nucleosynthesis network in novae

Nuclear ONe seed of white dwarf accreting solar-like matter (H dominant)

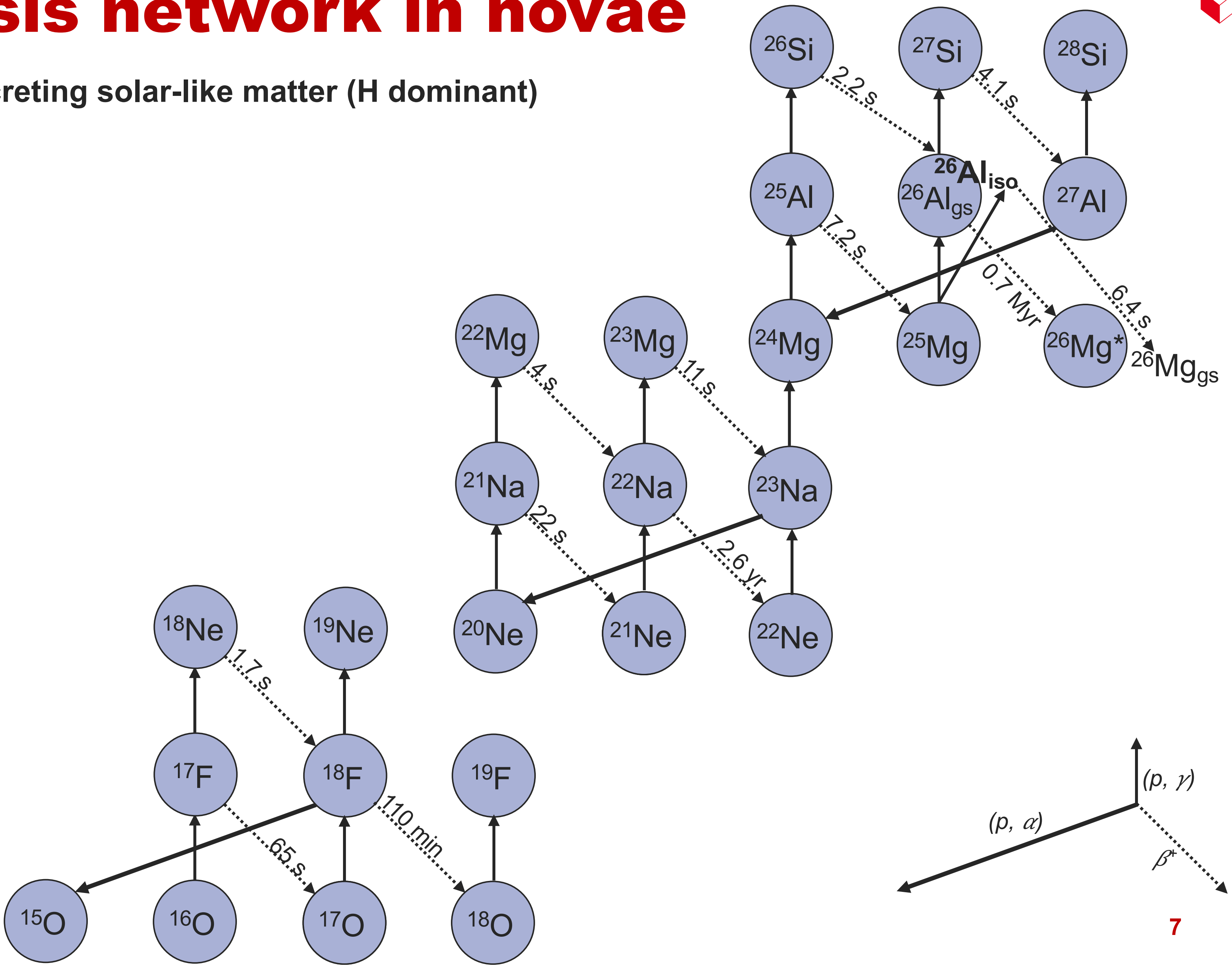

Nucleosynthesis network in novae

Nuclear ONe seed of white dwarf accreting solar-like matter (H dominant)

Radioelement

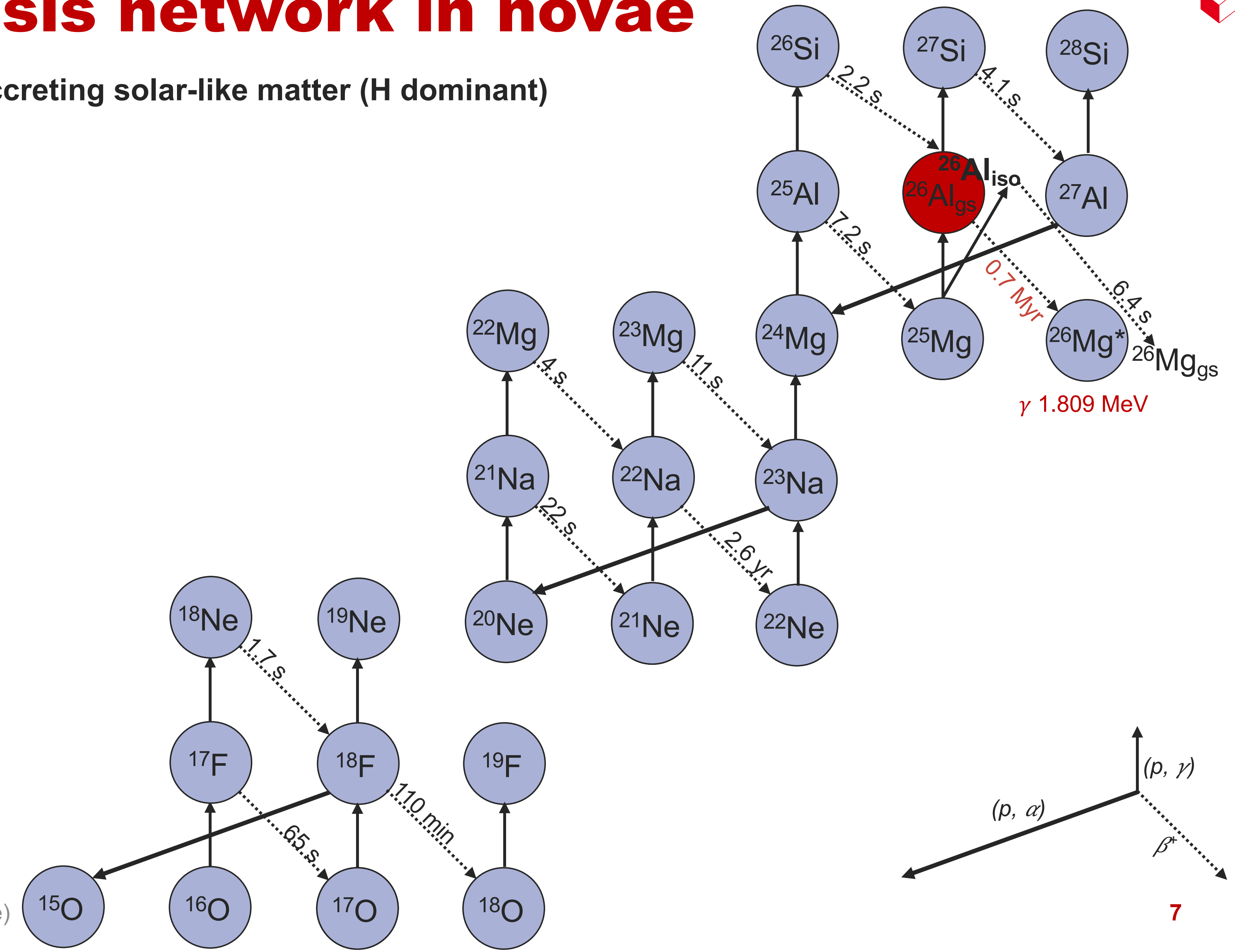

Nucleosynthesis network in novae

Nuclear ONe seed of white dwarf accreting solar-like matter (H dominant)

Radioelements

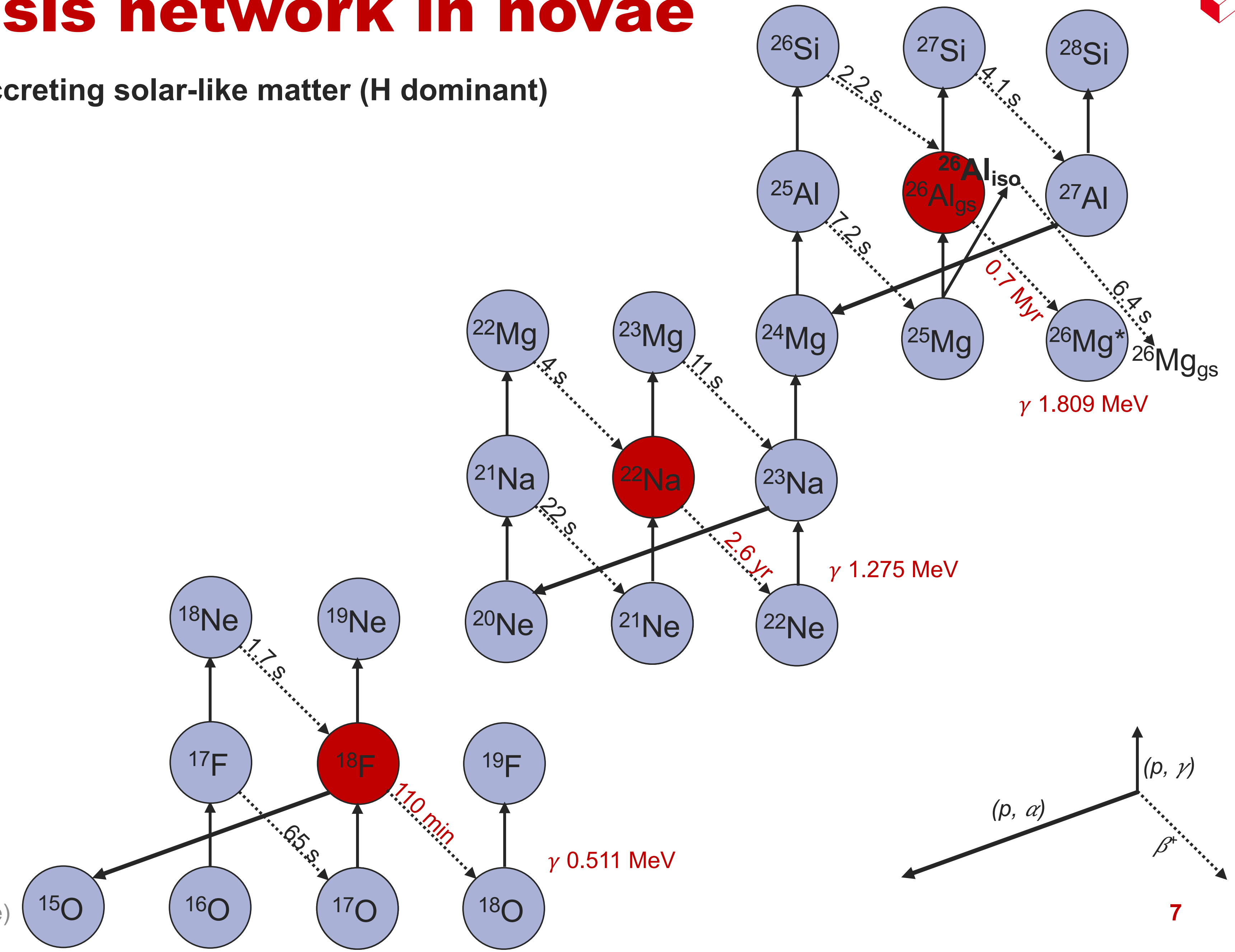

Nucleosynthesis network calculations

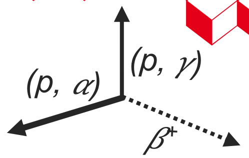

Abundance of ^{22}Na in novae

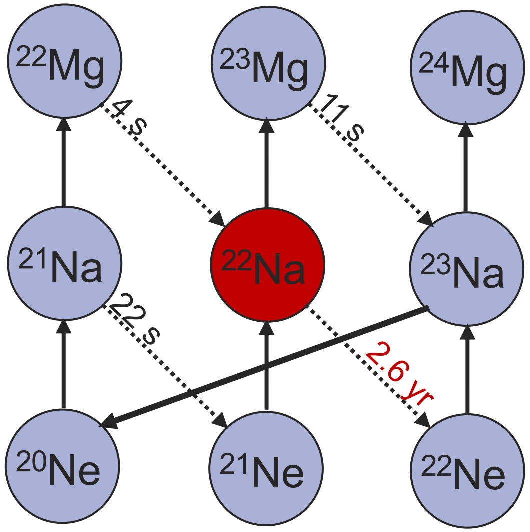

Nucleosynthesis network calculations

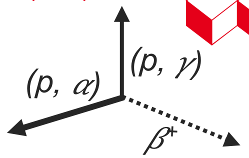

Abundance of ^{22}Na in novae: solver of an 8 ordinary differential equation system

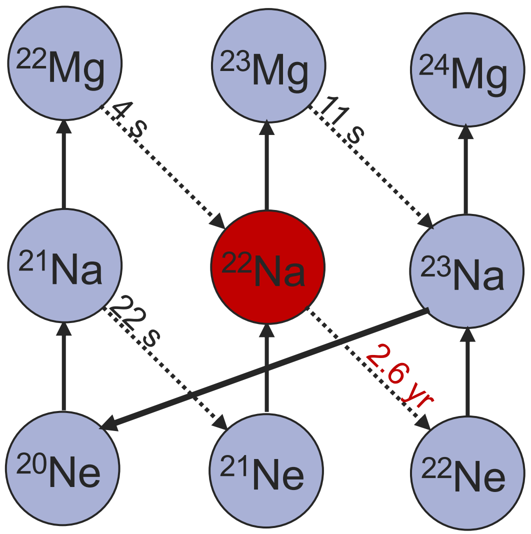

$$\frac{dy_{20Ne}}{dt} = -y_{20Ne} * y_H * <\sigma v>_{20Ne(p,\gamma)21Na} + y_{23Na} * y_H * <\sigma v>_{23Na(p,\alpha)20Ne}$$

$$\frac{dy_{21Ne}}{dt} = -y_{21Ne} * y_H * <\sigma v>_{21Ne(p,\gamma)22Na} + y_{21Na} * \frac{\ln(2)}{\tau_{21Na}}$$

$$\frac{dy_{22Ne}}{dt} = -y_{22Ne} * y_H * <\sigma v>_{22Ne(p,\gamma)23Na} + y_{22Na} * \frac{\ln(2)}{\tau_{22Na}}$$

$$\frac{dy_{21Na}}{dt} = -y_{21Na} * \left(y_H * <\sigma v>_{21Na(p,\gamma)22Mg} + \frac{\ln(2)}{\tau_{22Na}}\right) + y_{20Ne} * y_H * <\sigma v>_{20Ne(p,\gamma)21Na}$$

$$\frac{dy_{22Na}}{dt} = -y_{22Na} * \left(y_H * <\sigma v>_{22Na(p,\gamma)23Mg} + \frac{\ln(2)}{\tau_{22Na}}\right) + y_{21Ne} * y_H * <\sigma v>_{21Ne(p,\gamma)22Na} + y_{22Mg} * \frac{\ln(2)}{\tau_{22Mg}}$$

$$\frac{dy_{23Na}}{dt} = -y_{23Na} * y_H * <\sigma v>_{23Na(p,\alpha)20Ne} + y_{22Ne} * y_H * <\sigma v>_{22Ne(p,\gamma)23Na} + y_{23Mg} * \frac{\ln(2)}{\tau_{23Mg}}$$

$$\frac{dy_{22Mg}}{dt} = -y_{22Mg} * \frac{\ln(2)}{\tau_{22Mg}} + y_{21Na} * y_H * <\sigma v>_{21Na(p,\gamma)22Mg}$$

$$\frac{dy_{23Mg}}{dt} = -y_{23Mg} * \frac{\ln(2)}{\tau_{23Mg}} + y_{22Na} * y_H * <\sigma v>_{22Na(p,\gamma)23Mg}$$

Nucleosynthesis network calculations

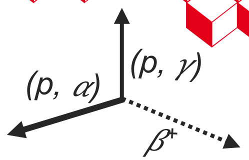

Abundance of ^{22}Na in novae: solver of an 8 ordinary differential equation system

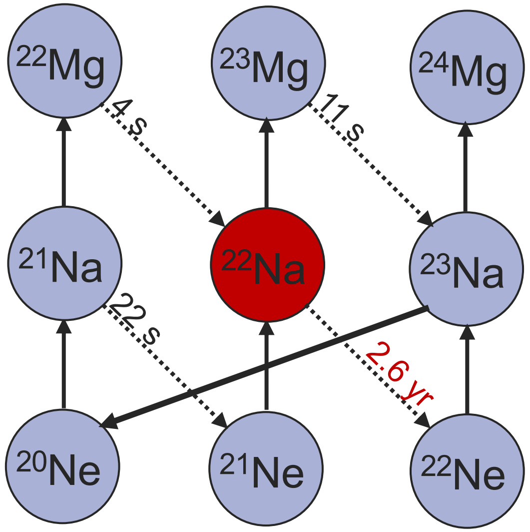

$$\frac{dy_{20Ne}}{dt} = -y_{20Ne} * y_H * <\sigma v>_{20Ne(p,\gamma)21Na} + y_{23Na} * y_H * <\sigma v>_{23Na(p,\alpha)20Ne}$$

$$\frac{dy_{21Ne}}{dt} = -y_{21Ne} * y_H * <\sigma v>_{21Ne(p,\gamma)22Na} + y_{21Na} * \frac{\ln(2)}{\tau_{21Na}}$$

$$\frac{dy_{22Ne}}{dt} = -y_{22Ne} * y_H * <\sigma v>_{22Ne(p,\gamma)23Na} + y_{22Na} * \frac{\ln(2)}{\tau_{22Na}}$$

$$\frac{dy_{21Na}}{dt} = -y_{21Na} * (y_H * <\sigma v>_{21Na(p,\gamma)22Mg} + \frac{\ln(2)}{\tau_{22Na}}) + y_{20Ne} * y_H * <\sigma v>_{20Ne(p,\gamma)21Na}$$

$$\frac{dy_{22Na}}{dt} = -y_{22Na} * (y_H * <\sigma v>_{22Na(p,\gamma)23Mg} + \frac{\ln(2)}{\tau_{22Na}}) + y_{21Ne} * y_H * <\sigma v>_{21Ne(p,\gamma)22Na} + y_{22Mg} * \frac{\ln(2)}{\tau_{22Mg}}$$

$$\frac{dy_{23Na}}{dt} = -y_{23Na} * y_H * <\sigma v>_{23Na(p,\alpha)20Ne} + y_{22Ne} * y_H * <\sigma v>_{22Ne(p,\gamma)23Na} + y_{23Mg} * \frac{\ln(2)}{\tau_{23Mg}}$$

$$\frac{dy_{22Mg}}{dt} = -y_{22Mg} * \frac{\ln(2)}{\tau_{22Mg}} + y_{21Na} * y_H * <\sigma v>_{21Na(p,\gamma)22Mg}$$

$$\frac{dy_{23Mg}}{dt} = -y_{23Mg} * \frac{\ln(2)}{\tau_{23Mg}} + y_{22Na} * y_H * <\sigma v>_{22Na(p,\gamma)23Mg}$$

Euler development *dY/dt = f(Y(t))* → *(1/dt – d/dY)(Y_{n+1} –Y_n) = f(Y_n)* *simple « Ax=B solver »*

Nucleosynthesis network calculations

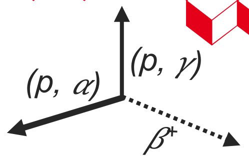

Abundance of ^{22}Na in novae: solver of an 8 ordinary differential equation system

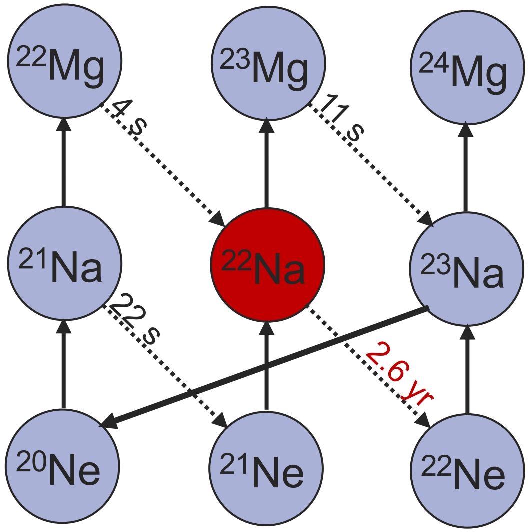

$$\frac{dy_{20Ne}}{dt} = -y_{20Ne} * y_H * <\sigma v>_{20Ne(p,\gamma)21Na} + y_{23Na} * y_H * <\sigma v>_{23Na(p,\alpha)20Ne}$$

$$\frac{dy_{21Ne}}{dt} = -y_{21Ne} * y_H * <\sigma v>_{21Ne(p,\gamma)22Na} + y_{21Na} * \frac{\ln(2)}{\tau_{21Na}}$$

$$\frac{dy_{22Ne}}{dt} = -y_{22Ne} * y_H * <\sigma v>_{22Ne(p,\gamma)23Na} + y_{22Na} * \frac{\ln(2)}{\tau_{22Na}}$$

$$\frac{dy_{21Na}}{dt} = -y_{21Na} * (y_H * <\sigma v>_{21Na(p,\gamma)22Mg} + \frac{\ln(2)}{\tau_{22Na}}) + y_{20Ne} * y_H * <\sigma v>_{20Ne(p,\gamma)21Na}$$

$$\frac{dy_{22Na}}{dt} = -y_{22Na} * (y_H * <\sigma v>_{22Na(p,\gamma)23Mg} + \frac{\ln(2)}{\tau_{22Na}}) + y_{21Ne} * y_H * <\sigma v>_{21Ne(p,\gamma)22Na} + y_{22Mg} * \frac{\ln(2)}{\tau_{22Mg}}$$

$$\frac{dy_{23Na}}{dt} = -y_{23Na} * y_H * <\sigma v>_{23Na(p,\alpha)20Ne} + y_{22Ne} * y_H * <\sigma v>_{22Ne(p,\gamma)23Na} + y_{23Mg} * \frac{\ln(2)}{\tau_{23Mg}}$$

$$\frac{dy_{22Mg}}{dt} = -y_{22Mg} * \frac{\ln(2)}{\tau_{22Mg}} + y_{21Na} * y_H * <\sigma v>_{21Na(p,\gamma)22Mg}$$

$$\frac{dy_{23Mg}}{dt} = -y_{23Mg} * \frac{\ln(2)}{\tau_{23Mg}} + y_{22Na} * y_H * <\sigma v>_{22Na(p,\gamma)23Mg}$$

Euler development *$dY/dt = f(Y(t))$* → *$(1/dt - d/dY)(Y_{n+1} - Y_n) = f(Y_n)$ simple « Ax=B solver »*

Initial conditions ONe white dwarf $\rho = 10^3$ g cm^{-3} with $Y_H^{constant} = 0.5$ $Y_{16O} = 0.25$ $Y_{20Ne} = 0.25$

Temperature profil

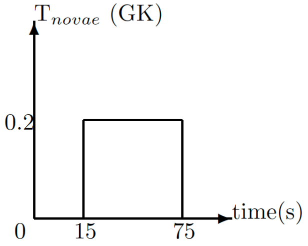

Nucleosynthesis network calculations

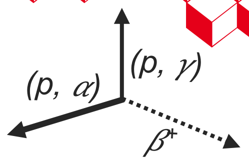

Abundance of ^{22}Na in novae: solver of an 8 ordinary differential equation system

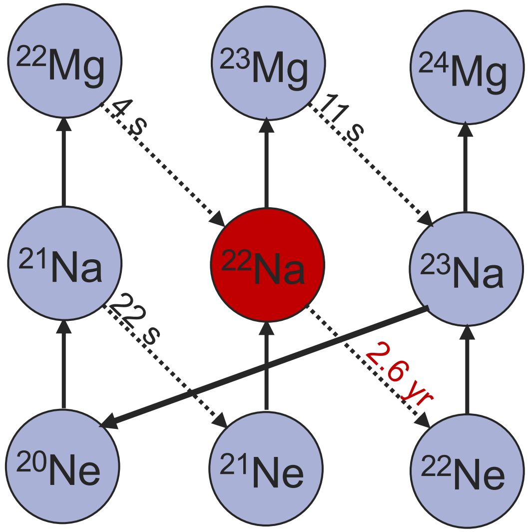

$$\frac{dy_{20Ne}}{dt} = -y_{20Ne} * y_H * <\sigma v>_{20Ne(p,\gamma)21Na} + y_{23Na} * y_H * <\sigma v>_{23Na(p,\alpha)20Ne}$$

$$\frac{dy_{21Ne}}{dt} = -y_{21Ne} * y_H * <\sigma v>_{21Ne(p,\gamma)22Na} + y_{21Na} * \frac{\ln(2)}{\tau_{21Na}}$$

$$\frac{dy_{22Ne}}{dt} = -y_{22Ne} * y_H * <\sigma v>_{22Ne(p,\gamma)23Na} + y_{22Na} * \frac{\ln(2)}{\tau_{22Na}}$$

$$\frac{dy_{21Na}}{dt} = -y_{21Na} * \left(y_H * <\sigma v>_{21Na(p,\gamma)22Mg} + \frac{\ln(2)}{\tau_{22Na}}\right) + y_{20Ne} * y_H * <\sigma v>_{20Ne(p,\gamma)21Na}$$

$$\frac{dy_{22Na}}{dt} = -y_{22Na} * \left(y_H * <\sigma v>_{22Na(p,\gamma)23Mg} + \frac{\ln(2)}{\tau_{22Na}}\right) + y_{21Ne} * y_H * <\sigma v>_{21Ne(p,\gamma)22Na} + y_{22Mg} * \frac{\ln(2)}{\tau_{22Mg}}$$

$$\frac{dy_{23Na}}{dt} = -y_{23Na} * y_H * <\sigma v>_{23Na(p,\alpha)20Ne} + y_{22Ne} * y_H * <\sigma v>_{22Ne(p,\gamma)23Na} + y_{23Mg} * \frac{\ln(2)}{\tau_{23Mg}}$$

$$\frac{dy_{22Mg}}{dt} = -y_{22Mg} * \frac{\ln(2)}{\tau_{22Mg}} + y_{21Na} * y_H * <\sigma v>_{21Na(p,\gamma)22Mg}$$

$$\frac{dy_{23Mg}}{dt} = -y_{23Mg} * \frac{\ln(2)}{\tau_{23Mg}} + y_{22Na} * y_H * <\sigma v>_{22Na(p,\gamma)23Mg}$$

Euler development *$dY/dt = f(Y(t))$* → *$(1/dt - d/dY)(Y_{n+1} - Y_n) = f(Y_n)$ simple « Ax=B solver »*

Initial conditions ONe white dwarf $\rho = 10^3$ g cm^{-3} with $Y_H^{constant} = 0.5$ $Y_{16O} = 0.25$ $Y_{20Ne} = 0.25$

Temperature profil

Simple Python recursive code

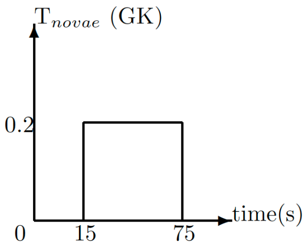

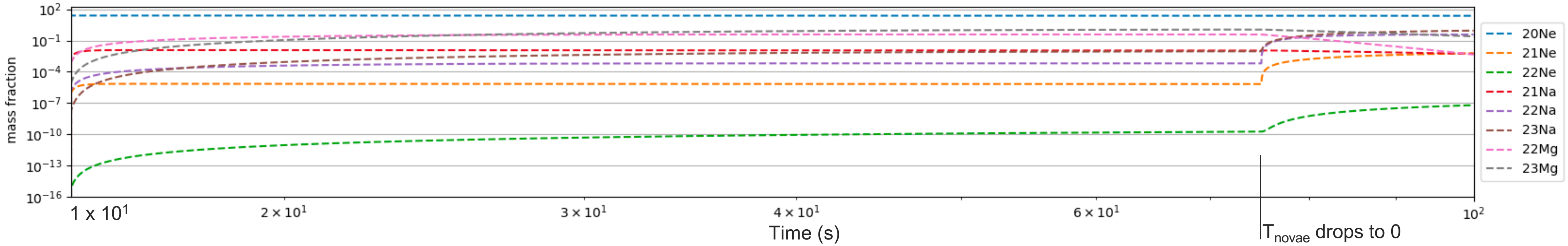

Nucleosynthesis network calculations

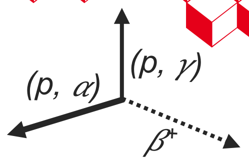

Abundance of ^{22}Na in novae: solver of an 8 ordinary differential equation system

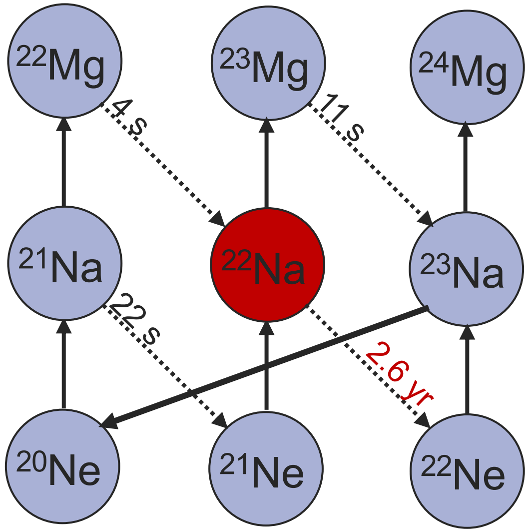

$$\frac{dy_{20Ne}}{dt} = -y_{20Ne} * y_H * < \sigma v >_{20Ne(p,\gamma)21Na} + y_{23Na} * y_H * < \sigma v >_{23Na(p,\alpha)20Ne}$$

$$\frac{dy_{21Ne}}{dt} = -y_{21Ne} * y_H * < \sigma v >_{21Ne(p,\gamma)22Na} + y_{21Na} * \frac{\ln(2)}{\tau_{21Na}}$$

$$\frac{dy_{22Ne}}{dt} = -y_{22Ne} * y_H * < \sigma v >_{22Ne(p,\gamma)23Na} + y_{22Na} * \frac{\ln(2)}{\tau_{22Na}}$$

$$\frac{dy_{21Na}}{dt} = -y_{21Na} * \left(y_H * < \sigma v >_{21Na(p,\gamma)22Mg} + \frac{\ln(2)}{\tau_{22Na}}\right) + y_{20Ne} * y_H * < \sigma v >_{20Ne(p,\gamma)21Na}$$

$$\frac{dy_{22Na}}{dt} = -y_{22Na} * \left(y_H * < \sigma v >_{22Na(p,\gamma)23Mg} + \frac{\ln(2)}{\tau_{22Na}}\right) + y_{21Ne} * y_H * < \sigma v >_{21Ne(p,\gamma)22Na} + y_{22Mg} * \frac{\ln(2)}{\tau_{22Mg}}$$

$$\frac{dy_{23Na}}{dt} = -y_{23Na} * y_H * < \sigma v >_{23Na(p,\alpha)20Ne} + y_{22Ne} * y_H * < \sigma v >_{22Ne(p,\gamma)23Na} + y_{23Mg} * \frac{\ln(2)}{\tau_{23Mg}}$$

$$\frac{dy_{22Mg}}{dt} = -y_{22Mg} * \frac{\ln(2)}{\tau_{22Mg}} + y_{21Na} * y_H * < \sigma v >_{21Na(p,\gamma)22Mg}$$

$$\frac{dy_{23Mg}}{dt} = -y_{23Mg} * \frac{\ln(2)}{\tau_{23Mg}} + y_{22Na} * y_H * < \sigma v >_{22Na(p,\gamma)23Mg}$$

Software freely available (WinNet, NuGrid, integrated MESA,…)

https://github.com/nuc-astro/WinNet

https://nugrid.github.io

https://docs.mesastar.org/en/24.08.1

Nuclear reaction rates

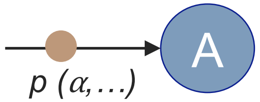

Reaction rate = < cross section σ x particle velocity distribution in plasma ν >

$$< \sigma v >= (\frac{8}{\pi \mu_{\mathrm{A,p}}})^{\frac{1}{2}} \times \frac{1}{(\mathrm{k_B T})^{\frac{3}{2}}} \times \int_0^{+\infty} \sigma(\mathrm{E}) \exp(-\frac{\mathrm{E}}{\mathrm{k_B T}}) \mathrm{E dE}$$

Nuclear reaction rates

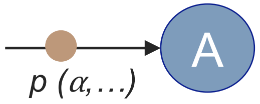

Reaction rate = < cross section σ x particle velocity distribution in plasma ν >

$$<\sigma v>=\left(\frac{8}{\pi\mu_{A,p}}\right)^{\frac{1}{2}}\times\frac{1}{(k_B T)^{\frac{3}{2}}}\times\int_0^{+\infty}\sigma(E)\exp\left(-\frac{E}{k_B T}\right)EdE$$

Charged particles

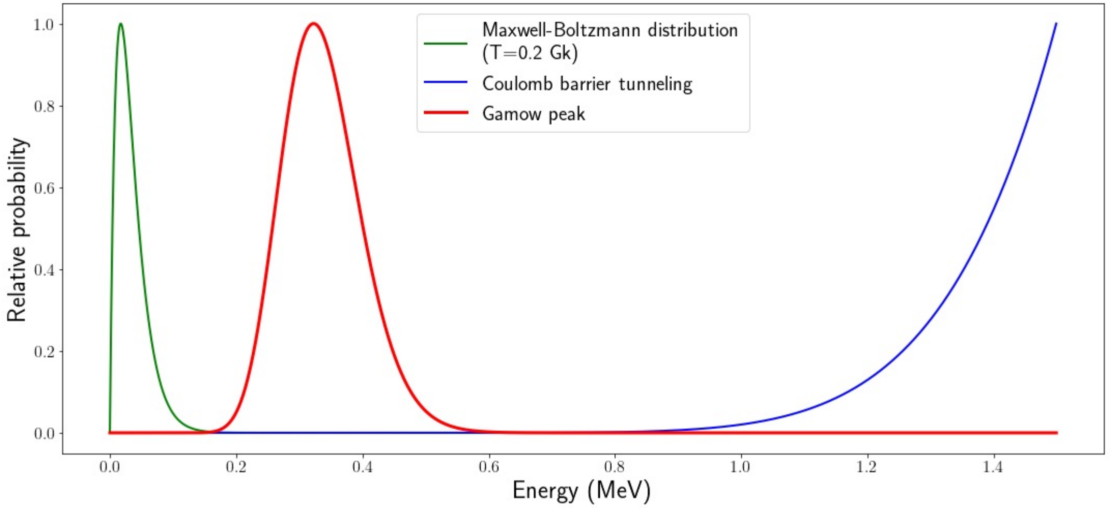

Nuclear reaction rates

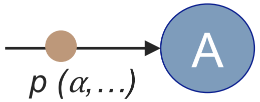

Reaction rate = < cross section σ x particle velocity distribution in plasma ν >

$$<\sigma v>=\left(\frac{8}{\pi\mu_{A,p}}\right)^{\frac{1}{2}}\times\frac{1}{(k_B T)^{\frac{3}{2}}}\times\int_0^{+\infty}\sigma(E)\exp\left(-\frac{E}{k_B T}\right)E\,dE$$

Charged particles

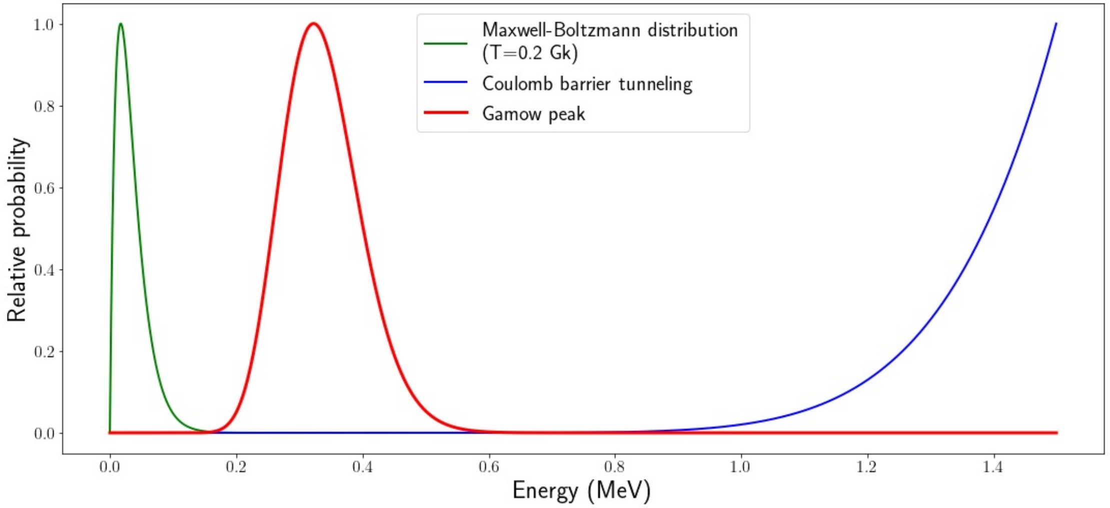

Gamow window $T \Leftrightarrow E_{cm}$

Energy region of compound system A+p where reaction most likely occurs at T

$$E_0 = 0.122(Z_p^2 Z_A^2 \mu_{A,p} T^2)^{\frac{1}{3}}$$

$$\Delta E_0 = 0.2368(Z_p^2 Z_A^2 \mu_{A,p} T^5)^{\frac{1}{6}}$$

Nuclear reaction rates (charged particles)

Reaction rate = < cross section σ x particle velocity distribution in plasma ν >

$$< \sigma v >= (\frac{8}{\pi \mu_{\mathrm{A,p}}})^{\frac{1}{2}} \times \frac{1}{(\mathrm{k_B T})^{\frac{3}{2}}} \times \int_0^{+\infty} \sigma(\mathrm{E}) \exp(-\frac{\mathrm{E}}{\mathrm{k_B T}}) \mathrm{EdE}$$

Nuclear reaction rates (charged particles)

Reaction rate = < cross section σ x particle velocity distribution in plasma ν >

$$< \sigma v >= (\frac{8}{\pi \mu_{A,p}})^{\frac{1}{2}} \times \frac{1}{(k_B T)^{\frac{3}{2}}} \times \int_0^{+\infty} \sigma(E) \exp(-\frac{E}{k_B T}) E dE$$

- In medium-hot stellar environments: **T ≲ 1 GK, *E_{cm}* ≲ MeV, *σ* << 1 mb**

$$\sigma_{BW}(E) = \pi \lambda\!\!\!^{-2} \omega \frac{\Gamma_a \Gamma_b}{(E - E_R)^2 + (\Gamma / 2)^2}$$

Breit-Wigner cross section

Nuclear reaction rates (charged particles)

Reaction rate = < cross section σ x particle velocity distribution in plasma ν >

$$<\sigma v>=\left(\frac{8}{\pi\mu_{A,p}}\right)^{\frac{1}{2}}\times\frac{1}{(k_B T)^{\frac{3}{2}}}\times\int_0^{+\infty}\sigma(E)\exp\left(-\frac{E}{k_B T}\right)E\,dE$$

- In medium-hot stellar environments: **T ≲ 1 GK, E_{cm} ≲ MeV, σ << 1 mb**

$$\sigma_{BW}(E)=\pi\lambda\!\!\!^{-2}\omega\frac{\Gamma_a\Gamma_b}{(E-E_R)^2+(\Gamma/2)^2}$$

Breit-Wigner cross section $\propto \Gamma_a, \Gamma_b$ (partial decay widths)

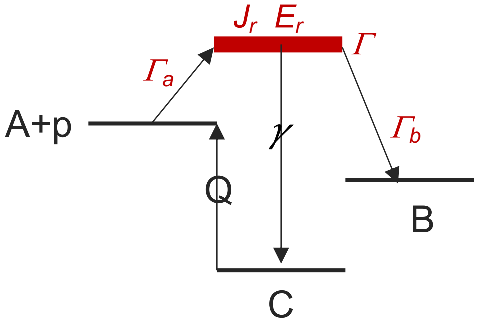

Nuclear reaction rates (charged particles)

Reaction rate = < cross section σ x particle velocity distribution in plasma ν >

$$< \sigma v >= \left(\frac{8}{\pi \mu_{A,p}}\right)^{\frac{1}{2}} \times \frac{1}{(k_B T)^{\frac{3}{2}}} \times \int_0^{+\infty} \sigma(E) \exp\left(-\frac{E}{k_B T}\right) E dE$$

- In medium-hot stellar environments: **T ≲ 1 GK, E_{cm} ≲ MeV, σ << 1 mb**

$$< \sigma \nu >_{tot} \propto \sum_r \omega\gamma_r \exp\left(-\frac{E_r}{k_B T}\right)$$

$$\sigma_{BW}(E) = \pi \bar{\lambda}^2 \omega \frac{\Gamma_a \Gamma_b}{(E - E_R)^2 + (\Gamma / 2)^2}$$

Breit-Wigner cross section $\propto \Gamma_a$, Γ_b (partial decay widths)

$\Gamma_b = CS_b \times \Gamma_{s.p., b}$

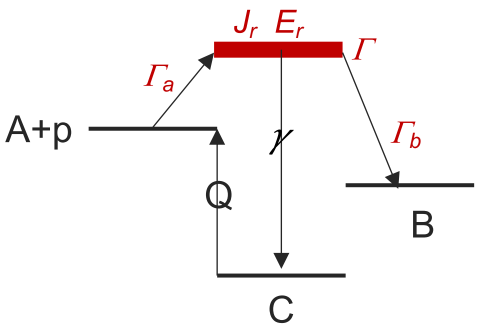

Nuclear reaction rates (charged particles)

Reaction rate = < cross section σ x particle velocity distribution in plasma ν >

$$<\sigma v>=\left(\frac{8}{\pi\mu_{\mathrm{A,p}}}\right)^{\frac{1}{2}}\times\frac{1}{(\mathrm{k_B T})^{\frac{3}{2}}}\times\int_0^{+\infty}\sigma(\mathrm{E})\exp\left(-\frac{\mathrm{E}}{\mathrm{k_B T}}\right)\mathrm{E}d\mathrm{E}$$

- In medium-hot stellar environments: **T ≲ 1 GK, E_{cm} ≲ MeV, σ << 1 mb**

$$<\sigma\nu>_{tot}\propto\sum_r\omega\gamma_r\exp\left(-\frac{E_r}{k_BT}\right)$$

$E_r = E_x - Q$ resonance energy

$$\sigma_{\mathrm{BW}}(E)=\pi\lambda^2\omega\frac{\Gamma_a\Gamma_b}{(E-E_R)^2+(\Gamma/2)^2}$$

Breit-Wigner cross section $\propto \Gamma_a, \Gamma_b$ (partial decay widths)

$\Gamma_b = CS_b \times \Gamma_{s.p., b}$

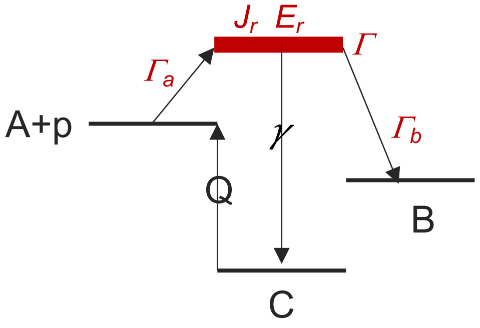

Nuclear reaction rates (charged particles)

Reaction rate = < cross section σ x particle velocity distribution in plasma ν >

$$<\sigma v>=(\frac{8}{\pi\mu_{A,p}})^{\frac{1}{2}}\times\frac{1}{(k_BT)^{\frac{3}{2}}}\times\int_0^{+\infty}\sigma(E)\exp(-\frac{E}{k_BT})EdE$$

- In medium-hot stellar environments: **T ≲ 1 GK, E_{cm} ≲ MeV, σ << 1 mb**

$$<\sigma\nu>_{tot}\propto\sum_r\omega\gamma_r\exp\left(-\frac{E_r}{k_BT}\right)$$

$E_r = E_x - Q$ resonance energy

$\omega\gamma_r$ resonance strength

$\omega \propto 2J_r+1$

$\gamma_r \propto (\Gamma = \hbar/\tau)$ x $BR_b(1-BR_b)$

$$\sigma_{BW}(E)=\pi\lambda^2\omega\frac{\Gamma_a\Gamma_b}{(E-E_R)^2+(\Gamma/2)^2}$$

Breit-Wigner cross section $\propto \Gamma_a, \Gamma_b$ (partial decay widths)

$\Gamma_b = CS_b \times \Gamma_{s.p.,b}$

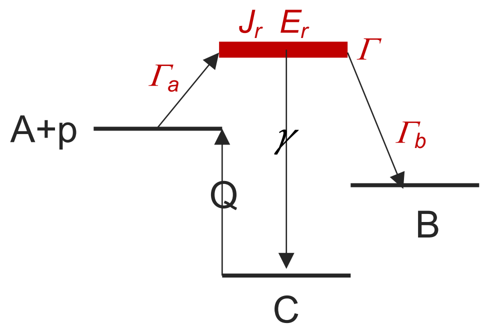

Nuclear reaction rates (charged particles)

Reaction rate = < cross section σ x particle velocity distribution in plasma ν >

$$<\sigma v>= (\frac{8}{\pi\mu_{A,p}})^{\frac{1}{2}} \times \frac{1}{(k_B T)^{\frac{3}{2}}} \times \int_0^{+\infty} \sigma(E)\exp(-\frac{E}{k_B T})EdE$$

- In medium-hot stellar environments: **T ≲ 1 GK, E_{cm} ≲ MeV, σ << 1 mb** → Resonance measurement

$$<\sigma\nu>_{tot} \propto \sum_r \boxed{\omega\gamma_r} \exp\left(-\frac{\boxed{E_r}}{k_B T}\right)$$

$E_r = E_x - Q$ resonance energy

$\omega\gamma_r$ resonance strength

$\omega \propto 2J_r+1$

$\gamma_r \propto (\Gamma = \hbar/\tau) \times BR_b(1-BR_b)$

$$\sigma_{BW}(E) = \pi\lambda^2\omega\frac{\boxed{\Gamma_a\Gamma_b}}{(E-E_R)^2+(\boxed{\Gamma}/2)^2}$$

Breit-Wigner cross section $\propto \Gamma_a, \Gamma_b$ (partial decay widths)

$\Gamma_b = CS_b \times \Gamma_{s.p.,b}$

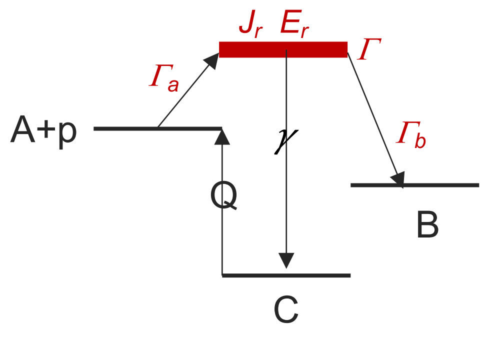

Measurement goals

E_r

$\omega\gamma_r$ or J_r

τ

BR_b or CS_b

Nuclear reaction rates (charged particles)

Reaction rate = < cross section σ x particle velocity distribution in plasma ν >

$$<\sigma v>= \left(\frac{8}{\pi\mu_{A,p}}\right)^{\frac{1}{2}} \times \frac{1}{(k_B T)^{\frac{3}{2}}} \times \int_0^{+\infty} \sigma(E)\exp\left(-\frac{E}{k_B T}\right) E dE$$

- In medium-hot stellar environments: **T ≲ 1 GK, E_{cm} ≲ MeV, σ << 1 mb** → Resonance measurement

$$<\sigma\nu>_{tot} \propto \sum_r \omega\gamma_r \exp\left(-\frac{E_r}{k_B T}\right)$$

$E_r = E_x - Q$ resonance energy

$\omega\gamma_r$ resonance strength

$\omega \propto 2J_r+1$

$\gamma_r \propto (\Gamma = \hbar/\tau) \times BR_b(1-BR_b)$

$$\sigma_{BW}(E) = \pi\lambda\!\!\!^{-2}\omega \frac{\Gamma_a\Gamma_b}{(E-E_R)^2+(\Gamma/2)^2}$$

Breit-Wigner cross section $\propto \Gamma_a, \Gamma_b$ (partial decay widths)

$\Gamma_b = CS_b \times \Gamma_{s.p.,b}$

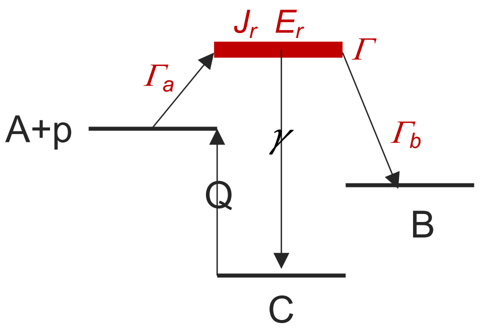

Measurement goals

E_r

$\omega\gamma_r$ or J_r

τ

BR_b or CS_b

- In hot stellar environments: **T > 1 GK, E_{cm} ~ MeV/u, σ ≳ 1 mb** → Cross section measurement

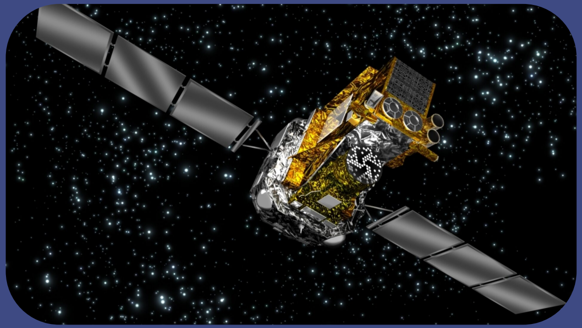

1. Astrophysical landscape

Few burning questions

Low energy γ–ray astronomy of novæ

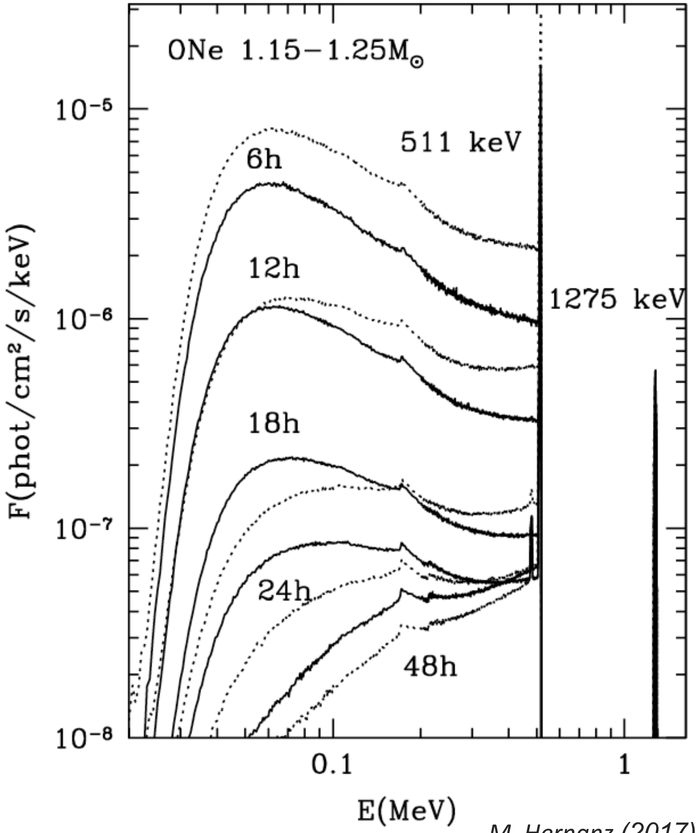

M. Hernanz (2017)

Low energy γ–ray astronomy of novæ

- **Short-lived** (~day) ^{18}F → ejecta stage

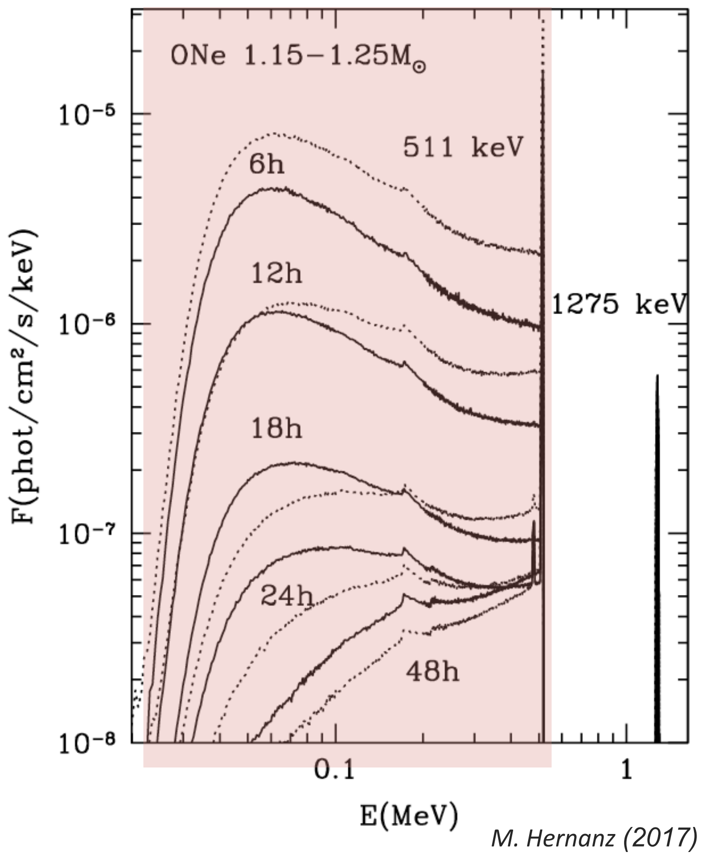

M. Hernanz (2017)

Low energy γ–ray astronomy of novæ

- **Short-lived** (~day) ^{18}F → ejecta stage

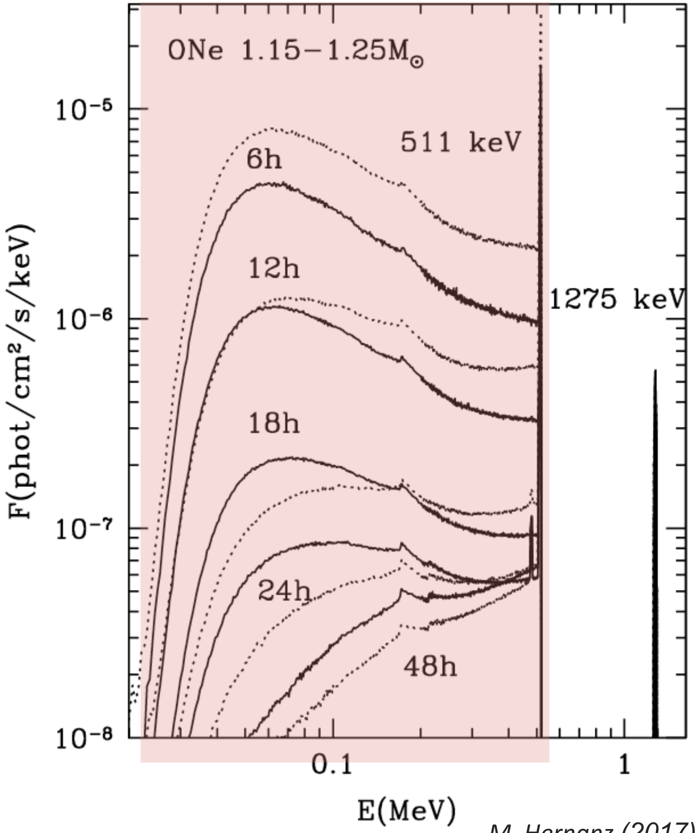

M. Hernanz (2017)

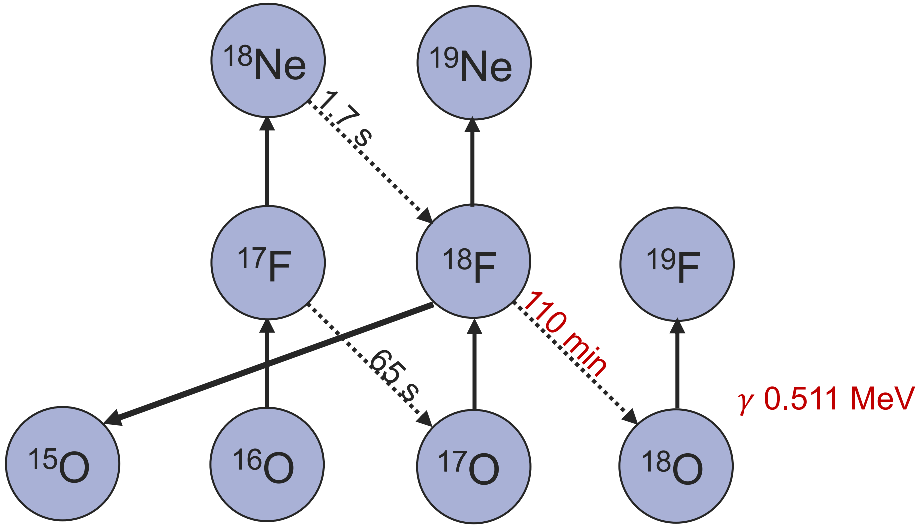

Low energy γ–ray astronomy of novæ

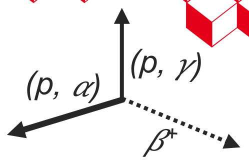

- **Short-lived** (~day) ^{18}F → ejecta stage
  Uncertainties in ^{18}F(p,α)^{15}O

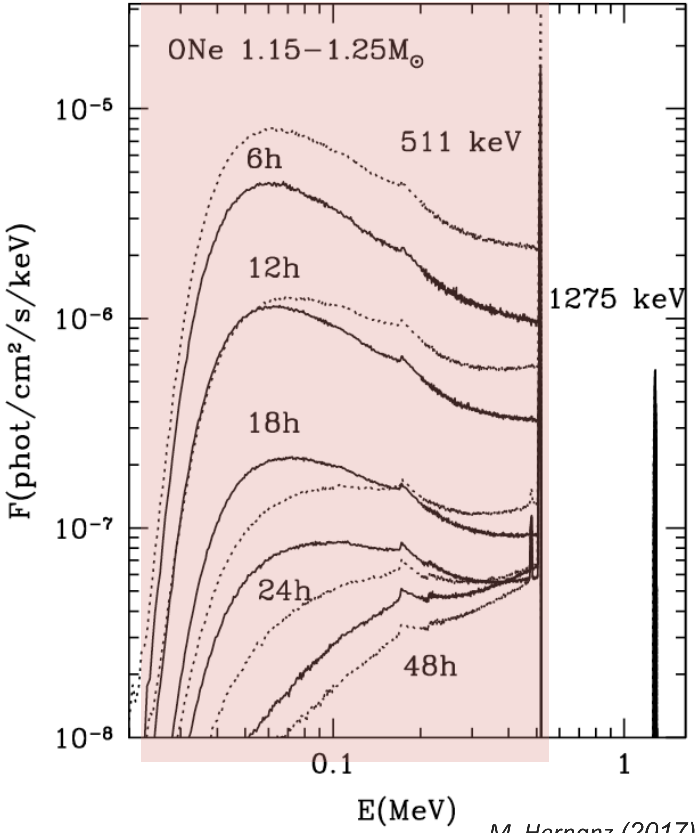

M. Hernanz (2017)

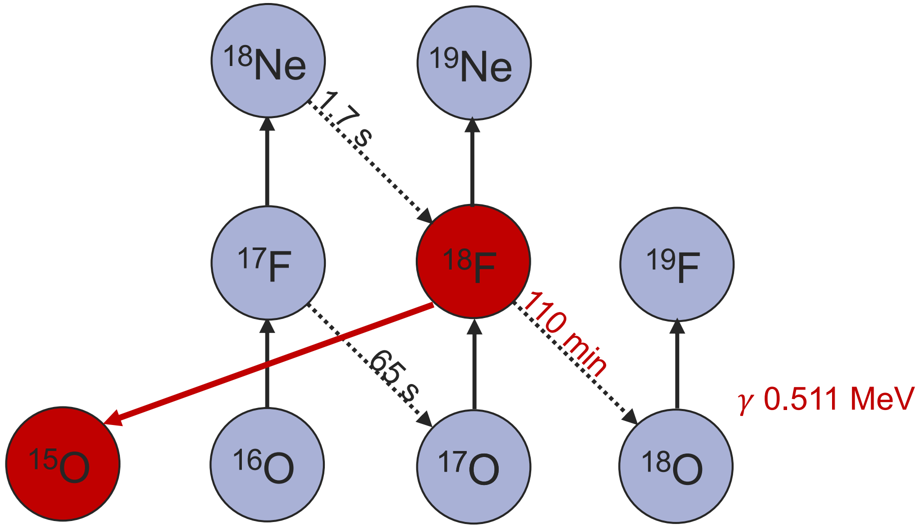

Low energy γ–ray astronomy of novæ

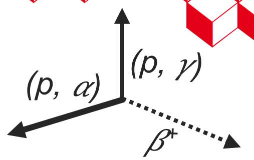

- **Short-lived** (~day) ^{18}F → ejecta stage
  Uncertainties in ^{18}F(p,α)^{15}O

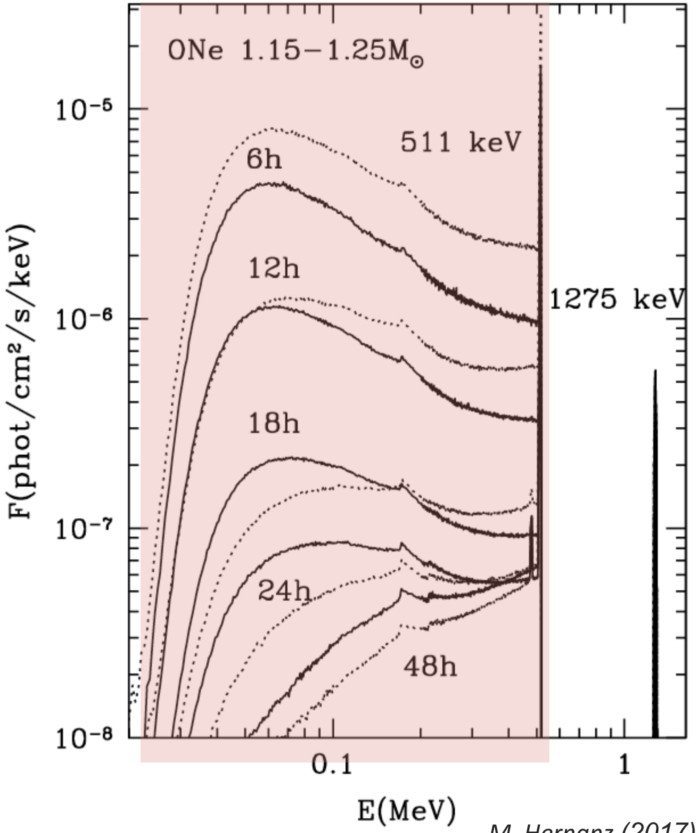

M. Hernanz (2017)

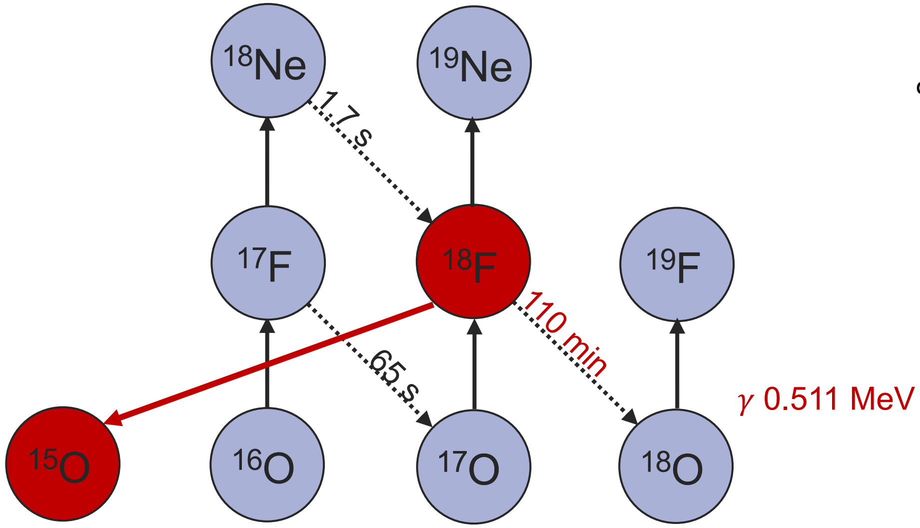

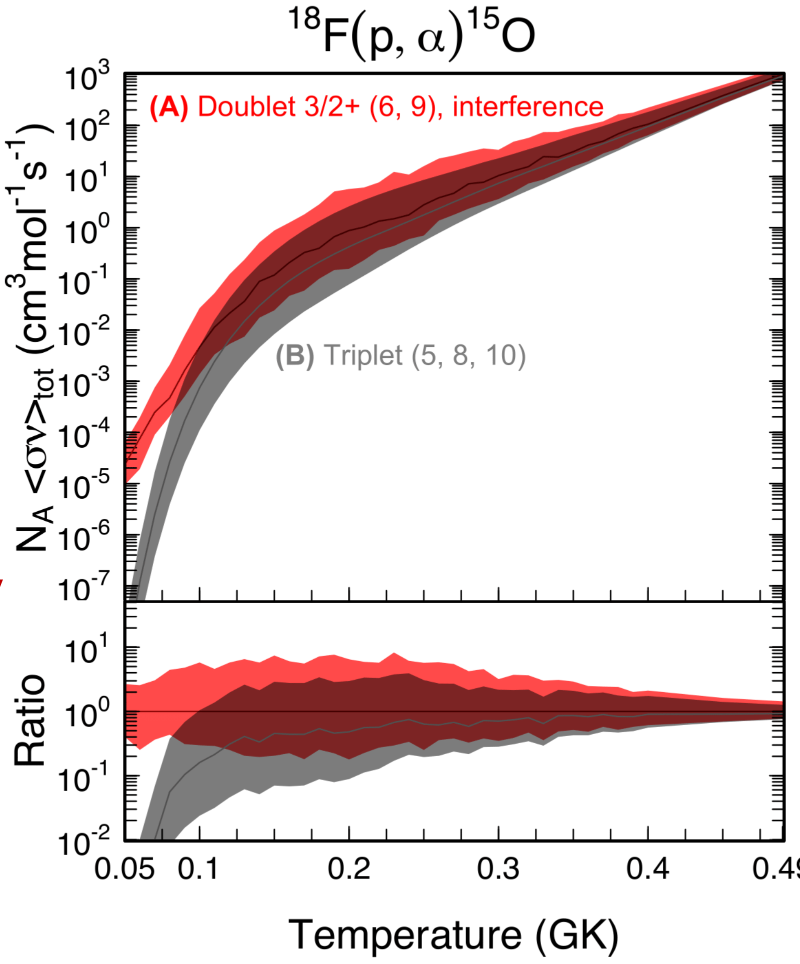

Low energy γ–ray astronomy of novæ

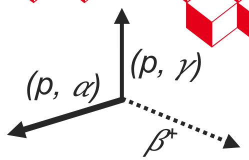

- **Short-lived** (~day) ^{18}F → ejecta stage
  Uncertainties in $^{18}F(p,\alpha)^{15}O$

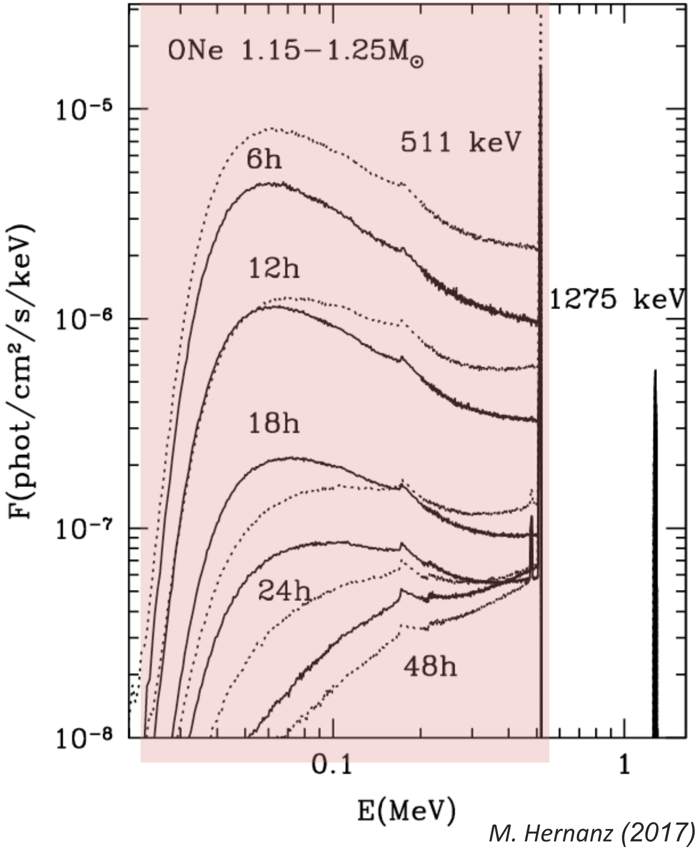

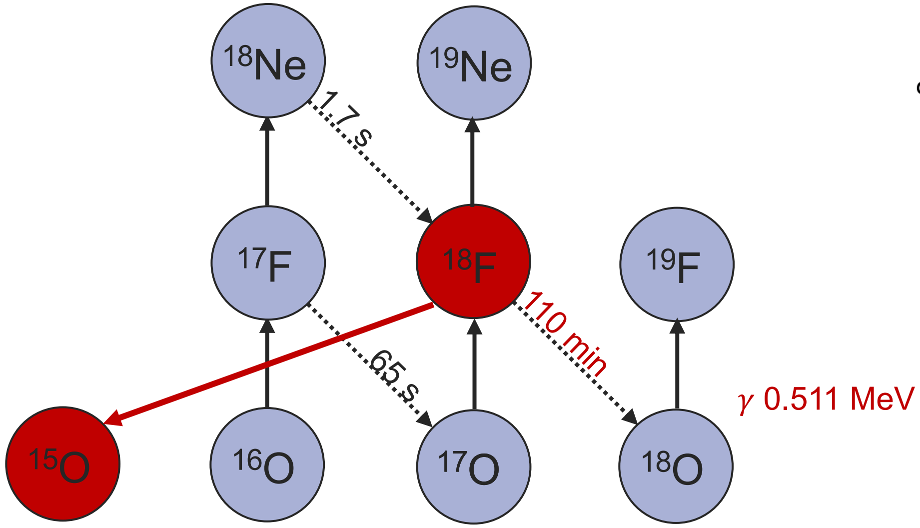

Maximum detectability distance
unc. x1.9

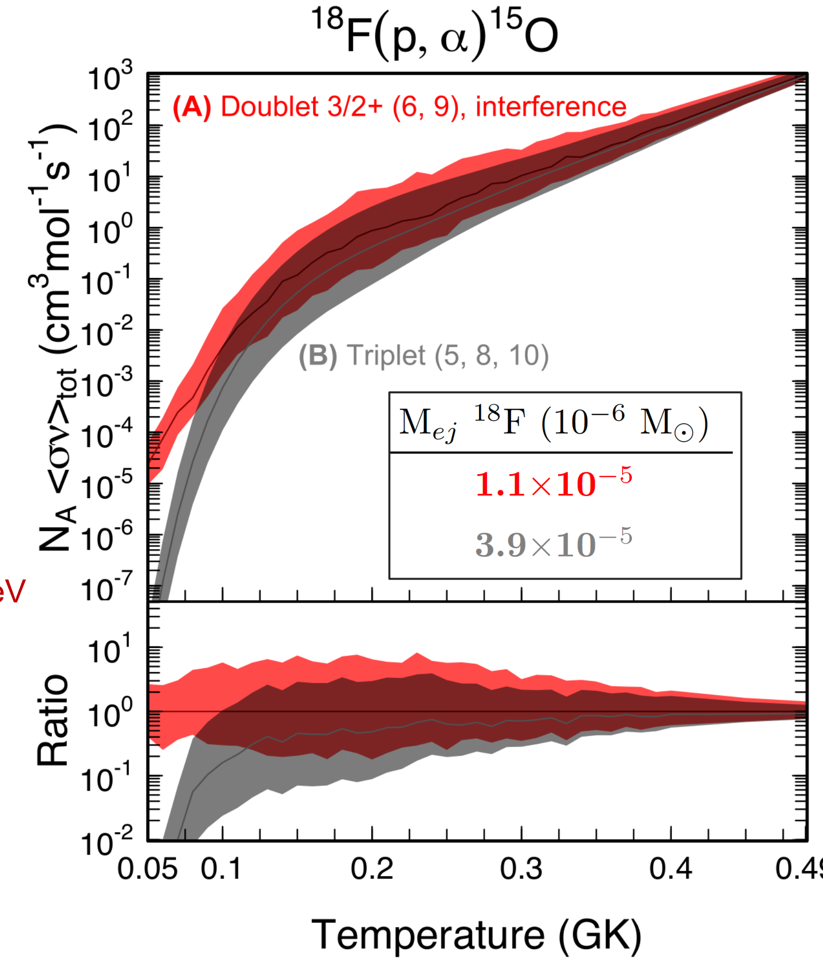

Low energy γ–ray astronomy of novæ

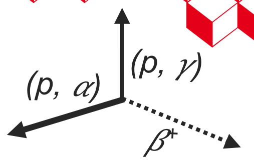

- **Short-lived** (~day) ^{18}F → ejecta stage
  Uncertainties in $^{18}F(p,\alpha)^{15}O$

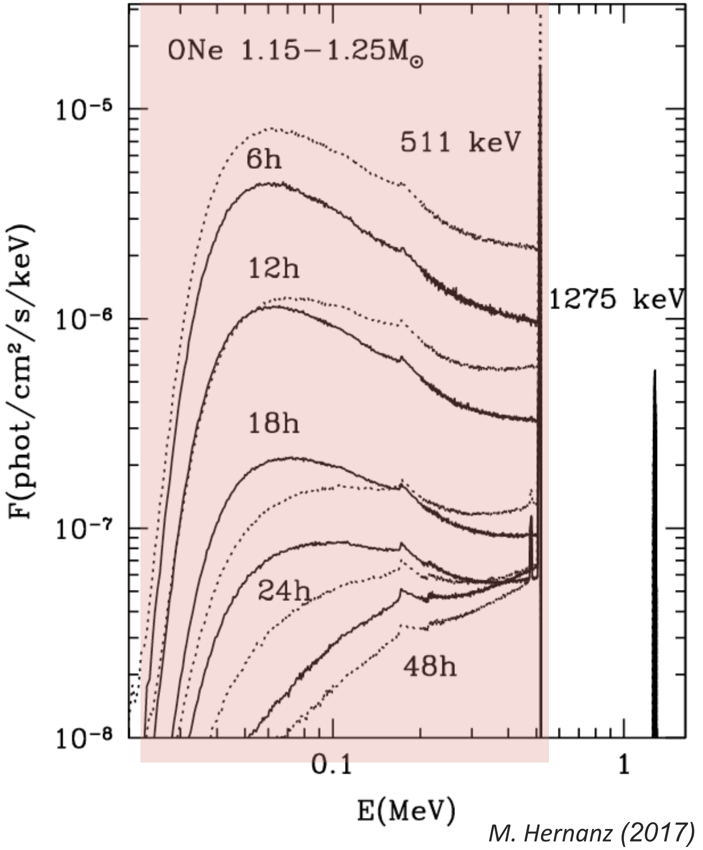

M. Hernanz (2017)

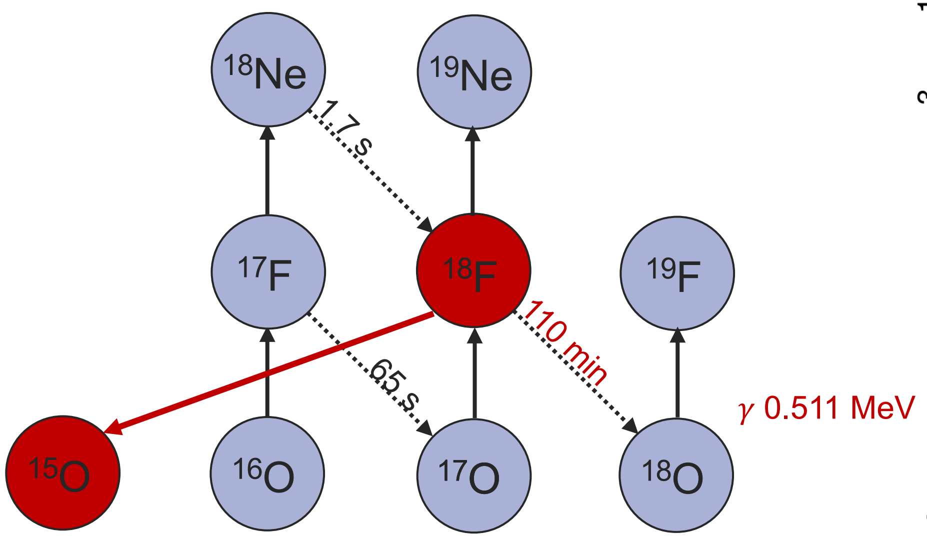

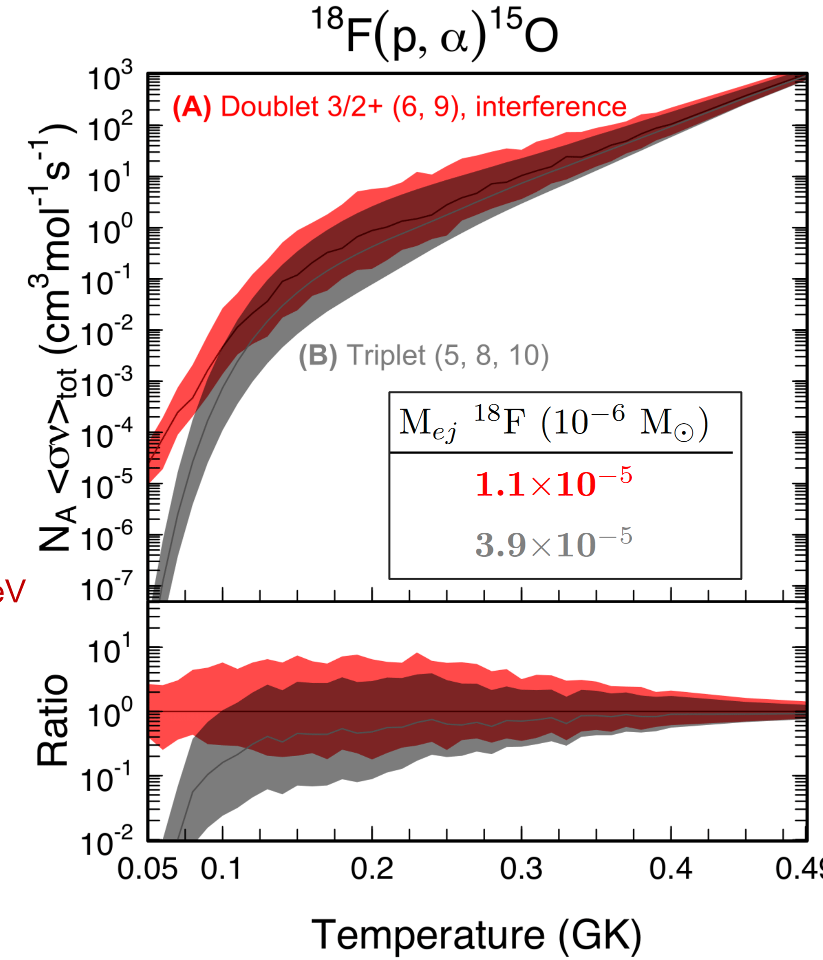

Maximum detectability distance unc. x1.9

Spectroscopy of ^{19}Ne (E_X>S_p)

Low energy γ–ray astronomy of novæ

- **Short-lived** (~day) ^{18}F → ejecta stage

Uncertainties in $^{18}F(p,\alpha)^{15}O$

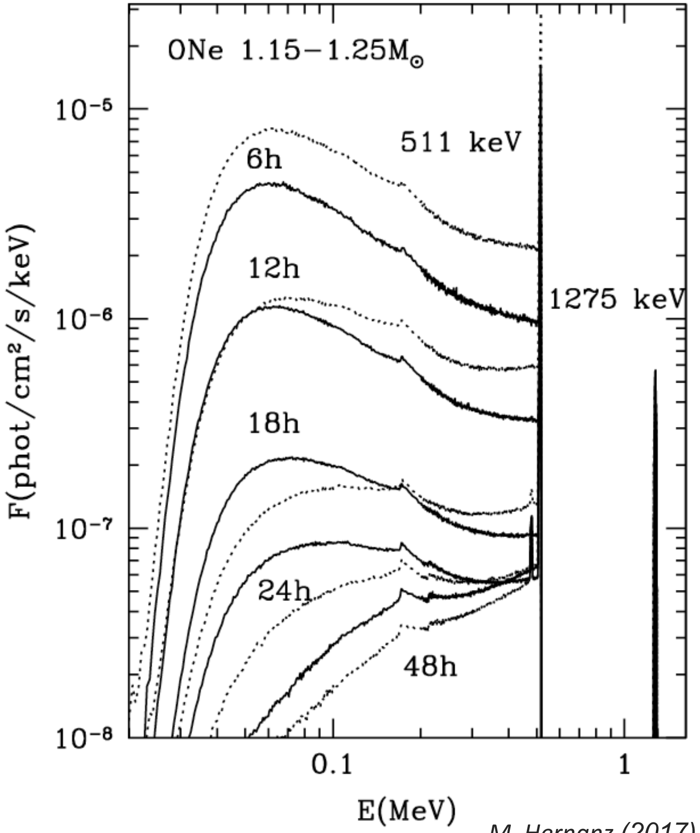

M. Hernanz (2017)

Low energy γ–ray astronomy of novæ

- **Short-lived** (~day) ^{18}F → ejecta stage
- **Medium-lived** (~year) ^{22}Na → novae properties

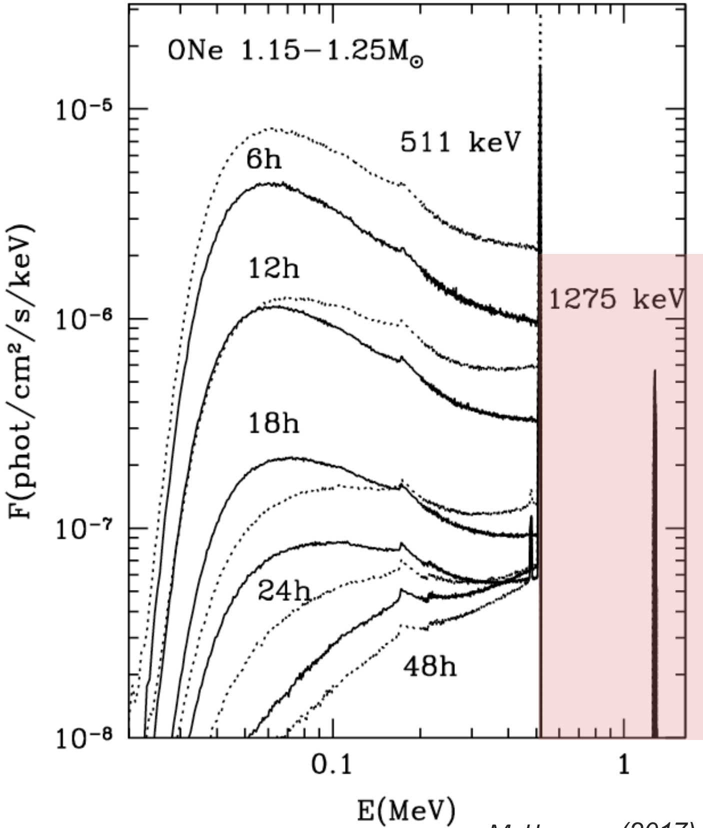

M. Hernanz (2017)

Uncertainties in $^{18}F(p,\alpha)^{15}O$

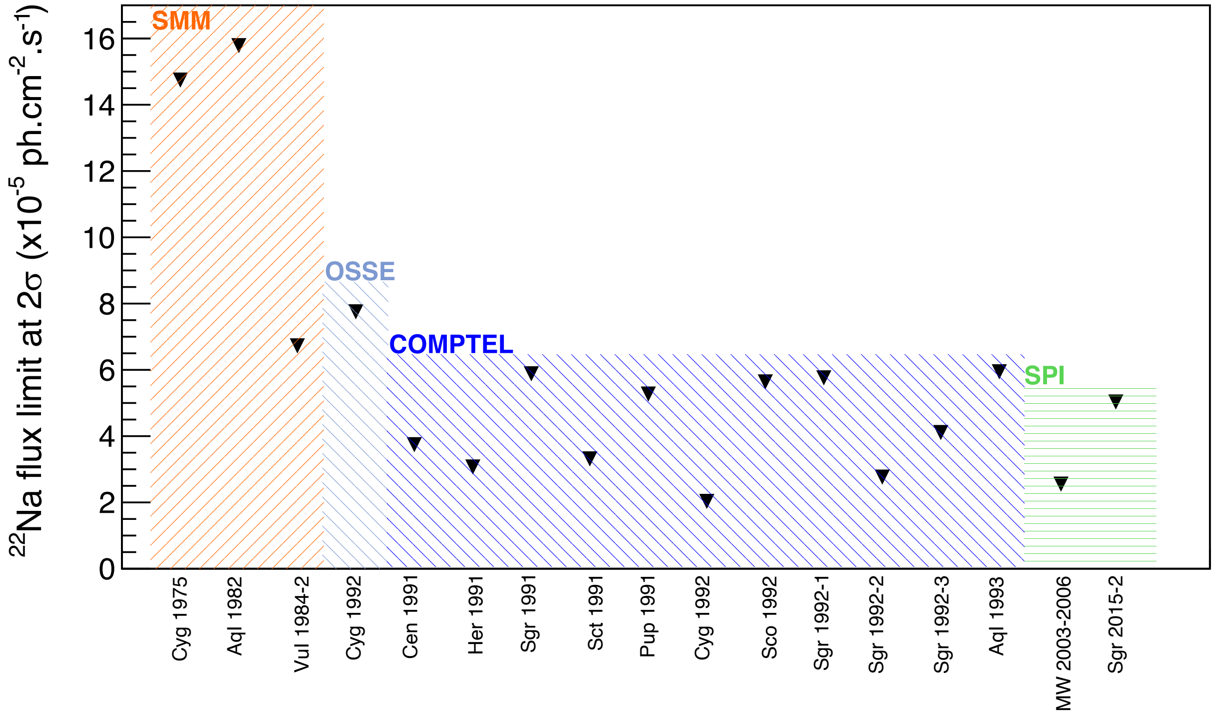

Low energy γ–ray astronomy of novæ

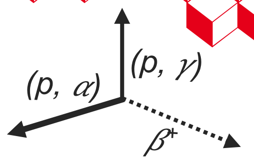

- **Short-lived** (~day) ^{18}F → ejecta stage
- **Medium-lived** (~year) ^{22}Na → novae properties

Uncertainties in ^{18}F(p,α)^{15}O

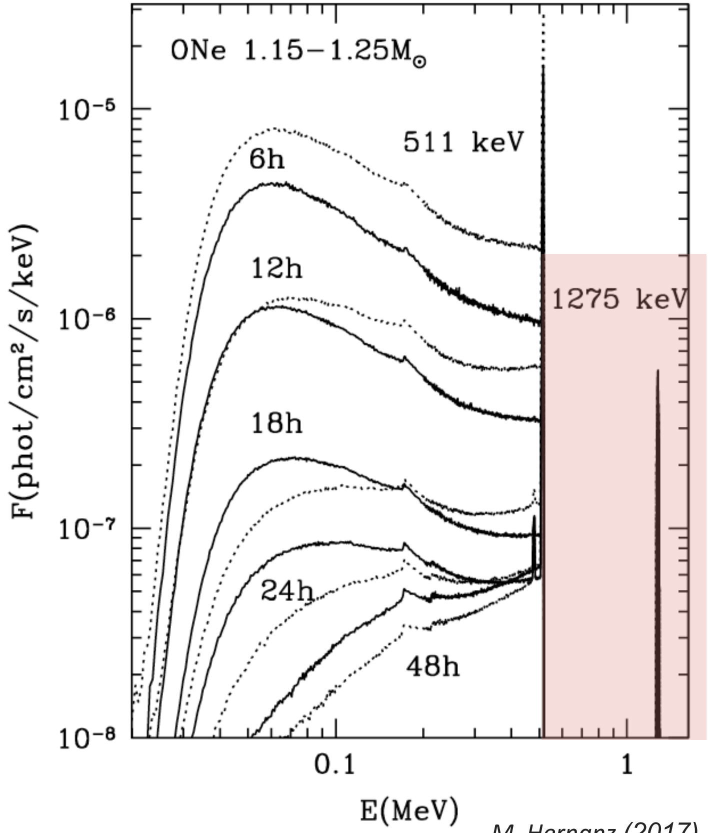

M. Hernanz (2017)

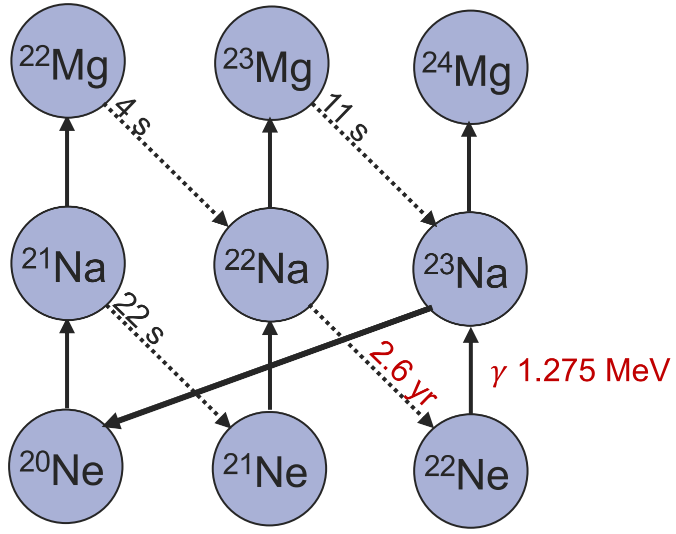

Low energy γ–ray astronomy of novæ

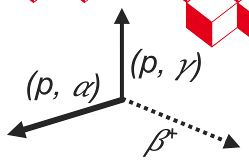

- **Short-lived** (~day) ^{18}F → ejecta stage
- **Medium-lived** (~year) ^{22}Na → novae properties

Uncertainties in $^{18}F(p,\alpha)^{15}O$
Uncertainties in $^{22}Na(p,\gamma)^{23}Mg$

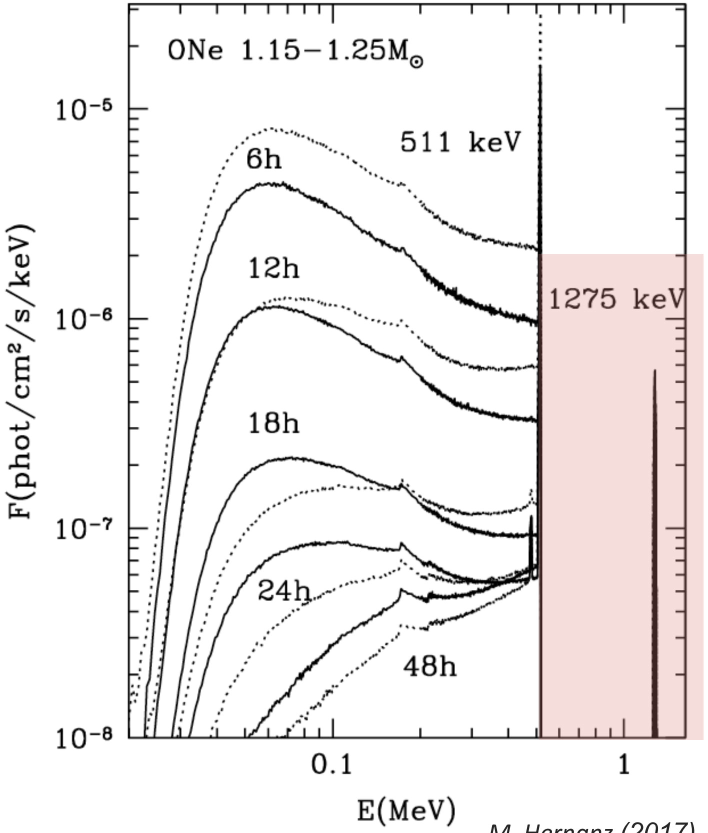

M. Hernanz (2017)

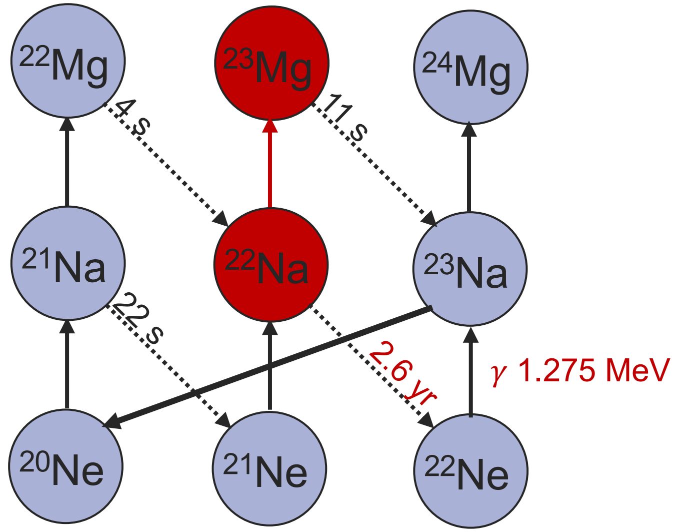

Low energy γ–ray astronomy of novæ

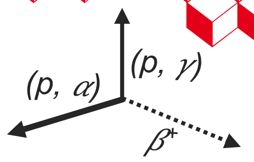

- **Short-lived** (~day) ^{18}F → ejecta stage
- **Medium-lived** (~year) ^{22}Na → novae properties

Uncertainties in $^{18}F(p,\alpha)^{15}O$
Uncertainties in $^{22}Na(p,\gamma)^{23}Mg$

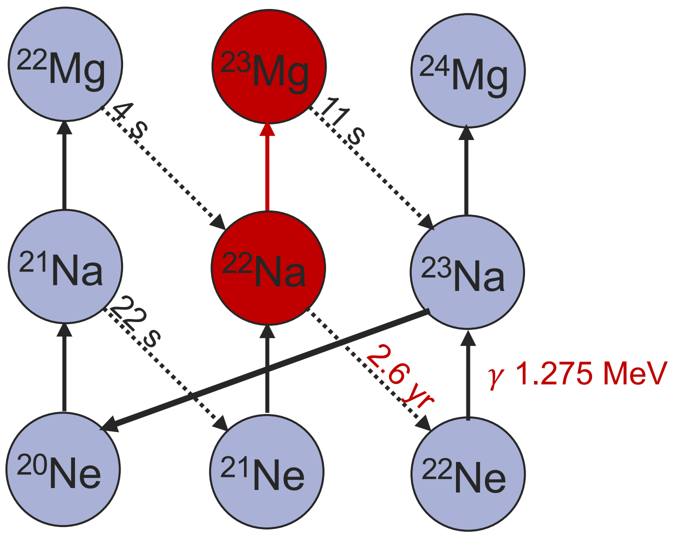

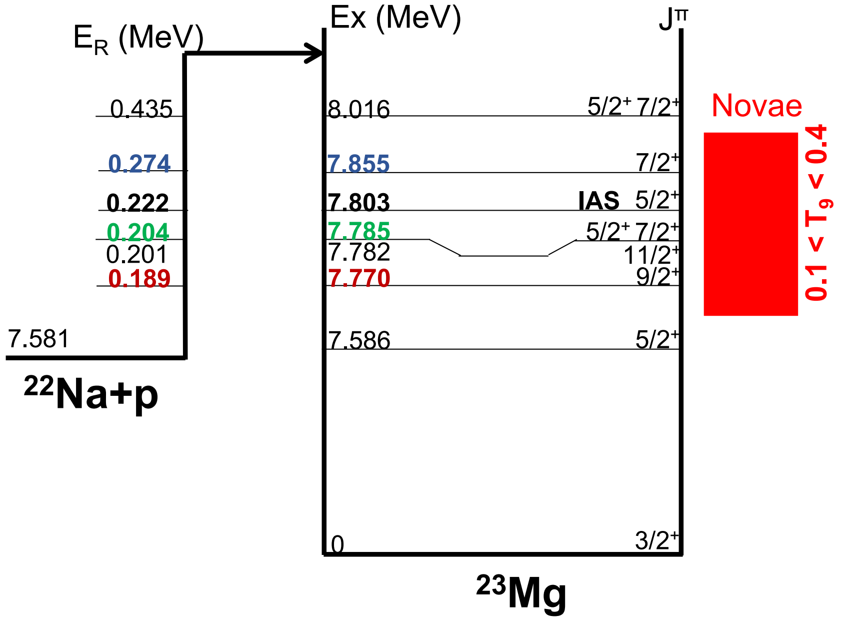

Low energy γ–ray astronomy of novæ

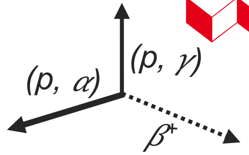

- **Short-lived** (~day) ^{18}F → ejecta stage
- **Medium-lived** (~year) ^{22}Na → novae properties

Uncertainties in $^{18}F(p,\alpha)^{15}O$

Uncertainties in $^{22}Na(p,\gamma)^{23}Mg$

Direct measurements of ωγ *Sallaska, Phys. Rev. L* ***105*** *(2010)*

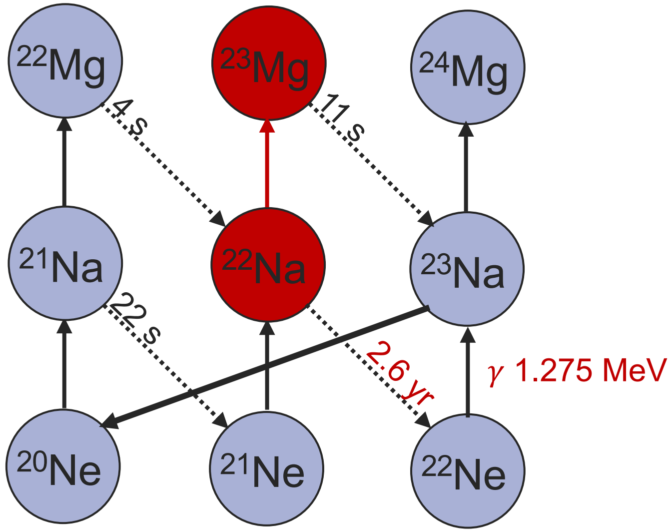

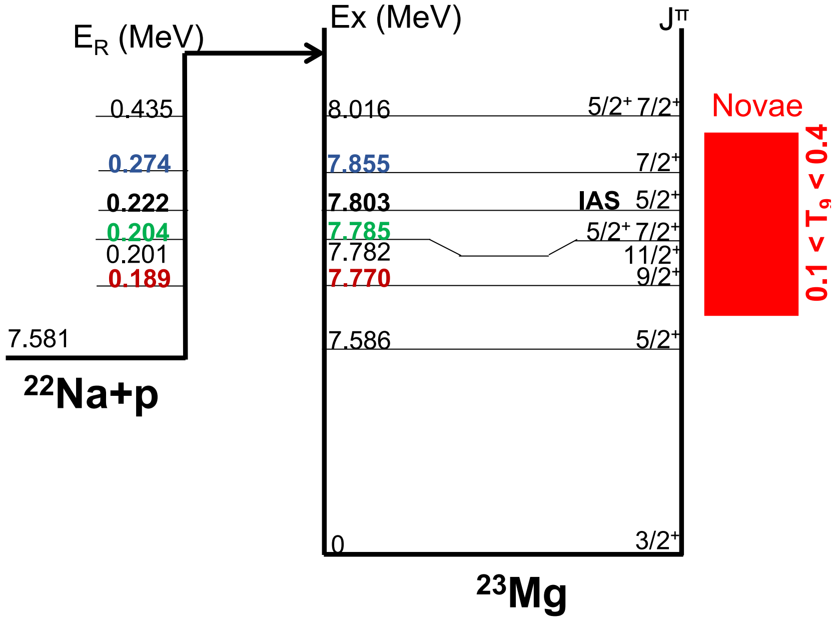

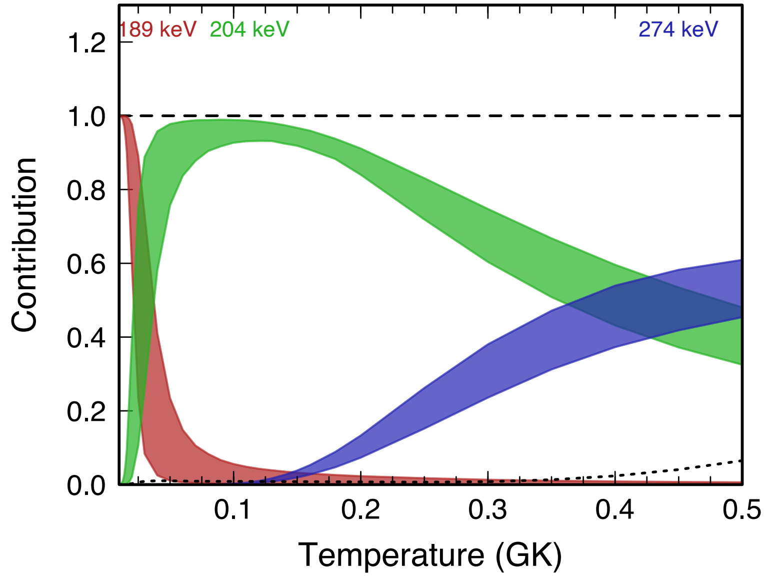

Dominant resonance in $^{23}Mg^*$
(E_x = 7.785 MeV, E_R = 0.204 MeV)

Low energy γ–ray astronomy of novæ

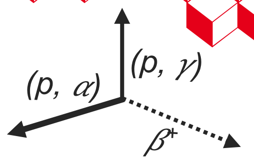

- **Short-lived** (~day) ^{18}F → ejecta stage
- **Medium-lived** (~year) ^{22}Na → novae properties

Uncertainties in $^{18}F(p,\alpha)^{15}O$
Uncertainties in $^{22}Na(p,\gamma)^{23}Mg$

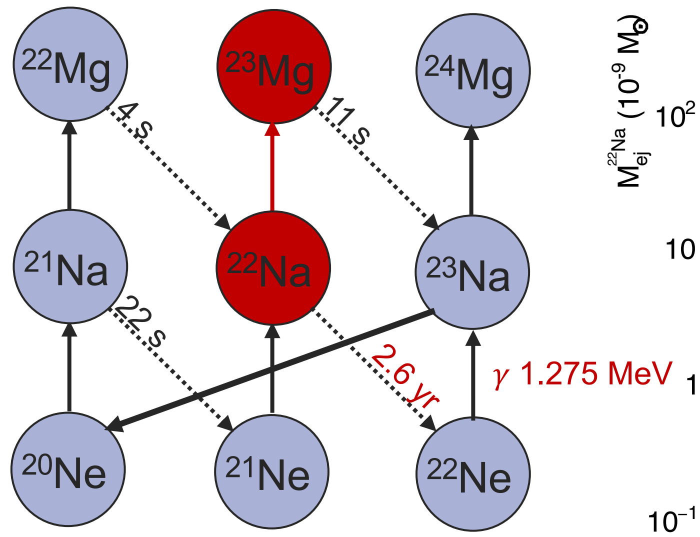

Dominant resonance (E_r = 0.204 MeV)

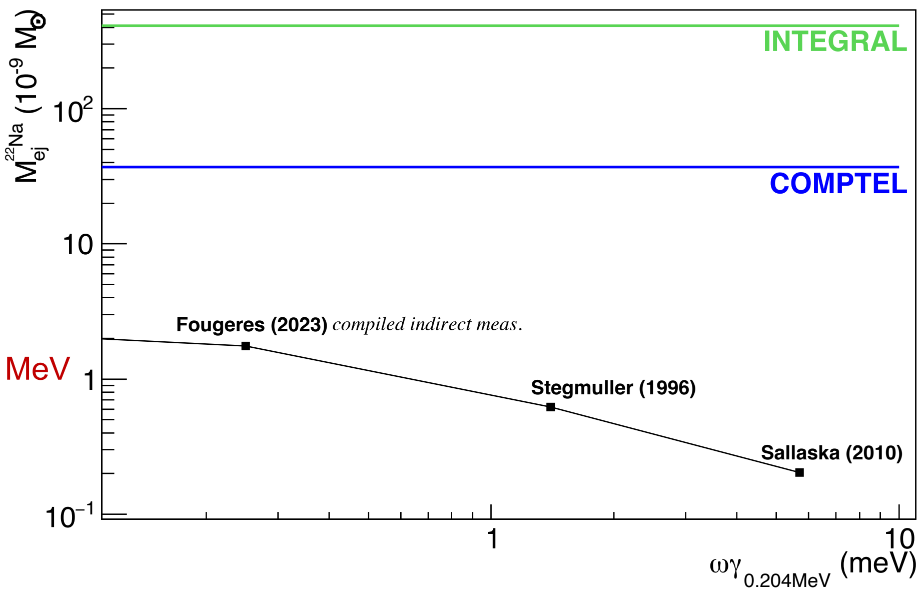

Ejected ^{22}Na mass uncertainties **x10**

Direct measurements of ***ωγ*** *Sallaska, Phys. Rev. L* ***105*** *(2010)*

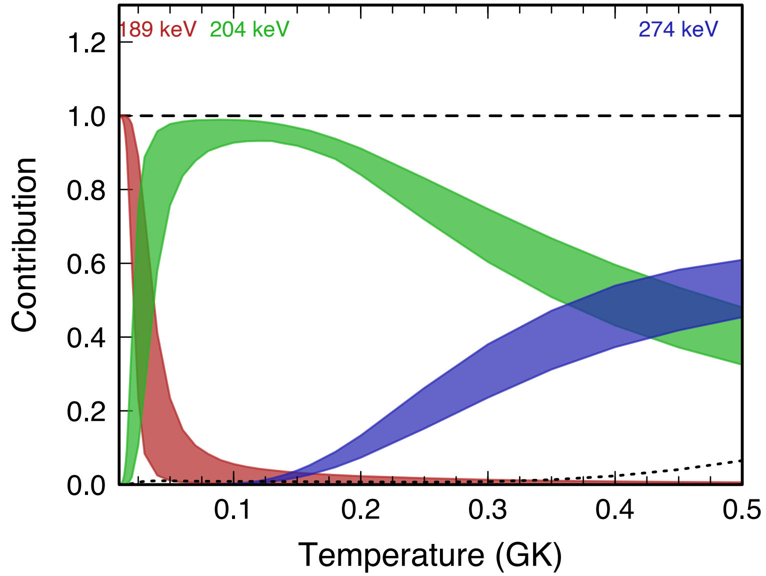

Dominant resonance in $^{23}Mg^*$
(E_x = 7.785 MeV, E_R = 0.204 MeV)

Low energy γ–ray astronomy of novæ

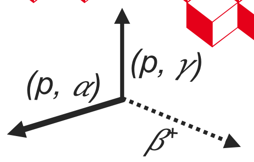

- **Short-lived** (~day) ^{18}F → ejecta stage — Uncertainties in ^{18}F(p,α)^{15}O
- **Medium-lived** (~year) ^{22}Na → novae properties — Uncertainties in ^{22}Na(p,γ)^{23}Mg

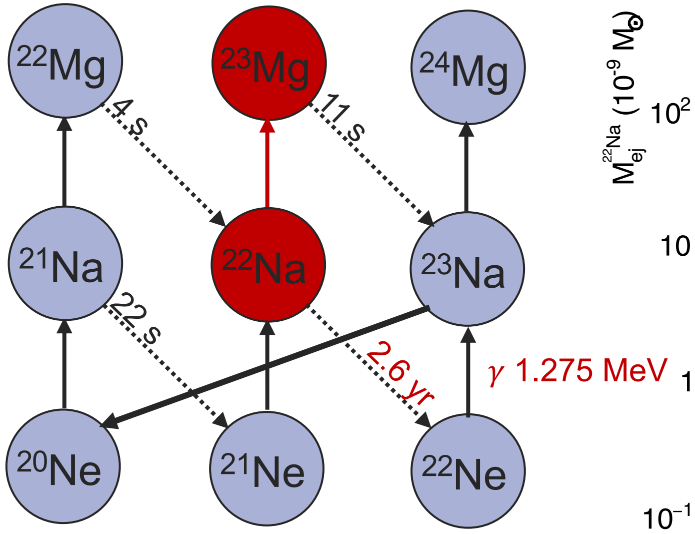

Dominant resonance (E_r = 0.204 MeV)

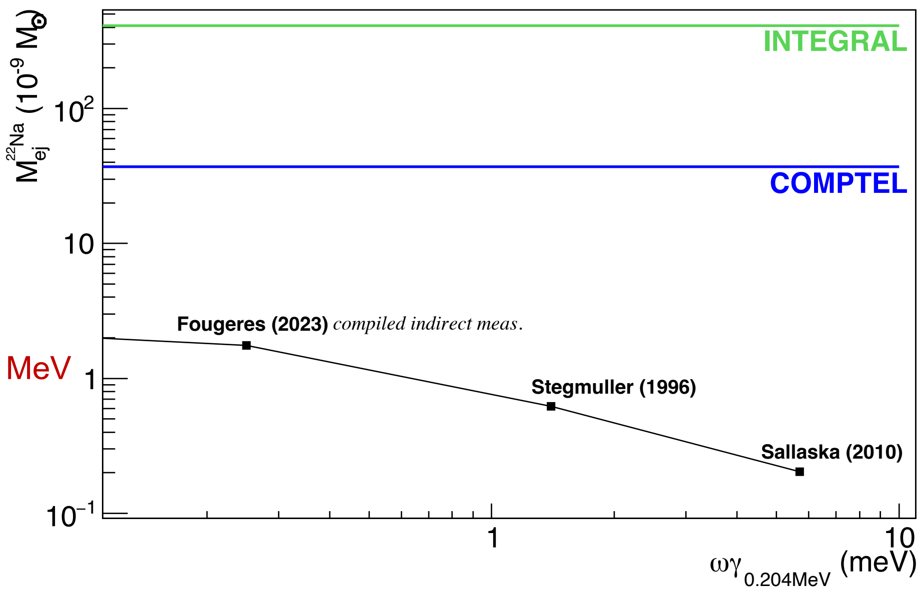

Ejected ^{22}Na mass uncertainties **x10**

Direct measurements of ωγ *Sallaska, Phys. Rev. L **105** (2010)*

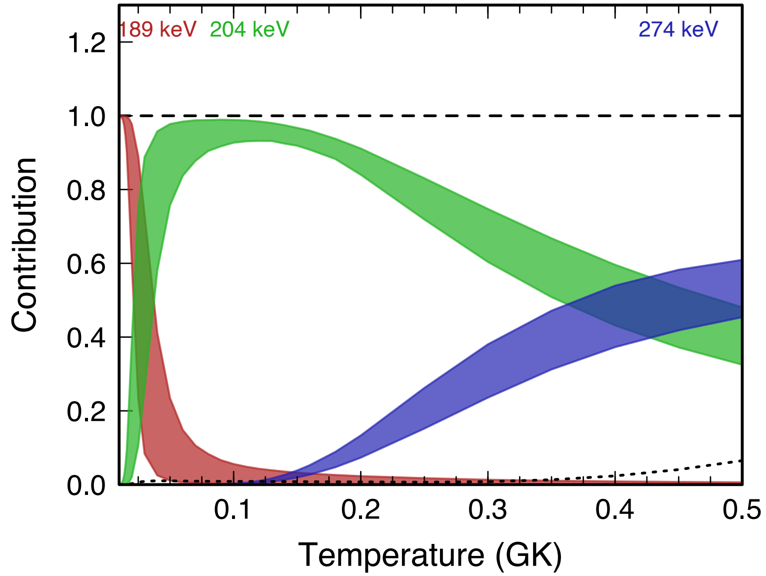

Dominant resonance in ^{23}Mg*
(E_x = 7.785 MeV, E_R = 0.204 MeV)

Resonance strength determination in ^{22}Na+p

Low energy γ–ray astronomy of novæ

- **Short-lived** (~day) ^{18}F → ejecta stage — Uncertainties in $^{18}F(p,\alpha)^{15}O$
- **Medium-lived** (~year) ^{22}Na → novae properties — Uncertainties in $^{22}Na(p,\gamma)^{23}Mg$
- **Long-lived** (>Myr) ^{26}Al → ongoing galactic nucleosynthesis and novae contribution

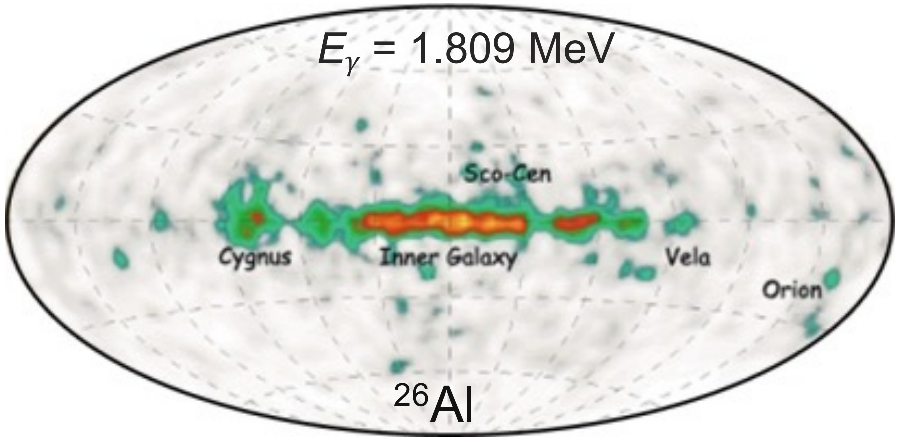

Plüschke et al. (2001)

Low energy γ–ray astronomy of novæ

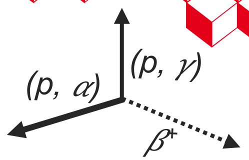

- **Short-lived** (~day) ^{18}F → ejecta stage — Uncertainties in ^{18}F(p,α)^{15}O
- **Medium-lived** (~year) ^{22}Na → novae properties — Uncertainties in ^{22}Na(p,γ)^{23}Mg
- **Long-lived** (>Myr) ^{26}Al → ongoing galactic nucleosynthesis and novae contribution

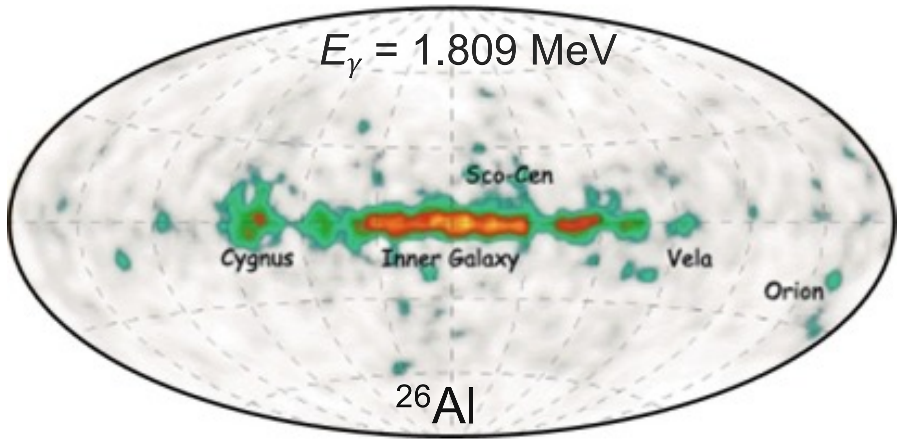

Plüschke et al. (2001)

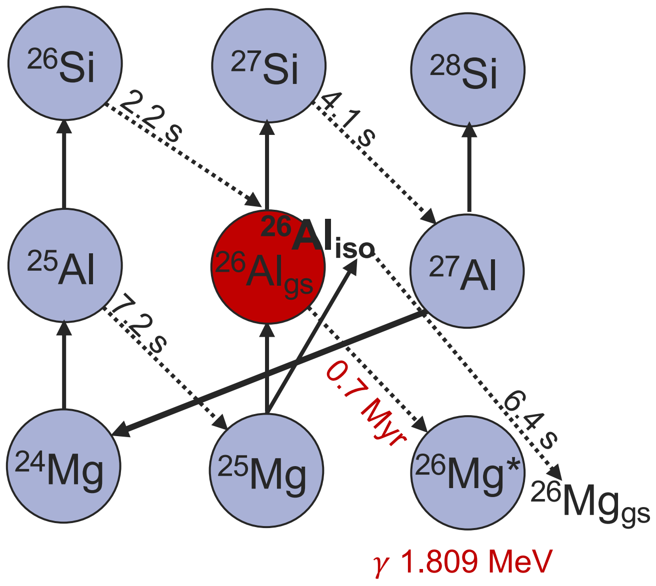

Low energy γ–ray astronomy of novæ

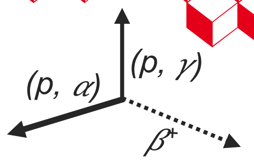

- **Short-lived** (~day) ^{18}F → ejecta stage — Uncertainties in ^{18}F(p,α)^{15}O
- **Medium-lived** (~year) ^{22}Na → novae properties — Uncertainties in ^{22}Na(p,γ)^{23}Mg
- **Long-lived** (>Myr) ^{26}Al → ongoing galactic nucleosynthesis and novae contribution — Uncertainties in ^{25}Al(p,γ)^{26}Si

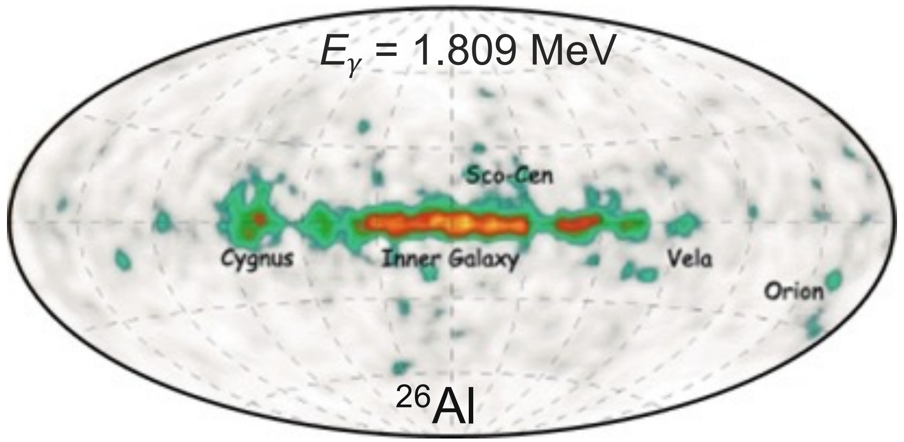

Plüschke *et al.* (2001)

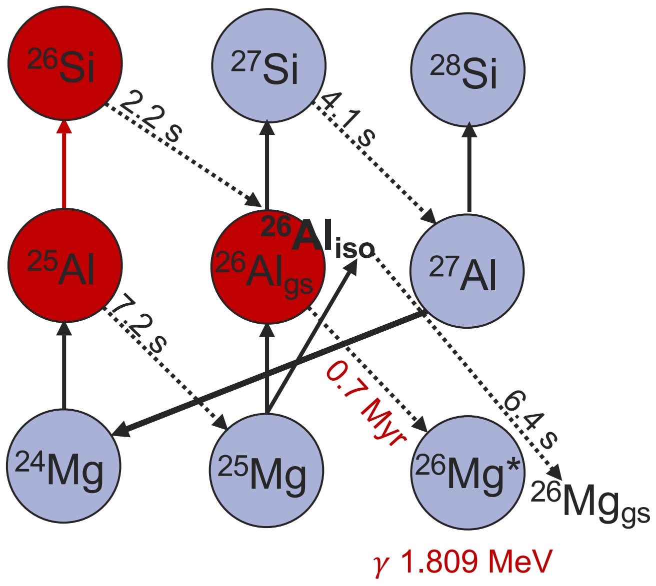

Novae contribution to ^{26}Al galactic production
10 – 30 %

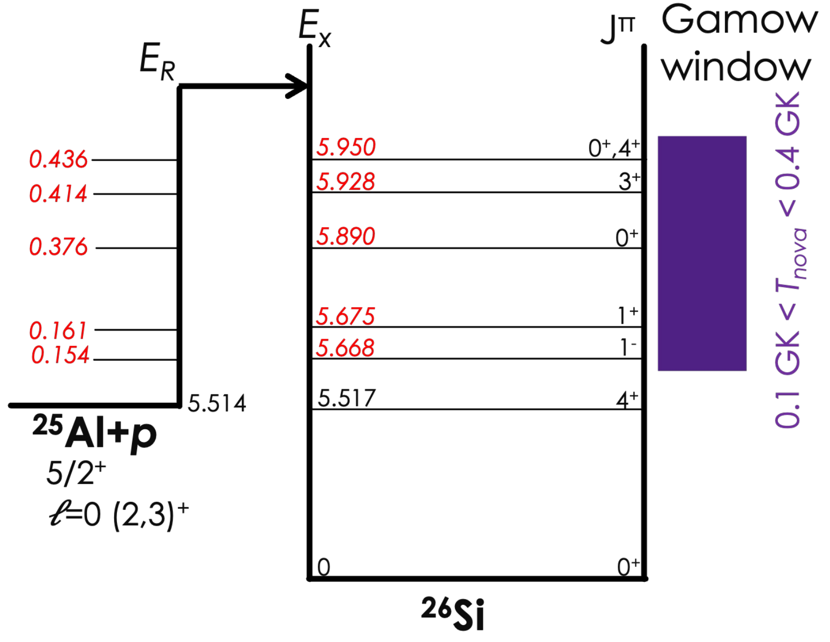

Low energy γ–ray astronomy of novæ

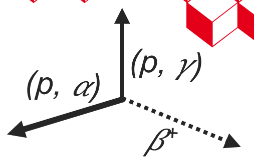

- **Short-lived** (~day) ^{18}F → ejecta stage — Uncertainties in $^{18}F(p,\alpha)^{15}O$
- **Medium-lived** (~year) ^{22}Na → novae properties — Uncertainties in $^{22}Na(p,\gamma)^{23}Mg$
- **Long-lived** (>Myr) ^{26}Al → ongoing galactic nucleosynthesis and novae contribution — Uncertainties in $^{25}Al(p,\gamma)^{26}Si$

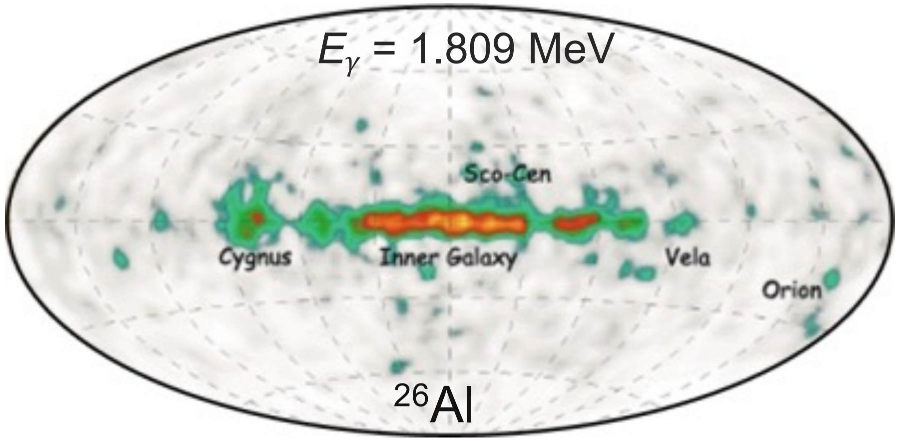

Plüschke *et al.* (2001)

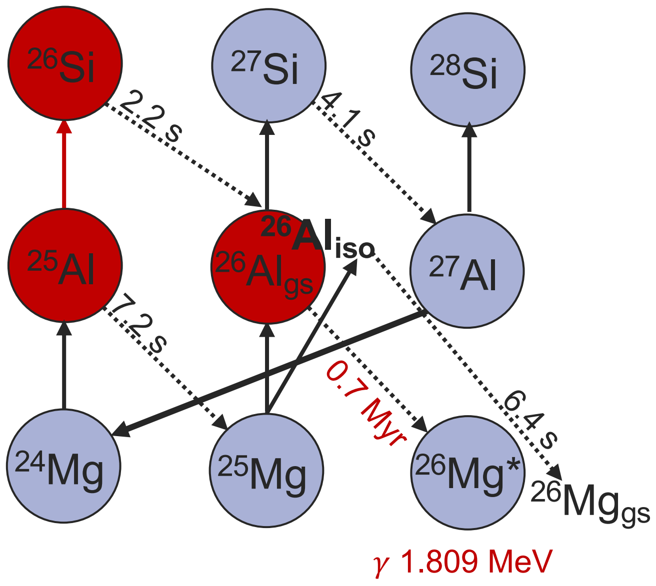

Novae contribution to ^{26}Al galactic production
10 – 30 %

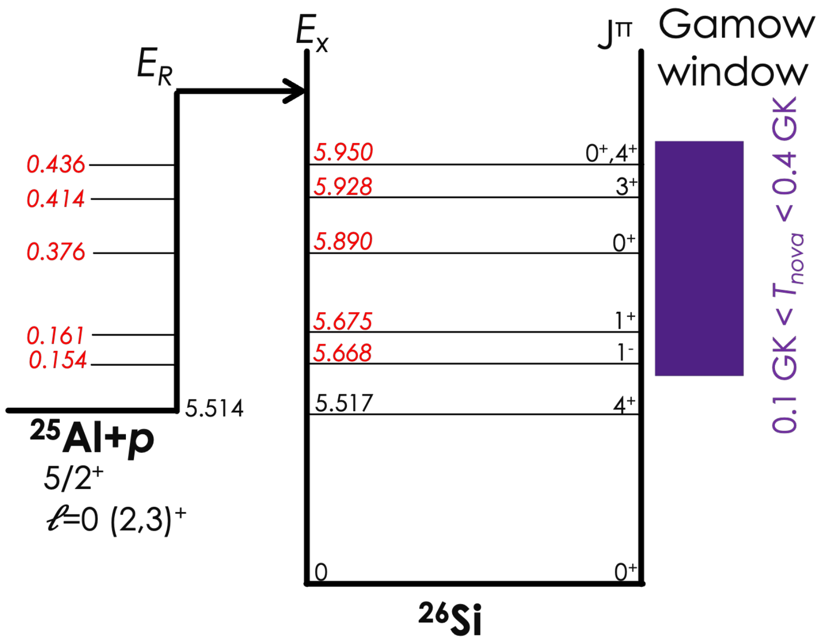

Resonance strength measurement in $^{25}Al+p$

2. Experimental methods

p-capture resonances

Identification of resonant states

$$< \sigma\nu >_{tot} \propto \sum_r \omega\gamma_r \exp\left(-\frac{\boxed{E_r}}{k_B T}\right)$$

Identification of resonant states

$$< \sigma\nu >_{tot} \propto \sum_r \omega\gamma_r \exp\left(-\frac{\boxed{E_r}}{k_B T}\right)$$

PhD *L. Dienis* → see her poster, E863 scheduled 2025

Aim high-resolution spectroscopy in ^{19}Ne at S_p=6.4 MeV

Identification of resonant states

$$< \sigma\nu >_{tot} \propto \sum_r \omega\gamma_r \exp\left(-\frac{E_r}{k_B T}\right)$$

PhD *L. Dienis* → see her poster, E863 scheduled 2025
Aim high-resolution spectroscopy in ^{19}Ne at S_p=6.4 MeV

Accessing (E_r, J, Γ_α) via resonant elastic scattering

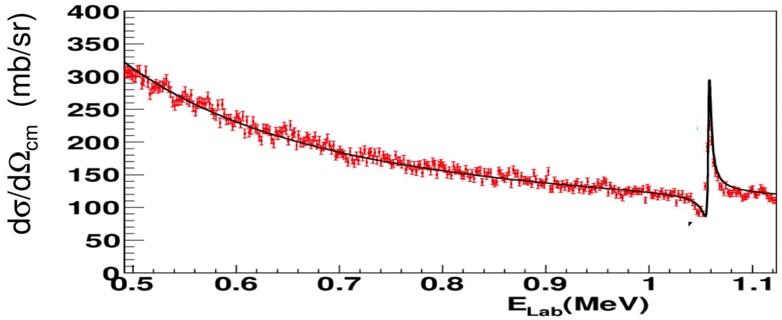

$^{18}F(p,\alpha)^{15}O$

Identification of resonant states

$$< \sigma\nu >_{tot} \propto \sum_r \omega\gamma_r \exp\left(-\frac{E_r}{k_B T}\right)$$

PhD *L. Dienis* → see her poster, E863 scheduled 2025

Aim high-resolution spectroscopy in ^{19}Ne at S_p=6.4 MeV

Accessing (E_r, J, Γ_α) via **resonant elastic scattering**

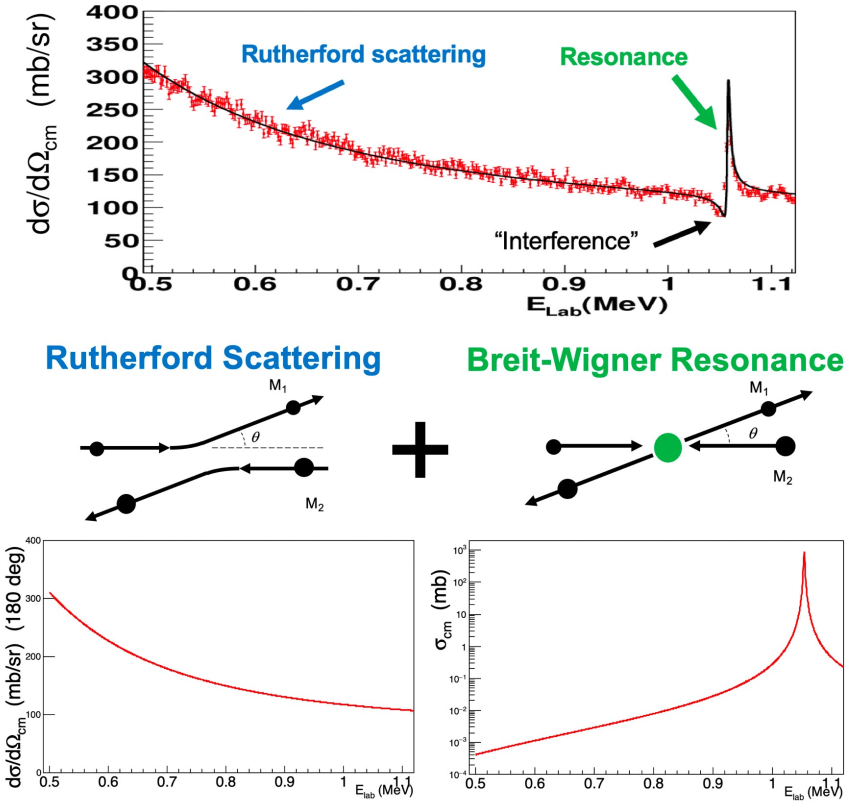

De Oliveira Santos, Prog. in Part. and Nuc. Phys., In press. hal-04673993 (2024)

Identification of resonant states

$$< \sigma\nu >_{tot} \propto \sum_r \omega\gamma_r \exp\left(-\frac{E_r}{k_B T}\right)$$

PhD *L. Dienis* → see her poster, E863 scheduled 2025
Aim high-resolution spectroscopy in ^{19}Ne at S_p=6.4 MeV

Accessing (E_r, J, Γ_α) via **resonant elastic scattering** via $\alpha(^{15}O,^{15}O)\alpha_{0deg}$ at 2 MeV/u

Identification of resonant states

$$<\sigma\nu>_{tot} \propto \sum_r \omega\gamma_r \exp\left(-\frac{E_r}{k_B T}\right)$$

PhD *L. Dienis* → see her poster, E863 scheduled 2025
Aim high-resolution spectroscopy in ^{19}Ne at S_p=6.4 MeV

Accessing (E_r, J, Γ_α) via **resonant elastic scattering** via $\alpha(^{15}O,^{15}O)\alpha_{0deg}$ at 2 MeV/u

^{15}O GANIL/SPIRAL1
10^6 pps, 2 MeV/u (spread 0.1%)
97% purity *Stefan (2014)*

Identification of resonant states

$$< \sigma\nu >_{tot} \propto \sum_r \omega\gamma_r \exp\left(-\frac{E_r}{k_B T}\right)$$

PhD *L. Dienis* → see her poster, E863 scheduled 2025
Aim high-resolution spectroscopy in ^{19}Ne at S_p=6.4 MeV

Accessing (E_r, J, Γ_α) via **resonant elastic scattering** via $\alpha(^{15}O,^{15}O)\alpha_{0deg}$ at 2 MeV/u

^{15}O GANIL/SPIRAL1
10^6 pps, 2 MeV/u (spread 0.1%)
97% purity *Stefan (2014)*

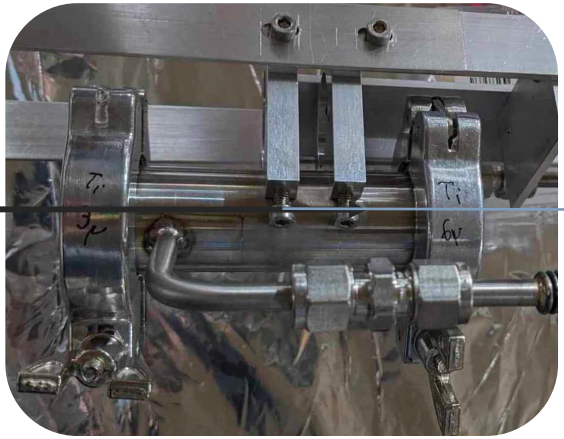

α

Gaseous target (α)
10^{20} at./cm^2
beam stopped in exit window

Identification of resonant states

$$< \sigma\nu >_{tot} \propto \sum_r \omega\gamma_r \exp\left(-\frac{\boxed{E_r}}{k_B T}\right)$$

PhD *L. Dienis* → see her poster, E863 scheduled 2025
Aim high-resolution spectroscopy in ^{19}Ne at S_p=6.4 MeV

Accessing (E_r, J, Γ_α) via **resonant elastic scattering** via $\alpha(^{15}O,^{15}O)\alpha_{0deg}$ at 2 MeV/u

^{15}O GANIL/SPIRAL1
10^6 pps, 2 MeV/u (spread 0.1%)
97% purity *Stefan (2014)*

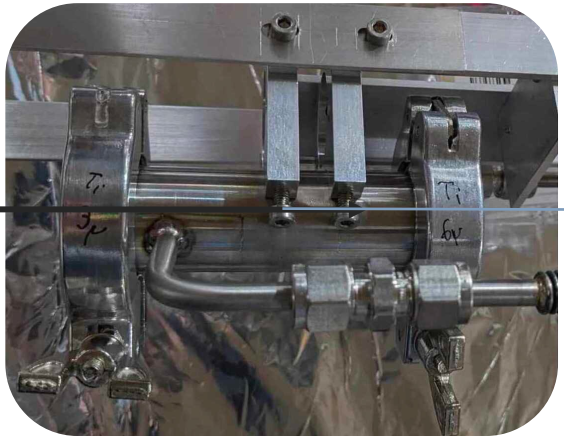

Gaseous target (α)
10^{20} at./cm^2
beam stopped in exit window

α

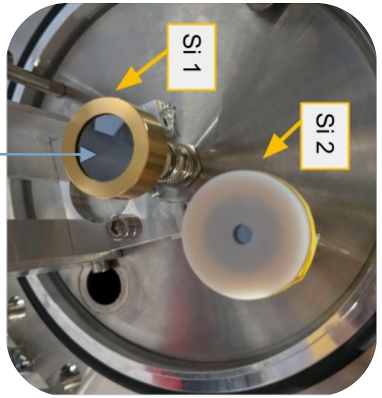

Si1 0deg detector
FWHM = 17 keV, **ΔΩ = 1.2 msr** (c.o.m.)
Si2 high-angle detector

Identification of resonant states

PhD *L. Dienis* → see her poster, E863 scheduled 2025
Aim high-resolution spectroscopy in ^{19}Ne at S_p=6.4 MeV

Accessing (E_r, J, Γ_α) via **resonant elastic scattering** via $\alpha(^{15}O,^{15}O)\alpha_{0deg}$ at 2 MeV/u

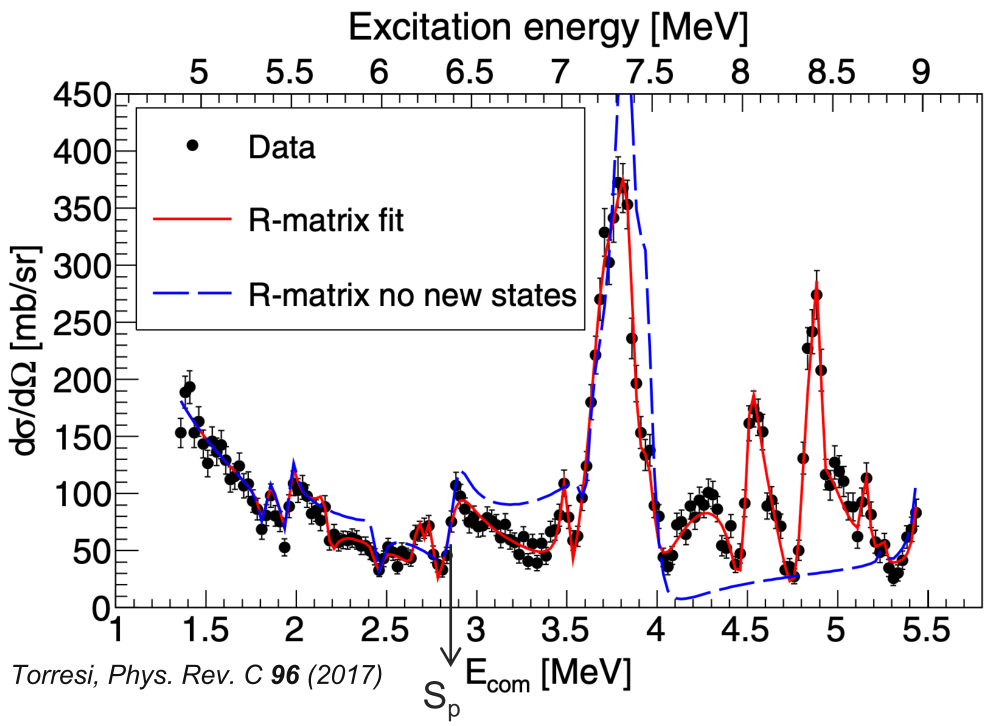

*Torresi, Phys. Rev. C **96** (2017)*

$^{18}F(p,\alpha)^{15}O$

Identification of resonant states

PhD *L. Dienis* → see her poster, E863 scheduled 2025
Aim high-resolution spectroscopy in ^{19}Ne at S_p=6.4 MeV

Accessing (E_r, J, Γ_α) via **resonant elastic scattering** via $\alpha(^{15}O,^{15}O)\alpha_{0deg}$ at 2 MeV/u

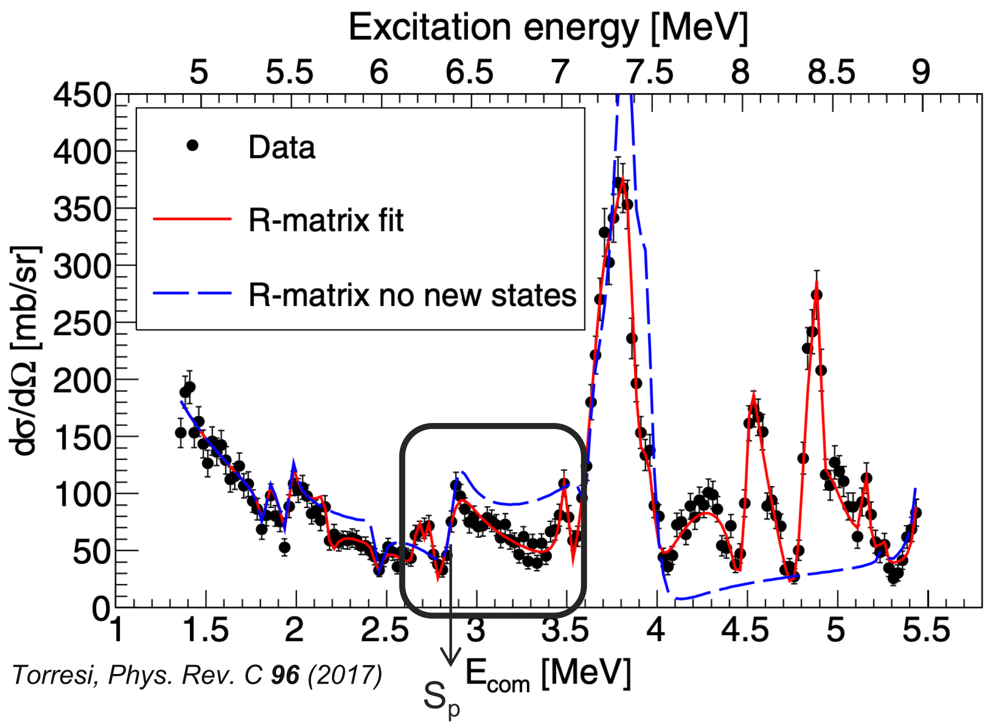

Torresi, Phys. Rev. C ***96*** *(2017)*

$^{18}F(p,\alpha)^{15}O$

Identification of resonant states

PhD *L. Dienis* → see her poster, E863 scheduled 2025
Aim high-resolution spectroscopy in ^{19}Ne at S_p=6.4 MeV

Accessing (E_r, J, Γ_α) via **resonant elastic scattering** via $\alpha(^{15}O,^{15}O)\alpha_{0deg}$ at 2 MeV/u

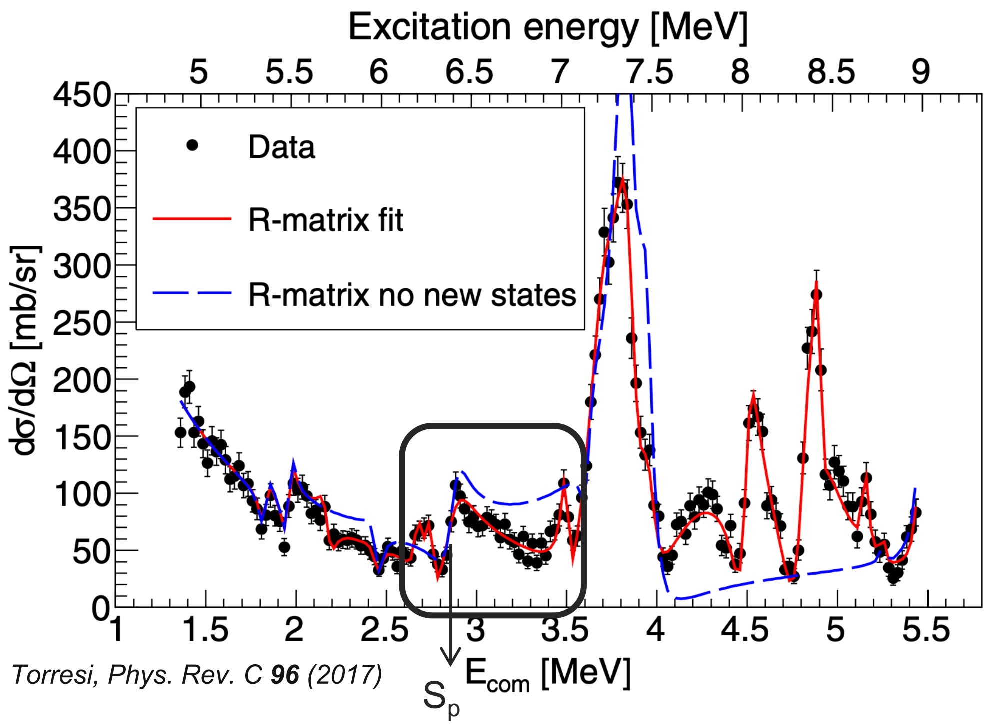

Torresi, Phys. Rev. C **96** (2017)

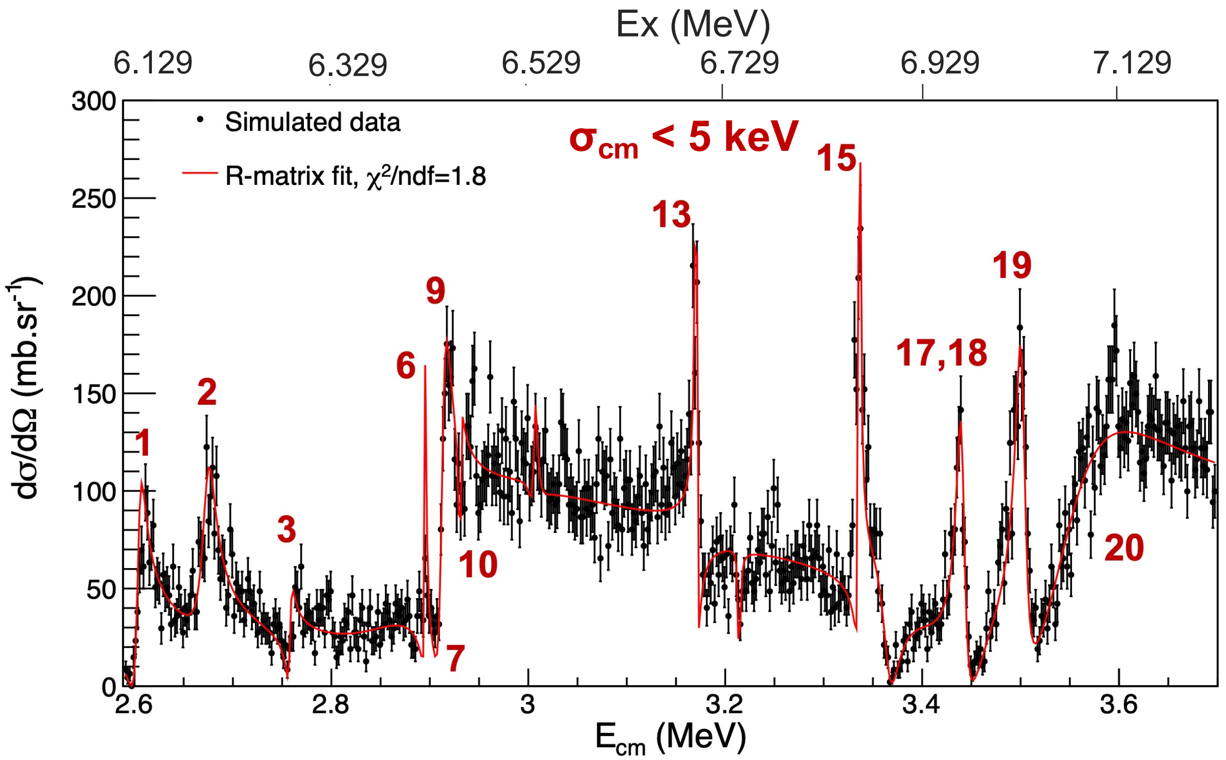

Accessing $\omega\gamma$ via angle-integrated measurement

$$< \sigma\nu >_{tot} \propto \sum_r \boxed{\omega\gamma_r} \exp\left(-\frac{E_r}{k_B T}\right)$$

Accessing $\omega\gamma$ via angle-integrated measurement

$$< \sigma\nu >_{tot} \propto \sum_r \boxed{\omega\gamma_r} \exp\left(-\frac{E_r}{k_B T}\right)$$

$$\omega\gamma = \frac{(2J+1)}{(2j+1)(2J_{^{25}Al}+1)} \frac{\Gamma_p \Gamma_\gamma}{\Gamma_{tot}}$$

Accessing $\omega\gamma$ via angle-integrated measurement

$$< \sigma\nu >_{tot} \propto \sum_r \boxed{\omega\gamma_r} \exp\left(-\frac{E_r}{k_B T}\right)$$

$$\omega\gamma = \frac{(2J+1)}{(2j+1)(2J_{^{25}Al}+1)} \frac{\Gamma_p \Gamma_\gamma}{\Gamma_{tot}}$$

Extension of recent method to measure C^2S_p (NSCL) via $d(^{26}Al,n\gamma)^{27}Si$ *Kankainen, EPJ **52** (2016)*

Accessing $\omega\gamma$ via angle-integrated measurement

$$< \sigma\nu >_{tot} \propto \sum_r \boxed{\omega\gamma_r} \exp\left(-\frac{E_r}{k_B T}\right)$$

$$\omega\gamma = \frac{(2J+1)}{(2j+1)(2J_{^{25}Al}+1)} \frac{\Gamma_p \Gamma_\gamma}{\Gamma_{tot}}$$

Extension of recent method to measure C^2S_p (NSCL) via $d(^{26}Al,n\gamma)^{27}Si$ *Kankainen, EPJ **52** (2016)*

Direct transfer $d(^{25}Al,n\gamma)^{26}Si$

Tagging of $^{26}Si^*$ on γ-ray transitions

Accessing $\omega\gamma$ via angle-integrated measurement

$$< \sigma\nu >_{tot} \propto \sum_r \boxed{\omega\gamma_r} \exp\left(-\frac{E_r}{k_B T}\right)$$

$$\omega\gamma = \frac{(2J+1)}{(2j+1)(2J_{^{25}Al}+1)} \frac{\Gamma_p \Gamma_\gamma}{\Gamma_{tot}}$$

Extension of recent method to measure C^2S_p (NSCL) via $d(^{26}Al,n\gamma)^{27}Si$ *Kankainen, EPJ* ***52*** *(2016)*

Direct transfer $d(^{25}Al,n\gamma)^{26}Si$

Tagging of $^{26}Si^*$ on γ-ray transitions → angle-integrated measurement of cross-section $\sigma_{transfer}$

$$N_\gamma = BR_\gamma \times \sigma^{exp}_{transfer} \times \epsilon^{tot}_{det.} N_{target} I_{beam} T_{UT}$$

Accessing $\omega\gamma$ via angle-integrated measurement

$$< \sigma\nu >_{tot} \propto \sum_r \boxed{\omega\gamma_r} \exp\left(-\frac{E_r}{k_B T}\right)$$

$$\omega\gamma = \frac{(2J+1)}{(2j+1)(2J_{^{25}Al}+1)} \frac{\Gamma_p \Gamma_\gamma}{\Gamma_{tot}}$$

Extension of recent method to measure C^2S_p (NSCL) via $d(^{26}Al,n\gamma)^{27}Si$ *Kankainen, EPJ* ***52*** *(2016)*

Direct transfer $d(^{25}Al,n\gamma)^{26}Si$

Tagging of $^{26}Si^*$ on γ-ray transitions → angle-integrated measurement of cross-section $\sigma_{transfer}$

$$N_\gamma = \boxed{BR_\gamma} \times \sigma^{exp}_{transfer} \times \epsilon^{tot}_{det.} N_{target} I_{beam} T_{UT}$$

$$BR_\gamma \rightarrow \frac{\Gamma_\gamma}{\Gamma_{tot}}$$

Accessing $\omega\gamma$ via angle-integrated measurement

$$< \sigma\nu >_{tot} \propto \sum_r \boxed{\omega\gamma_r} \exp\left(-\frac{E_r}{k_B T}\right)$$

$$\omega\gamma = \frac{(2J+1)}{(2j+1)(2J_{^{25}Al}+1)} \frac{\Gamma_p \Gamma_\gamma}{\Gamma_{tot}}$$

Extension of recent method to measure C^2S_p (NSCL) via $d(^{26}Al,n\gamma)^{27}Si$ *Kankainen, EPJ **52** (2016)*

Direct transfer $d(^{25}Al,n\gamma)^{26}Si$

Tagging of $^{26}Si^*$ on γ-ray transitions → angle-integrated measurement of cross-section $\sigma_{transfer}$

$$N_\gamma = \boxed{BR_\gamma} \times \boxed{\sigma^{exp}_{transfer}} \times \epsilon^{tot}_{det.} N_{target} I_{beam} T_{UT}$$

$$BR_\gamma \rightarrow \frac{\Gamma_\gamma}{\Gamma_{tot}} \qquad \sigma^{exp}_{transfer} \rightarrow C^2 S_p \times \sigma^{DWBA}_{transfer}$$

Accessing $\omega\gamma$ via angle-integrated measurement

$$< \sigma\nu >_{tot} \propto \sum_r \boxed{\omega\gamma_r} \exp\left(-\frac{E_r}{k_B T}\right)$$

$$\omega\gamma = \frac{(2J+1)}{(2j+1)(2J_{^{25}Al}+1)} \frac{\Gamma_p \Gamma_\gamma}{\Gamma_{tot}}$$

Extension of recent method to measure $\boldsymbol{C^2S_p}$ (NSCL) via d(^{26}Al,$n\gamma$)^{27}Si *Kankainen, EPJ* ***52*** *(2016)*

Direct transfer d(^{25}Al,$n\gamma$)^{26}Si

Tagging of ^{26}Si* on γ-ray transitions → angle-integrated measurement of cross-section σ_{transfer}

$$N_\gamma = \boxed{BR_\gamma} \times \boxed{\sigma^{exp}_{transfer}} \times \epsilon^{tot}_{det.} N_{target} I_{beam} T_{UT}$$

BR_γ → $\frac{\Gamma_\gamma}{\Gamma_{tot}}$

$\sigma^{exp}_{transfer}$ → $C^2 S_p \times \boxed{\sigma^{DWBA}_{transfer}}$ → FRESCO code

Accessing $\omega\gamma$ via angle-integrated measurement

$$< \sigma\nu >_{tot} \propto \sum_r \boxed{\omega\gamma_r} \exp\left(-\frac{E_r}{k_B T}\right)$$

$$\omega\gamma = \frac{(2J+1)}{(2j+1)(2J_{^{25}Al}+1)} \frac{\Gamma_p \Gamma_\gamma}{\Gamma_{tot}}$$

Extension of recent method to measure C^2S_p (NSCL) via $d(^{26}\text{Al},n\gamma)^{27}\text{Si}$ *Kankainen, EPJ* ***52*** *(2016)*

Direct transfer $d(^{25}\text{Al},n\gamma)^{26}\text{Si}$

Tagging of ^{26}Si* on γ-ray transitions → angle-integrated measurement of cross-section σ_{transfer}

$$N_\gamma = \boxed{BR_\gamma} \times \boxed{\sigma^{exp}_{transfer}} \times \epsilon^{tot}_{det.} N_{target} I_{beam} T_{UT}$$

$$BR_\gamma \rightarrow \frac{\Gamma_\gamma}{\Gamma_{tot}}$$

$$\sigma^{exp}_{transfer} \rightarrow \boxed{C^2S_p} \times \boxed{\sigma^{DWBA}_{transfer}}$$

$\sigma^{DWBA}_{transfer}$ → FRESCO code

$$C^2S_p \rightarrow \frac{\Gamma_p}{\Gamma_p^{s.p.}}$$

Accessing $\omega\gamma$ via angle-integrated measurement

$$< \sigma\nu >_{tot} \propto \sum_r \boxed{\omega\gamma_r} \exp\left(-\frac{E_r}{k_B T}\right)$$

$$\omega\gamma = \frac{(2J+1)}{(2j+1)(2J_{^{25}Al}+1)} \frac{\Gamma_p \Gamma_\gamma}{\Gamma_{tot}}$$

Extension of recent method to measure ***C*^{2}*S*$_p$** (NSCL) via d(^{26}Al,$n\gamma$)^{27}Si *Kankainen, EPJ **52** (2016)*

Direct transfer d(^{25}Al,$n\gamma$)^{26}Si

Tagging of ^{26}Si* on γ-ray transitions → angle-integrated measurement of cross-section σ_{transfer}

$$N_\gamma = \boxed{BR_\gamma} \times \boxed{\sigma^{exp}_{transfer}} \times \epsilon^{tot}_{det.} N_{target} I_{beam} T_{UT}$$

$$BR_\gamma \rightarrow \frac{\Gamma_\gamma}{\Gamma_{tot}}$$

$$\sigma^{exp}_{transfer} \rightarrow \boxed{C^2 S_p} \times \boxed{\sigma^{DWBA}_{transfer}}$$

$\sigma^{DWBA}_{transfer}$ → FRESCO code

$$C^2 S_p \rightarrow \frac{\Gamma_p}{\boxed{\Gamma_p^{s.p.}}}$$

$\Gamma_p^{s.p.}$ → DWU code

Accessing $\omega\gamma$ via angle-integrated measurement

$$< \sigma\nu >_{tot} \propto \sum_r \boxed{\omega\gamma_r} \exp\left(-\frac{E_r}{k_B T}\right)$$

$$\omega\gamma = \frac{(2J+1)}{(2j+1)(2J_{^{25}Al}+1)} \frac{\Gamma_p \Gamma_\gamma}{\Gamma_{tot}}$$

Extension of recent method to measure C^2S_p (NSCL) via d(^{26}Al,$n\gamma$)^{27}Si *Kankainen, EPJ **52** (2016)*

Direct transfer d(^{25}Al,$n\gamma$)^{26}Si

Tagging of ^{26}Si* on γ-ray transitions → angle-integrated measurement of cross-section $\sigma_{\mathrm{transfer}}$

$$N_\gamma = \boxed{BR_\gamma} \times \boxed{\sigma^{exp}_{transfer}} \times \epsilon^{tot}_{det.} N_{target} I_{beam} T_{UT}$$

$$BR_\gamma \rightarrow \frac{\Gamma_\gamma}{\Gamma_{tot}}$$

$$\sigma^{exp}_{transfer} \rightarrow \boxed{C^2 S_p} \times \boxed{\sigma^{DWBA}_{transfer}}$$

$\sigma^{DWBA}_{transfer}$ → FRESCO code

$$C^2 S_p \rightarrow \frac{\Gamma_p}{\boxed{\Gamma_p^{s.p.}}}$$

$\Gamma_p^{s.p.}$ → DWU code

$$\boxed{\omega\gamma = \frac{N_\gamma}{N_{target} I_{beam} \epsilon^{tot}_{det.} T_{UT}} \times \frac{\Gamma_p^{s.p.}}{\sigma^{DWBA}_{transfer}} \times \frac{(2J+1)}{(2j+1)(2J_{^{25}Al}+1)}}$$

Accessing $\omega\gamma$ via angle-integrated measurement

$$< \sigma\nu >_{tot} \propto \sum_r \boxed{\omega\gamma_r} \exp\left(-\frac{E_r}{k_B T}\right)$$

$$\omega\gamma = \frac{(2J+1)}{(2j+1)(2J_{^{25}Al}+1)} \frac{\Gamma_p \Gamma_\gamma}{\Gamma_{tot}}$$

Extension of recent method to measure ***C*²*S*ₚ** (NSCL) via $d(^{26}\mathrm{Al},n\gamma)^{27}\mathrm{Si}$ *Kankainen, EPJ **52** (2016)*

Direct transfer $d(^{25}\mathrm{Al},n\gamma)^{26}\mathrm{Si}$

Tagging of ^{26}Si* on γ-ray transitions → angle-integrated measurement of cross-section $\sigma_{\mathrm{transfer}}$

$$\mathrm{N}_\gamma = \boxed{\mathrm{BR}_\gamma} \times \boxed{\sigma^{\mathrm{exp}}_{\mathrm{transfer}}} \times \epsilon^{\mathrm{tot}}_{\mathrm{det.}} \mathrm{N}_{\mathrm{target}} \mathrm{I}_{\mathrm{beam}} \mathrm{T}_{\mathrm{UT}}$$

$$\mathrm{BR}_\gamma \rightarrow \frac{\Gamma_\gamma}{\Gamma_{\mathrm{tot}}}$$

$$\sigma^{\mathrm{exp}}_{\mathrm{transfer}} \rightarrow \boxed{C^2 S_p} \times \boxed{\sigma^{\mathrm{DWBA}}_{\mathrm{transfer}}}$$

$\sigma^{\mathrm{DWBA}}_{\mathrm{transfer}}$ → FRESCO code

$$C^2 S_p \rightarrow \boxed{\frac{\Gamma_{\mathrm{p}}}{\Gamma^{\mathrm{s.p.}}_{\mathrm{p}}}}$$

$\frac{\Gamma_{\mathrm{p}}}{\Gamma^{\mathrm{s.p.}}_{\mathrm{p}}}$ → DWU code

$$\omega\gamma = \frac{\mathrm{N}_\gamma}{\mathrm{N}_{\mathrm{target}} \mathrm{I}_{\mathrm{beam}} \epsilon^{\mathrm{tot}}_{\mathrm{det.}} \mathrm{T}_{\mathrm{UT}}} \times \frac{\Gamma^{\mathrm{s.p.}}_{\mathrm{p}}}{\sigma^{\mathrm{DWBA}}_{\mathrm{transfer}}} \times \frac{(2J+1)}{(2j+1)(2J_{^{25}Al}+1)}$$

Uncertainties = systematic ≲30% (from optical potentials) & statistical ($1/\sqrt{N_\gamma}$)

Experimental setup

Direct transfer $d(^{25}\mathrm{Al},n\gamma)^{26}\mathrm{Si}$

Extension of $d(^{26}\mathrm{Al},n\gamma)^{27}\mathrm{Si}$ *Kankainen, EPJ* ***52*** *(2016)*

$$\omega\gamma = \frac{\mathrm{N}_\gamma}{\mathrm{N}_{\mathrm{target}}\mathrm{I}_{\mathrm{beam}}\epsilon^{\mathrm{tot}}_{\mathrm{det.}}\,\mathrm{T}_{\mathrm{UT}}} \times \frac{\Gamma^{\mathrm{s.p.}}_{\mathrm{p}}}{\sigma^{\mathrm{DWBA}}_{\mathrm{transfer}}} \times \frac{(2J+1)}{(2j+1)(2J_{^{25}Al}+1)}$$

Experimental setup

Direct transfer $d(^{25}\text{Al},n\gamma)^{26}\text{Si}$
Extension of $d(^{26}\text{Al},n\gamma)^{27}\text{Si}$ *Kankainen, EPJ **52** (2016)*

$$\omega\gamma = \frac{N_\gamma}{N_{target} I_{beam} \epsilon^{tot}_{det.} T_{UT}} \times \frac{\Gamma_p^{s.p.}}{\sigma^{DWBA}_{transfer}} \times \frac{(2J+1)}{(2j+1)(2J_{^{25}Al}+1)}$$

@FRIB/ARIS *Fougères et al (2023)*

^{25}Al@**24MeV/u**
High-power primary beam ^{28}Si@**10kW**
Slow radioactive beam produced by fragmentation (thick Be + Al foils)
2x10^6 pps
>95% purity

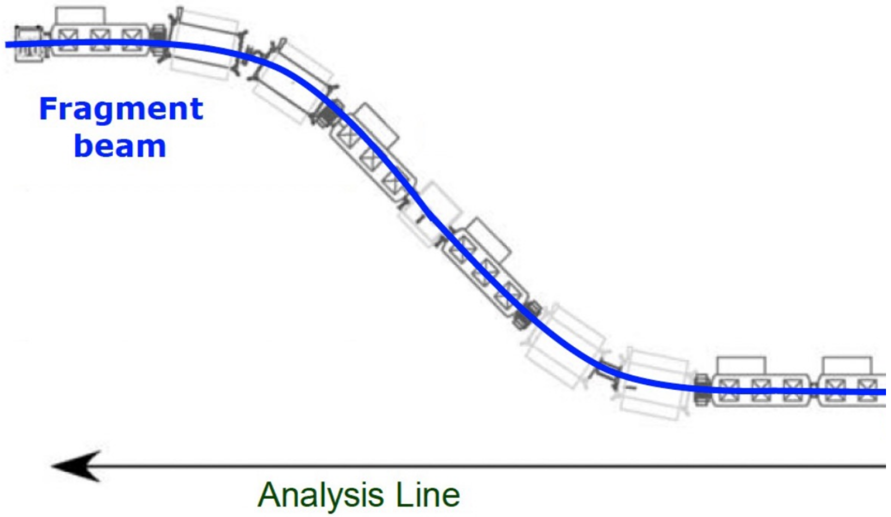

Experimental setup

Direct transfer $d(^{25}\text{Al},n\gamma)^{26}\text{Si}$

Extension of $d(^{26}\text{Al},n\gamma)^{27}\text{Si}$ *Kankainen, EPJ* ***52*** *(2016)*

$$\omega\gamma = \frac{N_\gamma}{N_{\text{target}} I_{\text{beam}} \epsilon^{\text{tot}}_{\text{det.}} T_{\text{UT}}} \times \frac{\Gamma_p^{\text{s.p.}}}{\sigma^{\text{DWBA}}_{\text{transfer}}} \times \frac{(2J+1)}{(2j+1)(2J_{^{25}Al}+1)}$$

@FRIB/ARIS *Fougères et al (2023)*

^{25}Al@**24MeV/u**

High-power primary beam ^{28}Si@**10kW**

Slow radioactive beam produced by fragmentation (thick Be + Al foils)

2x10^6 pps

>95% purity

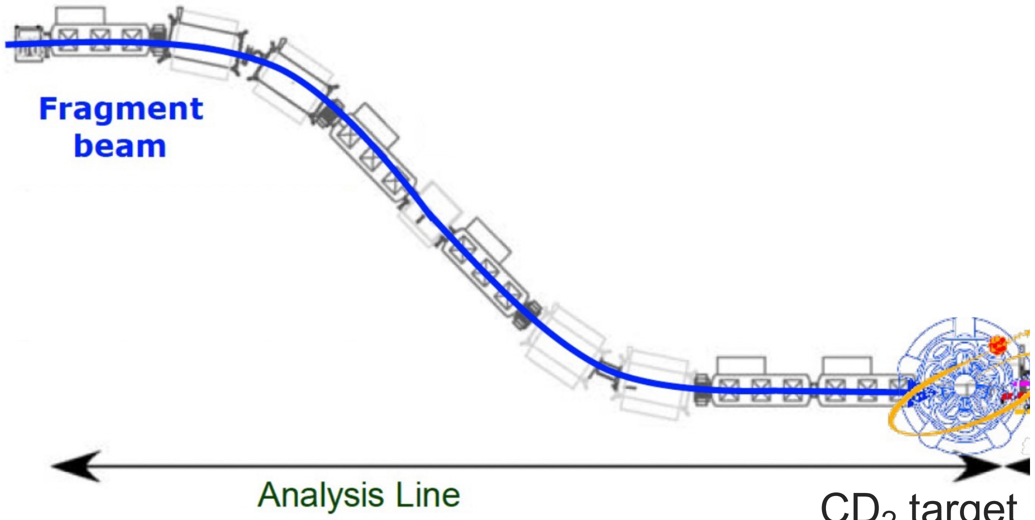

CD$_2$ target
thick (9.4 mg/cm^2)

Experimental setup

Direct transfer $d(^{25}Al,n\gamma)^{26}Si$
Extension of $d(^{26}Al,n\gamma)^{27}Si$ *Kankainen, EPJ* ***52*** *(2016)*

$$\omega\gamma = \frac{N_\gamma}{N_{target} I_{beam} \epsilon^{tot}_{det.} T_{UT}} \times \frac{\Gamma_p^{s.p.}}{\sigma^{DWBA}_{transfer}} \times \frac{(2J+1)}{(2j+1)(2J_{^{25}Al}+1)}$$

GRETINA **@FRIB/ARIS** *Fougères et al (2023)*

^{25}Al@**24MeV/u**
High-power primary beam ^{28}Si@**10kW**
Slow radioactive beam produced by fragmentation (thick Be + Al foils)
2x10^6 pps
>95% purity

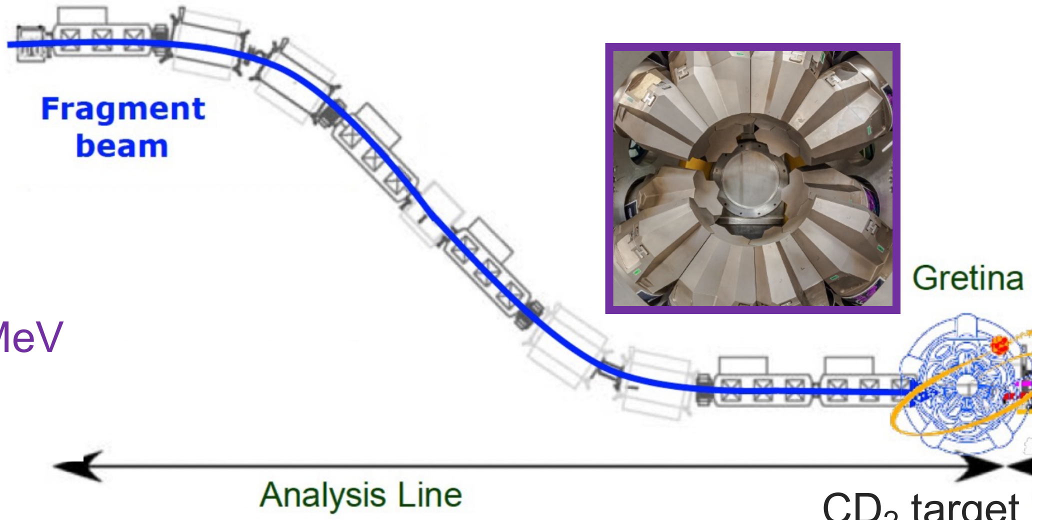

GRETINA@1.8MeV
FWHM_DC **0.7%**
efficiency **4.6%**

CD_2 target
thick (9.4 mg/cm^2)

^{25}Al(p,γ)^{26}Si

Experimental setup

Direct transfer $d(^{25}Al,n\gamma)^{26}Si$

Extension of $d(^{26}Al,n\gamma)^{27}Si$ *Kankainen, EPJ* ***52*** *(2016)*

$$\omega\gamma = \frac{N_\gamma}{N_{target} I_{beam} \epsilon^{tot}_{det.} T_{UT}} \times \frac{\Gamma^{s.p.}_{p}}{\sigma^{DWBA}_{transfer}} \times \frac{(2J+1)}{(2j+1)(2J_{^{25}Al}+1)}$$

GRETINA&S800@FRIB/ARIS *Fougères et al (2023)*

^{25}Al@**24MeV/u**

High-power primary beam ^{28}Si@**10kW**

Slow radioactive beam produced by fragmentation (thick Be + Al foils)

2x10^6 pps

>95% purity

S800 line

Lowest energy

Transmission **56%**

FP efficiency **65%**

GRETINA@1.8MeV

FWHM_DC **0.7%**

efficiency **4.6%**

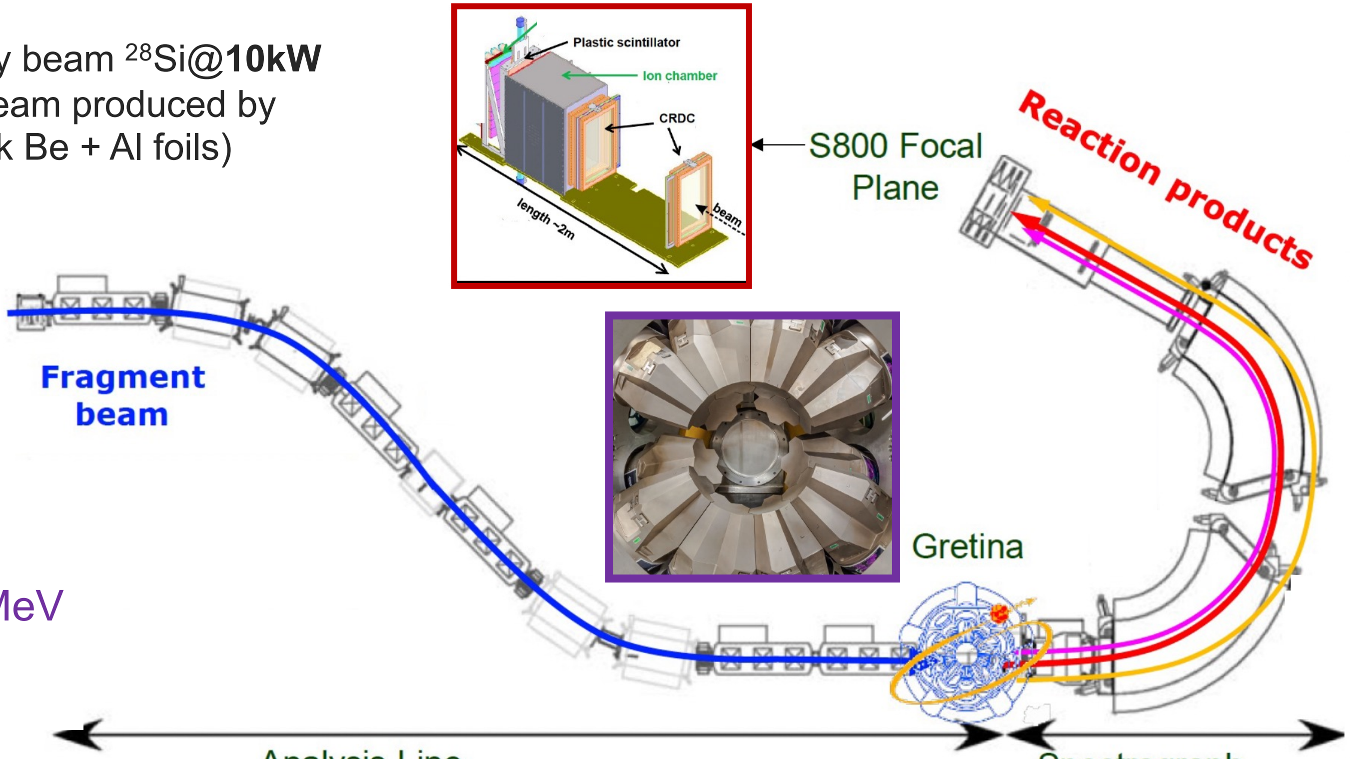

CD_2 target

thick (9.4 mg/cm^2)

$^{25}Al(p,\gamma)^{26}Si$

Experimental setup

Direct transfer $d(^{25}Al,n\gamma)^{26}Si$

Extension of $d(^{26}Al,n\gamma)^{27}Si$ *Kankainen, EPJ* ***52*** *(2016)*

$$\omega\gamma = \frac{N_\gamma}{N_{target} I_{beam} \epsilon^{tot}_{det.} T_{UT}} \times \frac{\Gamma_p^{s.p.}}{\sigma^{DWBA}_{transfer}} \times \frac{(2J+1)}{(2j+1)(2J_{^{25}Al}+1)}$$

GRETINA&S800@FRIB/ARIS *Fougères et al (2023)*

^{25}**Al@24MeV/u**

High-power primary beam ^{28}Si@**10kW**

Slow radioactive beam produced by fragmentation (thick Be + Al foils)

2×10^6 pps

>95% purity

S800 line

Lowest energy

Transmission **56%**

FP efficiency **65%**

GRETINA@1.8MeV

FWHM_DC **0.7%**

efficiency **4.6%**

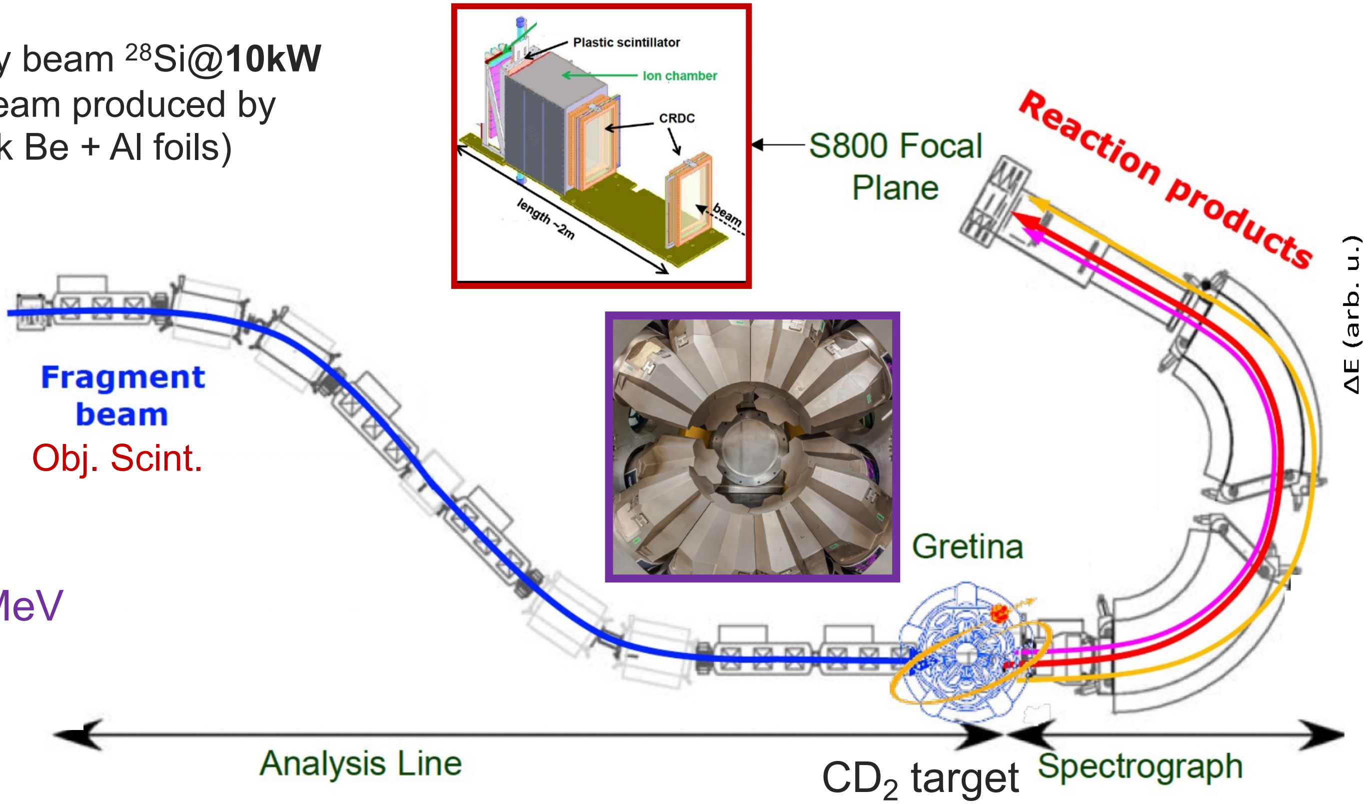

CD_2 target

thick (9.4 mg/cm^2)

Online PID

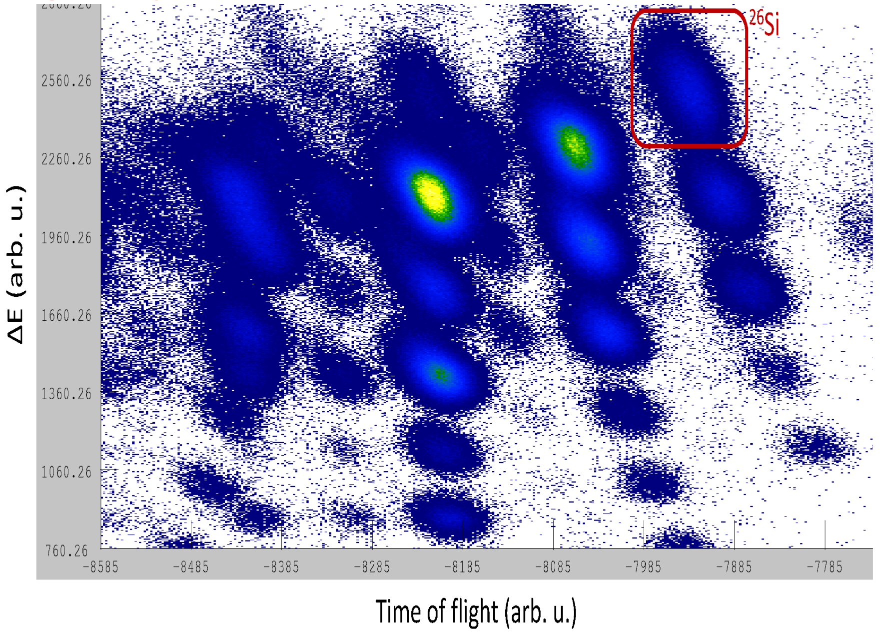

Focal Plane Scint. vs Obj. Scint.

$^{25}Al(p,\gamma)^{26}Si$

Experimental setup

Direct transfer $d(^{25}Al,n\gamma)^{26}Si$

Extension of $d(^{26}Al,n\gamma)^{27}Si$ *Kankainen, EPJ* ***52*** *(2016)*

$$\omega\gamma = \frac{N_\gamma}{N_{target} I_{beam} \epsilon^{tot}_{det.} T_{UT}} \times \frac{\Gamma_p^{s.p.}}{\sigma^{DWBA}_{transfer}} \times \frac{(2J+1)}{(2j+1)(2J_{^{25}Al}+1)}$$

GRETINA&S800@FRIB/ARIS *Fougères et al (2023)*

1st experiment supported by IRL NPA (FRIB & CNRS/IN2P3)

^{25}Al@**24MeV/u**

High-power primary beam ^{28}Si@**10kW**

Slow radioactive beam produced by fragmentation (thick Be + Al foils)

2x10⁶ pps

>95% purity

S800 line

Lowest energy

Transmission **56%**

FP efficiency **65%**

GRETINA@1.8MeV

FWHM_DC **0.7%**

efficiency **4.6%**

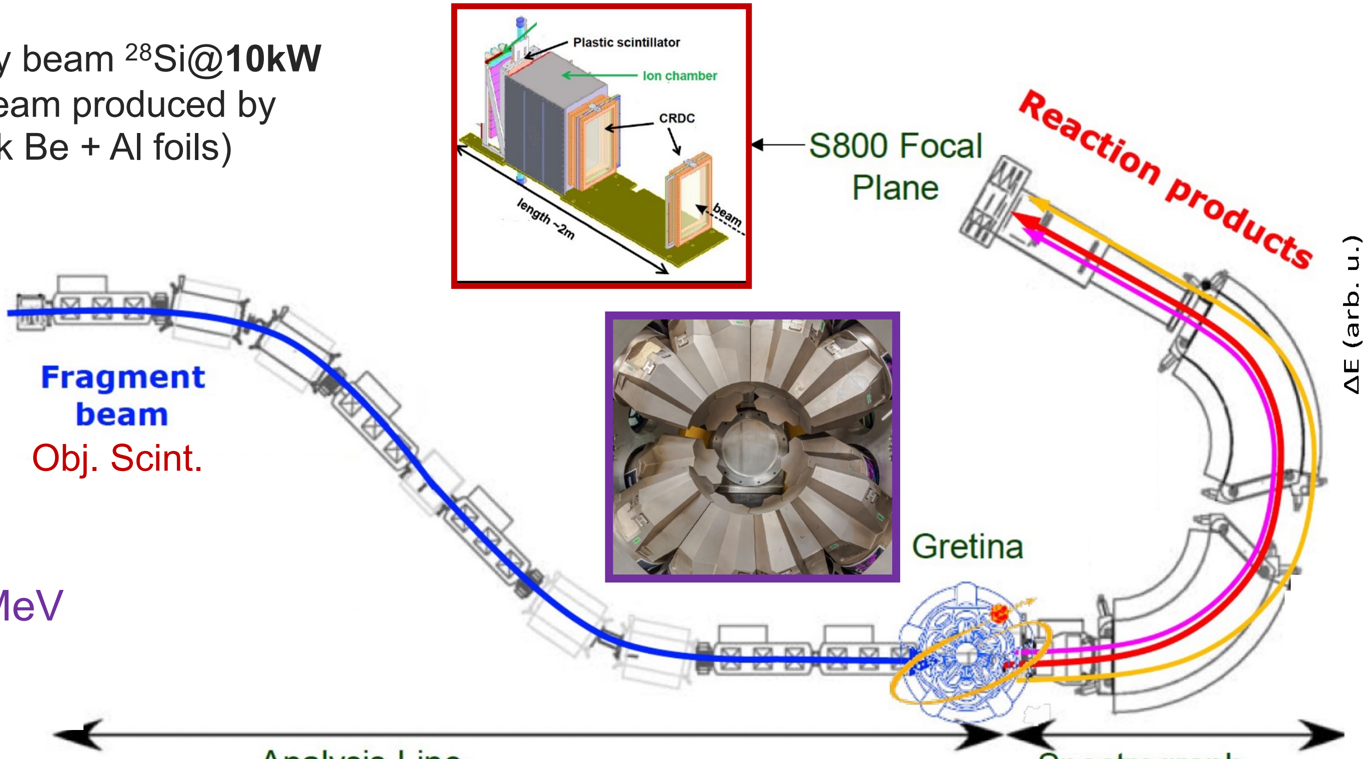

CD_2 target

thick (9.4 mg/cm²)

Online PID

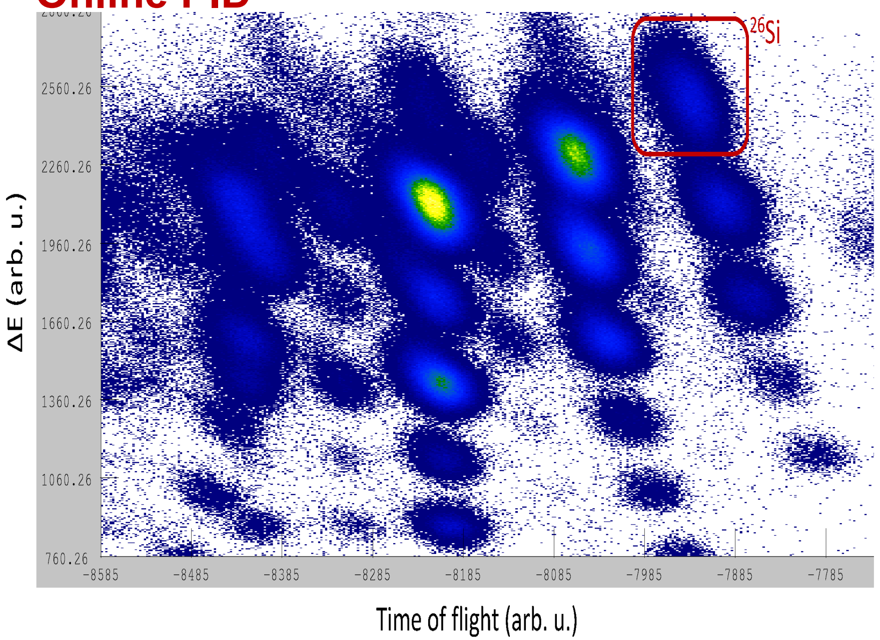

Focal Plane Scint. vs Obj. Scint.

Investigation of bound states

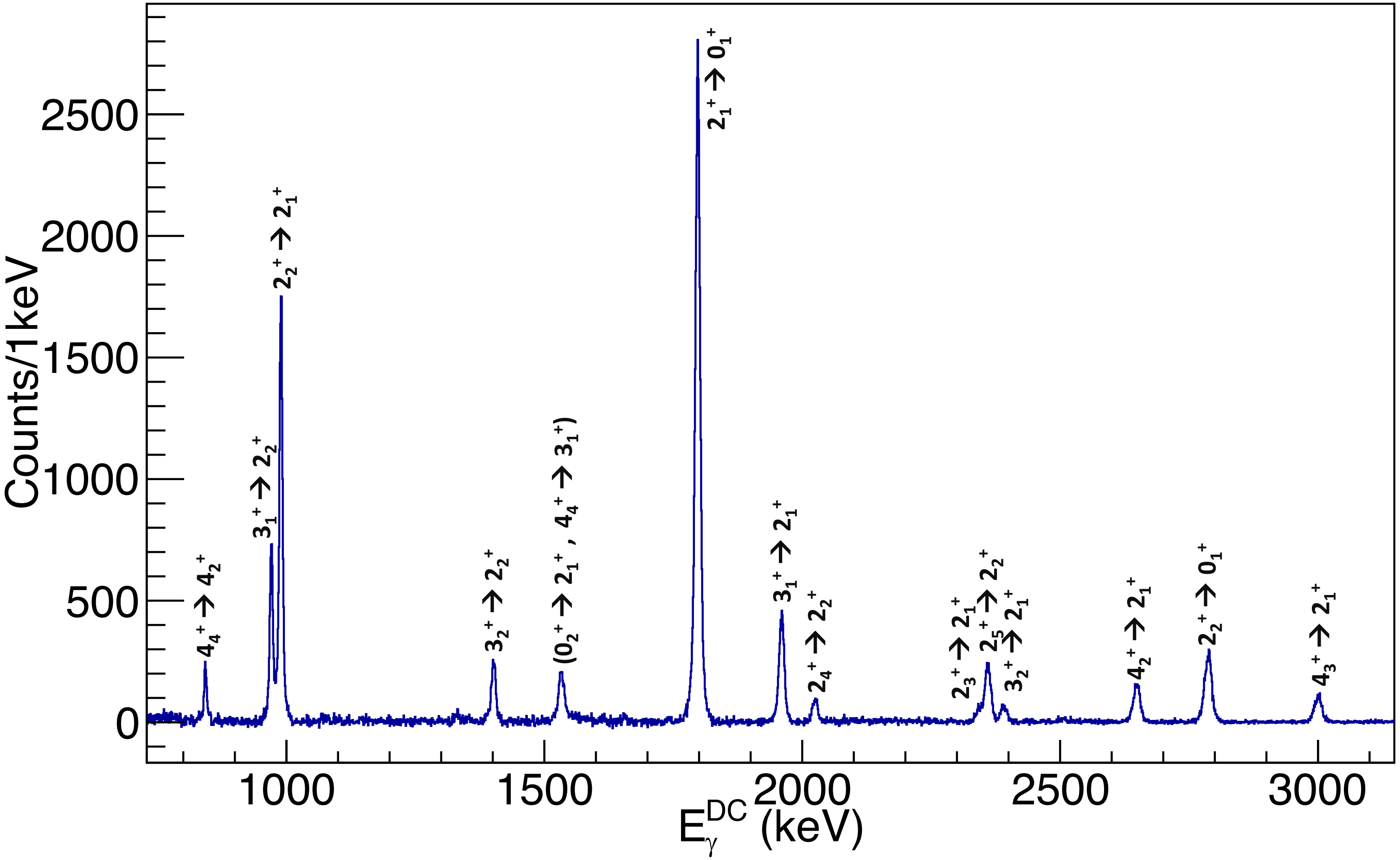

Investigation of bound states

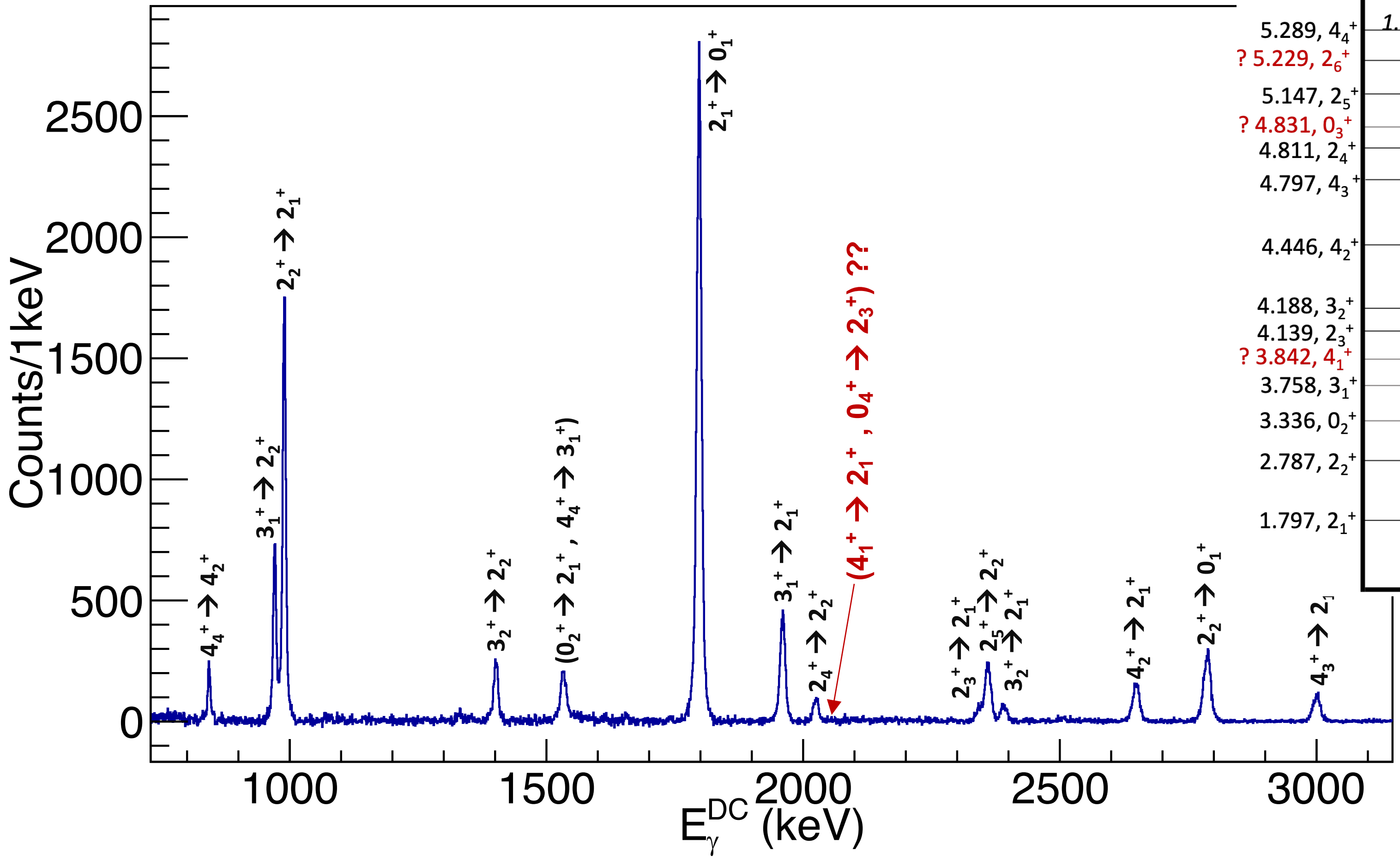

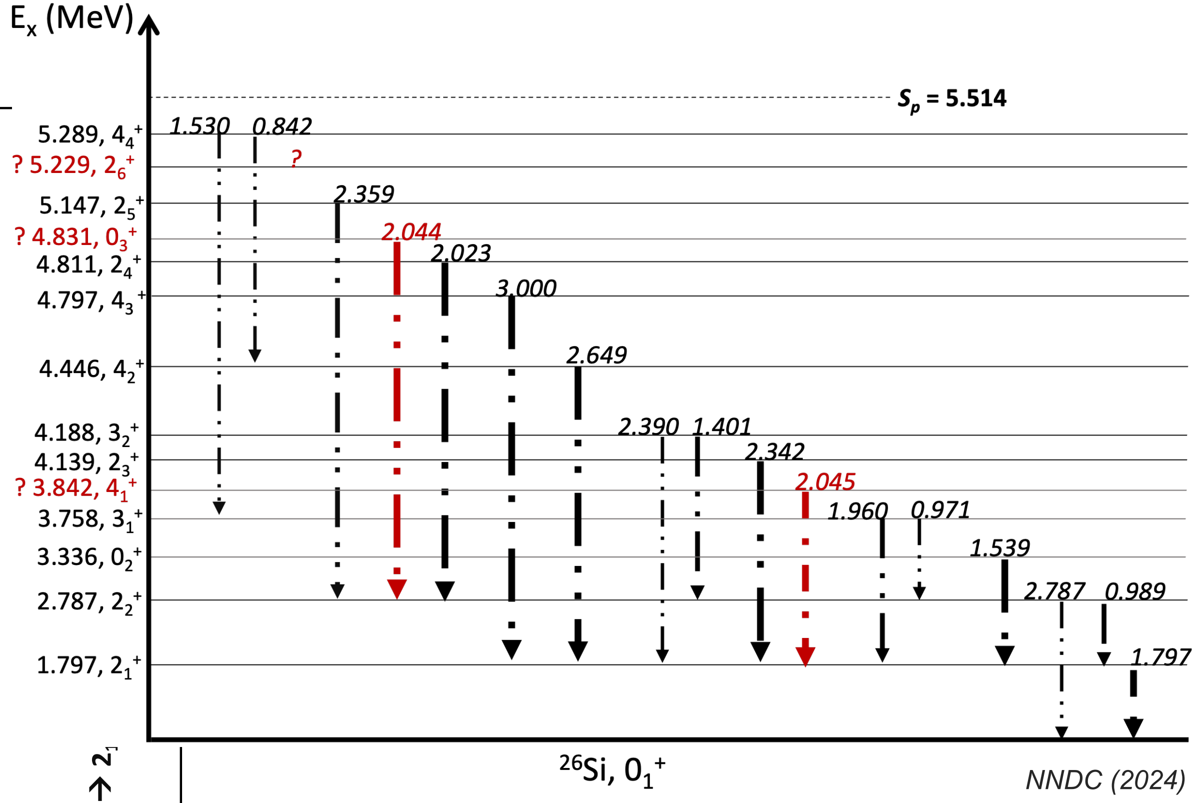

11 states identified among 14 referenced ones in ^{26}Si (<S_p)

$^{25}Al(p,\gamma)^{26}Si$

Investigation of bound states

Comparison with few analog states in ^{26}Mg *Burlein, PRC **29** (1984), Arciszewski NPA 430 (1984)*

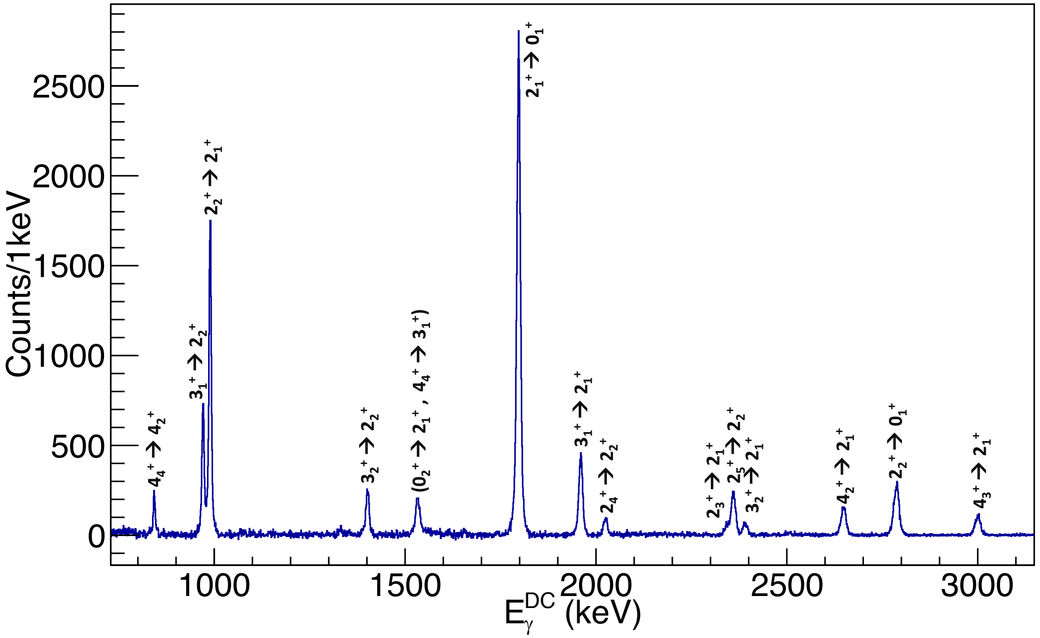

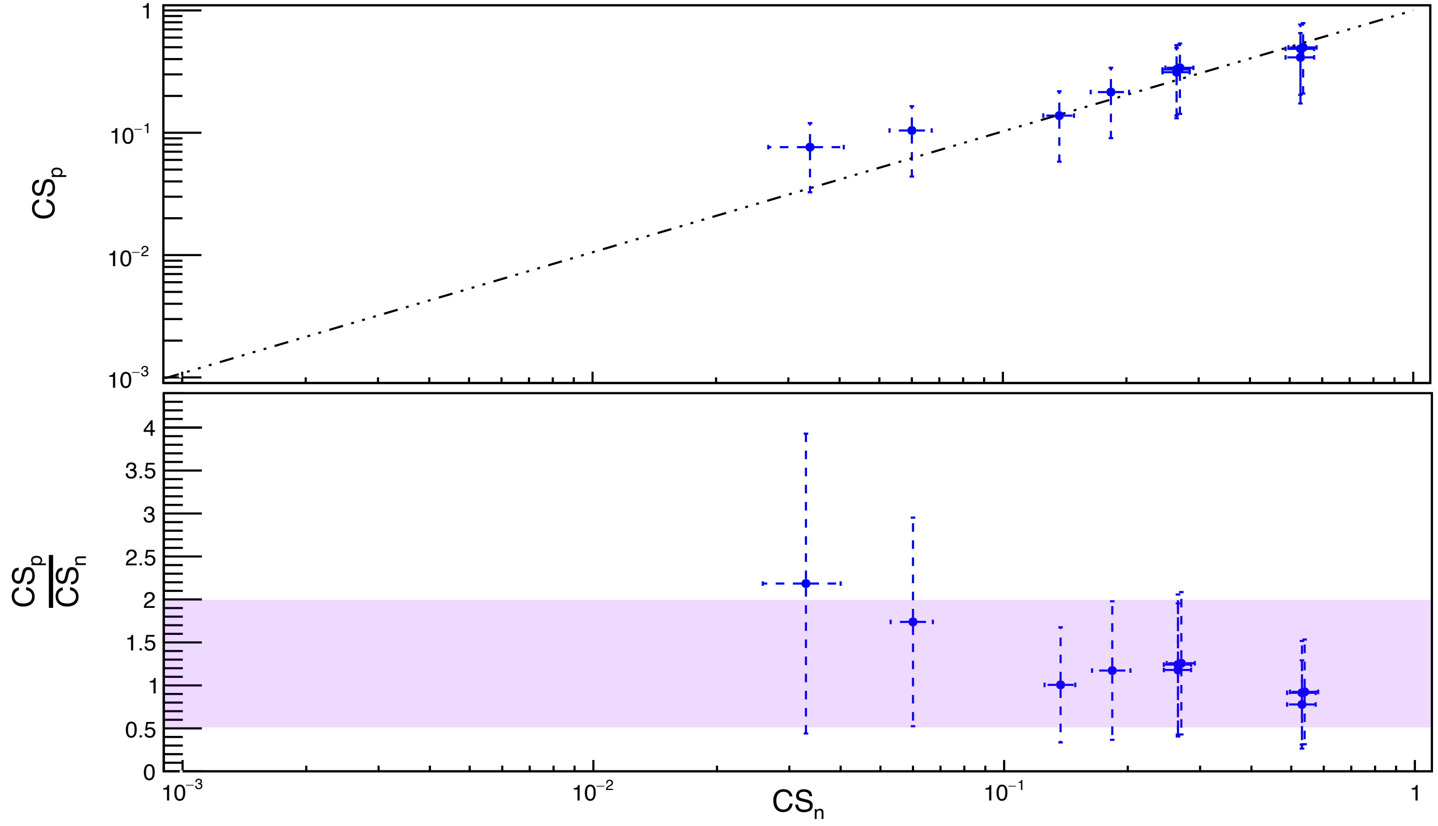

Investigation of bound states

Comparison with few analog states in ^{26}Mg *Burlein, PRC **29** (1984), Arciszewski NPA 430 (1984)*

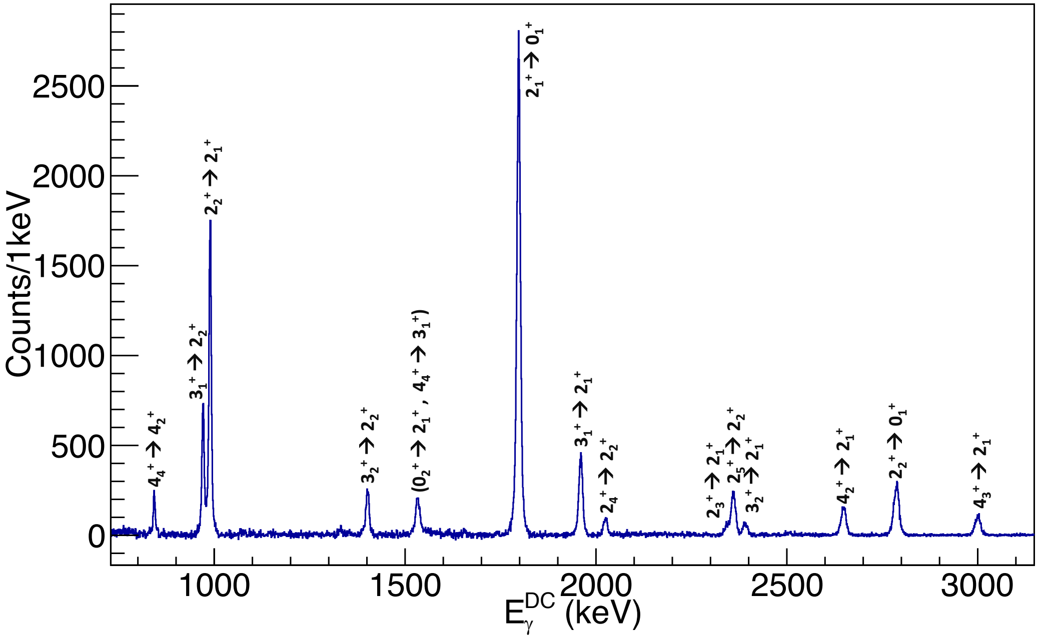

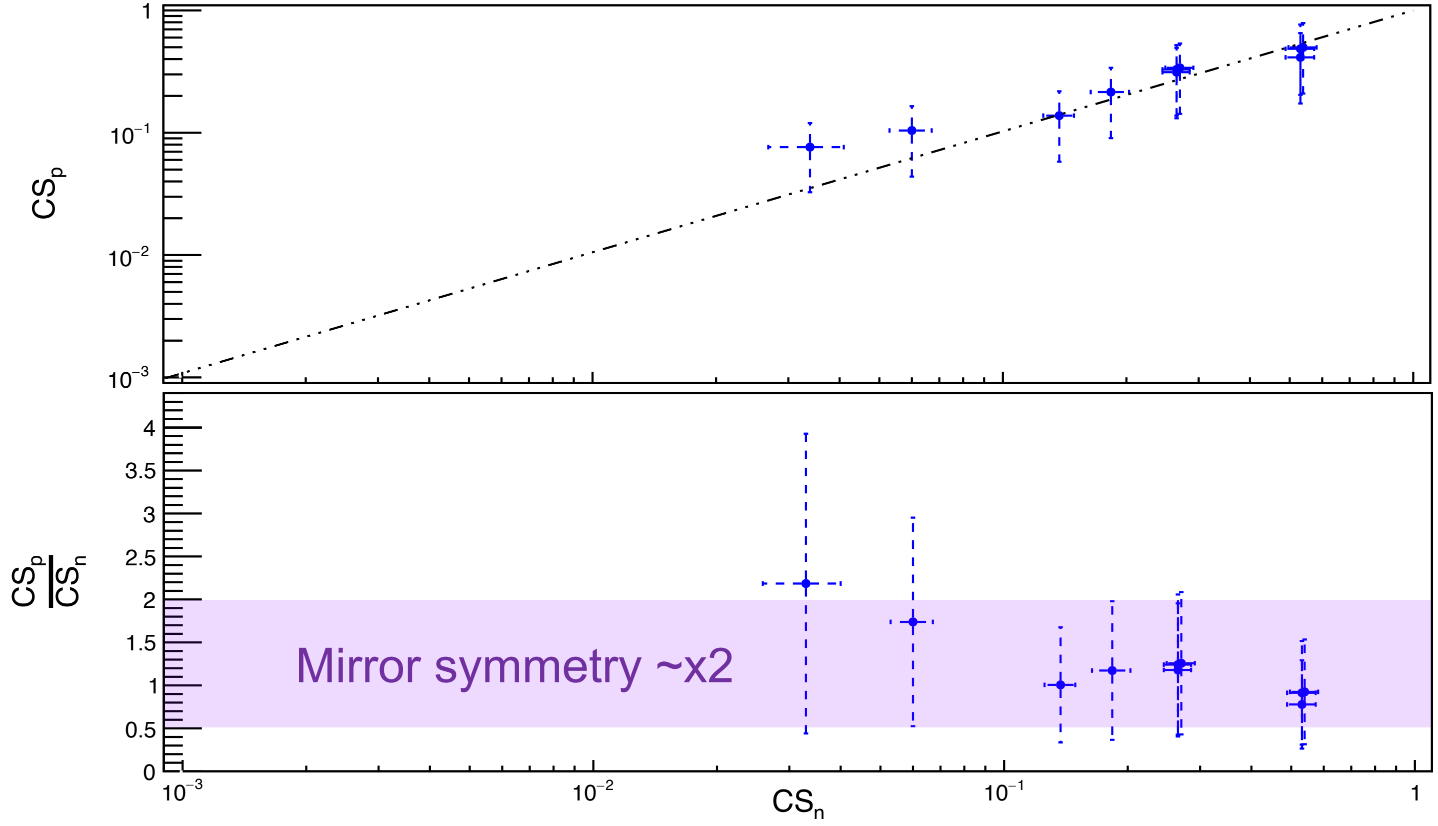

$^{25}Al(p,\gamma)^{26}Si$

Resonant states

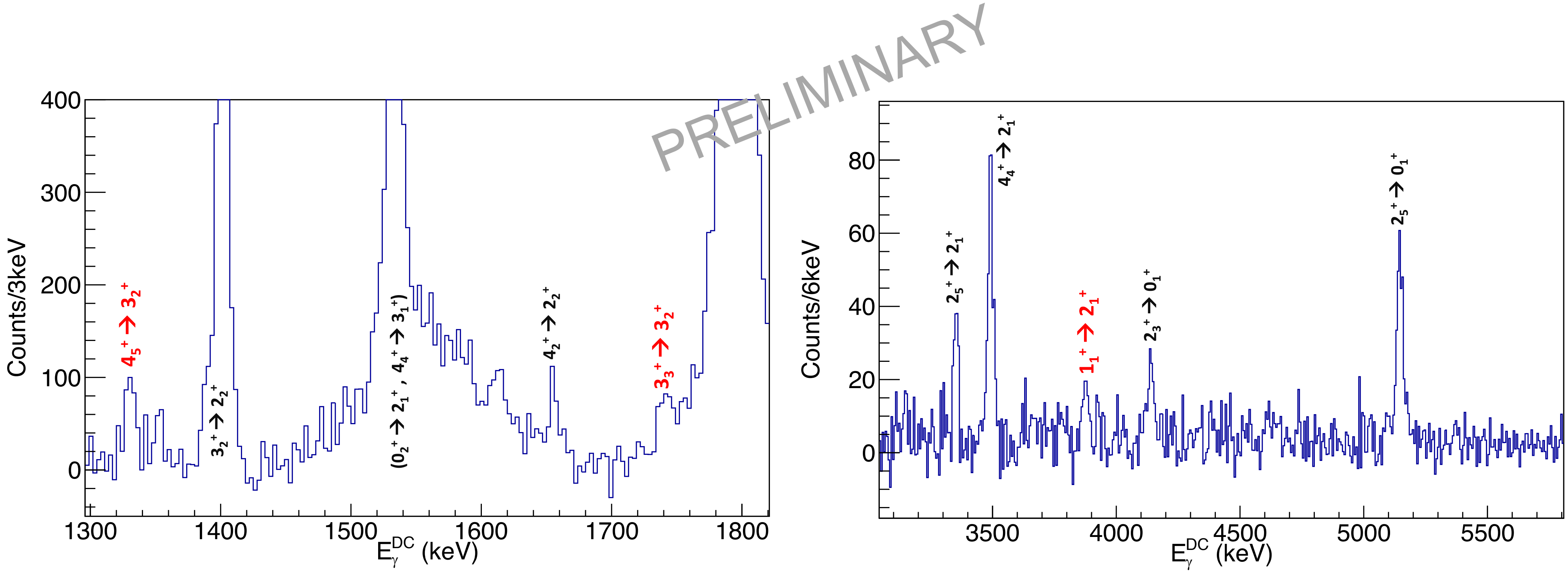

$^{25}Al(p,\gamma)^{26}Si$

Resonant states

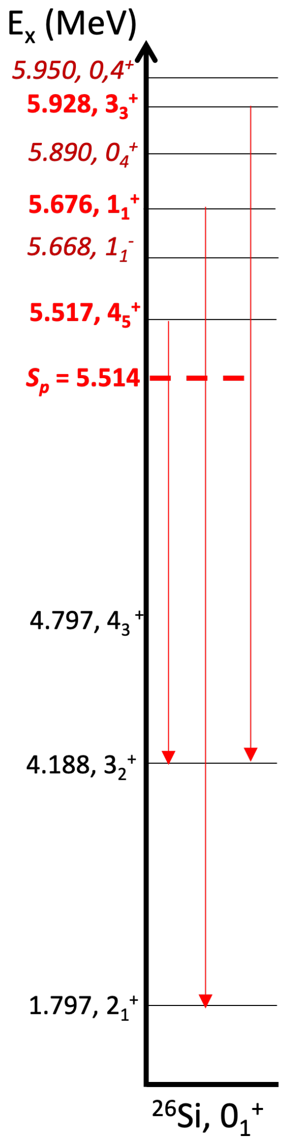

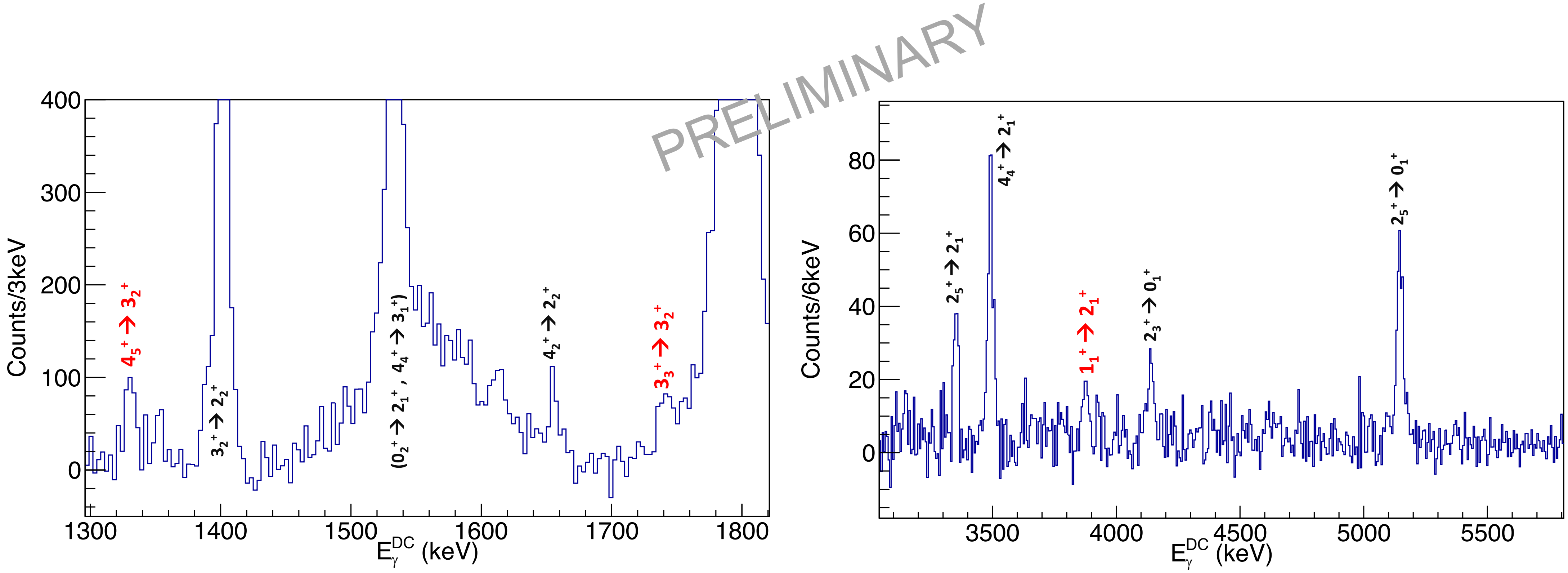

$^{25}Al(p,\gamma)^{26}Si$

Resonant states

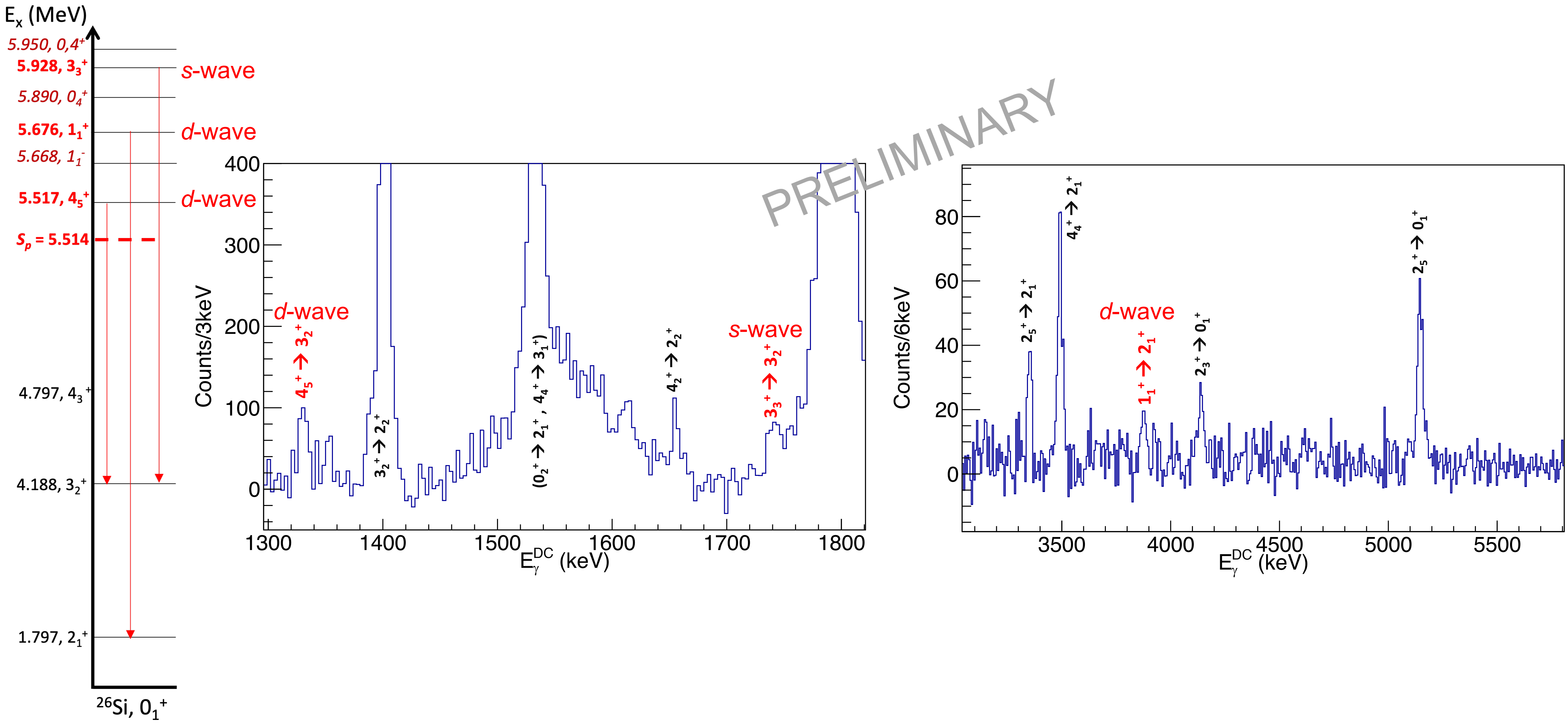

$^{25}Al(p,\gamma)^{26}Si$

Resonant states

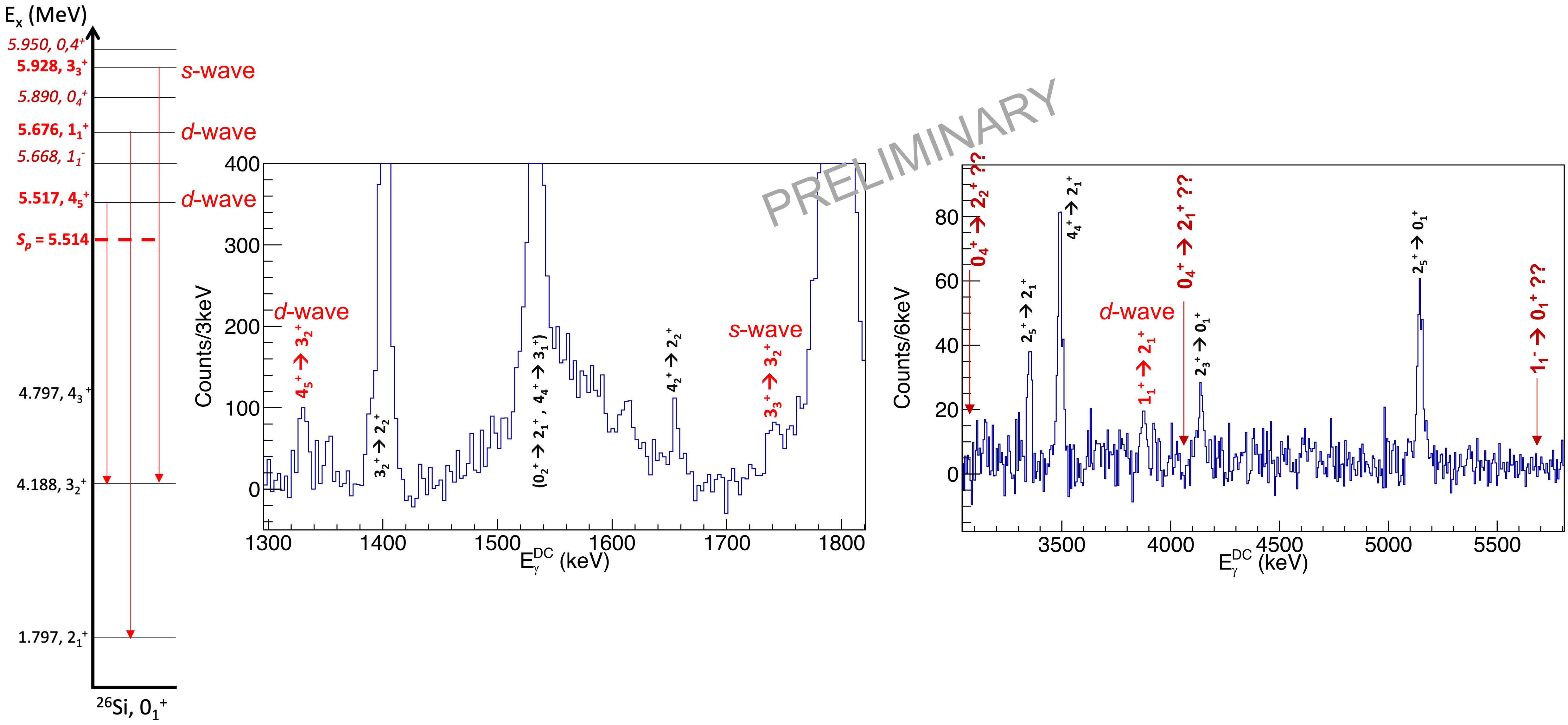

3 states identified among 6 of interest in ^{26}Si ($>S_p$)

$^{25}Al(p,\gamma)^{26}Si$

Resonant states

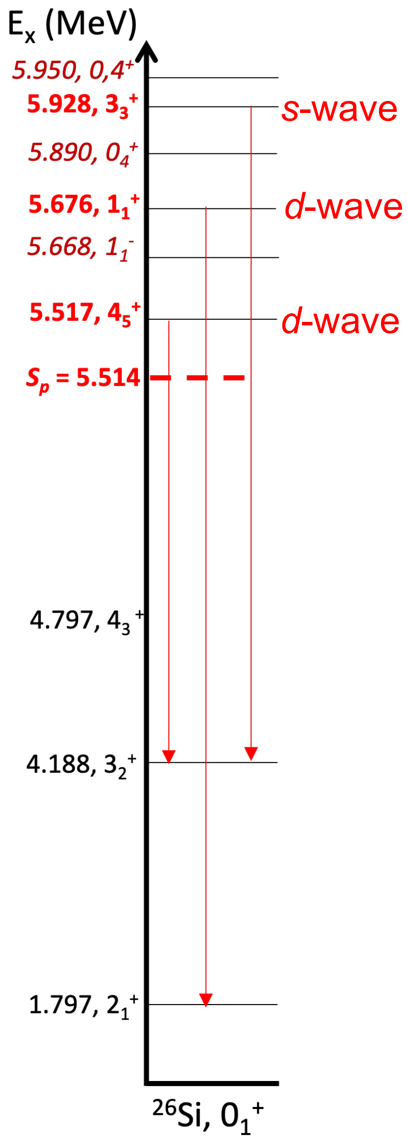

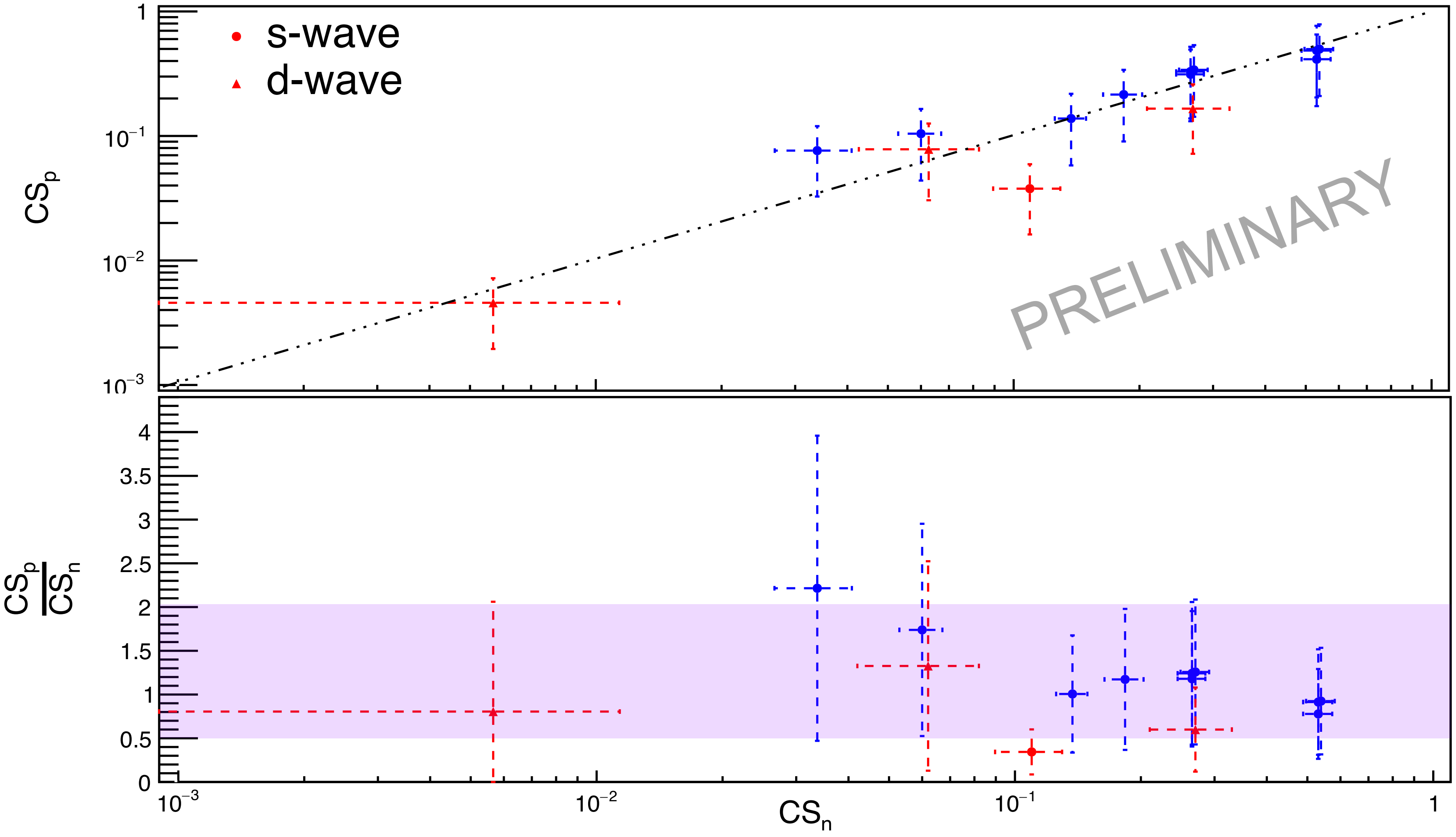

3 states identified among 6 of interest in ^{26}Si ($>S_p$)

$^{25}Al(p,\gamma)^{26}Si$

Resonant states

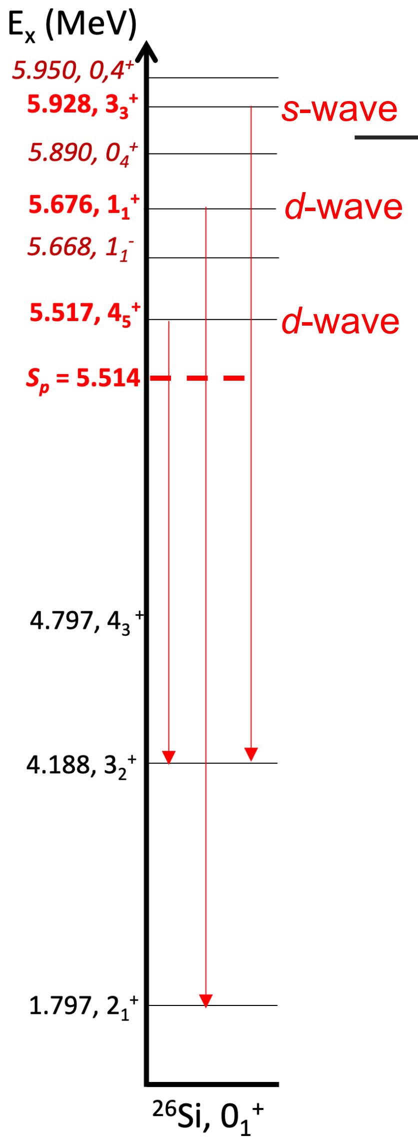

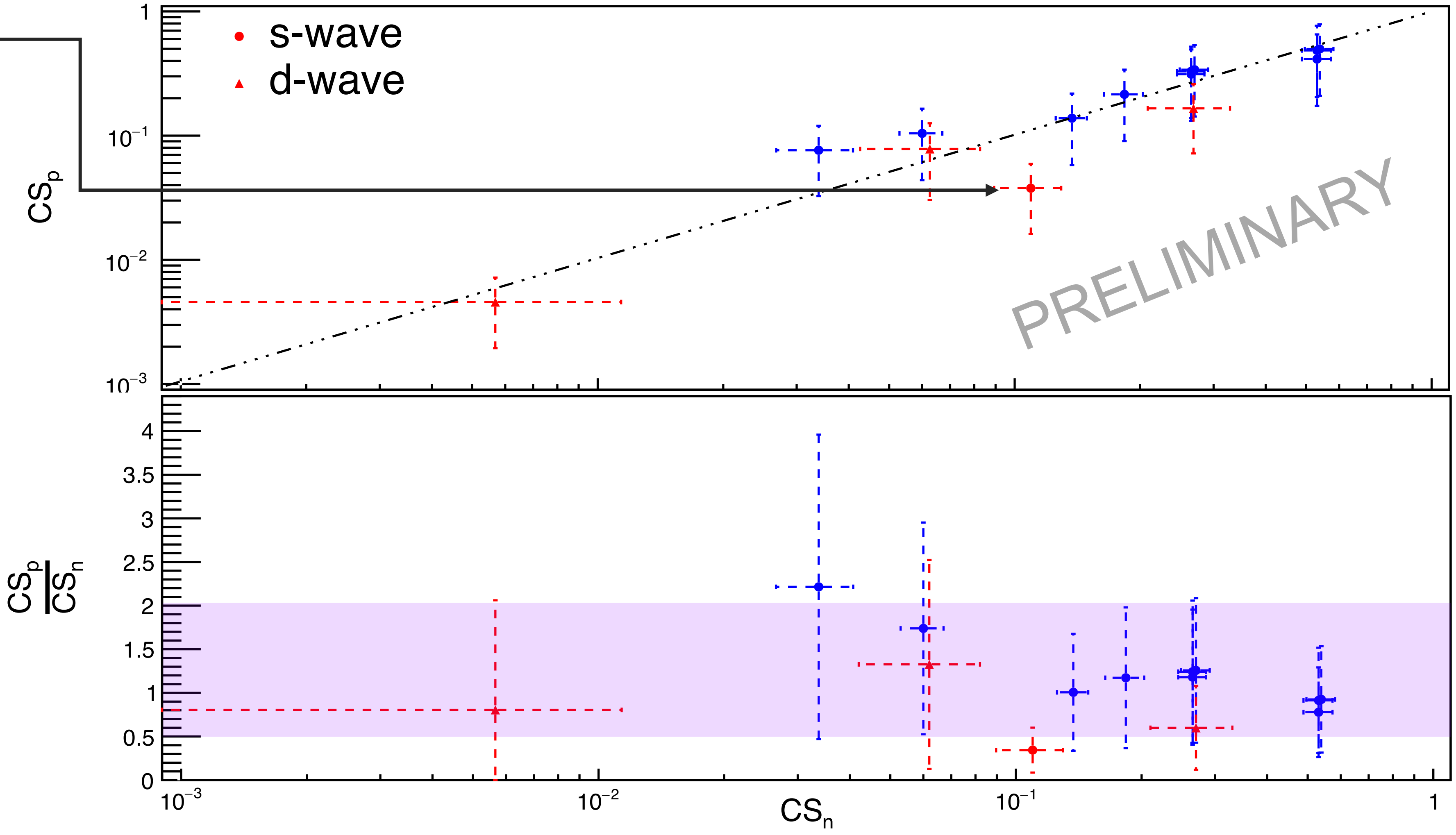

3 states identified among 6 of interest in ^{26}Si ($>S_p$)

$^{25}Al(p,\gamma)^{26}Si$

Resonant states

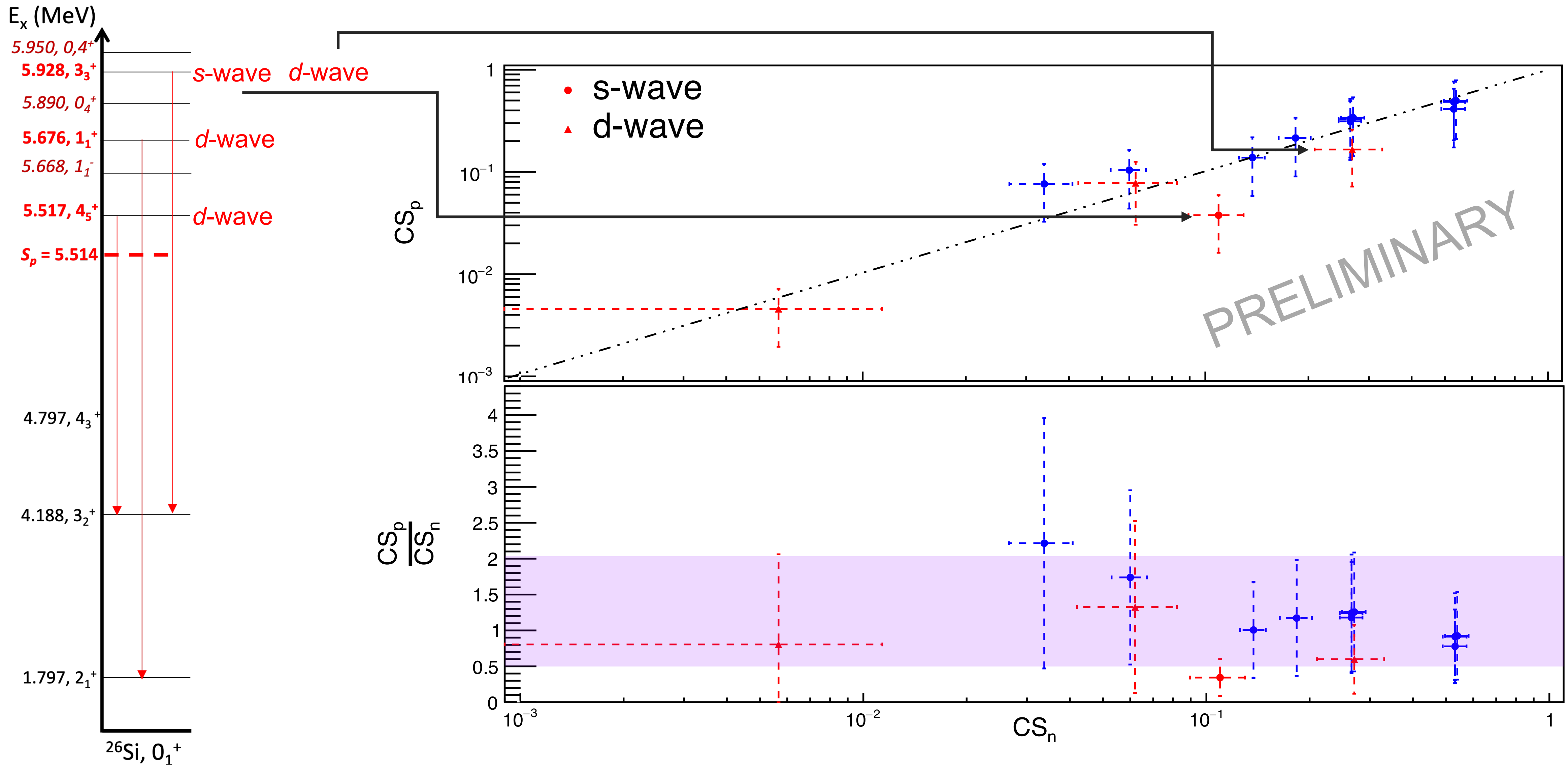

3 states identified among 6 of interest in ^{26}Si ($>S_p$)

Separation of *d*-wave contribution from the total cross section with angular distribution of γ-rays?

Spectroscopy of a resonant state

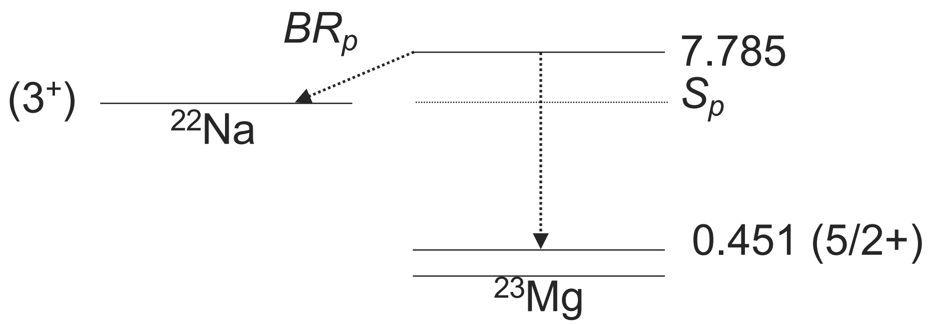

Spectroscopy of a resonant state

$$\omega\gamma = \frac{2J_{^{23}Mg}+1}{(2J_{^{22}Na}+1)(2J_p+1)} \times \frac{\hbar}{\tau} \times BR_p(1-BR_p)$$

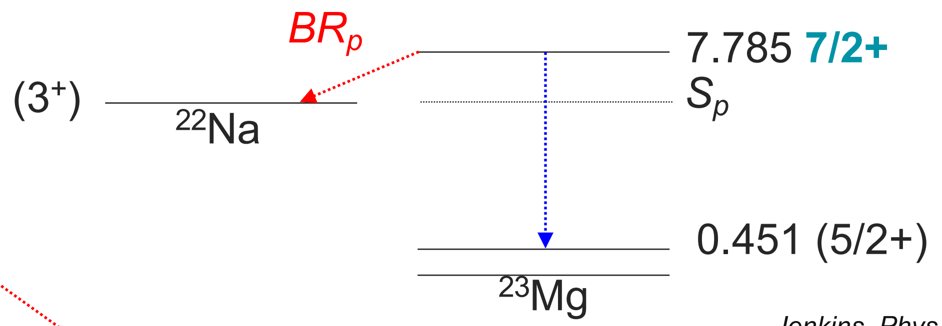

*Jenkins, Phys. Rev. L **92** (2004)*
*Fougères, EPJ Web Conf **279** (2023)*

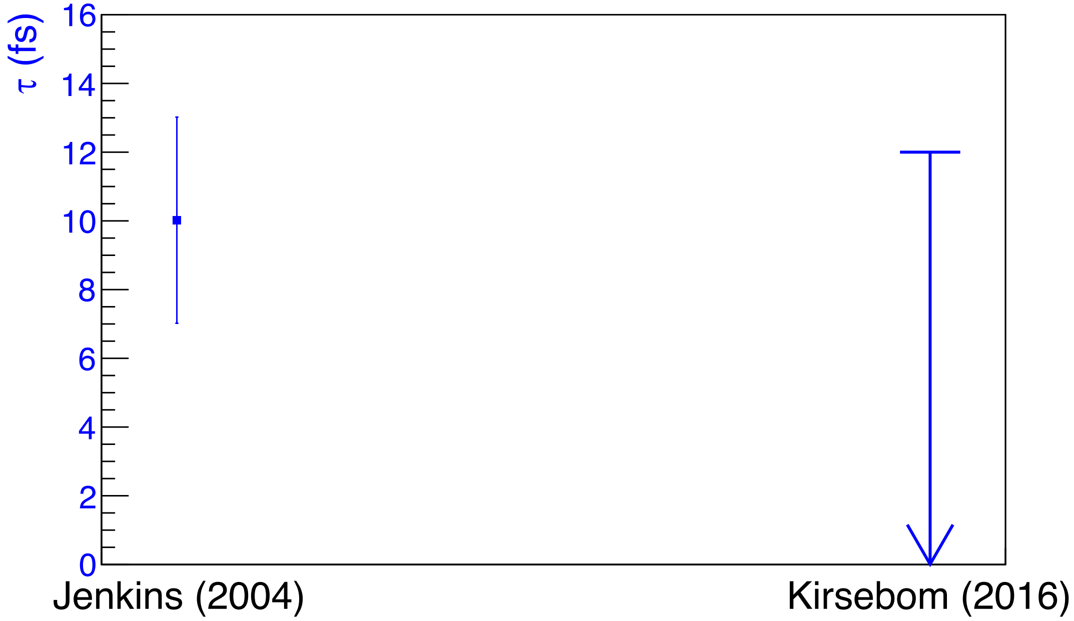

Reasonant state population

$^{3}He(^{24}Mg,^{4}He)^{23}Mg^{*}$

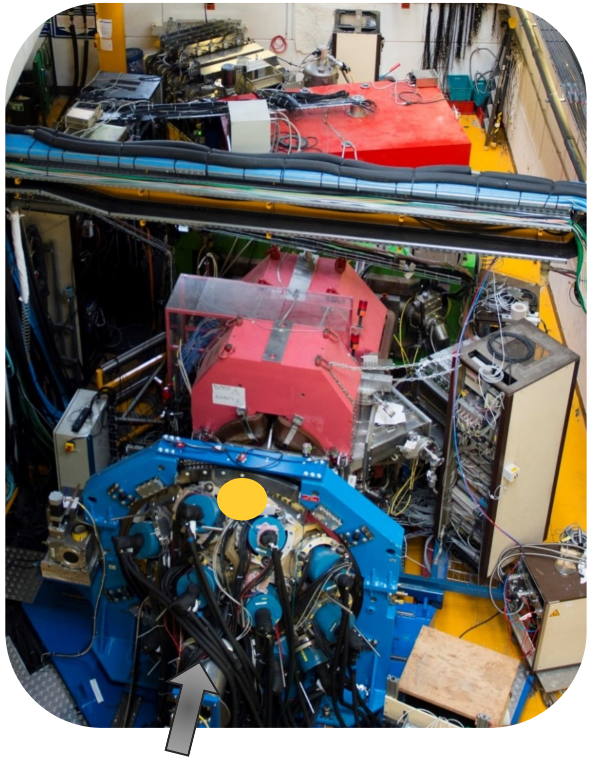

^{24}Mg at 4.6 MeV/u

Target + Beam Catcher

^{3}He surface implantation in gold

10^{17} at.cm^{-2}

Reasonant state population

$^{3}He(^{24}Mg,^{4}He)^{23}Mg^{*}$

$\beta_{ejectil}, \theta_{ejectil}, E_x^{\mathrm{VAMOS}}$

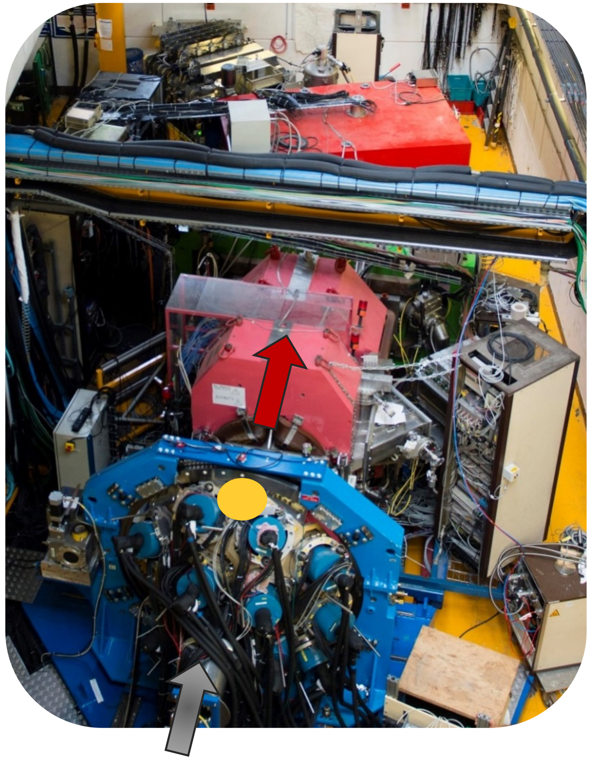

^{24}Mg at 4.6 MeV/u

VAMOS++
Zero-degree setup
α-reaction efficiency ~ 4 %
Resolution E_x = 250 keV, θ = 0.5 deg

Target + Beam Catcher
^{3}He surface implantation in gold
10^{17} at.cm^{-2}

Plastic photomultiplicator
Time of flight w.r.t cyclo. HF

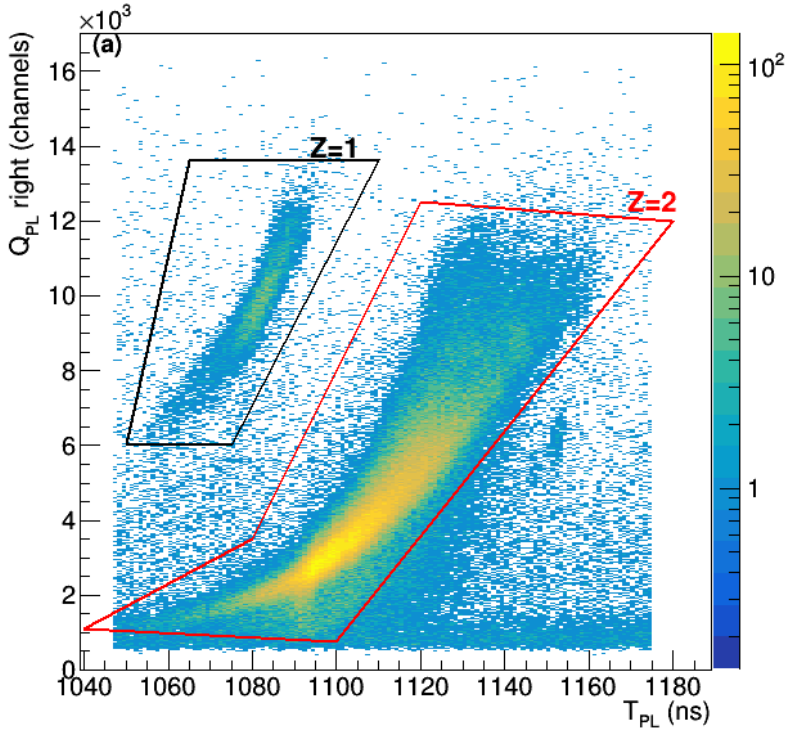

Reasonant state population

$^{3}He(^{24}Mg,^{4}He)^{23}Mg^{*}(\gamma)$

$\beta_{ejectil}, \theta_{ejectil}, E_x^{VAMOS}$

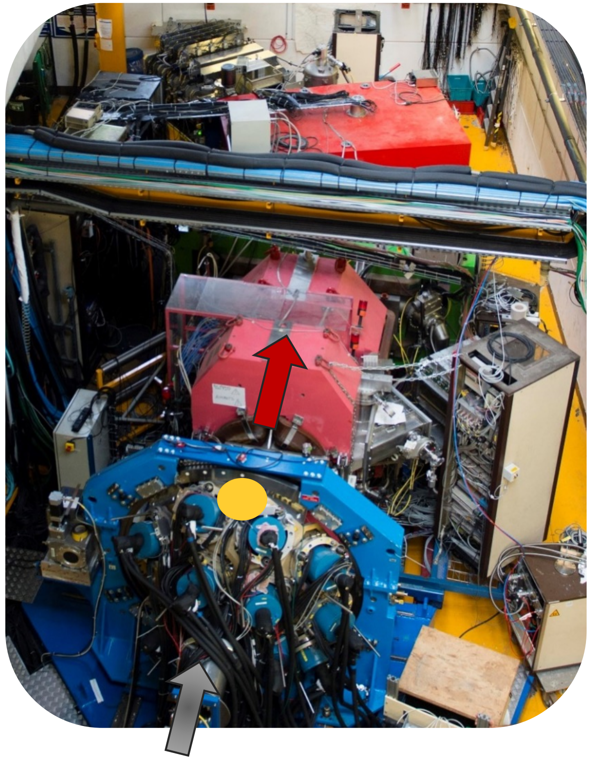

^{24}Mg at 4.6 MeV/u

VAMOS++
Zero-degree setup
α-reaction efficiency ~ 4 %
Resolution E_x = 250 keV, θ = 0.5 deg

^{3}He/gold Target
10^{17} at.cm^{-2}
Beam Catcher

AGATA
31 crystals X 36 segments

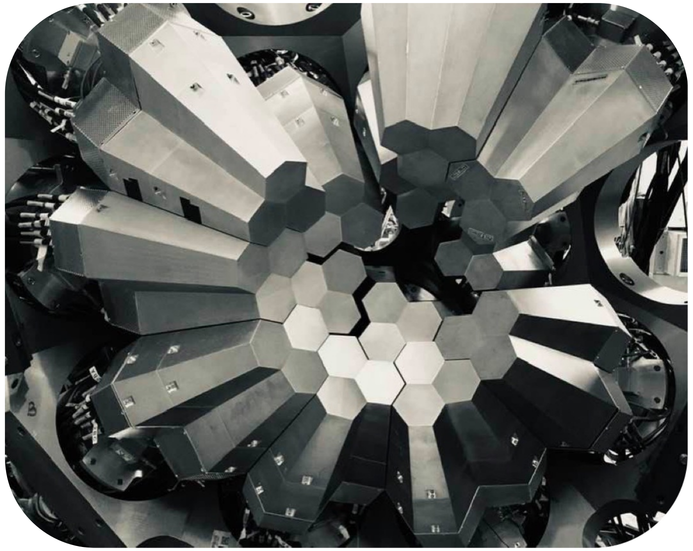

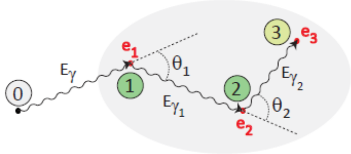

Compton tracking
global level

(X,Y,Z,E,t)$_i$

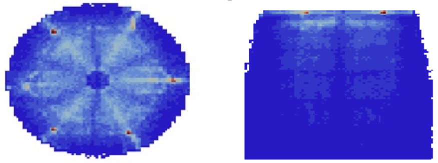

Pulse Shape Analysis
local level

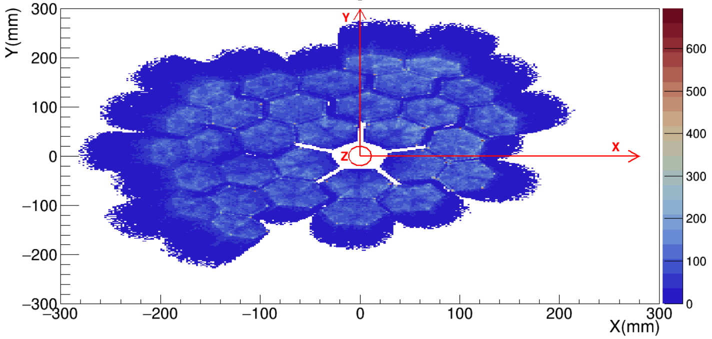

Reasonant state population

$^{3}He(^{24}Mg,^{4}He)^{23}Mg^{*}(\gamma)$

Doppler effect

$$E_\gamma = E_{\gamma,0}\frac{\sqrt{1-\beta^2}}{1-\beta\cos(\theta_{DS})}$$

$\beta_{ejectil}, \theta_{ejectil}, E_x{}^{VAMOS}$

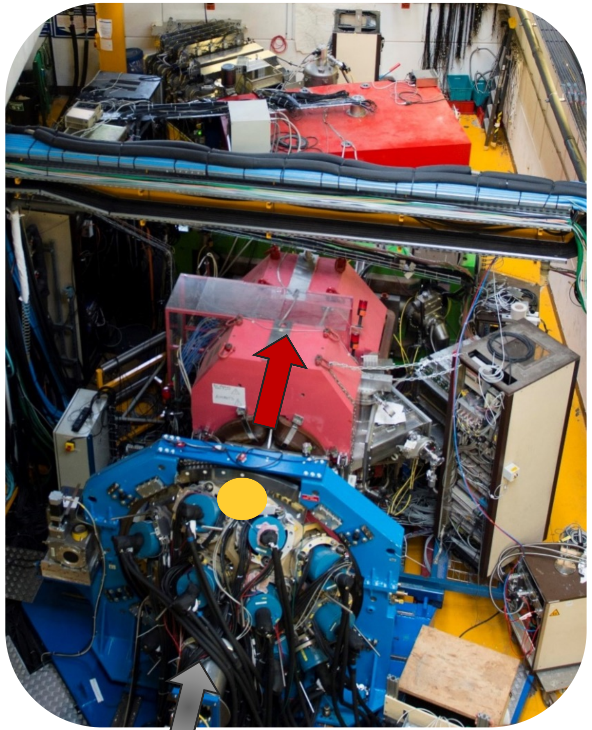

^{24}Mg at 4.6 MeV/u

VAMOS++
Zero-degree setup
α-reaction efficiency ~ 4
Resolution E_x = 250 ke

^{3}He/gold Target
10^{17} at.cm^{-2}
Beam Catcher

AGATA
31 crystals X 36 segments

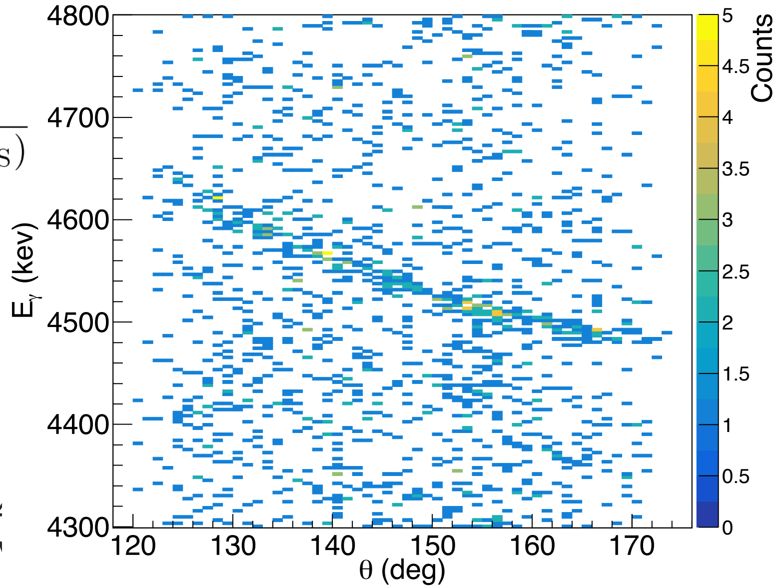

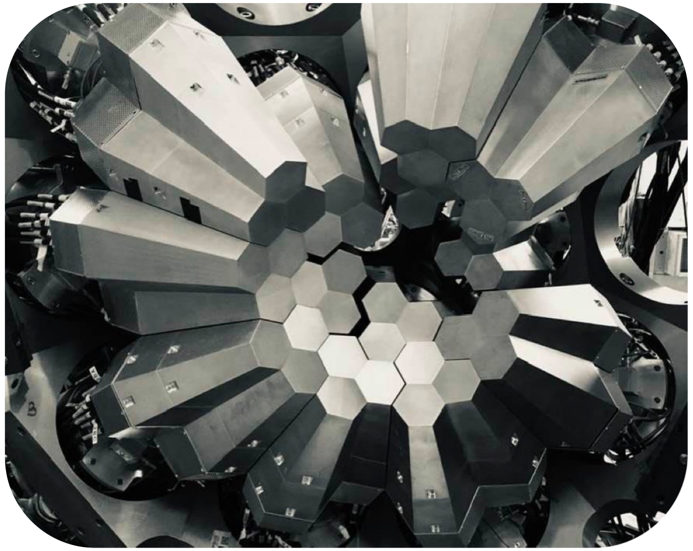

E_γ, θ_γ

Compton tracking
global level

$(Z,E,t)_i$

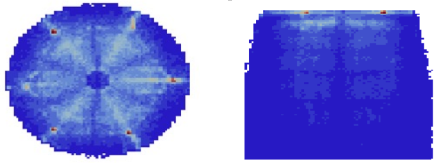

Pulse Shape Analysis
local level

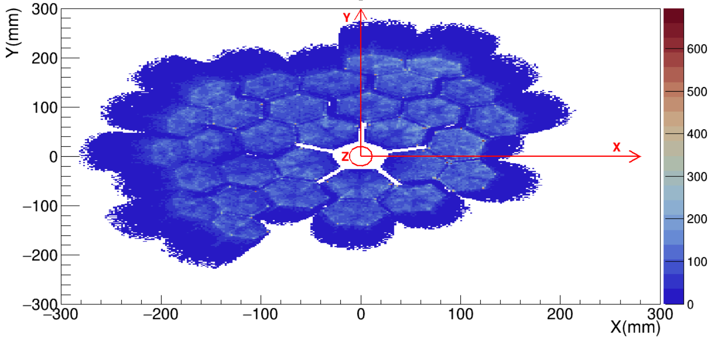

Reasonant state identification

^{3}He(^{24}Mg,^{4}He)^{23}Mg*(γ)

E_x^{VAMOS} E_γ^{DC}

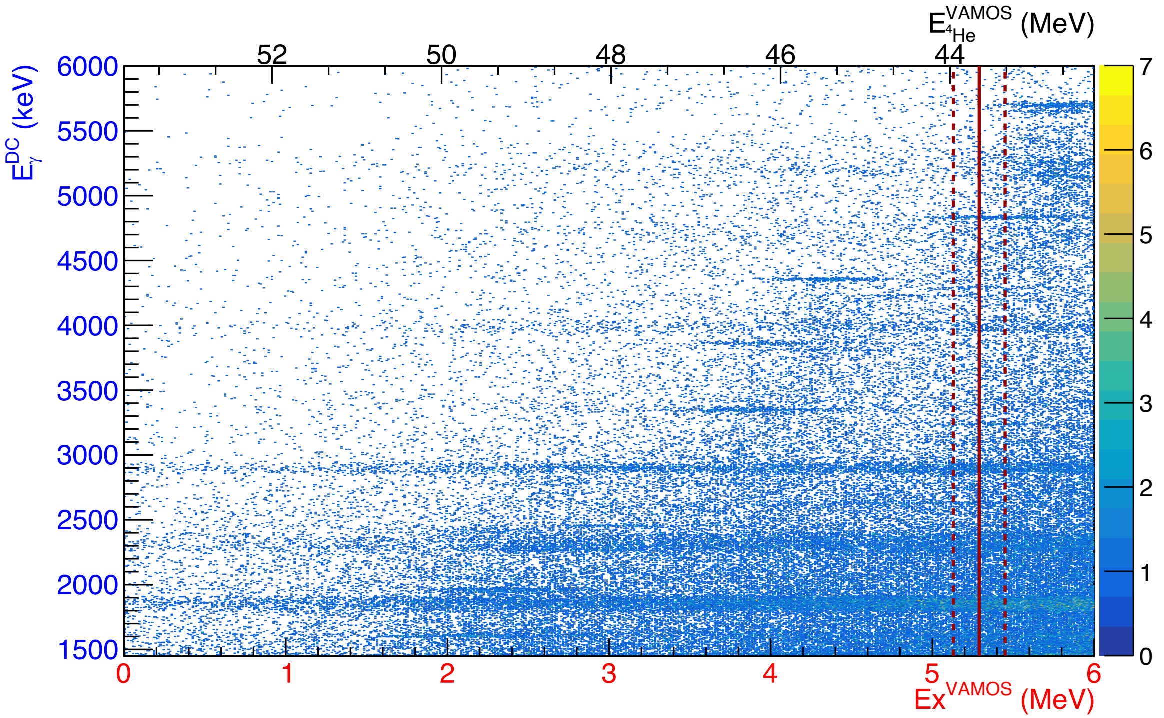

Reasonant state identification

$^{3}He(^{24}Mg,^{4}He)^{23}Mg^{*}(\gamma)$

E_x^{VAMOS} E_γ^{DC}

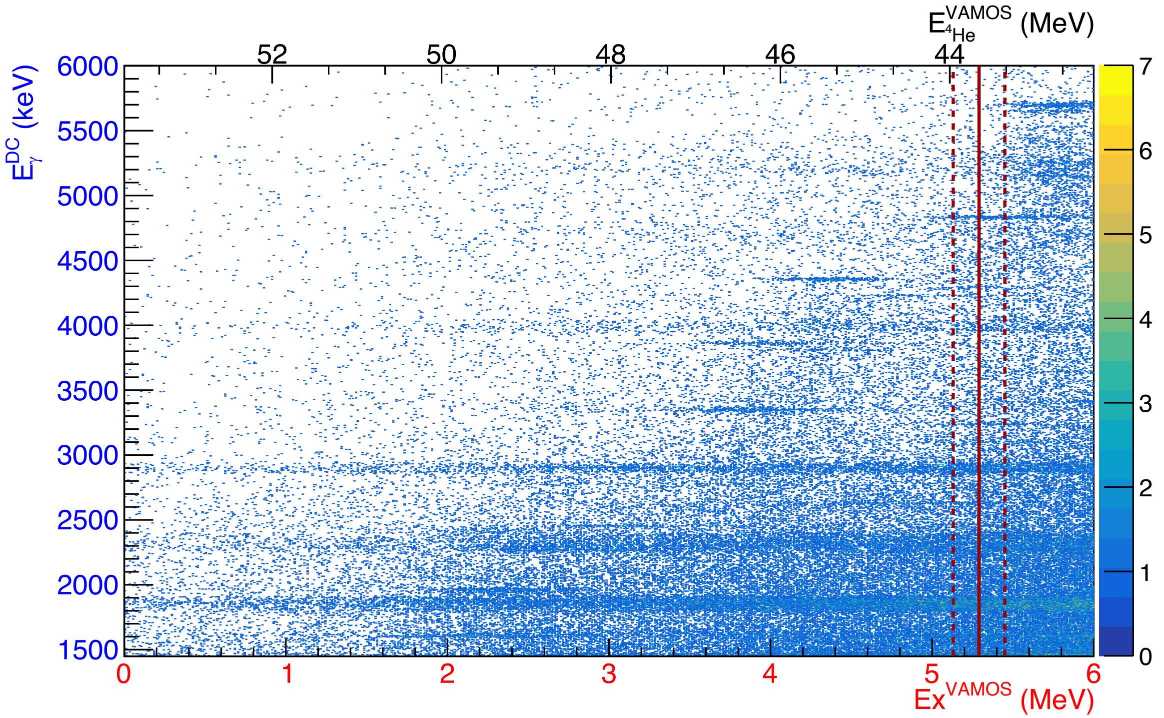

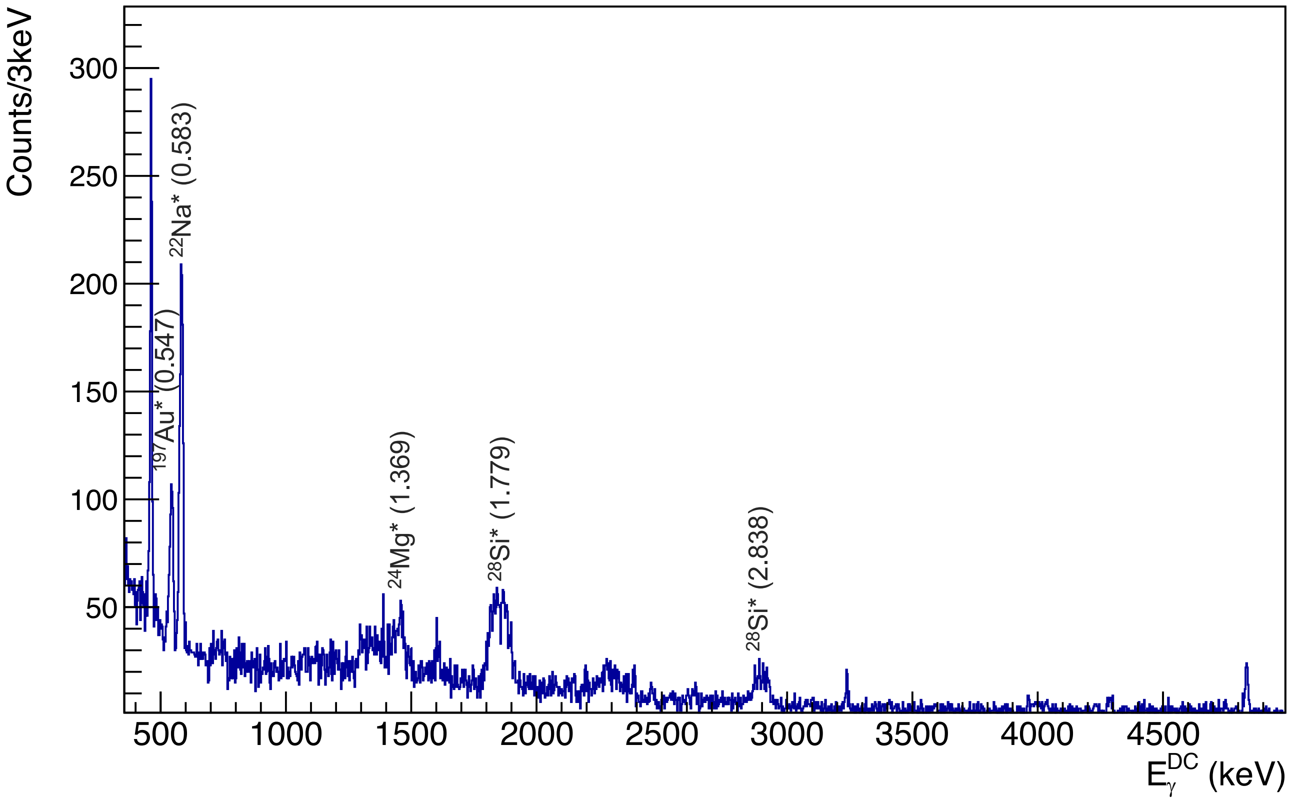

Reasonant state identification

^{3}He(^{24}Mg,^{4}He)^{23}Mg*(γ)

E_x^{VAMOS} E_γ^{DC}

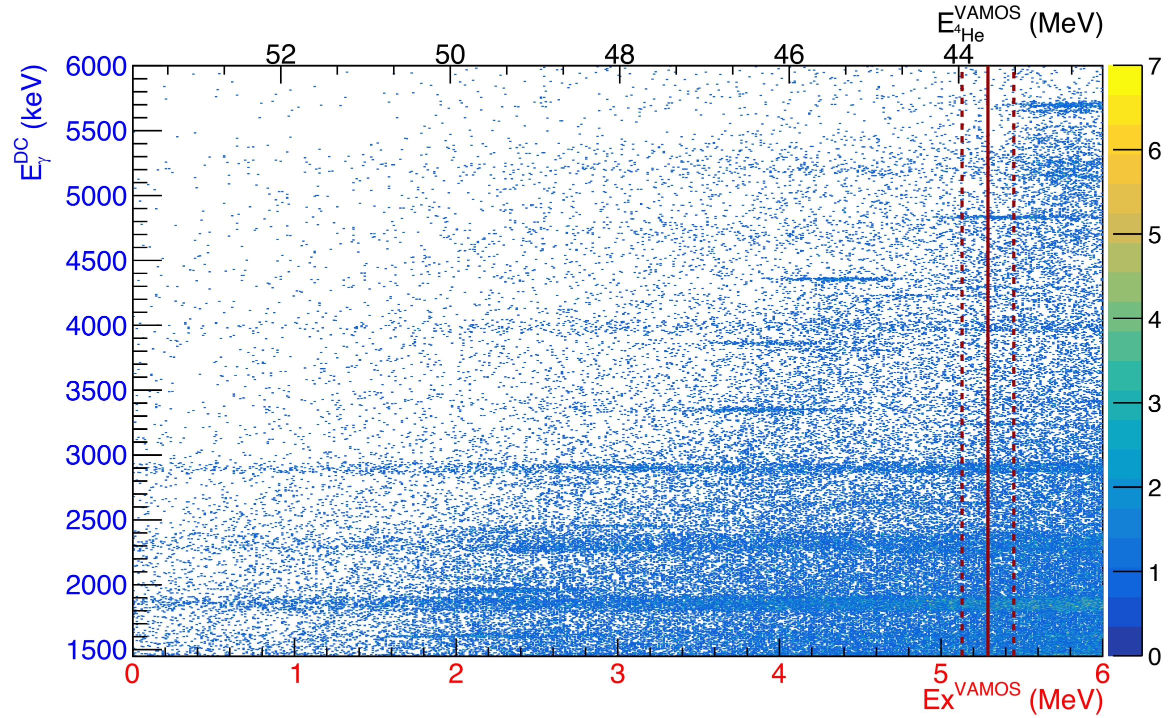

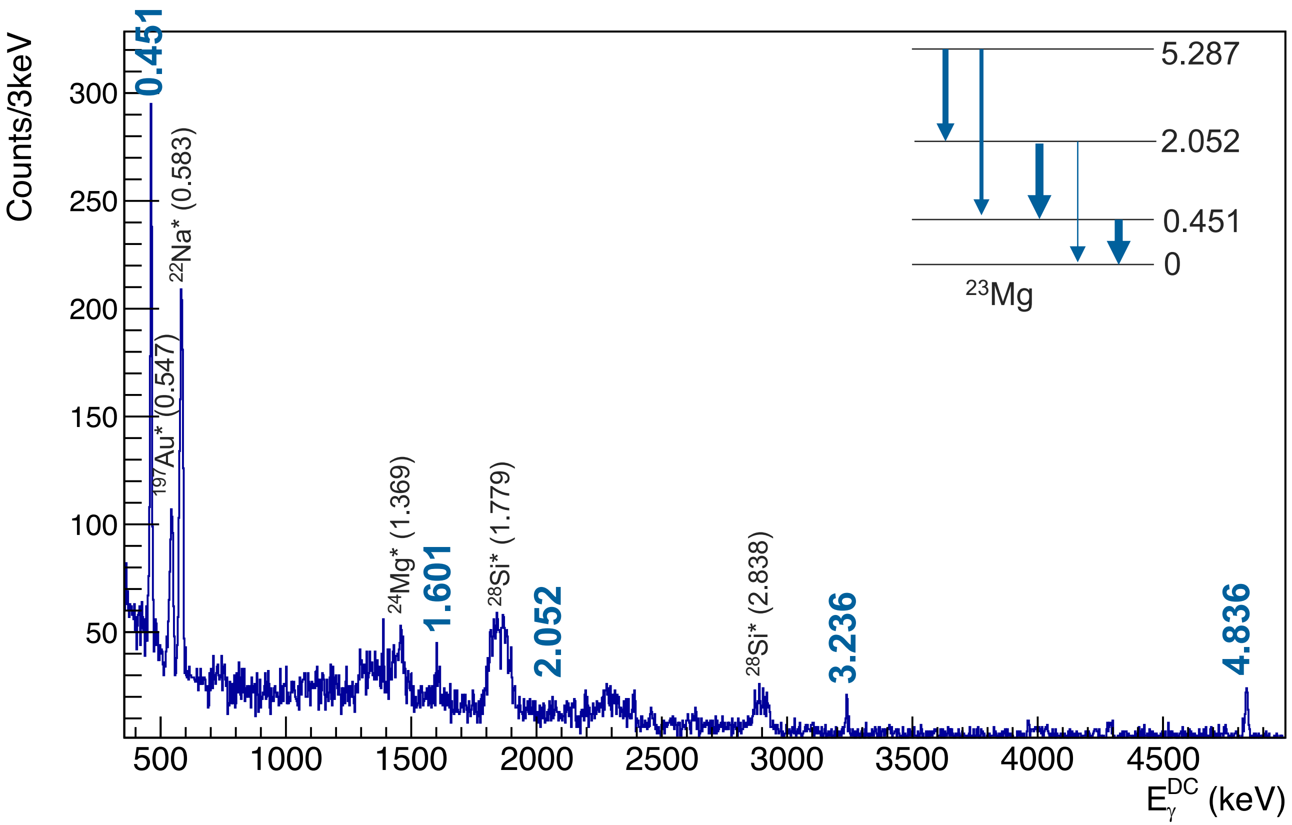

Accessing femtosecond nuclear lifetimes

$^{3}He(^{24}Mg,^{4}He)^{23}Mg^{*}(\gamma)$

(1) Particle-particle correlations

- β_{reac} from ($\beta_{beam}, \beta_{ejectil}, \theta_{ejectil}$) with 2-body kinematics
- β_{ems} from (E_{γ}, θ) with Doppler effect $\frac{R^2\cos(\theta) + \sqrt{1 + R^2\cos^2(\theta) - R^2}}{R^2\cos^2(\theta) + 1}$ $\quad R = \frac{E_{\gamma}}{E_{\gamma,0}}$

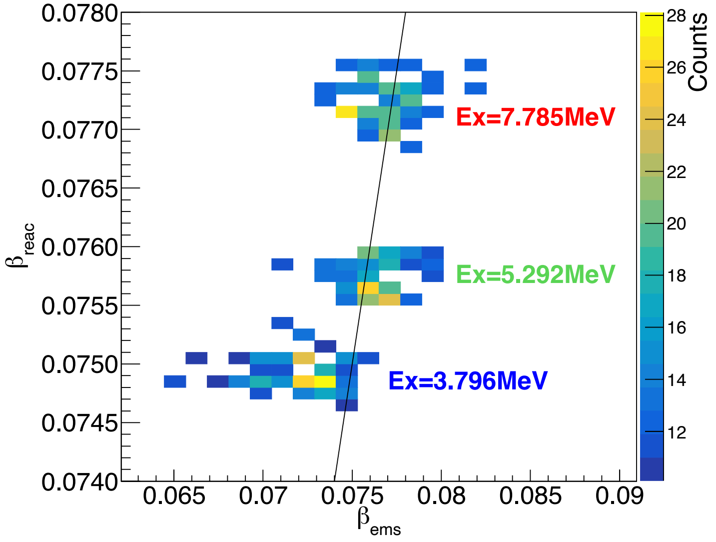

Accessing femtosecond nuclear lifetimes

$^{3}He(^{24}Mg,^{4}He)^{23}Mg^{*}(\gamma)$

(1) Particle-particle correlations

- β_{reac} from ($\beta_{beam}, \beta_{ejectil}, \theta_{ejectil}$) with 2-body kinematics
- β_{ems} from (E_{γ}, θ) with Doppler effect $\frac{R^2\cos(\theta) + \sqrt{1 + R^2\cos^2(\theta) - R^2}}{R^2\cos^2(\theta) + 1}$

(2) Angle-integrated velocity-difference profile

$\Delta\beta = \beta_{reac} - \beta_{ems}$

(3) χ^2 analysis

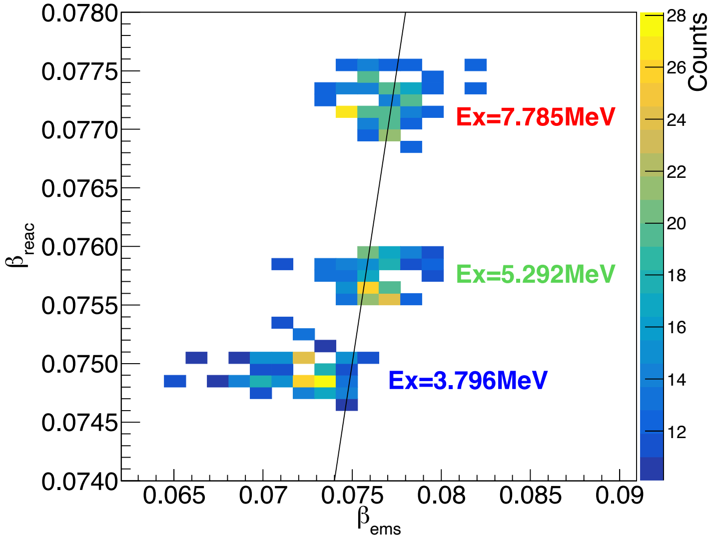

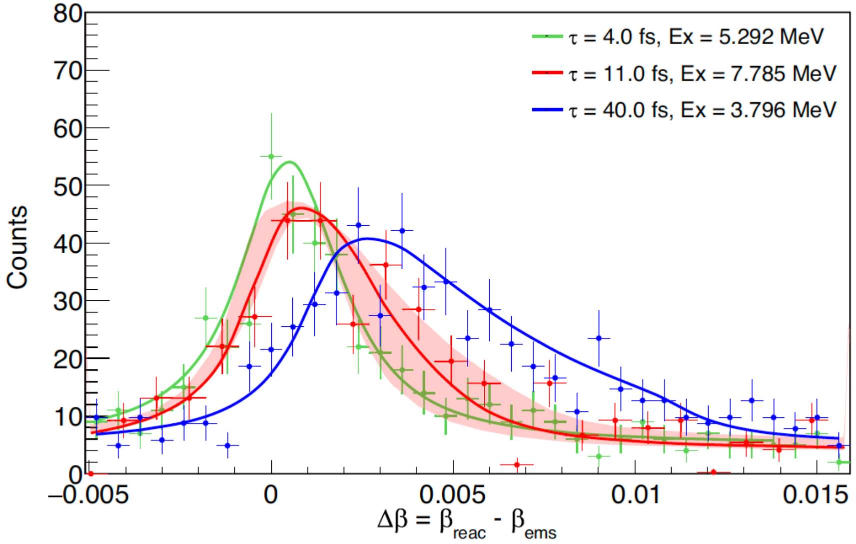

slowing-down in gold target

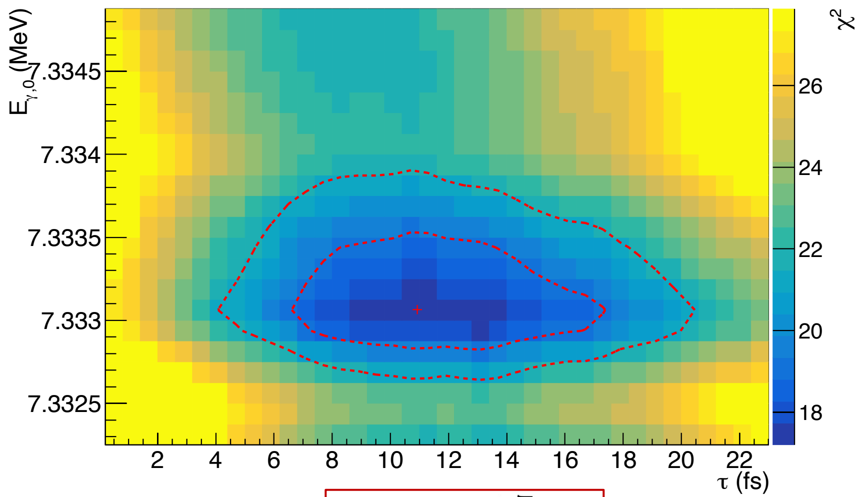

$\tau = 11^{+7}_{-5}$ fs

High energy and spatial resolution for particle- and γ–ray spectrometers

Fougères, Nat. Commun. **14** (2023)

Accessing *p*-branching-ratio

$^{3}He(^{24}Mg,^{4}He)^{23}Mg^{*}(p)$

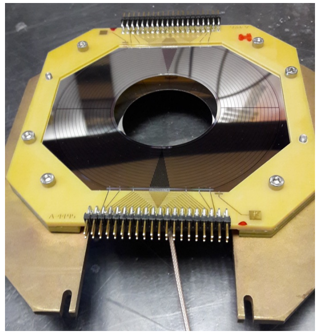

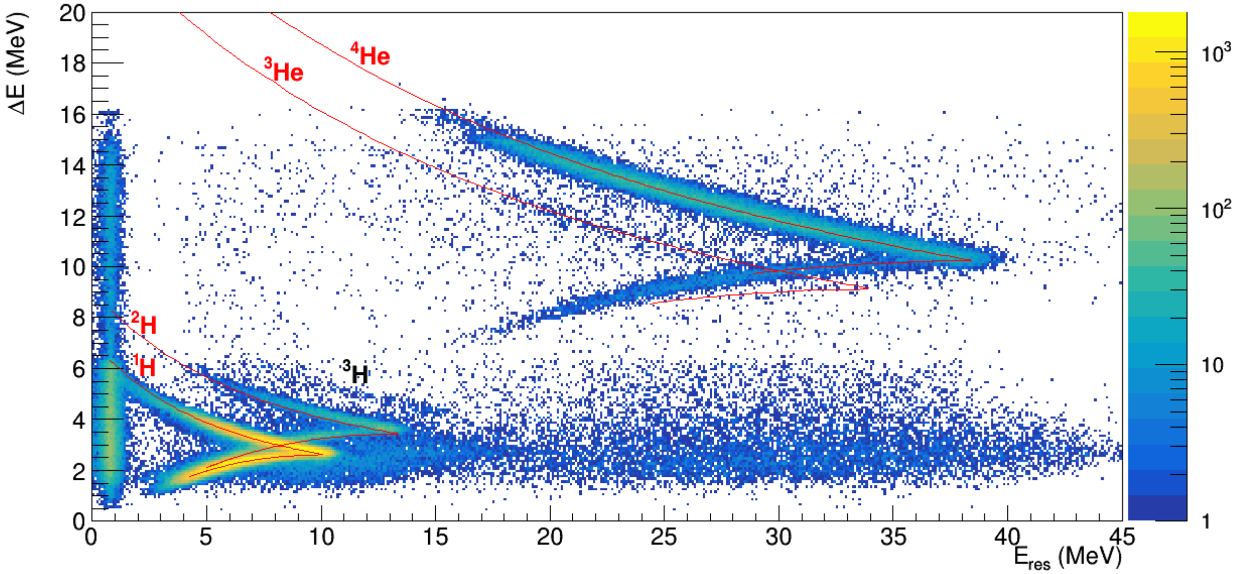

SPIDER

Si telescope ΔE-E

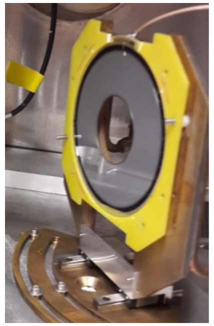

Accessing *p*-branching-ratio

$^{3}He(^{24}Mg,\mathbf{^{4}He})^{23}Mg^{*}(p)$

***p*-branching:** particle-particle correlation

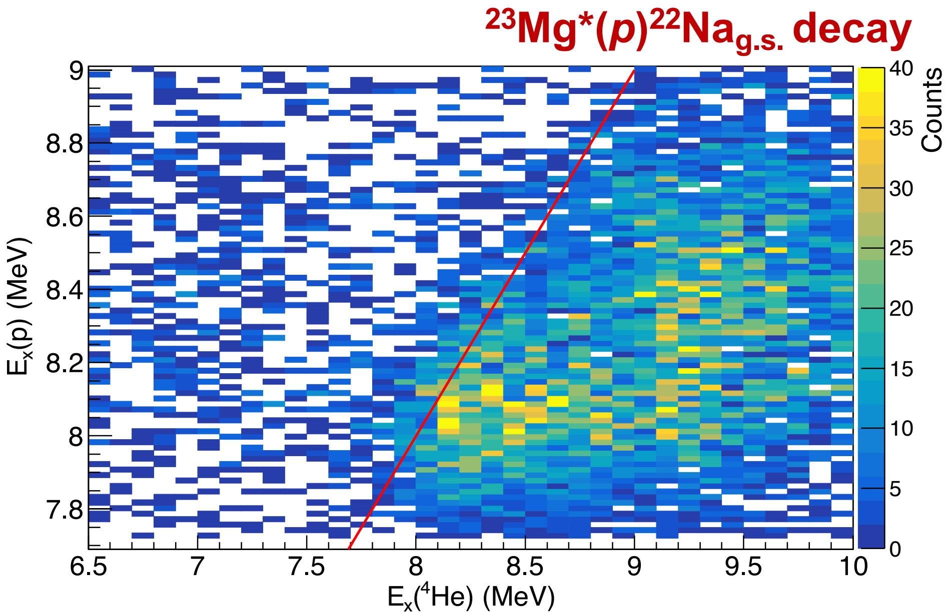

$^{22}Na(p,\gamma)^{23}Mg$

Accessing *p*-branching-ratio

$^{3}He(^{24}Mg,\mathbf{^{4}He})^{23}Mg^{*}(p)$

***p*-branching:** particle-particle correlation and quantification of excited state decay channels $BR_p = 1 / (1 + Counts_{Ex\&\gamma} / Counts_{Ex\&p})$

$^{23}Mg^{*}(p)^{22}Na_{g.s.}$ decay

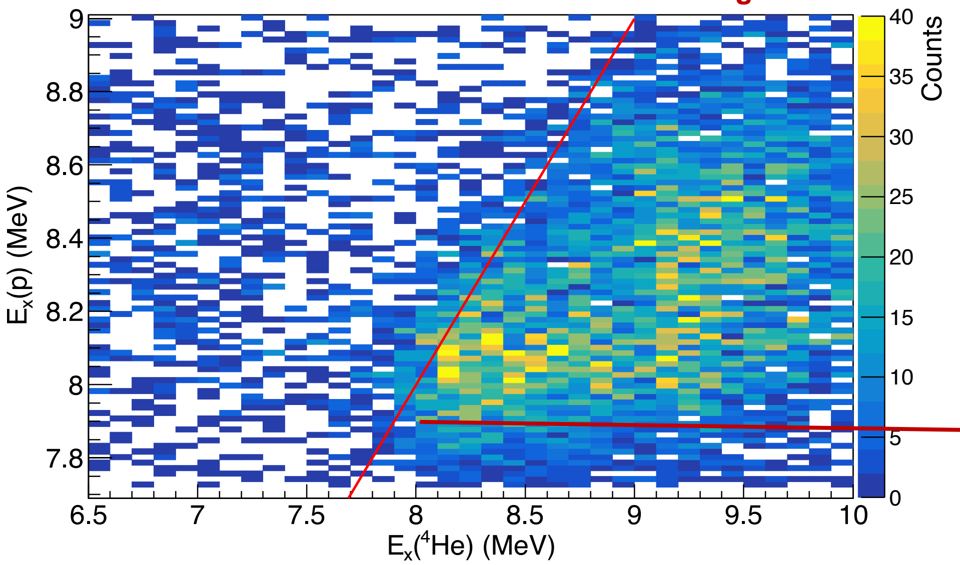

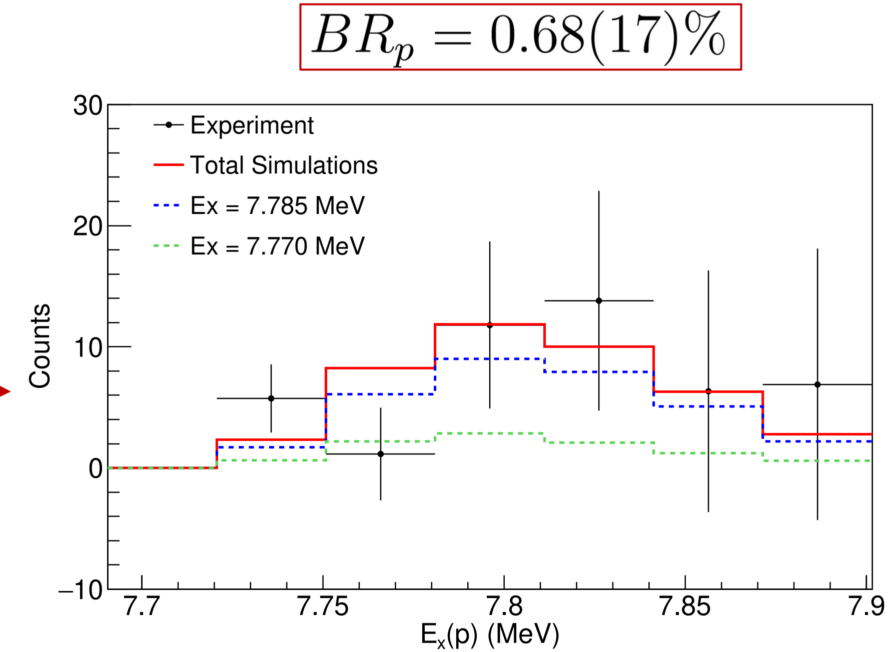

Fougères, Nat. Commun. ***14*** *(2023)*

3. Towards observations

Determination of reaction rates

E710 *C. Michelagnoli, F. de Oliveira Santos, C.Fougères, et al.*

^{3}He(^{24}Mg,^{4}He)^{23}Mg* @4.6MeV/u

(lifetime, p-branching) of p-unbound state

laboratoire commun CEA/DRF CNRS/IN2P3

Determination of reaction rates

E710 *C. Michelagnoli, F. de Oliveira Santos, C.Fougères, et al.*

$^{3}He(^{24}Mg,^{4}He)^{23}Mg^{*}$ @4.6MeV/u

(lifetime, *p*-branching) of *p*-unbound state

laboratoire commun CEA/DRF CNRS/IN2P3

$$\omega\gamma = 0.24^{+0.11}_{-0.04}\ \mathrm{meV}$$

Determination of reaction rates

E710 *C. Michelagnoli, F. de Oliveira Santos, C.Fougères, et al.*

$^{3}He(^{24}Mg,^{4}He)^{23}Mg^{*}$ @4.6MeV/u

(lifetime, *p*-branching) of *p*-unbound state

$$\omega\gamma = 0.24^{+0.11}_{-0.04}\ \mathrm{meV}$$

Monte-Carlo calculations

`RatesMC` on github *Longland, Nuc. Phys. A **240** (2010)*

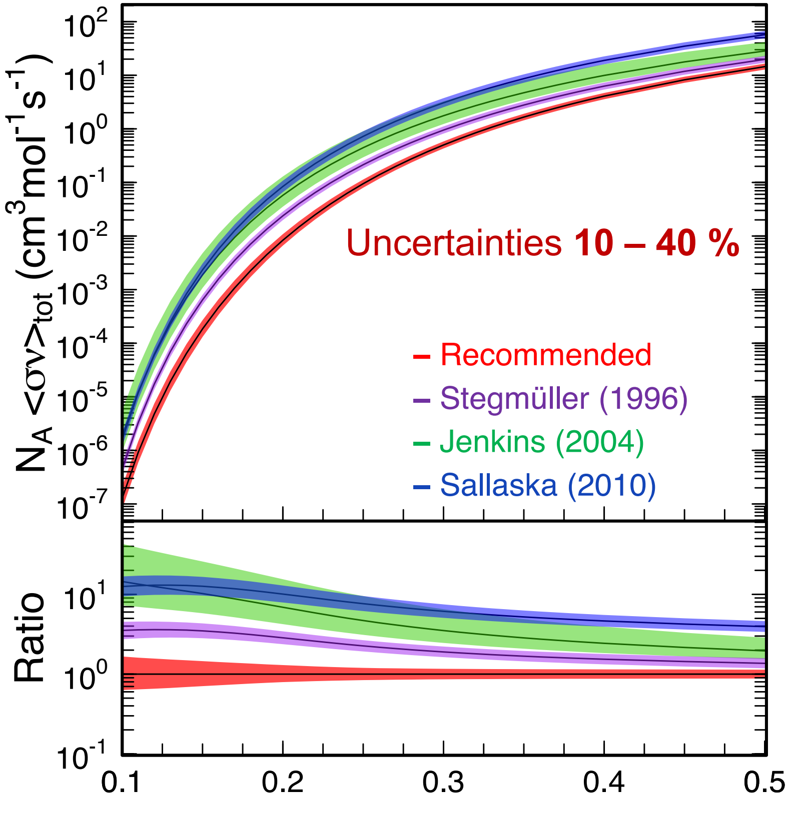

Determination of reaction rates

E710 *C. Michelagnoli, F. de Oliveira Santos, C.Fougères, et al.*

^{3}He(^{24}Mg,^{4}He)^{23}Mg* @4.6MeV/u

(lifetime, *p*-branching) of *p*-unbound state

$$\omega\gamma = 0.24^{+0.11}_{-0.04}\ \text{meV}$$

Monte-Carlo calculations

`RatesMC` on github *Longland, Nuc. Phys. A **240** (2010)*

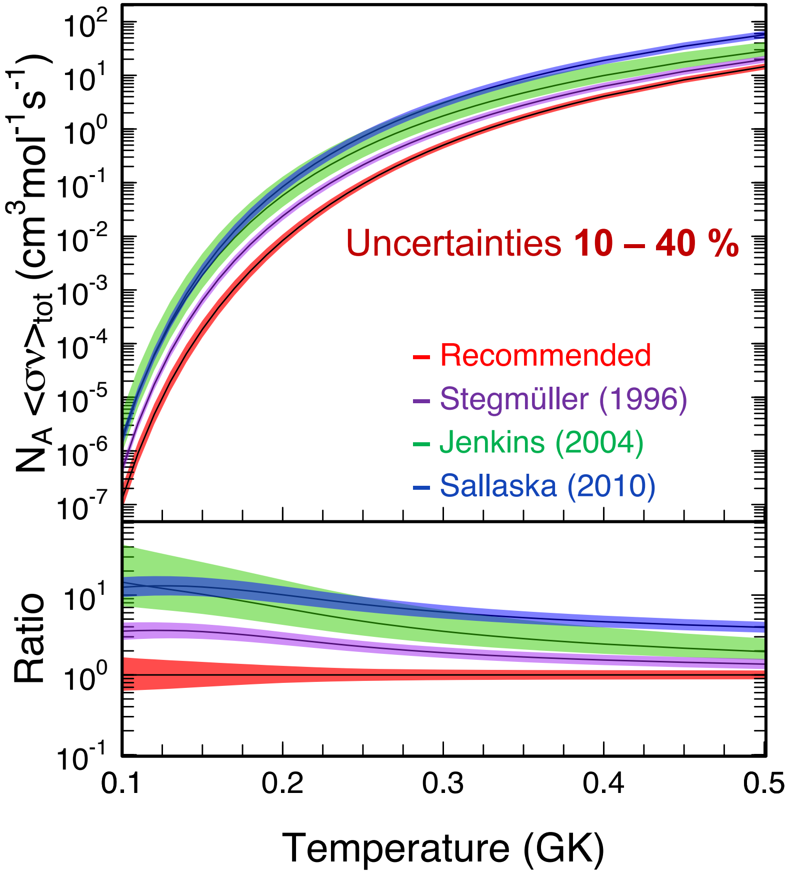

Impact on ejected ^{22}Na in novae?

Expectations in ONe novae (1)

Stellar modelling

MESA
Paxton, *Astrophys. J. Suppl. Ser.* **208** (2013)

SHIVA
José, *CRC Press* (2016)

Model	115a	115b	125	135
HD code	*MESA*	*SHIVA*	*SHIVA*	*SHIVA*
Input parameter M_{WD} ($M_\odot$)	1.15	1.15	1.25	1.35
R_{WD} (km)	4428	4334	3797	2258
T_{peak} (10^8 K)	2.12	2.27	2.48	3.13
M_{ejec} (10^{-5} $M_\odot$)	4.63	2.46	1.90	0.46
^{22}Na abundance in novae **X(^{22}Na)**	**3.1×10^{-4}**	**3.2×10^{-4}**	**3.7×10^{-4}**	**9.1×10^{-4}**

Fougères, *Nat. Commun.* **14** (2023)

Expectations in ONe novae (2)

Stellar modelling

Paxton, Astrophys. J. Suppl. Ser. ***208*** *(2013)*

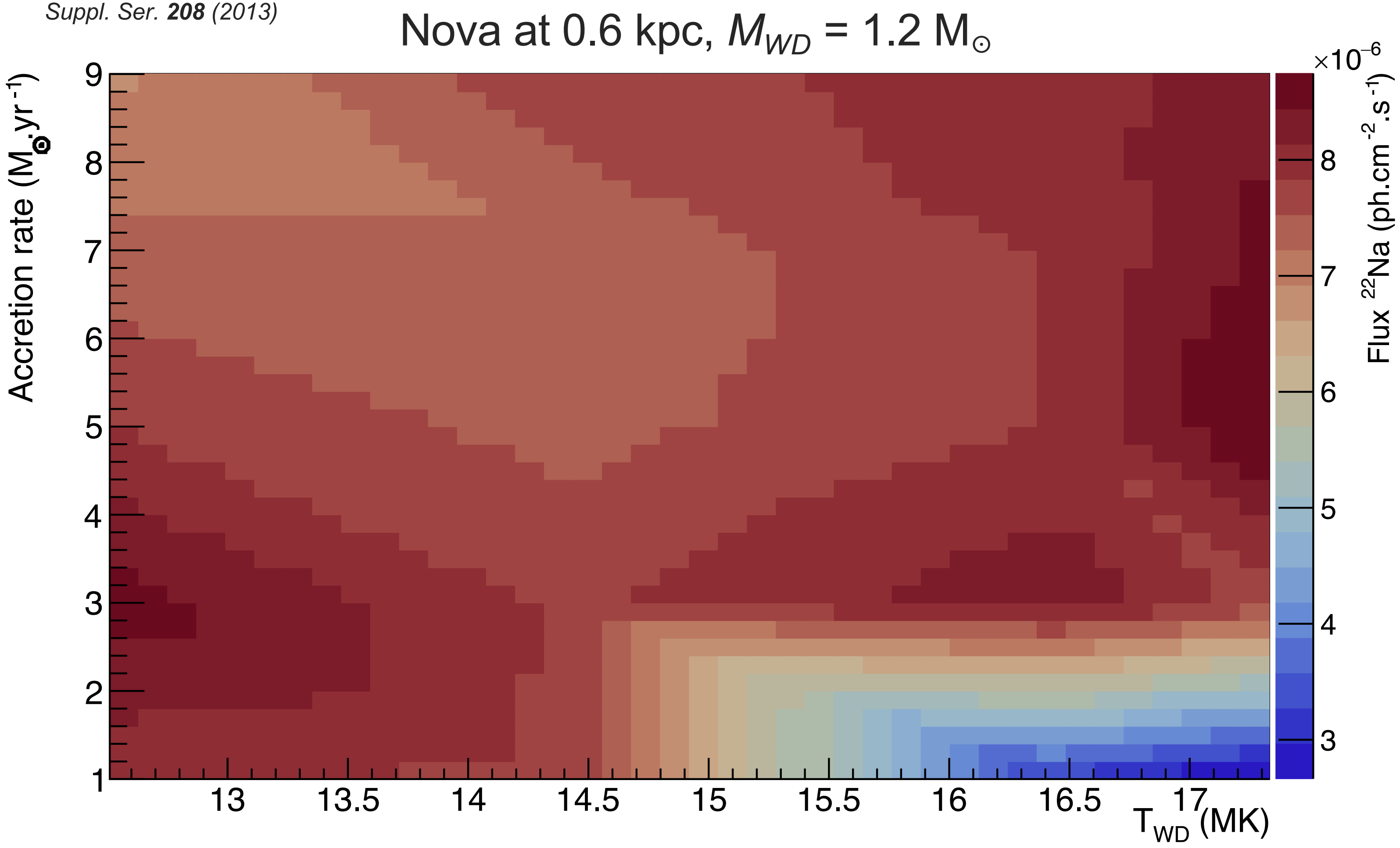

Expectations in ONe novae (2)

Stellar modelling MESA

Paxton, Astrophys. J. Suppl. Ser. **208** (2013)

Input parameter

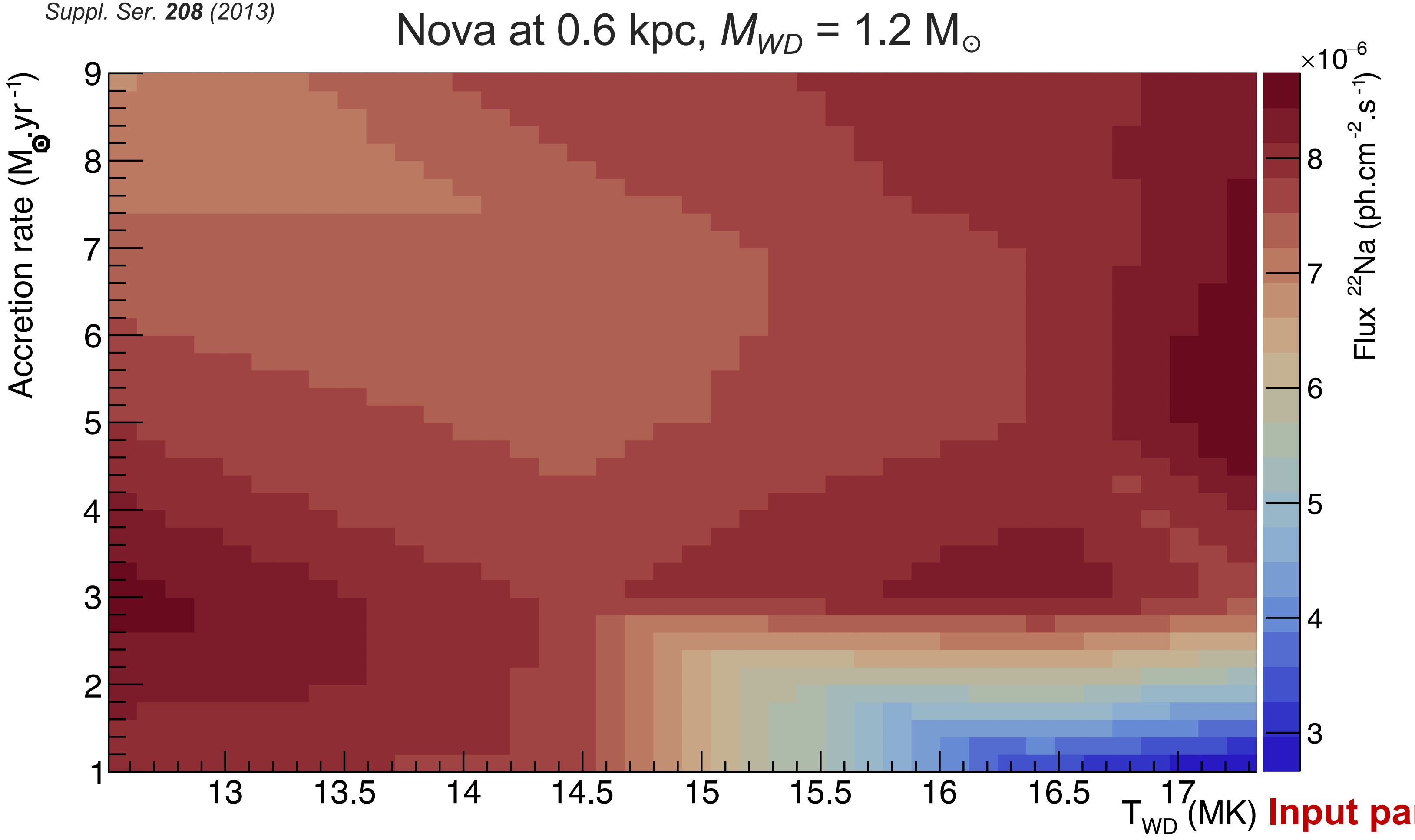

Input parameter

Expectations in ONe novae (2)

Stellar modelling MESA

Paxton, Astrophys. J. Suppl. Ser. **208** (2013)

Input parameter

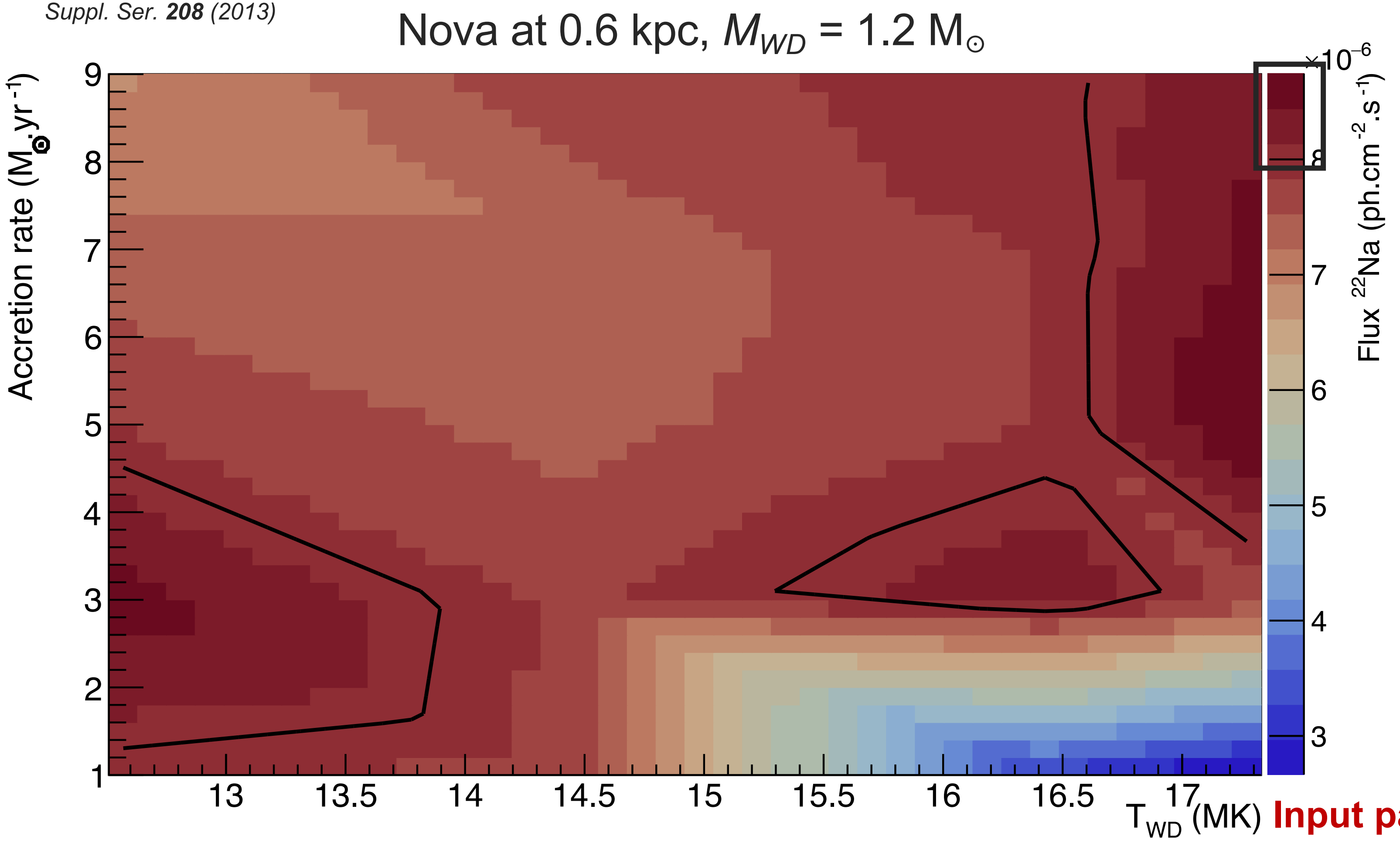

Input parameter

Constrain novae parameters with observed flux

Fougères, Nat. Commun. **14** (2023)

Future of low energy γ–ray astronomy (1)

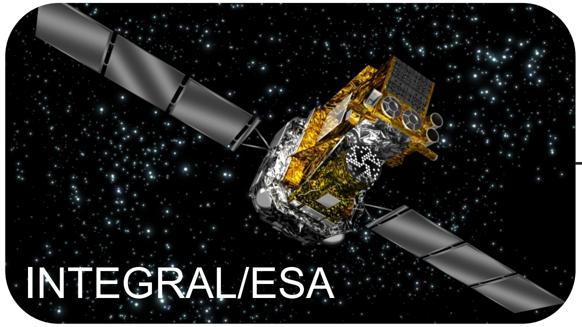

~ 2027

Photon sensitivity = 1.7×10^{-6} ph.cm^{-2}s^{-1}
Energy range = [0.2, 5] MeV

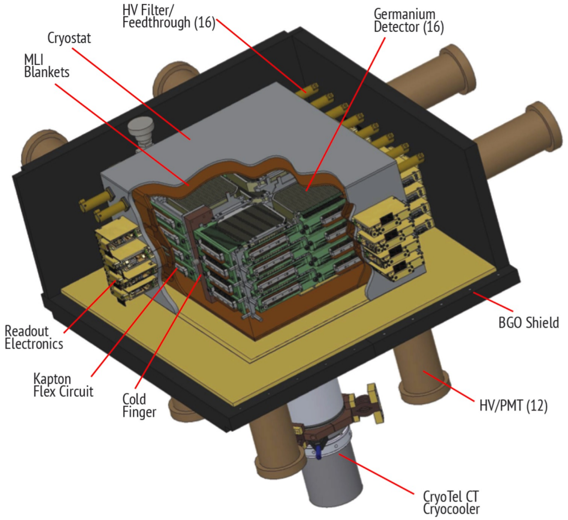

*Tomsick, Proc. Of Science **444** (2023)*

Future of low energy γ–ray astronomy (1)

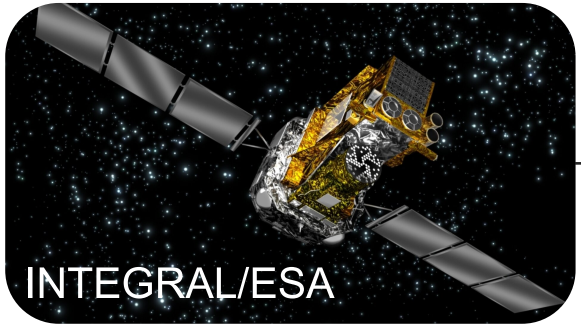

~ 2027

Photon sensitivity = 1.7×10^{-6} ph.cm^{-2}s^{-1}
Energy range = [0.2, 5] MeV

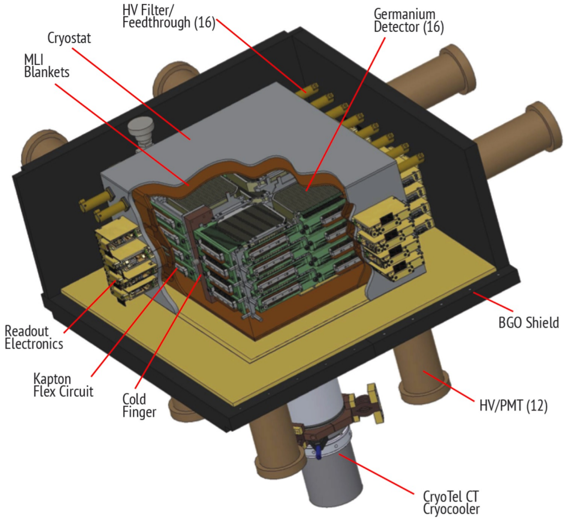

*Tomsick, Proc. Of Science **444** (2023)*

R.D.

« AMEGO/NASA »

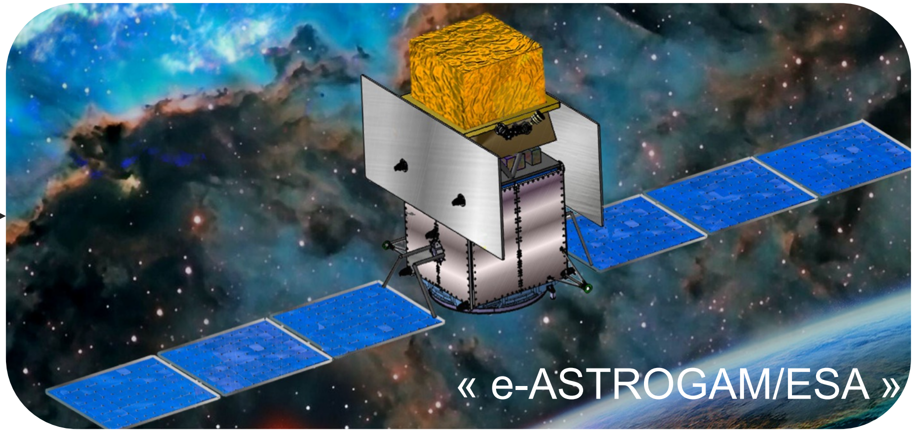

Photon sensitivity = 3×10^{-6} ph.cm^{-2}s^{-1}
Energy range = [0.3, 3000] MeV

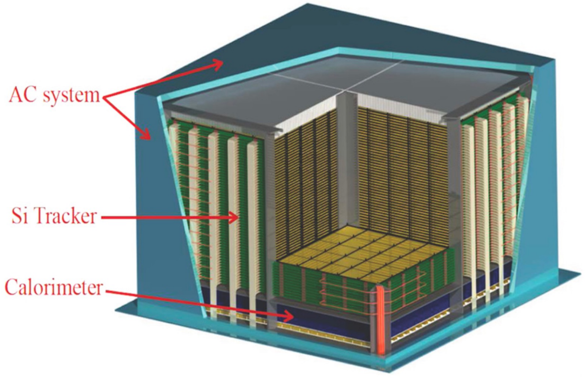

*De Angelis, Tatischeff, Journ. of High E. Astro. **19** (2018)*

Future of low energy γ–ray astronomy (2)

Survey of 8 observed ONe novae (60 yr) *Hachisu, Astrophys. J. Suppl. Ser.* ***242*** *(2019)* *José, CRC Press (2016)*

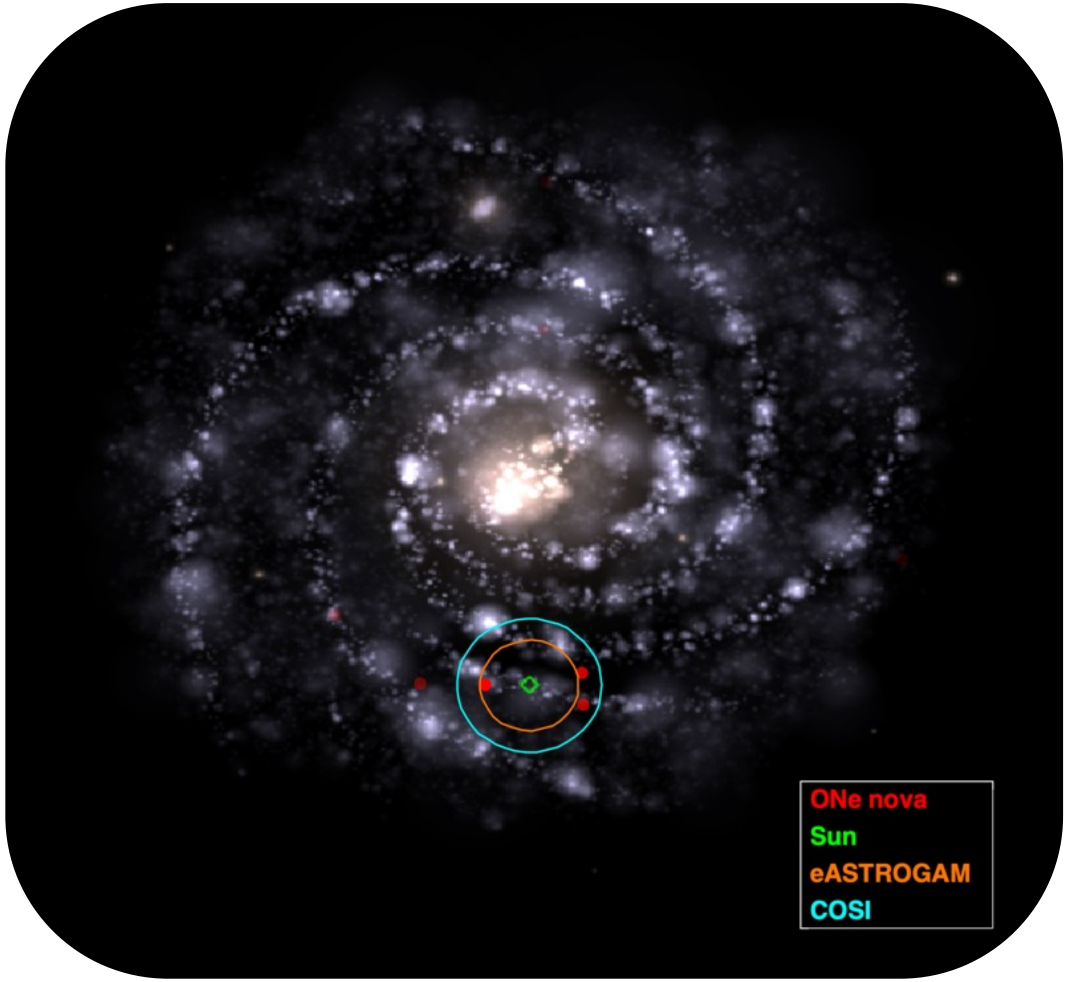

Future of low energy γ–ray astronomy (2)

Survey of 8 observed ONe novae (60 yr) *Hachisu, Astrophys. J. Suppl. Ser.* ***242*** *(2019)* *José, CRC Press (2016)*

^{22}Na γ–ray flux

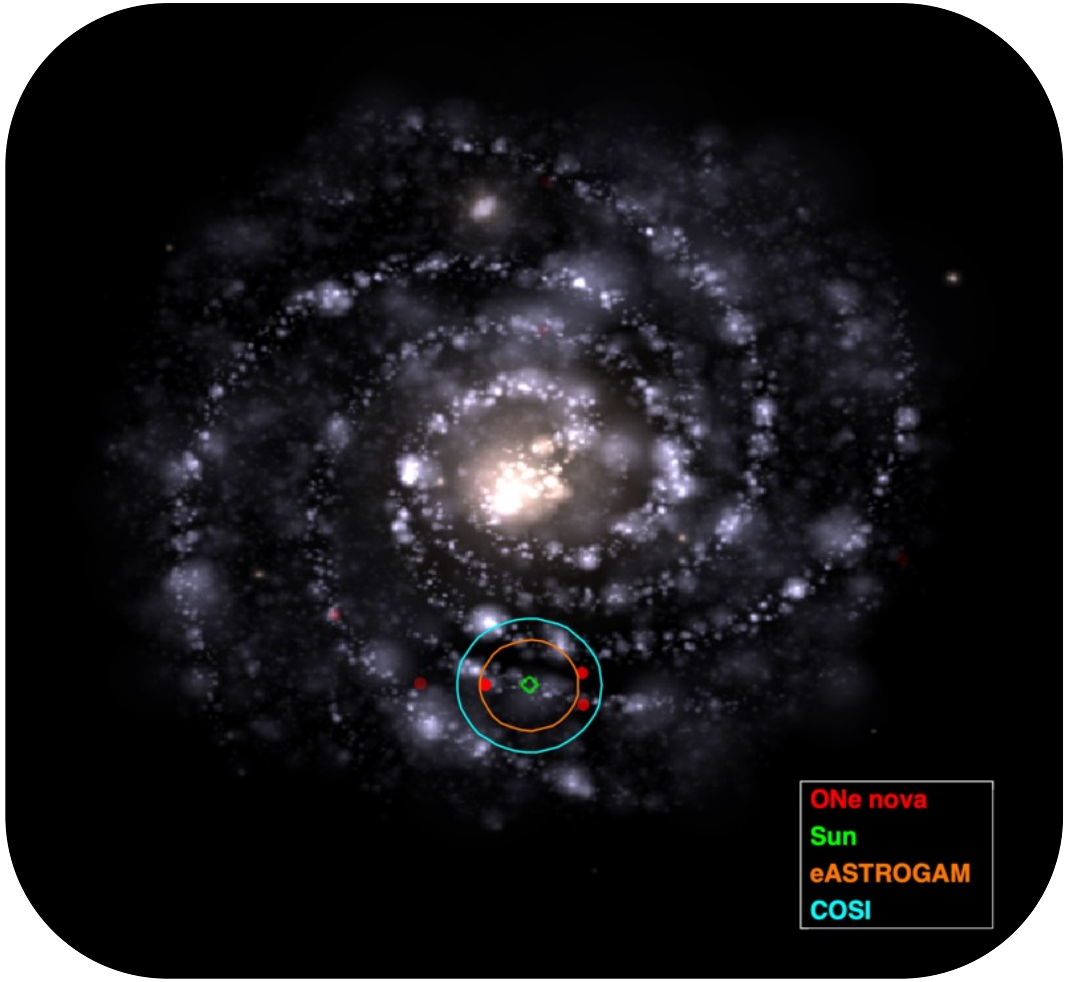

Future of low energy γ–ray astronomy (2)

Survey of 8 observed ONe novae (60 yr) *Hachisu, Astrophys. J. Suppl. Ser.* ***242*** *(2019)* *José, CRC Press (2016)*

^{22}Na γ–ray flux

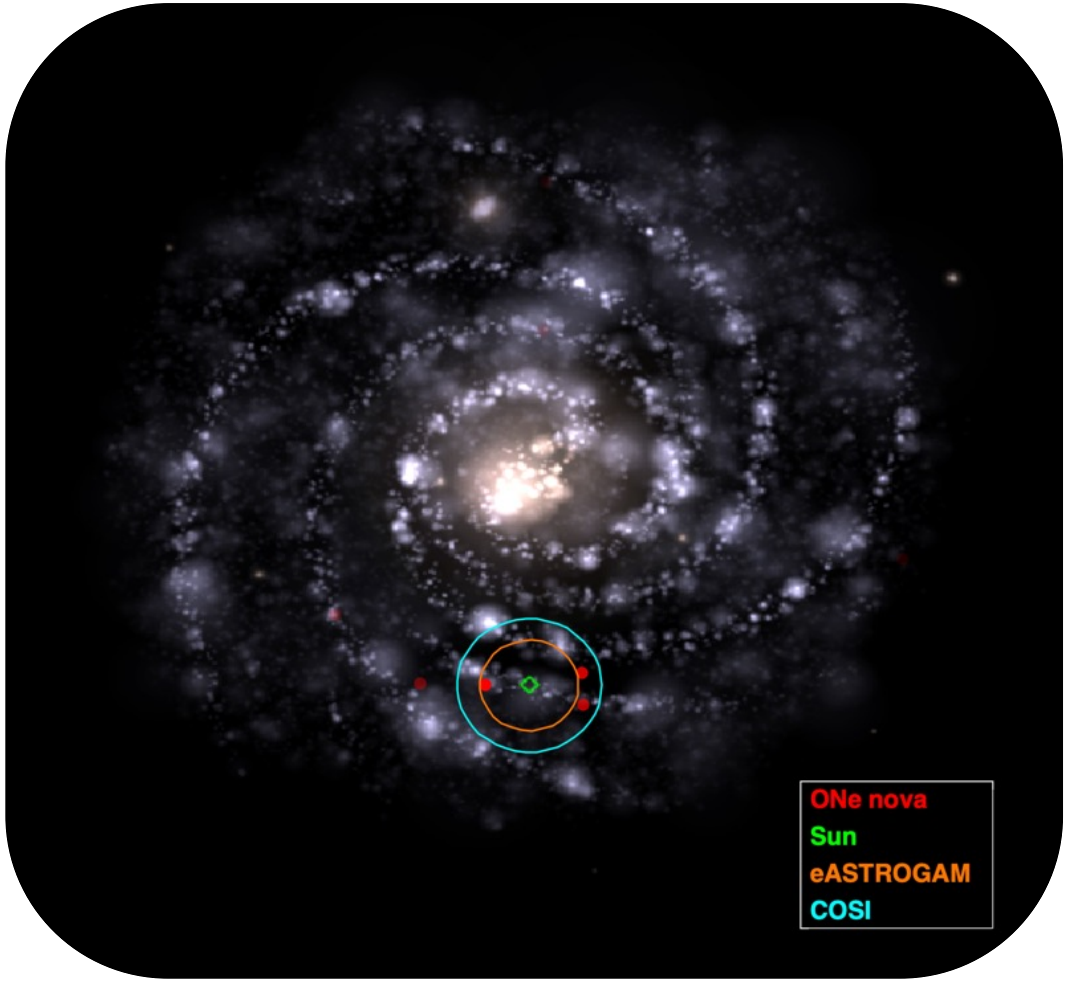

Limit in detection distance

e-ASTROGAM *De Angelis (2018)*

2.7(5) kpc

COSI *Tomsick (2020)*

4.0(7) kpc

Low limit in detection frequency

≥1 event / 60 yr

≥1 event / 20 yr

Future of low energy γ–ray astronomy (2)

Survey of 8 observed ONe novae (60 yr) *Hachisu, Astrophys. J. Suppl. Ser.* ***242*** *(2019)* *José, CRC Press (2016)*

^{22}Na γ–ray flux

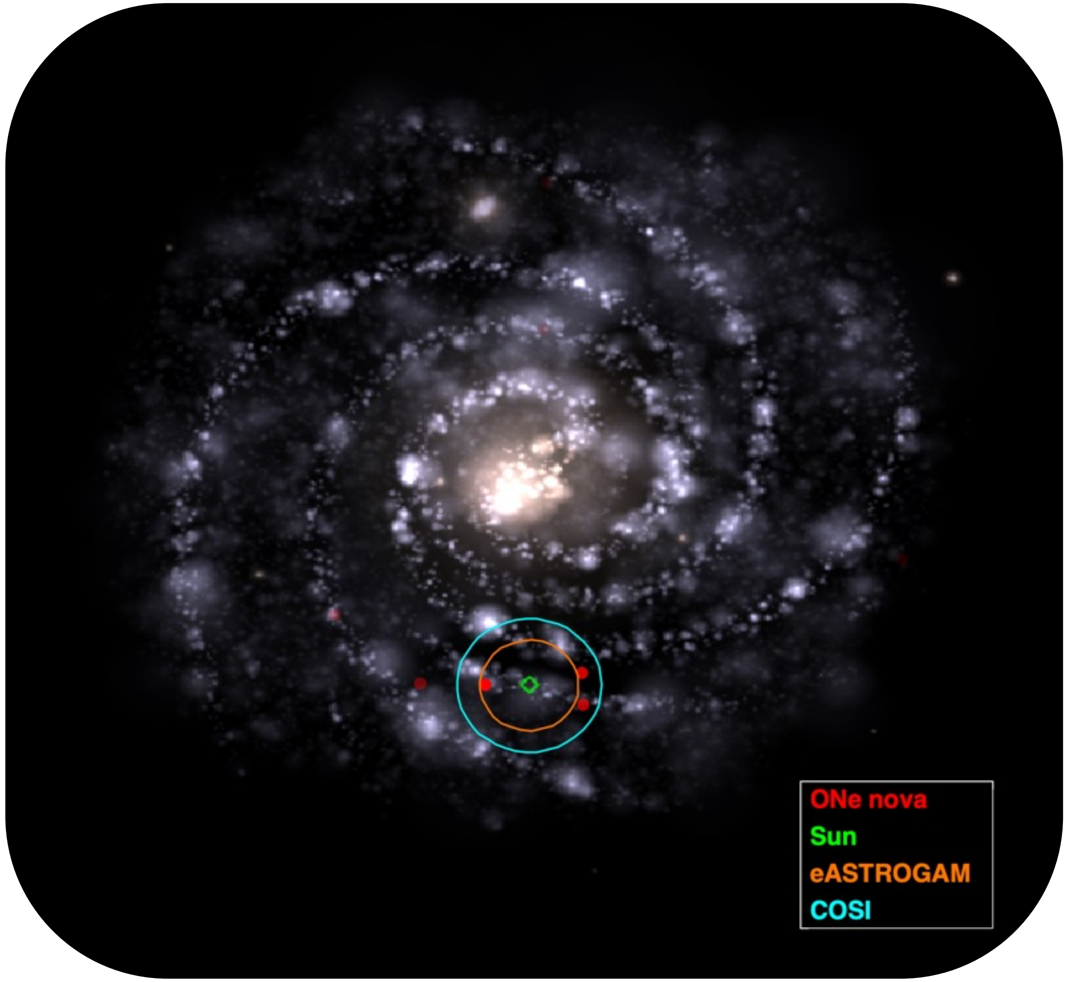

Limit in detection distance

e-ASTROGAM *De Angelis (2018)*

R_{det} *2.7(5) kpc*

COSI *Tomsick (2020)*

R_{det} *4.0(7) kpc*

Low limit in detection frequency

≥1 event / 60 yr

≥1 event / 20 yr

High limit

$F_{novae} \times (R_{det.} / R_{galaxy})^2$

Future of low energy γ–ray astronomy (2)

Survey of 8 observed ONe novae (60 yr) *Hachisu, Astrophys. J. Suppl. Ser.* ***242*** *(2019)* *José, CRC Press (2016)*

^{22}Na γ–ray flux

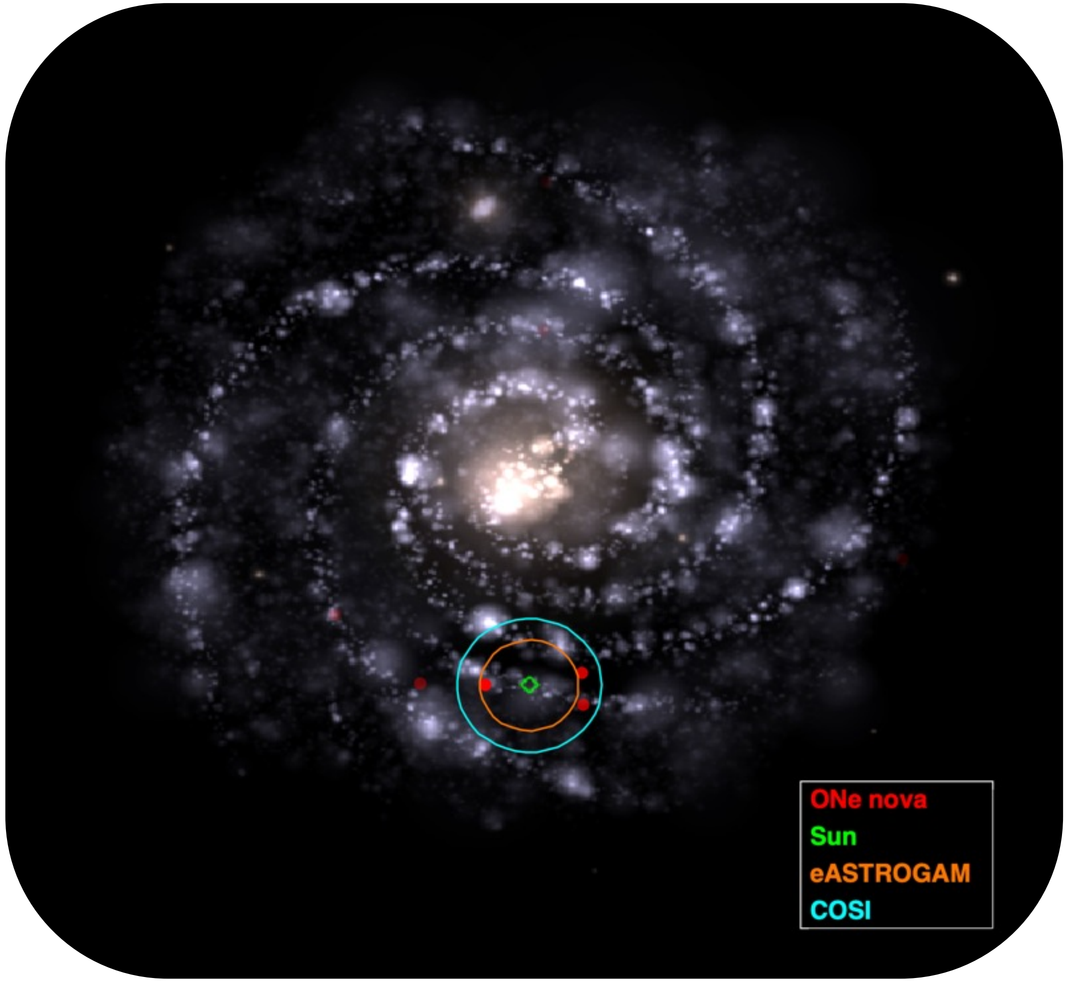

Limit in detection distance

e-ASTROGAM *De Angelis (2018)*

R_{det} *2.7(5) kpc*

COSI *Tomsick (2020)*

R_{det} *4.0(7) kpc*

Detection frequency

1 evt / 3 yr ≥ F ≥ 1 evt / 60 yr

3 evt / 4 yr ≥ F ≥ 1 evt / 20 yr

4. Future investigations?

Measurements of *p*–capture resonances strengths

Constraining sulphur Abundances in Novae presolar grains: $^{32}S/^{33}S$ strong hint of novae origin w.r.t. SNe II?

$^{33}Cl(p,\gamma)^{34}Ar$ **unc. rate >x2**

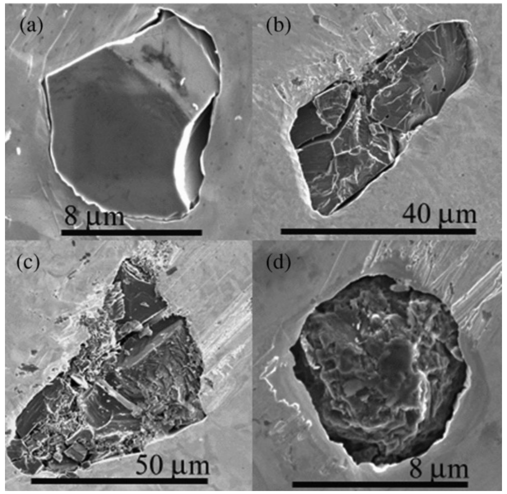

Measurements of *p*–capture resonances strengths

Constraining sulphur Abundances in Novae presolar grains: $^{32}S/^{33}S$ strong hint of novae origin w.r.t. SNe II?

$^{33}Cl(p,\gamma)^{34}Ar$ **unc. rate >x2**

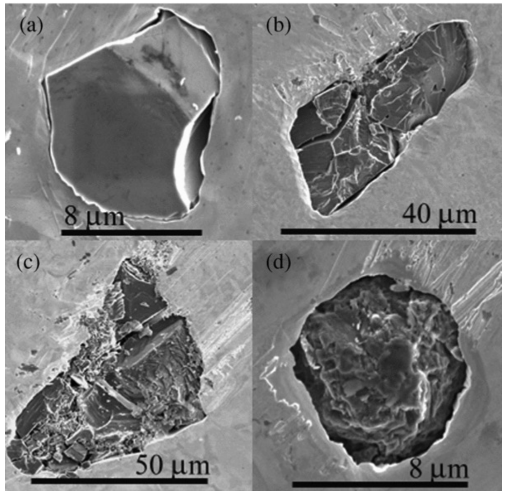

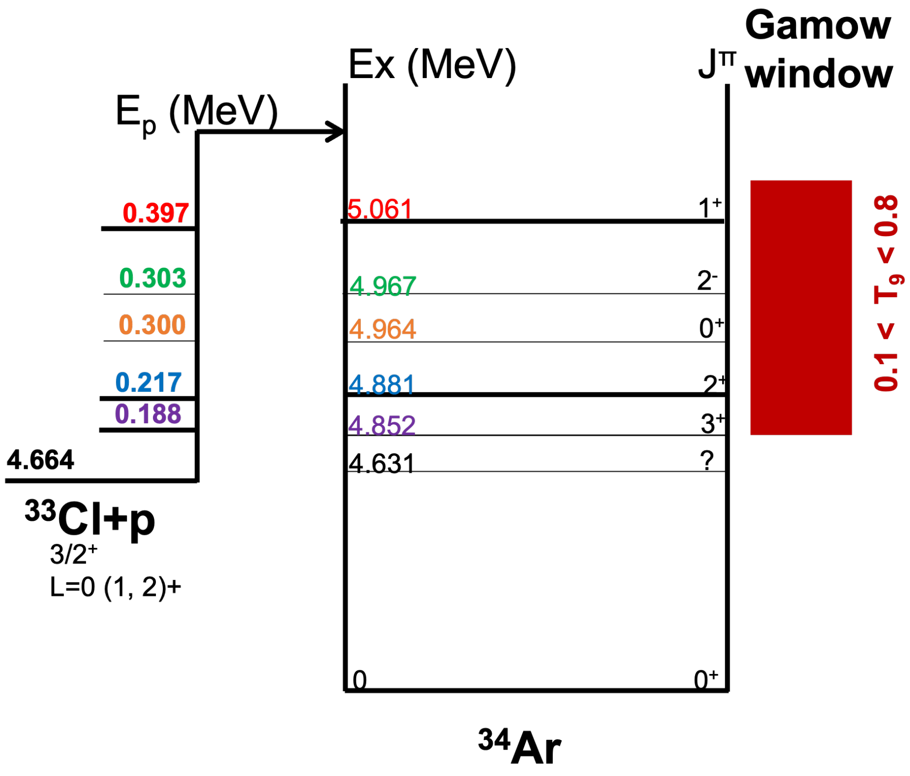

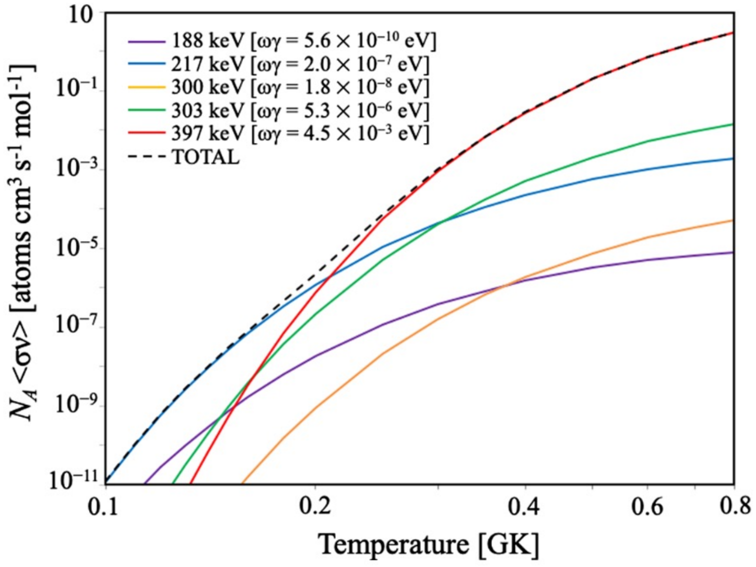

Kennington, Phys. Rev. L ***124*** *(2020)*

Measurements of *p*–capture resonances strengths

Constraining sulphur Abundances in Novae presolar grains: $^{32}S/^{33}S$ strong hint of novae origin w.r.t. SNe II?

$^{33}Cl(p,\gamma)^{34}Ar$ **unc. rate >x2**

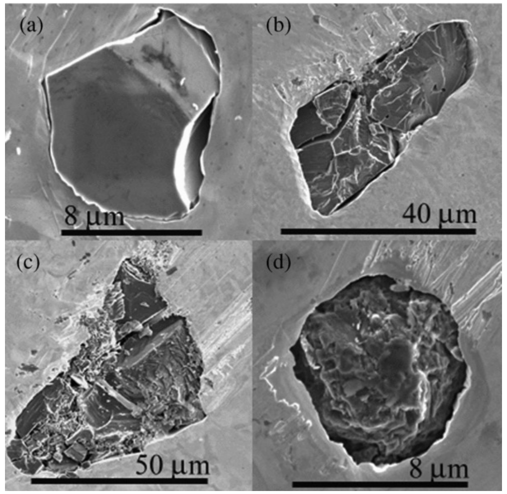

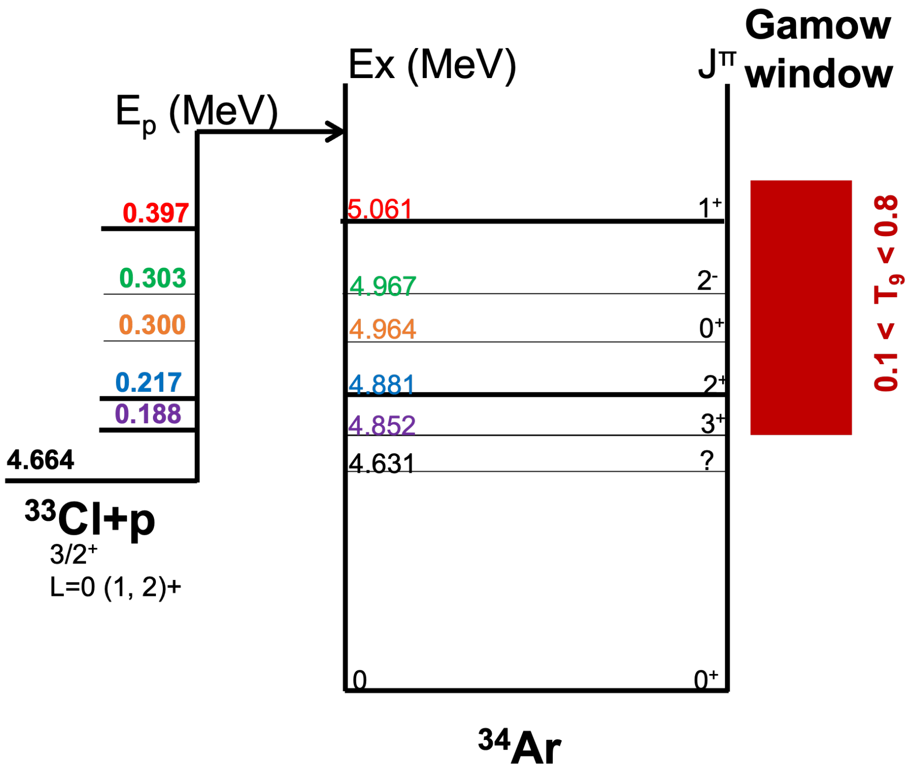

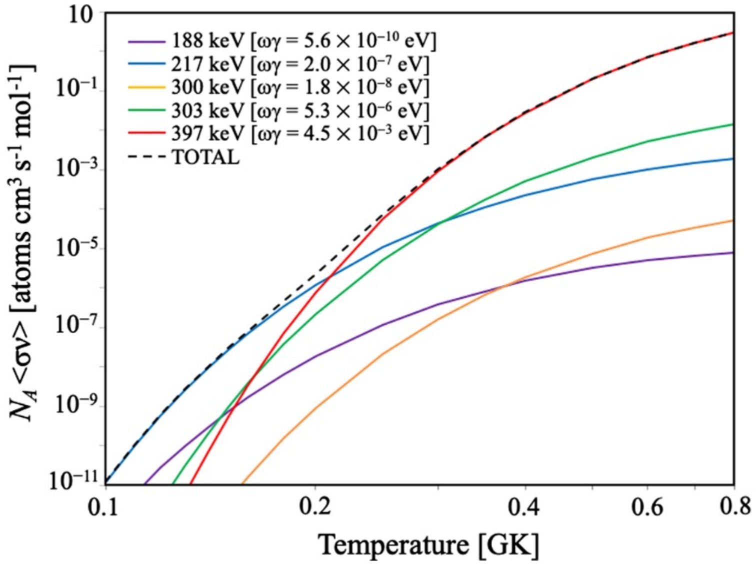

EXPERIMENTAL SETUP

- Radioactive fragmentation beam ^{33}Cl@20MeV/u → LISE/GANIL, ARIS/FRIB, …
- Particle recoil spectrometer → ZDD, S800, …
- γ–ray spectrometer → EXOGAM, GRETINA , …

Kennington, Phys. Rev. L ***124*** *(2020)*

Measurements of *p*–capture resonances strengths

Constraining sulphur Abundances in Novae presolar grains: $^{32}S/^{33}S$ strong hint of novae origin w.r.t. SNe II?

$^{33}Cl(p,\gamma)^{34}Ar$ **unc. rate >x2**

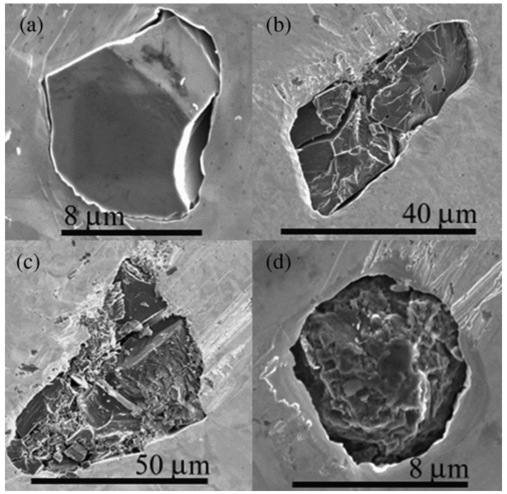

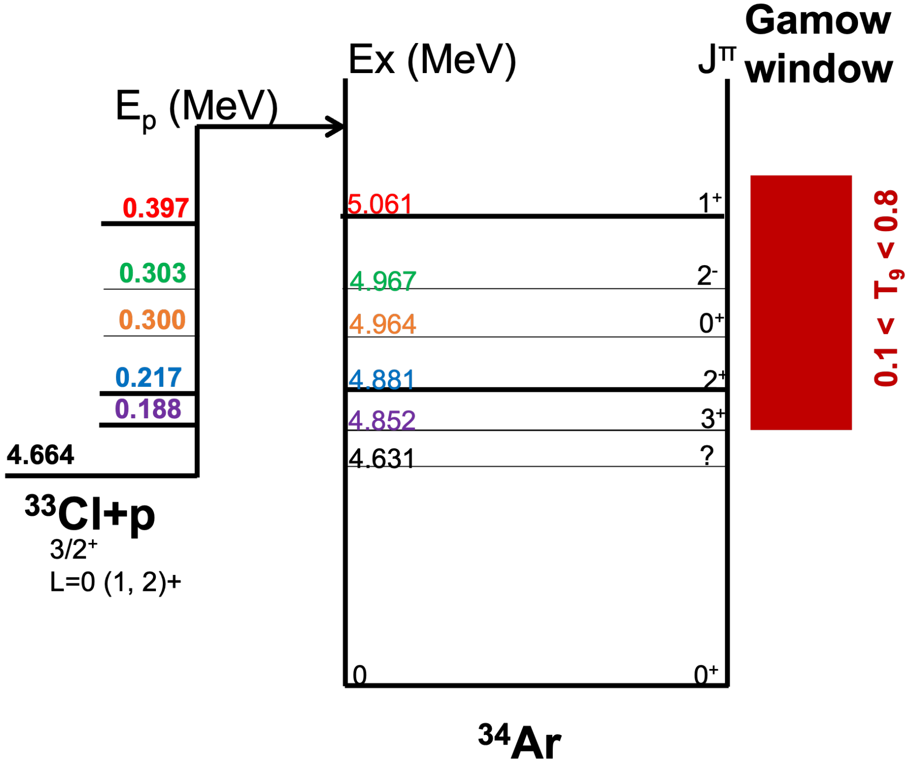

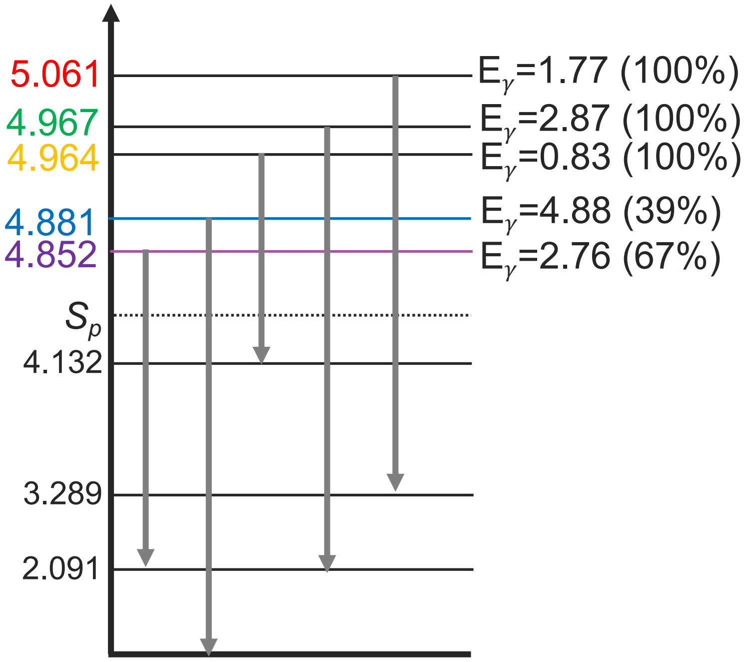

EXPERIMENTAL SETUP

- Radioactive fragmentation beam ^{33}Cl@20MeV/u → LISE/GANIL, ARIS/FRIB, …
- Particle recoil spectrometer → ZDD, S800, …
- γ–ray spectrometer → EXOGAM, GRETINA , …

Kennington, Phys. Rev. L ***124*** *(2020)*

Radiative spectroscopy of ^{34}Ar (E_X>S_p)

Another explosive site of interest: X-ray bursts

Explosive H-, He burning (T ≲ 2 GK)
Matter accretion at surface of compact star (NS)

Opened questions
Compact star mass?
Accretion?
Light Curve?
Heaviest element /
nucleosynthesis end?

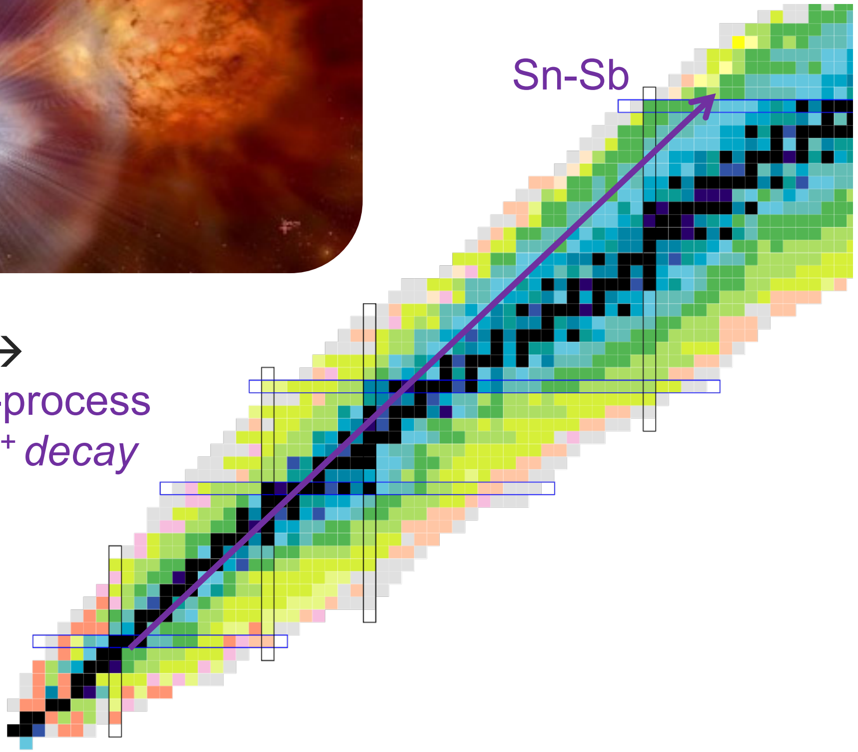

hot-CNO →
αp- and rp-process
(*α*/p,p/*γ*), β⁺ *decay*

Light curve

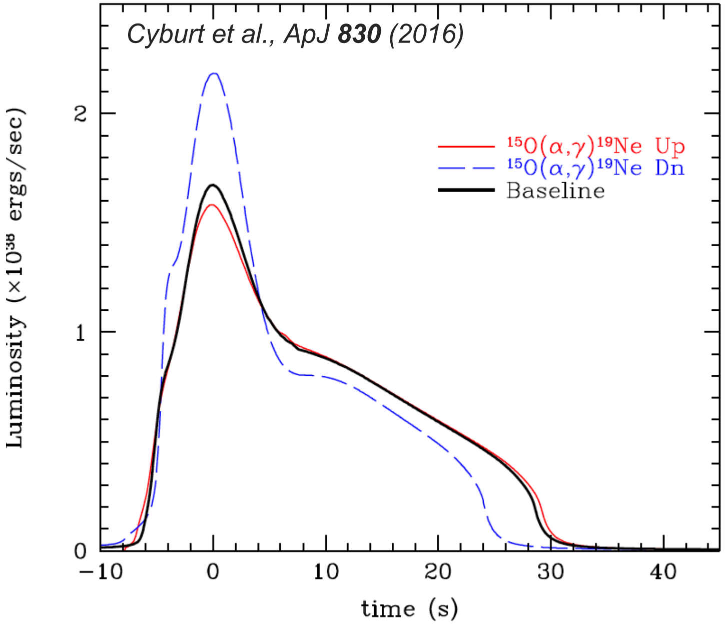

$^{15}O(\alpha,\gamma)^{19}Ne$ rate
Light Curve luminosity?
X-ray burst periodicity?
Flow hot-CNO → *rp*-process?

Spectroscopy of ^{19}Ne (E_X>S_α)

Spectroscopy of α–unbound ^{19}Ne* *F. de Oliveira Santos et al.*

Lifetime: particle-particle correlations and angle-integrated velocity-difference profile ($\Delta\beta = \beta_{reac} - \beta_{ems}$)
α-branching: particle-particle correlation and quantification of excited state decay channels $BR_\alpha = 1 / (1 + Counts_{Ex\&\gamma} / Counts_{Ex\&\alpha})$
Spin: angular distribution of particle decay

EXPERIMENTAL SETUP

- Stable beam ^{20}Ne@4MeV/u → GANIL, ATLAS, LEGNARO,…
- Particle spectrometer → VAMOS, FMA, PRIMSA, ..
- γ–ray spectrometer → AGATA, GRETINA

Spectroscopy of α–unbound ^{19}Ne* *F. de Oliveira Santos et al.*

Lifetime: particle-particle correlations and angle-integrated velocity-difference profile ($\Delta\beta = \beta_{reac} - \beta_{ems}$)
α-branching: particle-particle correlation and quantification of excited state decay channels $BR_\alpha = 1 / (1 + Counts_{Ex\&\gamma} / Counts_{Ex\&\alpha})$
Spin: angular distribution of particle decay

High energy and spatial resolution for particle- and γ–ray spectrometers

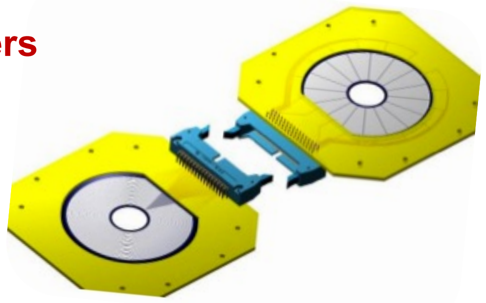

EXPERIMENTAL SETUP

- Stable beam ^{20}Ne@4MeV/u → GANIL, ATLAS, LEGNARO,…
- Particle spectrometer → VAMOS, FMA, PRIMSA, ..
- γ–ray spectrometer → AGATA, GRETINA

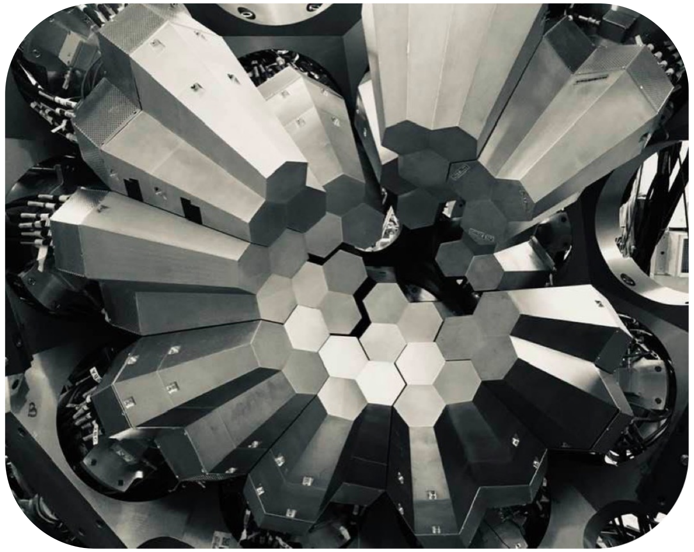

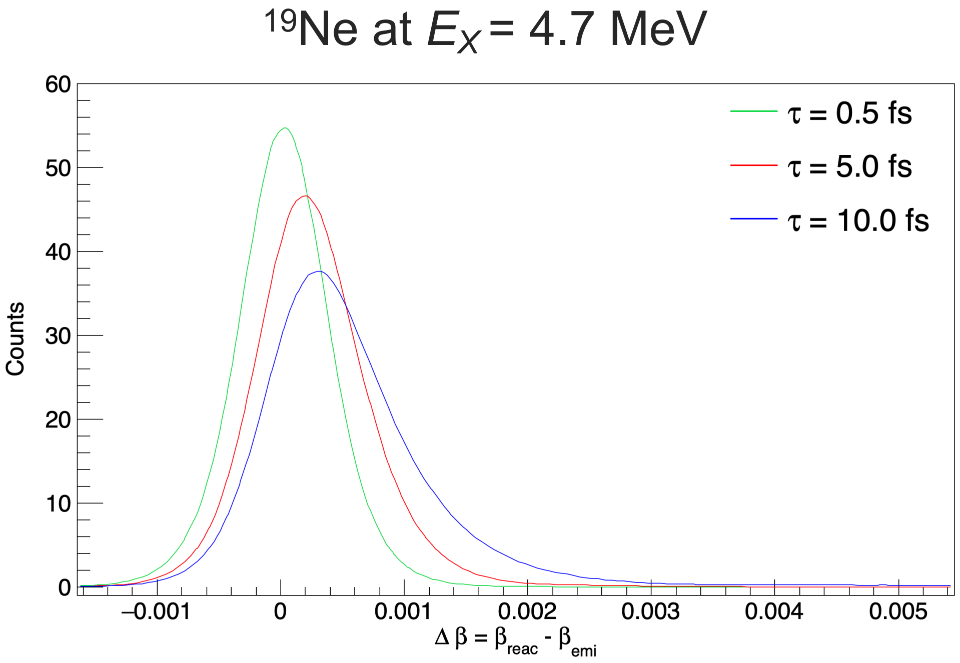

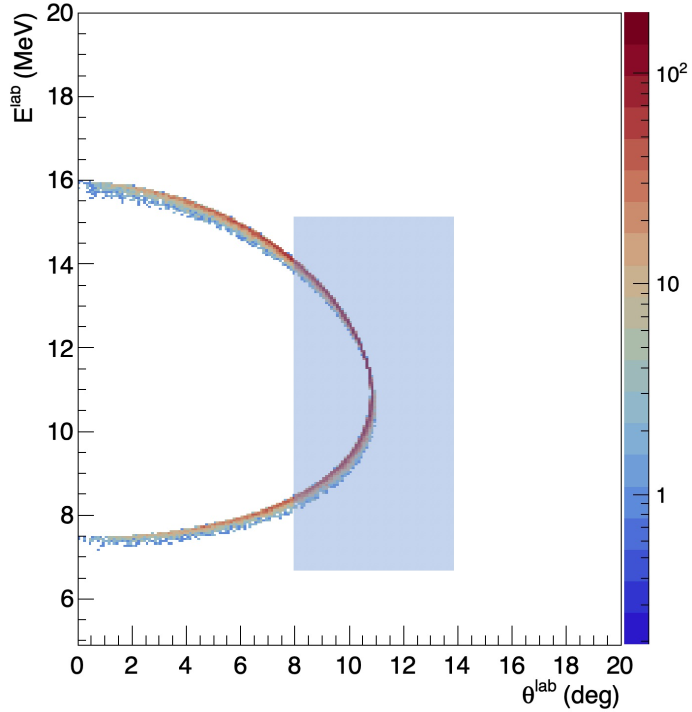

Another explosive site of interest: X-ray bursts

Explosive H-, He burning (T $\lesssim$ 2 GK)
Matter accretion at surface of compact star (NS)

hot-CNO →
αp- and rp-process
(α/p,p/γ), β⁺ decay

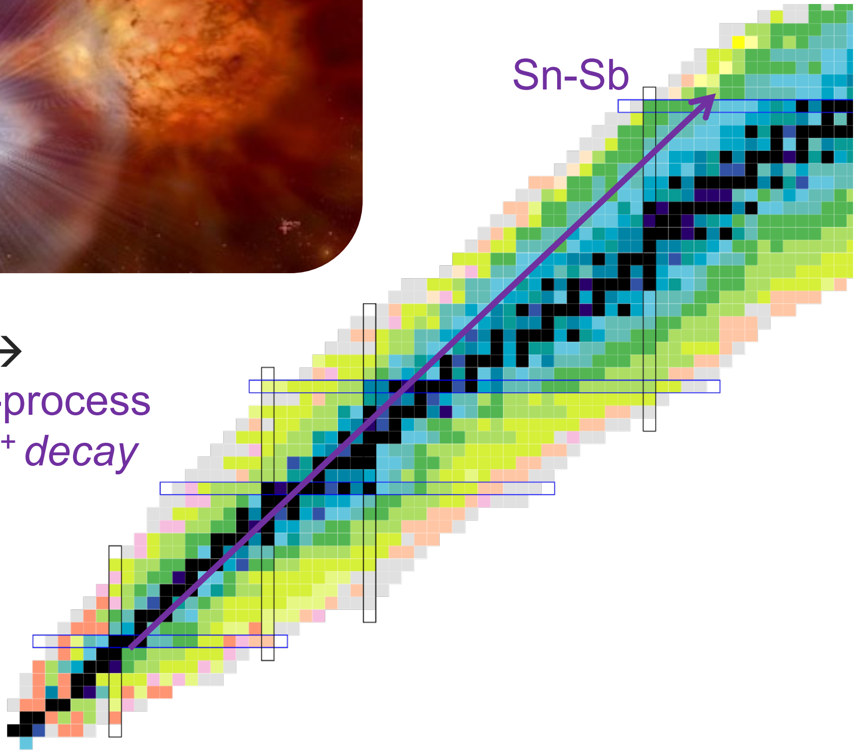

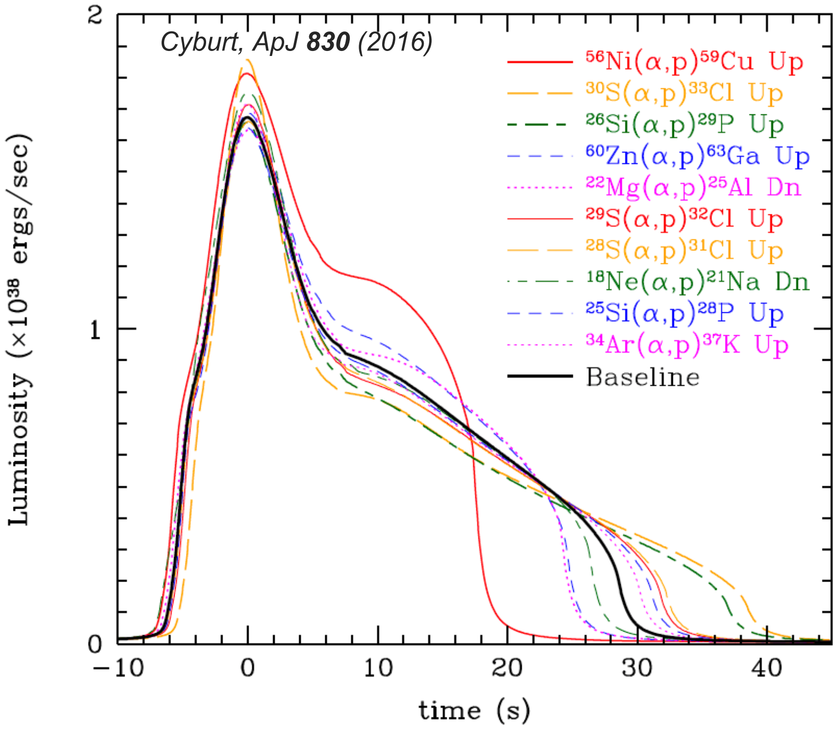

Direct α–capture cross sections measurements

Direct α–capture cross-section measurements

Direct cross section measurement at astrophysical energy with an active target in inverse kinematics

- Stellar environment T > 1 GK, E_{cm} ~ MeV/u ⇔ $\sigma \gtrsim 1$ mb
- High (thickness, efficiency)
- Excitation function in a single experiment

Direct α–capture cross-section measurements

Direct cross section measurement at astrophysical energy with an active target in inverse kinematics

- Stellar environment T > 1 GK, E_{cm} ~ MeV/u ⬄ $\sigma \gtrsim 1$ mb
- High (thickness, efficiency)
- Excitation function in a single experiment

Ionization chamber MUSIC *Carnelli, NIMA **799** (2015), Avila, Phys. Rev. C **94** (2016)*

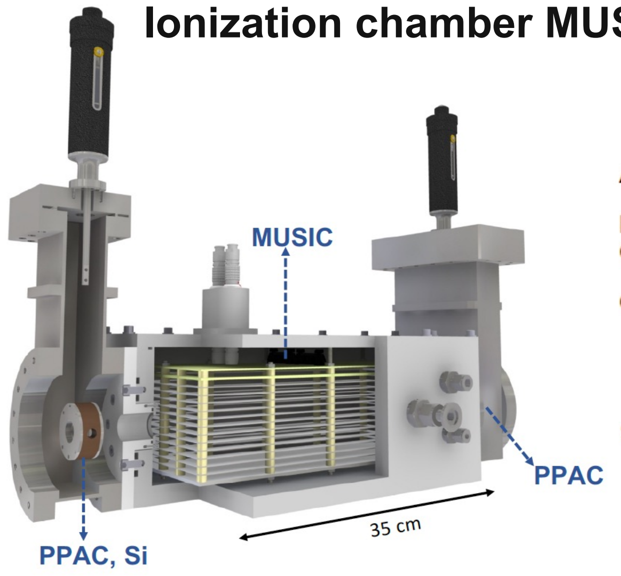

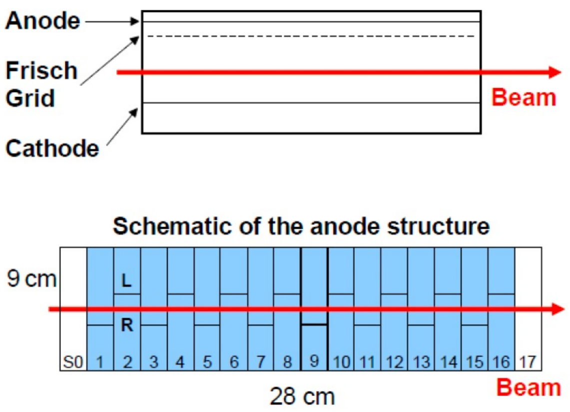

PPAC
Time of flight (radioactive beams)

Anode segmentation
Reaction at different energies

*Jayatissa, Phys. Rev. L **131** (2023)*

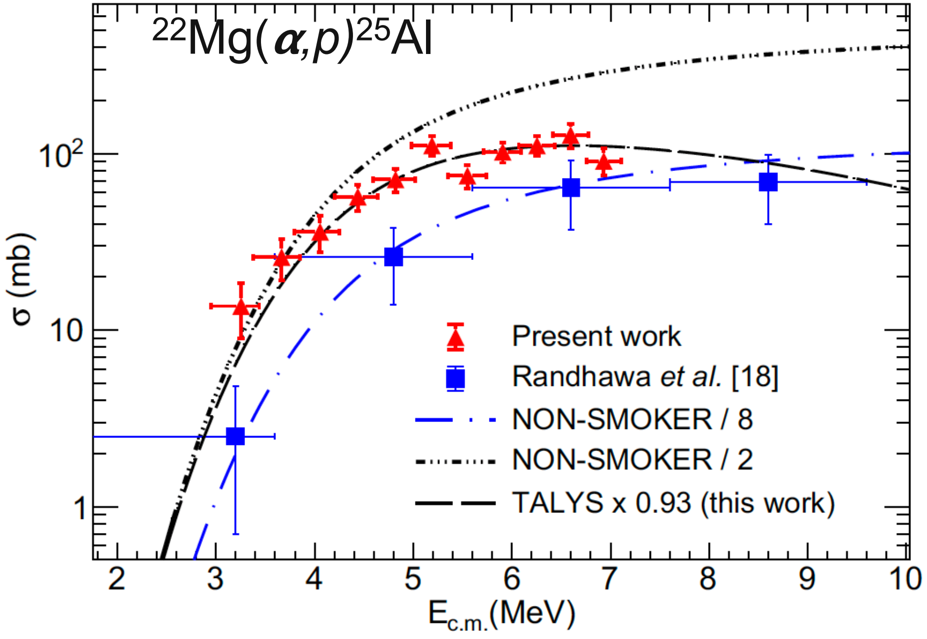

Direct α–capture cross-section measurements

Direct cross section measurement at astrophysical energy with an active target in inverse kinematics

- Stellar environment T > 1 GK, E_{cm} ~ MeV/u ⇔ $\sigma \gtrsim 1$ mb
- High (thickness, efficiency)
- Excitation function in a single experiment

Ionization chamber MUSIC *Carnelli, NIMA **799** (2015), Avila, Phys. Rev. C **94** (2016)*

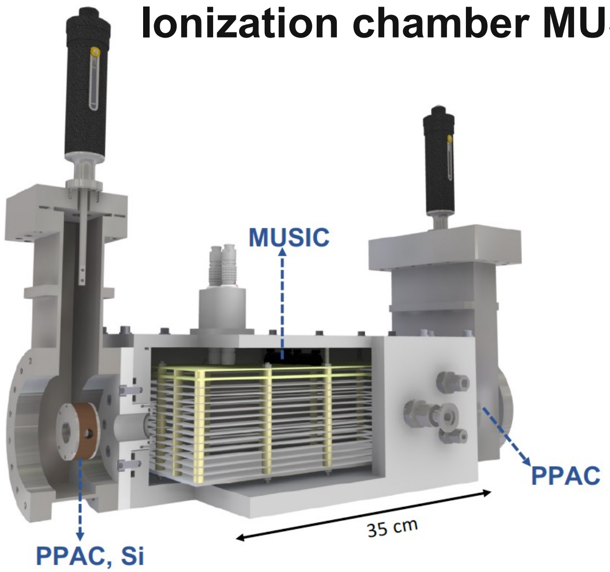

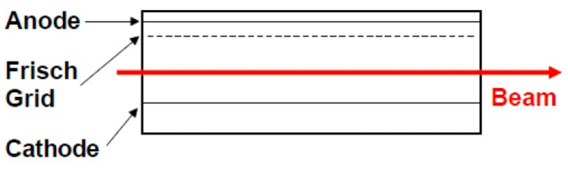

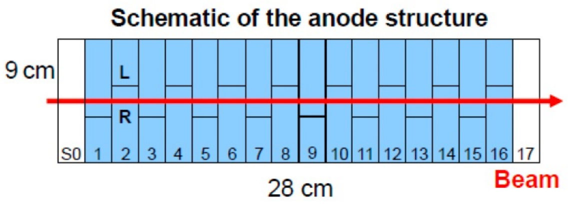

PPAC
Time of flight (radioactive beams)

Anode segmentation
Reaction at different energies

*Jayatissa, Phys. Rev. L **131** (2023)*

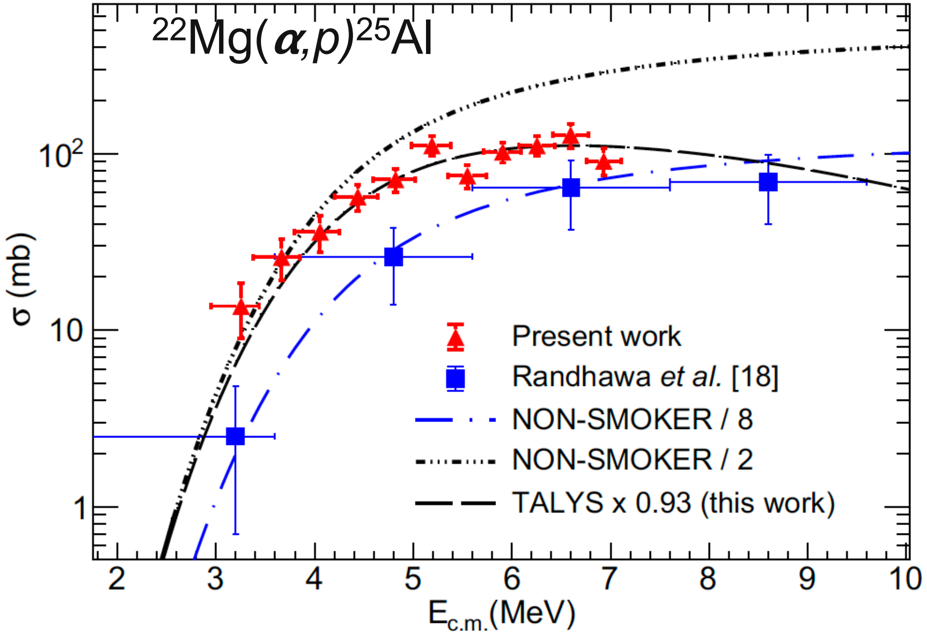

^{18}Ne(α,p)^{21}Na *N. de Séréville et al.*

EXPERIMENTAL SETUP

- Radioactive beam ^{18}Ne@2.7MeV/u → RAISOR/ANL, …
- Active gaseous target → MUSIC, …

Direct α–capture cross-section measurements

Direct cross section measurement at astrophysical energy with an active target in inverse kinematics

- Stellar environment T > 1 GK, E_{cm} ~ MeV/u ⇔ $\sigma \gtrsim 1$ mb
- High (thickness, efficiency)
- Excitation function in a single experiment

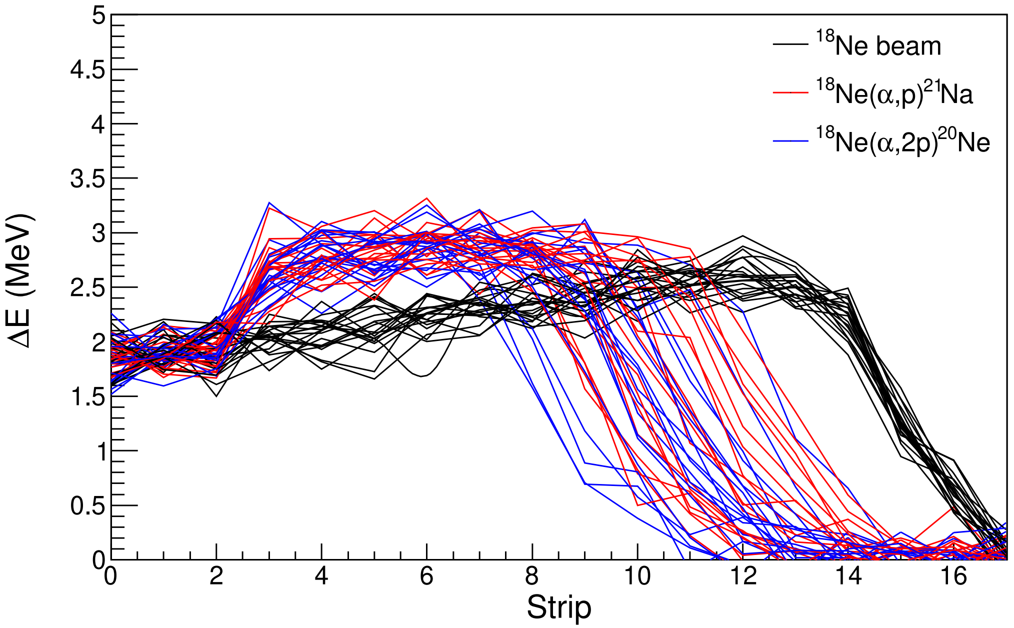

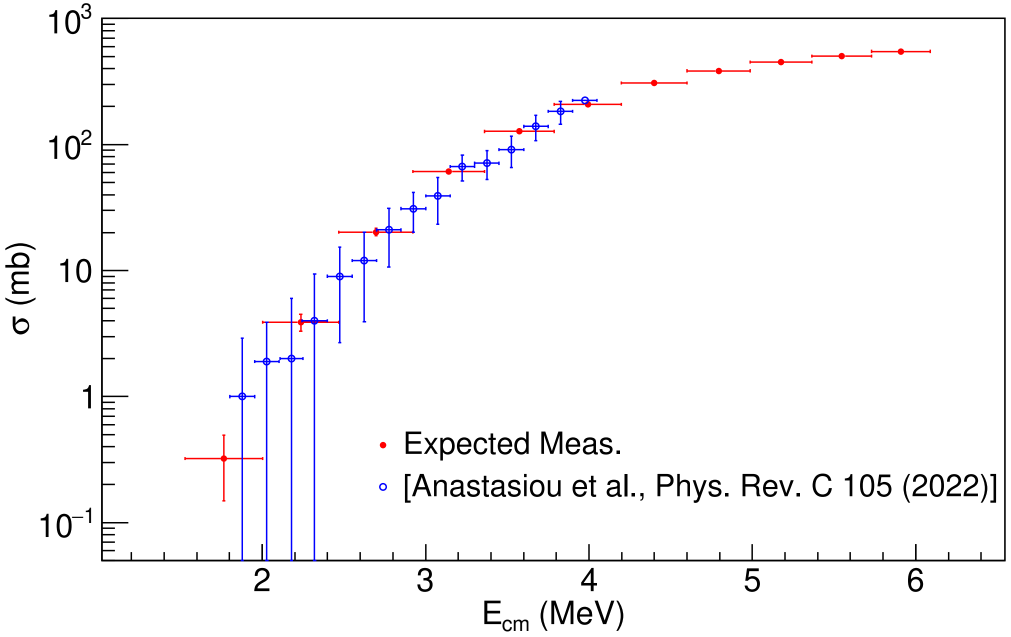

^{18}Ne(α,p)^{21}Na *N. de Séréville et al.*

EXPERIMENTAL SETUP

- Radioactive beam ^{18}Ne@2.7MeV/u → RAISOR/ANL, …
- Active gaseous target → MUSIC, …

The last words

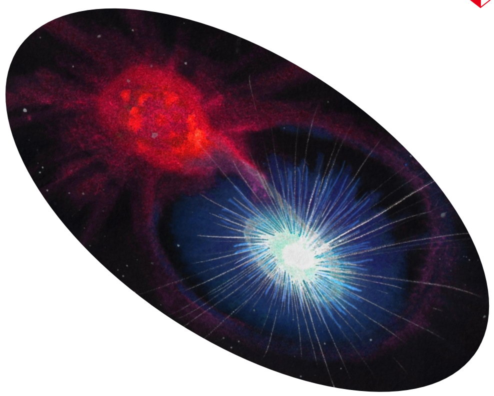

❑ **Need of nuclear data for processes involved in astrophysics**
High-resolution spectroscopy of compound nuclei
Direct access of resonances strengths

❑ **Active experimental programs**
@GANIL *p*-capture resonances & novae → resonant spectroscopy & ^{18}F in novae
@FRIB *p*-capture resonances & novae

❑ **Prospects for explosive nucleosynthesis in novae & X-ray bursts**
High-resolution spectroscopy of compound nuclei → high resolution γ–ray arrays
Direct cross-section measurements of α captures → active gaseous targets

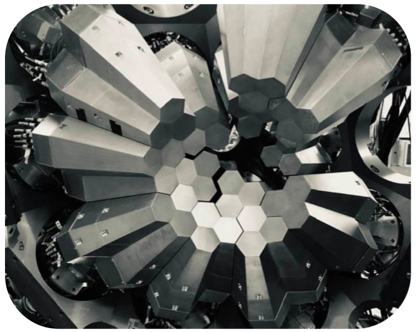

FRIB

laboratoire commun CEA/DRF CNRS/IN2P3

The last words

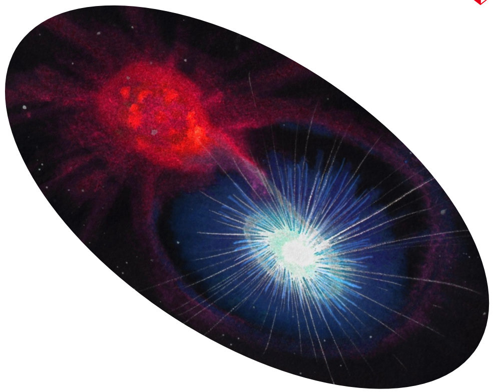

- **Need of nuclear data for processes involved in astrophysics**

High-resolution spectroscopy of compound nuclei
Direct access of resonances strengths

- **Active experimental programs**

@GANIL	*p*-capture resonances & novae	→ resonant spectroscopy & ^{18}F in novae
@FRIB	*p*-capture resonances & novae	

- **Prospects for explosive nucleosynthesis in novae & X-ray bursts**

High-resolution spectroscopy of compound nuclei → high resolution γ–ray arrays
Direct cross-section measurements of α captures → active gaseous targets

FRIB

Progress in explosive H-burning nucleosynthesis thanks to
(+) radioactive beam luminosity
(+) energy and spatial resolution of γ–ray and particle spectrometer

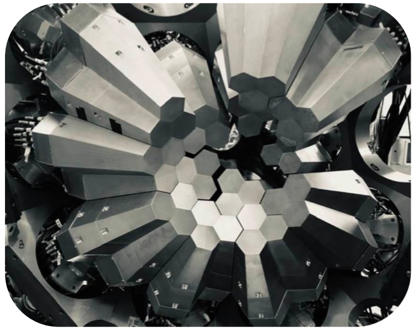

GANIL spiral2
laboratoire commun CEA/DRF CNRS/IN2P3

Search for ^{22}Na in novae supported by a novel method for measuring femtosecond nuclear lifetimes

Chloé Fougères, François de Oliveira Santos, Jordi José, Caterina Michelagnoli, Emmanuel Clément, Yung Hee Kim, Antoine Lemasson, Valdir Guimarães, Diego Barrientos, Daniel Bemmerer, Giovanna Benzoni, Andrew J. Boston, Roman Böttger, Florent Boulay, Angela Bracco, Igor Čeliković, Bo Cederwall, Michał Ciemala, Clément Delafosse, César Domingo-Pardo, Jérémie Dudouet, Jürgen Eberth, Zsolt Fülöp, Vicente González, Andrea Gottardo, Johan Goupil, Herbert Hess, Andrea Jungclaus, Ayşe Kaşkaş, Amel Korichi, Silvia M. Lenzi, Silvia Leoni, Hongjie Li, Joa Ljungvall, Araceli Lopez-Martens, Roberto Menegazzo, Daniele Mengoni, Benedicte Million, Jaromír Mrázek, Daniel R. Napoli, Alahari Navin, Johan Nyberg, Zsolt Podolyák, Alberto Pullia, Begoña Quintana, Damien Ralet, Nadine Redon, Peter Reiter, Kseniia Rezynkina, Frédéric Saillant, Marie-Delphine Salsac, Angel M. Sánchez-Benítez, Enrique Sanchis, Menekşe Şenyiğit, Marco Siciliano, Nadezda A. Smirnova, Dorottya Sohler, Mihai Stanoiu, Christophe Theisen, Jose J. Valiente-Dobón, Predrag Ujić & Magdalena Zielińska — Show fewer authors

laboratoire commun CEA/DRF CNRS/IN2P3

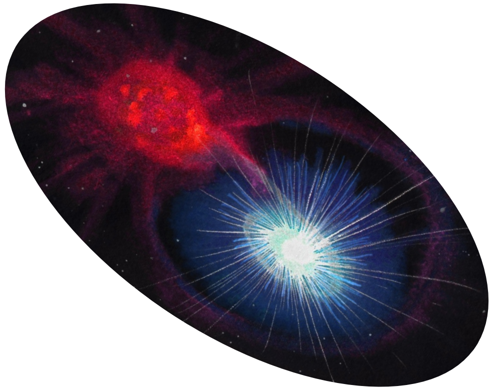

The collaboration

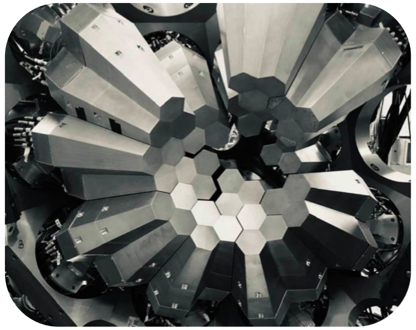

Angle-integrated measurement of the $d(^{25}\text{Al},n\gamma)^{26}\text{Si}$ transfer reaction to probe resonance strengths in $^{25}\text{Al}(p,\gamma)^{26}\text{Si}$ relevant for the production of ^{26}Al in novae
FRIB experiment with GRETINA - S800

C. Fougères[1,2], F. Hammache[3], F. de Oliveira Santos[4], N. de Séréville[3], C. Benetti[5], A. Gade[5], S. Gillespie[5], J. Swartz[5], J. Pereira[5], D. Weisshaar[5], S. M. Ali[5], H. Arora[5], M. L. Avila[1], L. Balliet[5], K. Bhatt[1], T. Beck[5], S. Ahn[6], J. Chung-Jung[5], L. Dienis[4], P. Farris[5], V. Girard-Alcindor[3], S. Giraud[5], J. Huffman[5], H. Jacob[3], D. Kim[6], M. Kuich[5], C. Maher[5], F. Montes[5], C. Müller-Gatermann[1], D. Neto[7], M. Portillo[5], B. M. Sherrill[5], O. B. Tarasov[5], A. Tumino[8], and R. Zegers[5]

FRIB

0. Appendices

Measurements of *p*–capture resonances strengths

Explosive H-, He burning (T ≲ 2 GK)
Matter accretion at surface of compact star (NS)

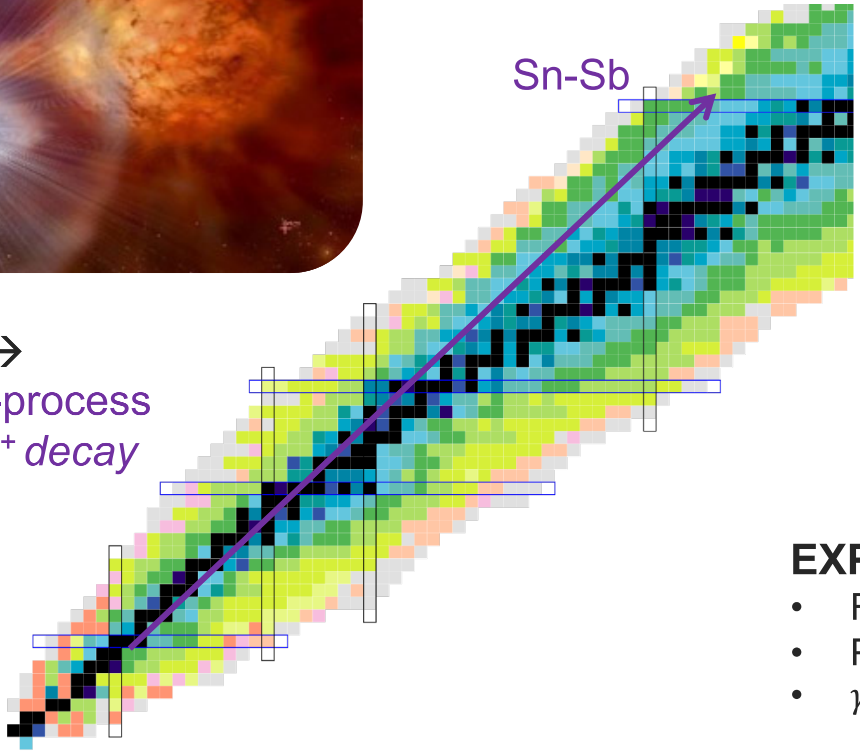

hot-CNO →
αp- and rp-process
(*α/p,p/γ*), *β⁺ decay*

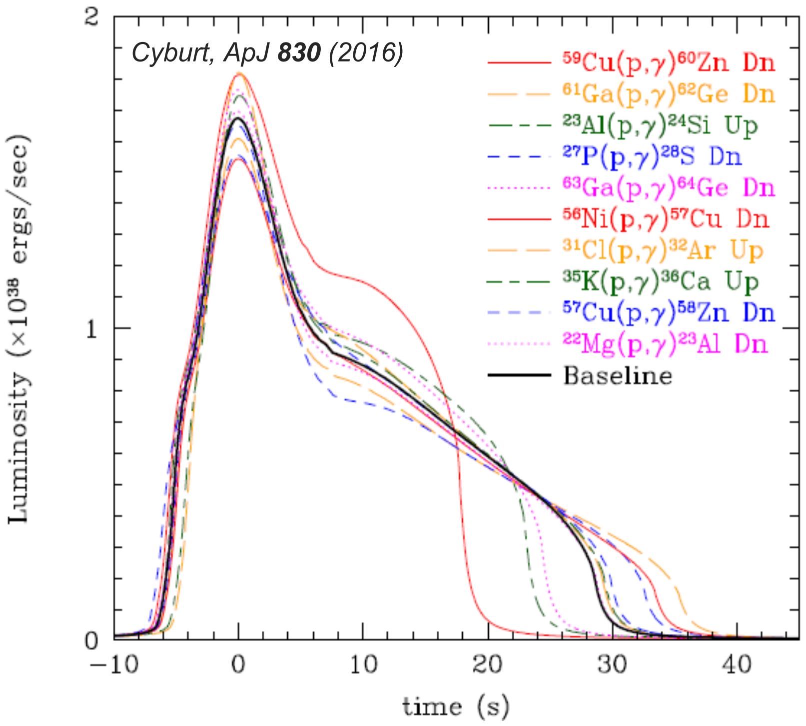

EXPERIMENTAL SETUP

- Radioactive beams @20MeV/u → ARIS/FRIB, …
- Particle spectrometer → S800, …
- *γ*–ray spectrometer → GRETINA , …

(*p*,*γ*) resonance strengths in X-ray bursts via angle-integrated transfer measurement *F. Hammache et al.*

$^{22}Na(p,\gamma)^{23}Mg$

Shell model insights

Spin consideration

γ-ray decay path → ***7/2+***

β-delayed probability

$\log_{10}(ft)$ = 3.305(23) vs {4.6(1), 3.9(1)} → ***(5/2, 7/2)+***

No mixing with the E_x = 7.801MeV IAS (*5/2+*) → ***7/2+***